THE UNIVERSITY OF
SYDNEY

Discovery and application of colorectal cancer protein markers for disease stratification

Jerry Zhou

A thesis submitted in fulfilment of the requirements

for the degree of Doctor of Philosophy

School of Molecular Bioscience

The University of Sydney

Sydney, Australia

March 2014

Table of contents

Chapter 3 Proteomic alterations during colorectal cancer progression

Declaration

All clinical colorectal cancer and normal mucosa samples were collected from Royal Prince Alfred Hospital and Concord Repatriation General Hospital. Surgical resections were performed by Prof. Michael J. Solomon, Prof. Leslie Bokey, Prof. Pierre Chapuis and their surgical team. Cancer histology was conducted by Clinical Associate Prof. Charles Chan, Joo-Shik Shin and their histopathology team. Experiments in Chapter 3 were funded by a Research Scholar Award from the Cancer Institute NSW. Protein identification by mass spectrometry in Chapter 3 was performed with assistance from Erin Sykes and Dr. Ben Crossett (Sydney University Proteome Research Unit, University of Sydney, NSW, Australia). Statistical analysis in Chapter 4 was conducted with assistance from Dr. Nicola J. Armstrong (School of Mathematics and Statistics, University of Sydney, NSW, Australia).

Jerry Zhou

Acknowledgements

I would like to thank the following people for their contribution towards my PhD because without their help and support this project would not have been possible.

My mentors Prof. Richard Christopherson and Dr. Larissa Belov: I am forever grateful for their guidance and support to make me the scientist I am today. I appreciate the freedom and trust Prof. Christopherson has given me to express myself in my work. His encouragement for my unconventional approach has reminded me of the reasons why I became a scientist. Dr. Belov has taught me the value of scientific integrity. She is both my harshest and most understanding critic. Her belief in me has made me continually strive to become a better scientist.

The dedicated people from Royal Prince Alfred Hospital: Prof. Michael Solomon, Prof. Soon Lee and Dr. Joo Shin.

The professional and friendly team from Concord Repatriation General Hospital: Prof. Stephen Clarke, Prof. Pierre Chapuis, Prof. Elie Leslie Bokey, Dr. Charles Chan, Ms Candice Clarke and Ms Gael Sinclair.

The post-doctorates: Dr. Kim Kaufman for her brilliant insights, Dr. Swetlana Mactier for her quirky anecdotes and Dr. Ben Crossett for his knowledge and encouragement.

Dr. Trisha Almazi for bringing warmth and enthusiasm to the lab, Dr. Pauline Huang for her wisdom and advice on all of life's little problems, and Dr. Zoe Che for being herself.

Duthika Mallawaaratchy for being the voice of reason, Meng-Ping Hsu for our shared love of food and Erin Sykes for her crazy stories.

To all the boys; Cody Finke, Ben Kroeger-Moore, Munther Alomari, David Gay and Kieran Matic, thanks for all the memorable testosterone fuelled adventures.

The past and present lab members who have continued to be awesome friends: Natalie Armacki, Elizabeth West, Sandra Wissmueller, Roselini Ngiono, Laura Mohr, Emily Heath and Philippa Kohnke.

My friends in SMB: Johanna, Tehara, Mia, Vicky, Nick, Michael, Brian, Anjali, Debbie, Taylor, David, Nestor, Sashi, Kavya, Chris, Wen, Christine, Sue Ling, Laura and Arlene.

I would like to thank the University of Sydney for their support through the University Post-graduate Award, the Cancer Institute NSW for their Research Scholar Award and the HUPO committee for the Travel Award in 2012.

And last but definitely not least, thanks to my family for their continued support.

Publications

Manuscripts

1. Zhou, J., Belov, L., Chan, C., Clarke, S.J., Christopherson, R.I. (2011) Colorectal cancer cell surface protein profiling using an antibody microarray and fluorescence multiplexing. J. Vis. Exp. (55), e3322, DOI:10.3792/3322
2. Belov, L., Zhou, J., Christopherson, R.I. (2010) Cell surface markers in colorectal cancer prognosis. Int. J. Mol. Sci. 12(1): 78-113
3. Zhou, J., Belov, L., Huang, P., Shin, J., Solomon, M.J., Chapuis, P.H., Bokey, L., Chan, C., Clarke, C., Clarke, S.J., Christopherson, R.I. (2010) Surface antigen profiling of colorectal cancer using antibody microarrays with fluorescence multiplexing. J. Immunol. Methods 355(1-2):40-51

Book Chapters

1. Wang, X. (Ed), Zhou, J., Belov, L., Christopherson, R.I. (2012) Bioinformatics of antibody microarray and multiplexing. Human Proteomics Bioinformatics. Springer Publisher.
2. Schwab, M. (Ed), Belov, L., Zhou, J., Christopherson, R.I. Colorectal cancer therapeutic antibodies. Springer Reference Live: Encyclopedia of Cancer. 19:22 Published 19 January 2010

Conference abstracts

Oral presentations

1. Zhou, J., Belov, L., Solomon, M.J., Chan, C., Clarke, C., Clarke, S.J., Christopherson, R.I. (2012) Multi-biomarker characterisation of colorectal cancer. Human Proteome Organisation (HUPO) 2012 annual world congress, Boston, United States of America
2. Zhou, J., Belov, L., Solomon, M.J., Chan, C., Clarke, C., Clarke, S.J., Christopherson, R.I. (2012) Colorectal cancer sub-classification using an antibody microarray. 17th Lorne Proteomic Symposium, Lorne, Australia
3. Zhou, J., Belov, L., Solomon, M.J., Chan, C., Clarke, C., Clarke, S.J., Christopherson, R.I. (2010) Surface profiling colorectal cancer and correlations with the microenvironment. The University of Sydney Cancer Research Network: Tumour Microenvironment Workshop, NSW, Australia
4. Zhou, J., Belov, L., Solomon, M.J., Chan, C., Clarke, C., Clarke, S.J., Christopherson, R.I. (2010) Colorectal cancer sub-classification using an antibody microarray. Postgraduate Cancer Research Symposium at the University of Sydney, NSW, Australia

Poster presentations

1. Zhou, J., Belov, L., Huang, P., Shin, J., Solomon, M.J., Chapuis, P.H., Bokey, L., Chan, C., Clarke, C., Clarke, S.J., Christopherson, R.I. (2012) Immunophenotyping of colorectal cancer cells correlating with disease stage and neutrophil to lymphocyte ratio, Proteomics and Beyond Symposium, Macquarie University, NSW, Australia
2. Zhou, J., Belov, L., Huang, P., Shin, J., Solomon, M.J., Chapuis, P.H., Bokey, L., Chan, C., Clarke, C., Clarke, S.J., Christopherson, R.I. (2012) Immunophenotyping of colorectal cancer cells and tumour-infiltrating T-cells, 3rd Sydney Cancer Conference, NSW, Australia
3. Zhou, J., Belov, L., Huang, P., Shin, J., Solomon, M.J., Chapuis, P.H., Bokey, L., Chan, C., Clarke, C., Clarke, S.J., Christopherson, R.I. (2012) Sub-classification of colorectal cancer using surface antigen antibody microarray and fluorescence multiplexing, 24th Lorne Cancer Conference, Lorne, Australia
4. Zhou, J., Belov, L., Huang, P., Shin, J., Solomon, M.J., Chapuis, P.H., Bokey, L., Chan, C., Clarke, C., Clarke, S.J., Christopherson, R.I. (2010) Sub-classification of colorectal cancer using surface antigen antibody microarray and fluorescence multiplexing, Human Proteome Organisation (HUPO) 2012 annual world congress, Sydney, Australia
5. Zhou, J., Belov, L., Huang, P., Shin, J., Solomon, M.J., Chapuis, P.H., Bokey, L., Chan, C., Clarke, C., Clarke, S.J., Christopherson, R.I. (2010) Sub-classification of colorectal cancer using surface antigen antibody microarray and fluorescence multiplexing, 2nd Sydney Cancer Conference, Sydney, Australia
6. Zhou, J., Belov, L., Christopherson, R.I. (2010) Multi-biomarker characterisation of colorectal cancer. Cancer Proteomic Conference, Berlin, Germany
7. Zhou, J., Belov, L., Christopherson, R.I. (2010) Multi-biomarker characterisation of colorectal cancer. 15th Lorne Proteomic Symposium, Lorne, Australia

Cover page illustration

1. Zhou, J. (2012) DotScan antibody microarray. Proteomics Clinical Applications 6(5-6): Cover

Abbreviations

2D electrophoresis	Two-dimensional electrophoresis
ACPS	Australian Clinicopathological Staging
ADH	Alcohol dehydrogenase
AJCC	American Joint Committee on Cancer
ANOVA	Analysis of variance
APC gene	Adenomatous polyposis coli gene
APS	Ammonium persulphate
ATP	Adenosine triphosphate
BSA	Bovine serum albumin
CA	Carbohydrate antigen
CD	Cluster of differentiation
CDK	Cyclin dependent kinase
CEA	Carcinoembryonic antigen
CK2	Casein kinase 2
CRC	Colorectal cancer
CREB	cAMP response element-binding
CSC	Cancer stem cell
CXC	Chemokine receptor
Cy Dye	Cyanine dye
DCC gene	Deleted in colorectal carcinoma gene
DIGE	Difference gel electrophoresis
DMF	Dimethylformamide
DMSO	Dimethyl sulfoixde
DNA	Deoxyribonucleic acid
DTT	Dithiothreitol
ECM	Extracellular matrix
EF-1α	Elongation factor Tu
EpCAM	Epithelial cell adhesion molecule
ER	Endoplasmic reticulum
ESI-QUAD-TOF	Electrospray ionisation-quadrupole-time of flight
FACS	Fluorescence activated cell sorting
FAP	Familial adenomatous polyposis
GAPDH	Glyceraldehyde-3-phosphate dehydrogenase
GRP	Glucose-regulated protein
HBSS	Hanks' balanced salt solution
HIF	Hypoxic inducible factor
HLA	Human leukocyte antigen
hnRNP	Heterogeneous nuclear ribonucleoprotein
HPLC	High-performance liquid chromatography
Hsp	Heat shock protein
ICAM	Intercellular adhesion molecule
IDA	Information dependent acquisition

IDH	Isocitrate dehydrogenase
IEF	Isoelectric focusing
IGF	Insulin-like growth factor
IHC	Immunohistochemistry
iTRAQ	Isobaric tag for relative and absolute quantitation
LC-MS	Liquid chromatography-mass spectrometry
LFA	Lymphocyte function-associated
MAPK	Mitogen-activated protein kinase
MHC	Major histocompatibility complex
MMP	Matrix metalloproteinase
MMR	Microsatellite mismatch repair
MnSOD	Manganese superoxide dismutase
mRNA	Messenger ribonucleic acid
MRPS22	28S ribosomal protein S22
MS	Mass-spectrometry
MS/MS	Tandem mass spectrometry
Muc1/EMA	Epithelial membrane antigen
NF-κB	Nuclear factor kappa-light-chain-enhancer of activated B cells
NK cell	Natural killer cell
NLR	Neutrophil to lymphocyte ratio
NPM	Nucleophosmin
PBS	Phosphate buffer saline
PCNA	Proliferating cell nuclear antigen
PCNP	PEST proteolytic signal containing nuclear protein
PDI	Disulfide-isomerase A3
PE	Phycoerythrin
PR	Proteinase
Prdx	Peroxiredoxin
PSA	Prostate specific antigen
RCN	Reticuloclabin
RNA	Ribonucleic acid
ROS	Reactive oxygen species
SDS	Sodium dodecyl sulfate
TAM	Tumour-associated macrophages
TCEP	Tris (2-carboxyethyl) phosphine
TGM	Transglutaminase
TIL	Tumour infiltrating lymphocytes
TNM	Tumour node metastasis
VEGF	Vascular endothelial growth factor
VLA	Very late activation
vWF	Von Willebrand factor
WDR	WD repeat-containing protein

Summary

Colorectal cancer (CRC) is a major cause of cancer mortality. Whereas some patients respond well to therapy, others do not, and thus more precise methods of CRC stratification are needed.

We analysed the intracellular protein expression from 28 CRC primary tumours and corresponding normal intestinal mucosa using saturation-DIGE/MS and Explorer antibody microarrays. Changes in protein abundance were identified at each stage of CRC. Proteins associated with proliferation, glycolysis, reduced adhesion, endoplasmic reticulum stress, angiogenesis, and response to hypoxia represent changes to CRC and its microenvironment during development. Molecular changes in CRC cells and their microenvironment can be incorporated into clinico-pathological data to help sub-classify tumours and personalise treatment.

DotScan antibody microarray analysis was used to profile the surface proteome of cells derived from 50 CRC samples and corresponding normal intestinal mucosa. Fluorescence multiplexing enabled the analysis of two different sub-populations of cells from each sample: $EpCAM^+$ cells (CRC cells in the tumours or normal epithelial cells in normal mucosa) and $CD3^+$ T-cells (tumour-infiltrating lymphocytes). Unsupervised hierarchical clustering of the CRC and T-cell surface profiles defined four clinically relevant clusters, which showed some correlation with histopathological and clinical characteristics such as cancer cell differentiation, peri-tumoural inflammation and stimulation of infiltrating T-cells. The observed relationship between the surface antigen expression profiles of patients' CRC cells and their corresponding tumour infiltrating T-cells suggests that CRC surface proteins may play a direct role in influencing the activity (and hence surface protein expression) of neighbouring T-cells and/or *vice versa*. We conclude that the application of surface profiling may provide improved patient stratification, allowing more reliable prediction of disease progression and patient outcome.

Chapter 1

General introduction

1.1 Colorectal cancer overview

Colorectal cancer (CRC) is a cancer of epithelial origin, localised to the large intestine and rectum. It has the highest incidence of all malignant cancers in Australia (excluding skin cancers other than melanoma) and accounts for 9.3 per cent of all cancer related deaths in this country (Statistics from Australian Institute of Health and Welfare. Cancer in Australia: an overview, 2012). Treatment of patients with primary CRC is often restricted to surgical resection of the tumour. The risk of recurrence and the decision for adjuvant therapy following surgery depend on a number of prognostic factors for relapse and survival, i.e. clinico-pathological staging based on the extent of tumour invasion, involvement of regional lymph nodes and metastatic spread to other organs (Figure 1.1).

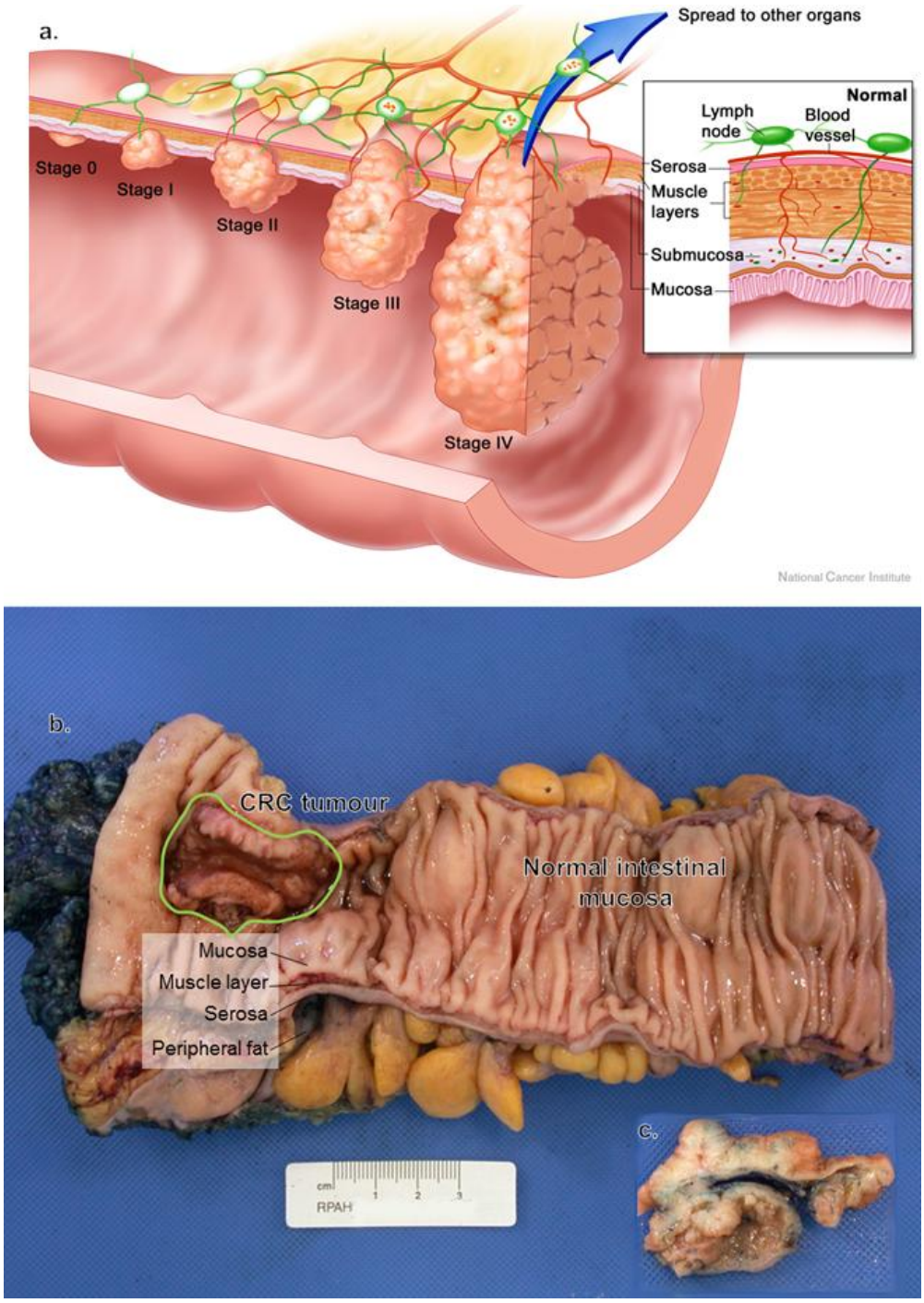

Figure 1.1 a) Graphical representation of CRC progression. Stage 0 (*tumour-in-situ*) adenoma initiates at the innermost layer of the colon/rectum, the mucosal surface. Malignant stage I tumours propagate outwards beyond the mucosa into the submuscosa but not beyond the muscularis properia. Stage II tumours invade beyond the muscularis properia into the subserosa and serosa. Stage III tumours are characterised by the presence of cancer cells in one or more local and/or regional lymph nodes. Stage IV tumours have metastasised into distant organs. (Image from National Cancer Institute colon and rectal cancer: www.cancer.gov/cancertopics/types/colon-and-rectal). b) Adenocarcinoma of the transverse colon. The fungating ACPS B1 adenocarcinoma projects into the lumen but has not caused obstruction (circled in green). c) Transverse slice of the primary tumour. The serosa is painted blue for orientation and to visualise tumour infiltration (photo taken at The Royal Prince Alfred Hospital).

If metastasis has occurred, the patient 5-year survival rate falls dramatically from 90% to less than 10% (O'Connell et al., 2004). Stage C patients (30 – 60%) survive the first 5 years depending on the number of involved lymph nodes and the benefit of adjuvant chemotherapy. For stage B patients (without lymph node involvement), the use of adjuvant chemotherapy remains controversial (Kopetz et al., 2008). This is because the clinical course for individuals remains difficult to predict, largely due to prognostically heterogeneous groups within same-stage tumours. Therefore, there is a need for more reliable methods of CRC stratification to predict CRC progression, identify patients at risk of recurrence and those most likely to benefit from adjuvant therapy.

1.2 Tumour microenvironment

The evolution of CRC from an adenomatous polyp to metastatic disease is dependent not only on progressive accumulation of genetic and epigenetic abnormalities (Moyret-Lalle et al., 2008), but also on the complex interactions of different sub-populations of cells within the tumour microenvironment (cancer cells, normal stromal cells, infiltrating leukocytes and the soluble factors they produce) (McAllister and Weinberg, 2010).

The stroma consists of the non-malignant cells of the tumour: fibroblasts, infiltrating leukocytes and cells of the blood vessels. The tumour stroma plays an essential role in the development of CRC and is referred to as a “reactive stroma” (Kalluri and Zeisberg, 2006). This reactive stroma is associated with an increased number of fibroblasts, enhanced capillary density and deposition of a new extracellular matrix (ECM) rich in type-1-collagen and fibrin. There is evidence indicating that the primary neoplasm and the reactive stroma communicate in a reciprocal way via the basement membrane (Kalluri and Zeisberg, 2006). A loss of basement membrane components due to degradation by proteolytic enzymes and/or

a lack of biosynthesis are correlated with tumour progression. For example, Type VII collagen is lost early in the development of several cancers (Havenith et al., 1988). Similarly, laminin-5 is commonly lost in colon carcinomas but not in pre-malignant tumours (Sordat et al., 1998). These modifications of the basement membrane occur simultaneously to changes in trans-membrane adhesive receptors expressed by tumour cells in response to degradation of ECM. Metabolism of ECM molecules is an important aspect of tissue homeostasis and determines how cells respond to acute and chronic stresses. Various types of proteinases participate in ECM turnover, but matrix metalloproteinases (MMPs) are the principal ECM-degrading enzymes. These enzymes have a central role in cancer progression, given that ECM degradation products can influence stroma-cancer cell interactions. In particular, metastatic colon cancer cells are able to induce the expression and/or secretion of MMP-2 and MMP-9 in stromal cells, either via direct contact, or via a paracrine regulation (Mook et al., 2004).

Inflammatory reactions in tumours can have a positive influence on survival (Klintrup et al., 2005) or alternatively can be associated with development of metastases and disease progression (Jedinak et al., 2010). The presence of large numbers of tumour infiltrating lymphocytes (TILs) at the invasive tumour front has been associated with a good prognosis for CRC patients (Katz et al., 2009). Patients with high levels of $CD3^+$, $CD8^+$, $CD25^+$, $CD45RO^+$ or $CD71^+$ TILs appear to have a better clinical course (Lee et al., 2010) than those with low levels, particularly in early disease stages (Deschoolmeester et al., 2010). The importance of the intra-tumoural location, immunophenotype and density of these infiltrates has been demonstrated (Halama et al., 2009, Pages et al., 2008).

The role of tumour-associated macrophages (TAM) in tumourigenesis is complex because TAMs can either prevent or promote tumour development. While Foressell *et al.* showed that a dense TAM infiltration at the tumour front positively influenced prognosis in colon cancer

(Forssell et al., 2007), strong pro-tumourigenic effects of TAMs in CRC have also been reported (Jedinak et al., 2010, Kaler et al., 2010). It has been suggested that the balance between pro- and anti-tumourigenic properties of TAMs may depend on their interaction with cancer cells, other stromal cells, and the tumour microenvironment (Jedinak et al., 2010) or be influenced by the degree of cell-cell contact (Forssell et al., 2007).

1.3 The current state of cancer classification

The role of the histopathologist is no longer limited to issuing an accurate tissue diagnosis, but is increasingly directed towards the provision of prognostic information and additional findings directly relevant to patient management. This ongoing refinement of reporting is heavily dependent on the fundamental role of the pathologist in the accurate classification of disease. Classification is more than the naming of disease entities or even the collation of their particular diagnostic features. It includes the elucidation of clinico-pathological correlations that are the starting point for investigation of the causation, evolution and natural history of the disease. It is necessary for a disease to be properly classified to achieve effective clinical management and meaningful laboratory investigation of the underlying mechanisms. The classification of cancer has traditionally been based mainly on microscopic morphology, supplemented in more complex forms of malignancy, by immunohistochemistry and sometimes molecular approaches.

In the case of CRC, both clinical management and research have continued for many decades to classify CRC based on histological features, such as tumour grade (differentiation) and tumour stage (Table 1.1) (Newland et al., 1981, Fielding et al., 1991) that is based on depth of tumour invasion, involvement of regional lymph nodes and metastatic spread to other organs (Compton, 2003). These staging systems offer systematic evaluation of tumours and

provide the basis for prediction of survival and choice of initial treatment. By placing patients into groups with different risks of disease progression, clinico-pathological staging has become widely accepted and is comparatively easy to perform. However, these anatomically based staging systems have limited use beyond local therapies (surgical resection, radio-frequency ablation, regional radiotherapy) and have proven to be unreliable in intermediate stage B and C patients, where tumours of similar histological appearance can follow different clinical courses and show different responses to therapy (Eschrich et al., 2005).

Table 1.1 The main CRC stratification systems used in Australia. Duke's classification is the oldest CRC staging method. The American Joint Committee on Cancer (AJCC) system and TNM (tumour node metastasis) staging are extensions based on the original Duke's methods. The Australian clinico-pathological staging (ACPS) system has been adopted by several Australian Hospitals, in particular Concord Repatriation General Hospital that developed a more specific version of the ACPS in 1971.

2011 7th edition TNM classification of malignant tumours	**AJCC stage**	**TNM stage**	**ACPS (Concord sub-stage)**	**Duke's classifi-cation**
Tumour confined to mucosa (*cancer-in-situ*)	Stage 0	Tis N0M0	A1	
Tumour invades submucosa	Stage I	T1 N0M0	A2	A
Tumour invades muscularis properia		T2 N0M0	A3	B1
Tumour invades subserosa or beyond (without other organs involved)	Stage IIA	T3 N0M0	B1	B2
Tumour invades adjacent organs or perforates the serosa	Stage IIB	T4 N0M0	B2	B3
Metastasis to 1 to 3 local lymph nodes	Stage IIIA	T-2 N1M0	C1	C3
Metastasis to 1 to 3 regional lymph nodes	Stage IIIB	T3-4 N1M0	C2	C2-3
Metastasis to 4 or more regional lymph nodes	Stage IIIC	Any T N2M0	D1	C1-3
Distant metastases present	Stage IV	Any T any N M1	D2	D

The introduction of molecular factors has complicated the situation, as well as providing new opportunities for predicting prognosis. The genetic evolution of CRC was understood to proceed on the basis of a relatively uniform and linear sequence of steps, with *APC* inactivation initiating adenomas and additional genetic changes, notably *KRAS* mutation, and *TP53* inactivation, promoting the emergence of increasingly aggressive sub-clones

(Vogelstein et al., 1988). The condition familial adenomatous polyposis (FAP), caused by germ-line mutation of APC, was perceived as the hereditary counterpart to sporadic CRCs (Fodde et al., 2001). These genetic biomarkers have shown great potential in predicting specific phenotypes in hereditary CRC patients (i.e. those with FAP); however, it remains difficult to correlate phenotype in sporadic CRC with its cellular genotype (Soravia et al., 1998). Sporadic CRC represents 90% of all cases, exhibiting a wide diversity of cellular dysfunctions (Steinert et al., 2002), even between histologically identical tumours.

In the search for tumour progression markers, there has been a concerted effort to define gene expression profiles at the transcript level (Ross et al., 2000, Scherf et al., 2000). However, it is clear that mRNA expression data alone are insufficient to predict functional outcomes for the cell. For instance, mRNA expression data provide very little information about activation state, post-translational modification or localisation of corresponding proteins. Moreover, there are numerous reports highlighting the disparity between mRNA transcript and protein expression levels (Gygi et al., 1999). The inherent advantage of proteomics is that the identification of proteins is itself the biological endpoint. Comparative studies of protein expression in normal and disease tissue have led to the identification of aberrantly expressed proteins that may assist in diagnosis, outcome prediction and drug development (Hanash, 2003).

1.4 Protein biomarkers

Despite the discovery of a range of intra- and extra-cellular protein biomarkers for CRC and continuing efforts to discover potentially prognostic and predictive markers using various approaches (Alfonso et al., 2008, Andre et al., 2006, Barderas et al., 2010, Friedman et al., 2004, Gil-Bazo, 2007, Habermann et al., 2008, Jimenez et al., 2010, Luque-Garcia et al.,

2010), the translation of this increasing volume of differential proteomic data into patient care remains a major challenge. This is partly due to the heterogeneous nature of CRC (Hlubek et al., 2007, Li et al., 2007b) and the complexity of processes involved in its development and spread, but also to challenges in detecting and characterising glycoproteins and low abundance proteins (Ahn et al., 2009, Rho et al., 2008) in complex mixtures. In addition, validation of candidate proteins as prognostic markers is time-consuming and expensive, and recent critical reviews of differentially expressed proteins from comparative proteomic studies have suggested that reported proteins may be associated with general cellular stress response, rather than being disease-specific biomarkers (Petrak et al., 2008, Wang et al., 2009). The development of a reliable assay for CRC stratification, determining prognosis and guiding post-surgical therapy, therefore remains elusive. There is a general consensus that individual biomarkers cannot provide enough prognostic information to replace histopathological staging and that the application of multiple biomarkers will be required; innovative approaches are needed to translate accumulating data into a useful method for sub-classifying CRC patients for disease stage and those likely to benefit from available treatment.

The metastatic potential of CRC may already be encoded in the primary tumour (Yamasaki et al., 2007), and molecular staging using a classifier based on 43 genes has yielded more reliable prognostic information than the traditional clinical staging, particularly for intermediate stage B and C patients (Eschrich et al., 2005). While genomics and mRNA expression based technologies will continue to contribute substantially to biology and medicine, there are limits to the type and amount of information such studies can provide. Comparisons of transcript and corresponding protein expression have shown that mRNA and protein levels are not necessarily correlative (Steiner and Witzmann, 2000, Celis et al., 2000). In addition, proteomics can provide information on the post-translational modifications such

as phosphorylation (Mann, 2006, Rush et al., 2005, Dwek et al., 2001) or glycosylation (Dwek et al., 2001). Moreover, since almost all therapeutic intervention strategies involve targeting and modulating protein function and activity, it is imperative that analyses of mechanism underlying tumourigenesis include proteomics. Identification of disease signatures based on protein expression profiles in primary CRC tissue may provide a more accurate representation of disease progression and metastasis, and enable these signatures to be used to predict patient recovery and survival after surgical removal of the primary CRC. The use of immunohistochemistry for analysis of CRC tissue sections for multiple potentially prognostic/predictive markers (Fernebro et al., 2004, Lyall et al., 2006) has the advantage of revealing antigen location in sections; however the method is relatively low throughput, expensive, labour-intensive, and quantification is difficult. The use of high throughput techniques, such as Saturation-DIGE and antibody microarrays, enable analysis of a large number of samples simultaneously.

1.5 Proteomic techniques

Sample preparation determines the success or failure of protein expression profiling in tumour tissue. Factors such as time between surgical removal and sample processing impact significantly on the integrity of the proteins. To obtain the most accurate representation of the cancer proteome, samples should be assessed and sliced immediately by the pathologist and snap-frozen at -80°C within 12 h of surgical removal to avoid protein degradation. To ensure that experimental findings relate directly to changes in the cancer cells, it is desirable that the cancer cells are free of contaminating serum proteins, haemopoietic cells, stroma and necrotic tissue. Depending on tissue type, enrichment for specific sub-populations of cells has been performed using techniques such as micro-dissection (Lawrie and Curran, 2005, Sheehan et

al., 2008), fluorescence activated cell sorting (FACS) (Dalerba et al., 2007b) or antibody-conjugated magnetic beads (Dalerba et al., 2007b, Kaufman et al., 2010).

Traditionally, proteome profiling of complex mixtures, such as whole-cell lysates, has involved the combination of two-dimensional electrophoresis (2DE) protein profiling with mass spectrometry (MS) for protein identification (Friedman et al., 2004, Alfonso et al., 2005). 2DE separates proteins by charge in the first dimension and molecular weight in the second dimension, enabling visualisation of thousands of proteins in a single experiment. However, owing to the complexity of whole cells or tissues, a single separation strategy such as 2DE will probably reveal only a subset of the total proteome. The problems associated with solubility of various classes of proteins, can further reduce the window of proteins that can be recovered for identification.

Advances in 2DE technology, such as the multiplexing of samples for DIGE analysis have enabled the user to identify protein abundance changes with a higher degree of confidence than with the use of the standard 'one sample per gel' method. This has resulted in less variation between gels, and requires fewer replicates to be confident that an observed difference is genuine (Shaw et al., 2003). Conventional DIGE technology utilises three mass- and charge-matched cyanine dyes (Cy2, Cy3, and Cy5) that, as N-hydroxy-succinmidyl esters, undergo nucleophilic substitution with ε-amine groups of lysine residues of proteins. The dye to protein ratio must be kept low (approximately 5%) in order to avoid multiple dye additions on each protein molecule that would give rise to multiple spots per protein on a 2D gel. Saturation of lysine would produce more reliable results but is not a practical solution as most proteins have a typically high lysine content (e.g., 10.1% across eight random proteins (Lehninger, 1972) it would be difficult to force the labelling reaction to saturation without the need for excessive amounts of reagent. To improve sensitivity, it would be preferable to label an alternative, less prevalent, amino acid to saturation. Saturation-labelling technology (GE

Healthcare Amersham) uses one such amino acid, cysteine, which is less prevalent in proteins than lysine (e.g., 2.47% across eight random proteins (Lehninger, 1972)), yet also has chemistry amenable to chemical modification through reaction with its thiol group. Saturation-labelling delivers all the advantages of conventional DIGE with improved sensitivity of detection (Shaw et al., 2003). By labelling the proteins to saturation the amount of sample required is reduced from 50 -100 µg for conventional DIGE to 5 – 10 µg for saturation-DIGE. Although saturation DIGE has led to the discovery of a number of differentially expressed proteins in CRC (Alfonso et al., 2008), there are inherent limitations in this method; in particular, up to 40% of high-molecular-weight material becomes insoluble upon labelling and some proteins lacking cysteine residues are not labelled with the saturation-labelling dyes, resulting in the loss of a subset of proteomic data.

Mass spectrometry (MS) has increasingly become the method of choice for analysis of complex protein samples. MS-based proteomics is a discipline made possible by the availability of gene and genome sequence databases and technical and conceptual advances in many areas. The classical proteomic quantification methods utilise high-resolution protein separation (e.g. 2D gels), which limits their applicability to abundant and soluble proteins; and second, they do not reveal the identity of the underlying protein. Recent developments in modern LC-MS/MS techniques have overcome these problems by enabling proteome-wide quantification (Bantscheff et al., 2007, Ong and Mann, 2005). Many of these advances can be achieved through improved MS instrumentation, more intelligent algorithms and software. Most of these methods employ differential stable isotope labelling to create a specific mass tag, which can be introduced into proteins or peptides. In contrast, label-free quantification approaches aim to correlate the mass spectrometric signal of intact proteolytic peptides or the number of peptide sequencing events with the relative or absolute protein quantity directly

(Old et al., 2005). A multitude of methods has emerged for the analysis of simple and complex proteomes using quantitative mass spectrometry, and the field is beginning to learn for which type of study these methods can be meaningfully applied. However, significant further improvements to experimental strategies are required particularly for the quantitative analysis of post-translational modifications.

Antibody microarrays hold great promise as a valuable tool for cancer research. The low volume requirement and the multiplexing capability of microarrays enable optimal use of precious clinical samples, and because the assays are rapid and amenable to automation, large sample sets required for biomarker studies can be processed and analysed (Sutandy et al., 2013). The first model to demonstrate the application of antibody microarrays employed the "analyte-labelled" assay format. In this format, proteins are pre-labelled with biotin before antibody capture, and once bound they can be detected after incubation with a secondary labelled binder (Haab, 2005). Using this format, Knezevic *et al.* (Knezevic et al., 2001) found changes in protein expression during cancer cell development. This approach enables the simultaneous analysis of hundreds of different proteins on the same slide, and allows for fluorescence multiplexing, i.e., the comparison of two or more samples labelled with different fluorophores, on the same microarray. However, this method lacks specificity in protein target labelling and has poor sensitivity for low-abundance proteins (Sutandy et al., 2013). Moreover, targeted protein labelling may lead to epitope destruction by some chemical reactions (Poetz et al., 2005). Therefore, the sensitivity of analyte-labelling microarrays is highly dependent on the selection of high-affinity antibodies recognising antigen epitopes unaffected by the labelling.

A novel application of antibody microarrays is the surface antigen profiling of whole cells using the DotScan antibody microarray (Zhou et al., 2010, Zhou et al., 2011). The DotScan CRC antibody microarray allows rapid immunophenotyping of 122 surface antigens on a

population of disaggregated live tumour cells in suspension, requiring 4×10^6 cells per assay. Density of cell binding per antibody dot depends on the proportion of positive cells in the population, level of antigen expression and affinity of the antibody. The optical binding pattern reflects the immunophenotype of the mixed cell population, while the CD3-Phycoerythrin (PE) and EpCAM-Alexa Fluor 647 staining allow for the detection of T-cells and cancer/epithelial cells, respectively. This approach generates dot patterns that define the surface immunophenotype of each sub-population of captured cells.

1.6 Aims

This PhD project aims to apply proteomic analysis to the stratification of CRC. We hope to obtain expression profiles from intracellular- and surface-proteins in CRC cells that can be used to generate "disease signatures" correlating with CRC stage, invasion, metastasis and patient outcome.

Access to fresh surgically resected CRC tissue has enabled us to obtain an accurate representation of the cancer cell proteome. We have developed a cell disaggregation method for CRC and normal intestinal mucosa tissue, to yield viable single cells for downstream analysis.

To gain a better understanding of the processes involved in CRC tumourigenesis and provide additional markers for classification, CRC tumours from every ACP stage were disaggregated and depleted of $CD45^+$ leukocytes to enable identification of differentially expressed proteins in CRC using Saturation DIGE (GE Healthcare Amersham) and Explorer antibody microarrays (FullMoon).

Changes in the cell surface proteome of CRC cells and tumour infiltrating T-cells (TILs) from different patients may enable the sub-classification of clinico-pathologically similar CRC tumours. In addition, correlations between the surface profiles of cancer cells and TILs from the same patient may reflect the influence on CRC tumours of their stromal microenvironment, and the contribution leukocytes make to tumourigenesis. The immunophenotypes of cancer cells and T-cell sub-populations from 50 CRC tumours have been determined with the DotScan antibody microarray (Medsaic Pty Ltd).

Chapter 2

Material and methods

The discovery and analysis of cancer biomarkers is a multi-phased process (Figure 2.1). In this PhD project we have utilised two proteomic analysis techniques, saturation-DIGE/MS and Explorer antibody microarrays, to profile the CRC proteome and identify protein alterations during CRC progression. A third technique, DotScan antibody microarrays, was used to profile the surface antigen expression on CRC cells and tumour-infiltrating T-cells. This high throughput immuno-assay has been used to generate disease signatures for the sub-classification of CRC and prediction of overall survival. Figure 2.2 summaries the work flow for this PhD project.

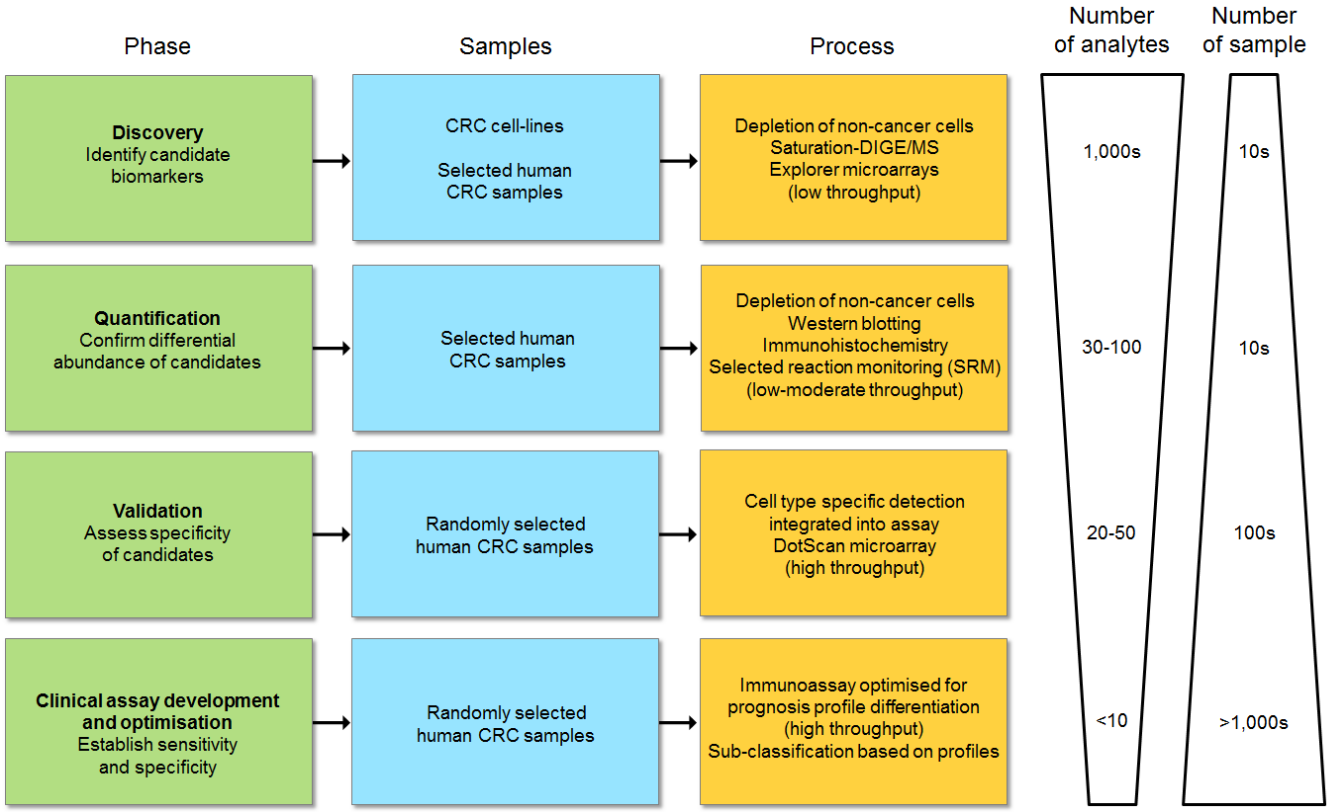

Figure 2.1 Work flow for the identification of novel protein biomarkers. 'Number of analytes' refers to the number of proteins evaluated as candidate biomarkers in each phase of development. 'Number of samples' refers to the number of samples required for each phase. DIGE, two-dimensional fluorescence difference gel electrophoresis; MS, mass spectrometry.

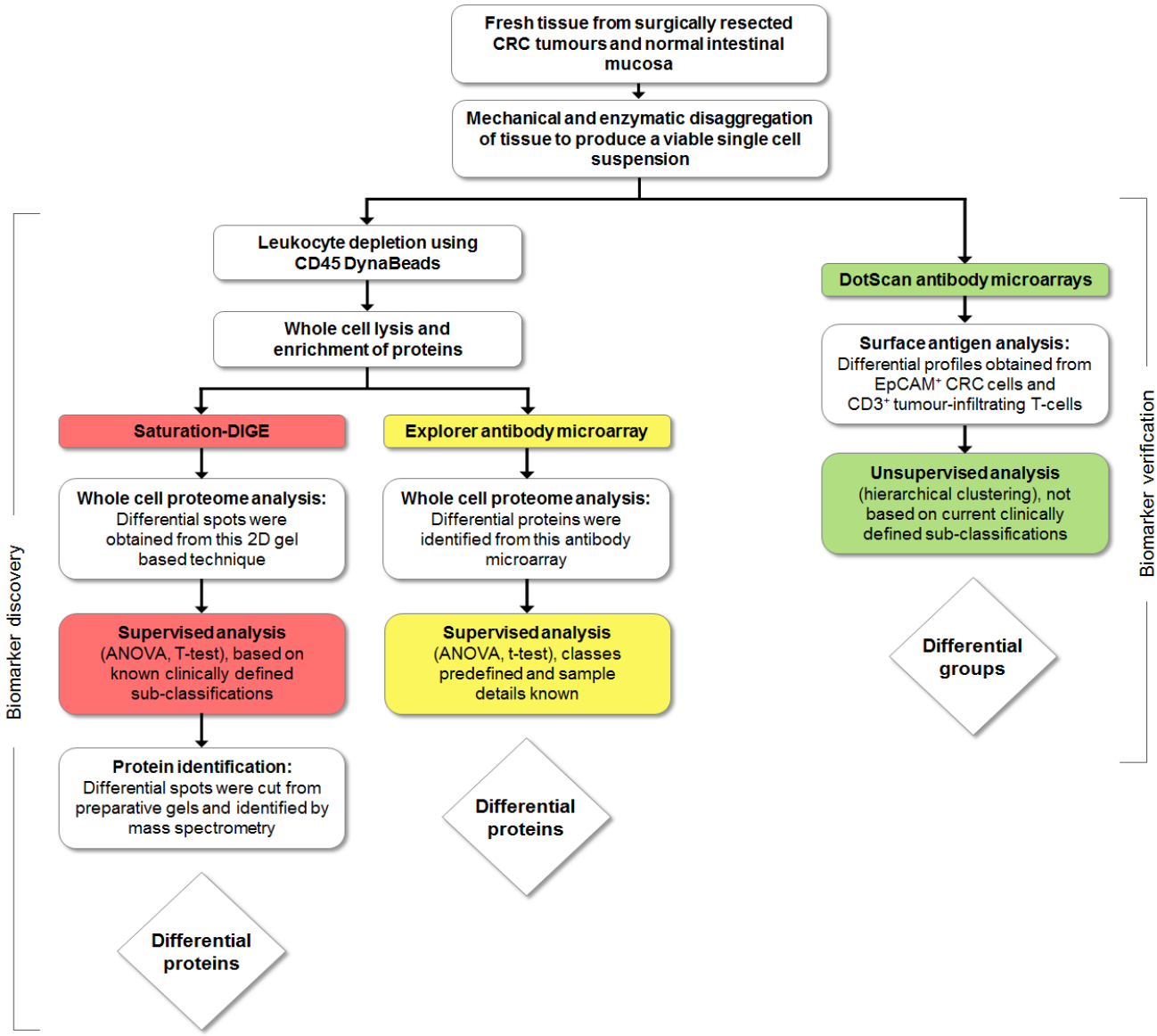

Figure 2.2 Workflow for identification of CRC biomarkers

2.1 Materials

Table 2.1 List of materials/equipment and the company supplier

Materials and equipment	Company
15 ml Falcon tubes	BD Biosciences (Franklin Lakes, NJ, USA)
2-D Cleanup Kit	Bio-Rad (Hercules, CA, USA)
2-D Quant Kit	Bio-Rad (Hercules, CA, USA)
50 ml Falcon tubes	BD Biosciences (Franklin Lakes, NJ, USA)
Agilent 1100 HPLC system	Agilent (Palo Alto, CA, USA)
Airpure® biological safety cabinet class II	Westinghouse (Butler County, PA, USA)
Analyst OS 2.0 software	AB Sciex (Foster City, CA, USA)
Antibody array assay kit	Full Moon BioSystems (Sunnyvale, CA, USA)
C18 separation nanocolumn ZORBAX 300SB-C18	Agilent (Palo Alto, CA, USA)
C18 trap column ZORBAX 300SB-C18	Agilent (Palo Alto, CA, USA)
C18 Zip-tip	Merck Millipore (Billerica, MA, USA)
CD45-Dynabead	Invitrogen Life Technologies (Carlsbad, CA, USA)
Centrifuge 5810 R	Eppendorf (Hamburg, Germany)
Cryo freezing contrainer	Nalgene (Rochester, NY, USA)
CyDye DIGE fluor labeling kit for scarce samples	GE Healthcare (Buckinghamshire, UK)
Cyrovial tubes	Greiner bio-one (Kremsmuenster, Austria)
DotReaderTM	Medsaic (Sydney, NSW, Australia)
DotScanTM microarray wash tray	Medsaic (Sydney, NSW, Australia)
DotScanTM antibody microarray kit	Medsaic (Sydney, NSW, Australia)
Eppendof tubes	Greiner (Frickenhausen, Germany)
Explorer antibody microarray	Full Moon BioSystems (Sunnyvale, CA, USA)
Filcon filter (200 µm)	BD Biosciences (Franklin lakes, NJ, USA)
Filcon filter (50 µm)	BD Biosciences (Franklin lakes, NJ, USA)
GS-800 calibrated densitometer	Bio-Rad (Hercules, CA, USA)
Haemocymeter Technocolour Neubar	Hirschmann (Eberstadt, Germany)
Harris uni-core 2 mm (spot cutter)	Electron Microscopy Sciences (Hatfield, PA, USA)
ImageQuant TL software	GE Healthcare (Buckinghamshire, UK)
Light microscope	Nikon (Tokyo, Japan)
LoBind plate	Eppendorf (Hamburg, Germany)
LoBind tube	Eppendorf (Hamburg, Germany)
MultiExperiment Viewer v4.4	TM4 Microarray Software Suite (Boston, MA, USA)
Nanodrop 3300	Thermo Fisher Scientific (Waltham, MA, USA)
Nikon TMS microscope	Nikon (Kanagawa, Japan)
Probot microfraction collector	Dionex/LC Packings (Lane Cove, NSW, Australia)
Progenesis SameSpot	Nonlinear Dynamics (Newcastle, UK)
Protean plus dodeca cell	Bio-Rad (Hercules, CA, USA)
Protein extraction kit	Full Moon BioSystems (Sunnyvale, CA, USA)
ProteinPilot 3.0	AB Sciex (Foster City, CA, USA)

Materials and equipment	Company
QSTAR Elite mass spectrometer	AB Sciex (Foster City, CA, USA)
ReadyStripTM IPG strip, 17 cm, pH 3-10 Non-linear	Bio-Rad (Hercules, CA, USA)
Strong cation exchange column	Agilent (Palo Alto, CA, USA)
Surgical blades	Livingstone International (Toronoto, Canada)
Terumo® Syringe (10 mL)	Terumo Medical Co. (Tokyo, Japan)
Typhoon FLA 9000 biomolecular imager	GE Healthcare (Buckinghamshire, UK)
Vacuum centrifuge	Thermo Fisher Scientific (Waltham, MA, USA)

2.2 Reagents

Table 2.2 List of reagents and the company of purchase

Reagent	Company
3-[(3-Cholamidopropyl) dimethylammonium]-1-propanesulfonate (CHAPS)	Sigma-Aldrich (St. Louis, MO, USA)
4-(2-hydroxyethyl)piperazine-1-ethanesulfonic acid (HEPES)	Sigma-Aldrich (St. Louis, MO, USA)
85% phosphoric acid	Sigma-Aldrich (St. Louis, MO, USA)
Acetonitrile	Sigma-Aldrich (St. Louis, MO, USA)
Agarose	Sigma-Aldrich (St. Louis, MO, USA)
AlexaFluor647-conjugated EpCAM	BioLegend (San Diego, CA, USA)
Ammonium Biocarbonate	Sigma-Aldrich (St. Louis, MO, USA)
Ammonium persulphate (APS)	Sigma-Aldrich (St. Louis, MO, USA)
Ammonium sulphate	Sigma-Aldrich (St. Louis, MO, USA)
Ampholyte (broad range pH 3-10)	Bio-Rad (Hercules, CA, USA)
Benzonase Nuclease (ultrapure) >99%	Sigma-Aldrich (St. Louis, MO, USA)
Bovine serum albumin (BSA)	Sigma-Aldrich (St. Louis, MO, USA)
Bovine serum albumin (BSA)	Sigma-Aldrich (St. Louis, MO, USA)
Bromophenol blue	Sigma-Aldrich (St. Louis, MO, USA)
Collagenase type 4	Worthington Biochemical Corporation (Lakewood Township, NJ, USA)
Coomassie Brilliant Blue G250	Sigma-Aldrich (St. Louis, MO, USA)
Cy3-streptavidin	GE Healthcare (Buckinghamshire, UK)
Deoxyribonuclease 1 (DNAse)	Sigma-Aldrich (St. Louis, MO, USA)
Dimethyl sulphoxide (DMSO)	Sigma-Aldrich (St. Louis, MO, USA)
Dimethylformamide (DMF)	Sigma-Aldrich (St. Louis, MO, USA)
Disodium hydrogen orthophosphatedodecahydrate Anhydrous	Univar (Redmond, WA, USA)
Dithiothreitol (DTT)	Sigma-Aldrich (St. Louis, MO, USA)
Ethylenediaminetetraacetic acid (EDTA)	Univar (Redmond, WA, USA)
Fetal calf serum (FCS)	Gibco/Invitrogen (Carlsbad, CA, USA)
Fetuin	Sigma-Aldrich (St. Louis, MO, USA)
Formaldehyde 37%	Sigma-Aldrich (St. Louis, MO, USA)
Formic acid	Sigma-Aldrich (St. Louis, MO, USA)
Glycine	Univar (Redmond, WA, USA)
GluFib	Sigma-Aldrich (St. Louis, MO, USA)
Hanks' balanced salt solution (HBSS)	Sigma-Aldrich (St. Louis, MO, USA)
Heat-inactivated AB serum 2%	Gibco/Invitrogen (Carlsbad, CA, USA)
Methyl alcohol (methanol), absolute	Sigma-Aldrich (St. Louis, MO, USA)
Mineral Oil	Sigma-Aldrich (St. Louis, MO, USA)
Phosphate	Univar (Redmond, WA, USA)

Reagent	Company
Phycoerythrin-conjugated CD3	Beckman Coulter (Brea, CA, USA)
Potassium chloride (KCl)	Univar (Redmond, WA, USA)
Potassium di-hydrogen orthophosphate	Univar (Redmond, WA, USA)
Renin	Sigma-Aldrich (St. Louis, MO, USA)
RPMI 1640 with 2 mM Hepes	Sigma-Aldrich (St. Louis, MO, USA)
Sequencing grade trypsin	Promega (Fitchburg, WI, USA)
Sodium chloride (NaCl)	Univar (Redmond, WA, USA)
Sodium dodecyl sulfate (SDS)	Sigma-Aldrich (St. Louis, MO, USA)
Sypro Ruby	Sigma-Aldrich (St. Louis, MO, USA)
Tetramethylethylenediamine (TEMED)	Sigma-Aldrich (St. Louis, MO, USA)
Thiourea	Sigma-Aldrich (St. Louis, MO, USA)
Tris-(2-carboxyethyl) phosphine hydrochloride (TCEP)	Sigma-Aldrich (St. Louis, MO, USA)
Tris (hydroxymethyl) aminomethane (Tris)	Univar (Redmond, WA, USA)
Trypan blue solution 0.4%	Sigma-Aldrich (St. Louis, MO, USA)
Urea	Sigma-Aldrich (St. Louis, MO, USA)

2.3 General solutions

2.3.1 Tissue disaggregation and storage

Collagenase solution pH 7.4

Collagenase (2 % (v/v))	500 mg
RPMI 1640 medium	25 ml

DNAse solution

DNAse I (0.1% (w/v))	10 mg
MilliQ water	1 ml

Cell storage solution

DMSO (20% (v/v))	2 ml
Made up in foetal calf serum (FCS)	8 ml

Added to cell in FCS 1:1 volume

HEPES-HBSS pH 7.3

Hanks' balanced salt solution (HBSS)

HEPES (25 mM)	12 g
MilliQ water	1 L

10 × Phosphate buffer saline (PBS) pH 7.5

Sodium chloride (80 g/L)	80 g
Potassium chloride (2 g/L)	2 g
Potassium di-hydrogen orthophosphate (14 mM)	2 g
Di-sodium hydrogen orthophosphate-dodecahydrate (43mM)	6.1 g
MilliQ water	1 L

Dilute 1 in 10 in MilliQ water for general use (1×PBS)

2.3.2 Leukocyte depletion with CD45 DynaBeads

Dynabead buffer 1

EDTA (1 mM)	29.2 mg
BSA	0.1g
1 × PBS	100 ml

Tris-HCl stock solution pH 8

Tris (100 mM)	12.1 g
MilliQ water	Up to 1 L

Dissolve, check pH, adjust to pH 8. Store at 4 – 8^{o}C up to 1 month

Cell lysis buffer pH 8

100 mM Tris-HCl pH 8 stock (30 mM)	6 ml
Urea (7 M)	8.41
Thiourea (2 M)	3.041 g
CHAPS (4% (w/v)	800 mg
MilliQ water	Up to 20 ml

Dissolve. Adjust to pH 8 with 1M HCl. Aliquot and store at -20^{o}C for up to 3 months

2.3.3 Saturation-DIGE for analytical and preparative gels

DTT (dithiothreitol) stock solution

DTT (1 M)	3.09 g
MilliQ water	Up to 20 ml

Aliquot and store at -20^{o}C

TCEP (Tris (2-carboxyethyl) phosphine) reducing solution

TCEP (2 mM for analytical gel)	5 mg
MilliQ water	8.7 ml

TCEP (20 mM for preparative gel)	5 mg
MilliQ water	870 µl

Use immediately (unstable)

1 × Sample buffer

Urea (7 M)	16.82 g
Thiourea (2 M)	6.08 g
CHAPS (4% (w/v)	1.6 g
MilliQ water	Up to 40 ml

Stop mixture

Immediately before use add

Ampholyte (2% (v/v)	4.5 µl
DTT (130 mM)	4.5 µl
1 × sample buffer	445.5 µl

Use immediately and discard any unused material

Rehydration solution

Immediately before use add

Ampholyte (1% (v/v))	10 µl
DTT stock (13 mM)	13 µl
1 × sample buffer	977 µl

Use immediately and discard any unused material

IPG equilibration solution

1 M Tris-HCl pH8 stock (0.1M)	10 ml
Urea (6 M)	36 g
Glycerol (30% (v/v))	30 ml
SDS (2% (w/v))	2 g

MilliQ water ..... Up to 100 ml

Prepare DTT-free stock and store at room temperature for up to 6 months.

Immediately before use add

1M DTT stock (0.5% (w/v)) ..... 32.5 µl per ml of DTT free stock

Use immediately and discard any unused material

5 × Gel buffer pH 8.8

Tris (1.87 M) ..... 227 g

MilliQ water ..... Up to 1 L

Adjust to pH 8.8 with 1M HCl

Glycerol solution

Glycerol (50% (w/v)) ..... 500 g

MilliQ water ..... Up to 500 ml

APS (ammonium persulphate) solution

APS (10 % (w/v)) ..... 0.1 g

MilliQ water ..... 1 ml

Store at -20^{o}C

10 – 18 % (w/v) acrylamide gel recipe for 12 gels

10 % (w/v) light gel

5 × gel buffer (45.8 mM) ..... 70 ml

Acrylamide/Bis (10% (v/v)) ..... 88 ml

MilliQ water ..... 192 ml

APS (0.05% (w/v)) ..... 560 µl

TEMED (0.1% (v/v)) ..... 56 µl

18% (w/v) heavy gel

5 × gel buffer (45.8 mM)	70 ml
Acrylamide/bis (18% (v/v))	158 ml
Glycerol (17.4% (v/v))	122 ml
APS (0.05% (w/v))	560 µl
TEMED (0.1% (v/v))	56 µl

SDS stock solution

SDS (20% (w/v))	200 g
MilliQ water	1 L

10 × Tris-glycine running buffer

Glycine (192 mM)	576 g
Tris-HCl pH 8 (24.8 mM)	132 g
20% SDS stock solution (5% (v/v))	200 ml
MilliQ water	4 L

Overlay solution

Agarose (0.5 % (w/v))	0.25 g
Bromophenol blue (0.001 % (w/v))	0.5 mg
1 × Tris-glycine running buffer pH 8	Up to 50 ml

Fix/wash

Methanol (10% (v/v))	50 ml
Acetic acid (7% (v/v))	35 ml
MilliQ water	Up to 500 ml

Coomassie Blue stock solution

Ammonium sulphate (17% (w/v))	50 g
85% Phosphoric acid (3% (v/v))	6 ml
Coomassie G-250 (0.1% (w/v))	0.5 g in 10 ml water
MilliQ water	500 ml

Coomassie destain/gel storage solution

Acetic acid (2.5 % (v/v))	5 ml
MilliQ water	500 ml

2.3.4 Peptide digestion

1 M stock ammonium bicarbonate

Ammonium bicarbonate	0.79 g
MilliQ water	10 ml

20 mM working ammonium bicarbonate solution

1 M stock ammonium bicarbonate	20 µl
MilliQ water	1 ml

Destain

20 mM ammonium biocarbonate (12 mM)	6 ml
Acetonitrile (40% (v/v))	4 ml
MilliQ water	10 ml

Resuspension buffer

Acetic acid (50 mM)	30 mg
MilliQ water	10 ml

Trypsin solution

Trypsin (12 ng/µl)	20 µg
Resuspension buffer	166.7 µl
Heat at 30°C for 15 min	
NH_4HCO_3 (50 mM)	Dilute 1:10
Aliquot and store at -80°C	

2.5% (v/v) formic acid stock

100 % formic acid	25 µl
MilliQ water	975 µl

Zip Tip wetting solution

2.5% Formic acid (0.1% (v/v))	40 µl
Acetonitrile (50% (v/v))	500 µl
MilliQ water	460 µl

Zip Tip wash/HPLC solution

Formic acid (0.1% (v/v))	40 µl
MilliQ water	960 µl

Zip Tip elution solution

Formic acid (0.1% (v/v))	40 µl
Acetonitrile (70% (v/v))	700 µl
MilliQ water	260 µl

SCX buffer A pH 2.5

Acetonitrile (25% (v/v))	250 ml
Formic acid (0.05% (v/v))	0.5 ml
MilliQ water	Up to 1 L

SCX buffer B pH 2.5

Acetonitrile (25% (v/v))	250 ml
Ammonium formate (0.5 M)	31.5 g
Formic acid (2% (v/v))	20 ml
MilliQ water	Up to 1 L

LC-MS standard

BSA (1 pmol/µl)	10 µl
Fetuin (200 fmol/µl)	2 µl
GluFib (1 pmol/µl)	1 µl
Renin (100 fmol/µl)	10 µl
Acetonitrile (5% (v/v))	50 µl
Formic acid (0.1% (v/v))	1 µl
MilliQ water	926 µl

Aliquot and freeze. For QSTAR make dilution 1:10 with addition of 45 µl of 0.1% (v/v) formic acid, load 5 µl on standard 30 min gradient.

Solvent B

Formic acid (0.1% (v/v))	0.1 ml
Acetonitrile	100 ml

2.3.4 Explorer antibody microarray

Buffer 1

EDTA (1 mM)	29.2 mg
BSA (0.1% (w/v))	0.1 g
PBS	100 ml

2.3.5 DotScan antibody microarray

DotScan fixative solution

Formaldehyde (3.7 % (v/v))	370 µl
PBS	10 ml

DotScan blocking buffer pH 7.3

BSA (2 % (w/v))	0.2 g
Heat-inactivated AB serum (0.02 % (v/v))	2 µl
PBS	10 ml

Multiplexing solution

Phycoerythrin-anti-CD3 (1:7.5 dilution)	20 µl
Alexa Fluor 647-anti-EpCAM (1:15 dilution)	10 µl
Heat-inactivated AB serum 1.5 % (v/v)	2 µl
DotScan blocking buffer	150 µl

2.4 Methods

2.4.1 Tissue disaggregation and storage

Surgically resected samples were collected from the Royal Prince Alfred Hospital (Camperdown, NSW, Australia) and Concord Repatriation Hospital (Concord West, NSW, Australia) with ethical approval under protocol No. X08-164 by NSW Local Health District.

The optimisation of solid tumour and normal intestinal mucosal tissue disaggregation was discussed in detail in Zhou, Honours thesis (Zhou, 2008). Surgically resected CRC tumours were selected and sliced by the pathologist, while control samples were taken from healthy intestinal mucosa at least 10 cm from the primary tumour site. Samples were stored in Hanks' balanced salt solution pH 7.3 (HBSS) at 4°C for no more than 12 h after resection. Clinical samples were sliced into 2 mm strips and incubated with collagenase solution at 37°C for 1 h. Semi-digested tissue was passed through a fine wire mesh strainer using a plunger from a 10 ml syringe, cells were washed through with HBSS. The cell suspension was then passed through 200 µm and 50 µm Filcon filters resulting in a single cell suspension. The cells were pelleted (400 × g, 20°C, 5 min) and resuspended in cell storage solution for long term storage and lysis of red blood cells (up to 1 year, -80°C). A total of 254 CRC patient samples was collected and processed for cryostorage over a period of 4 years (2008 – 2012).

2.4.2 Leukocyte depletion with CD45 Dynabeads

For $CD45^+$ leukocyte depletion, the cryostored cell suspension was thawed in a 37°C water bath and washed with HBSS. The Trypan blue exclusion procedure was used to determine cell viability and numbers. Cell suspensions (10 µl) were mixed with equal volumes of Trypan blue and 10 µl was pipetted into the haemocytometer chamber. A Nikon TMS

microscope (Nikon, Kanagawa, Japan) was used to determine cell density and viability. Viable cell density (i), dead cell density (ii), viability (iii), were determined using the following equations.

$$X_v\,(\text{cells/mL}) = (C_{av} \times D) / 10^{-4} \qquad \text{(i)}$$

$$X_d\,(\text{cells/mL}) = (C_{ad} \times D) / 10^{-4} \qquad \text{(ii)}$$

$$V\,[\%] = C_{av}/(C_{av}+C_{ad}) \qquad \text{(iii)}$$

X_v – Viable cell density (cells/mL)

X_d – Dead cell density (cells/mL)

C_{av} – Average number of viable cells per haemocytometer square (1 mm^2)

C_{ad} – Average number of dead cells per haemocytometer square (1 mm^2)

D – Dilution factor (cell solution/Trypan blue) = 2

10^{-4} – volume of haemocytometer cell (mL)

Approximately 180 µl of CD45 Dynabead solution density was used per 10^7 viable cells. CD45 Dynabeads were pre-washed in buffer 1 and recovered using magnets before being resuspended in 180 µl of buffer 1. The cell suspension (10^7 viable cells per 1 ml of HBSS) was incubated with 10 µl heat-inactivated AB serum for 5 min at 4°C before adding the CD45-Dynabeads, then incubated for 45 min at 4°C with gentle rotation. The cell/bead suspension was diluted into 12 ml of buffer 1 and gently mixed by pipetting, and placed on a magnet for 10 min to separate the $CD45^+$ cells bound to beads from unbound cells. The unbound fraction was transferred to a centrifuge tube and spun (400 × g, 5 min, 25°C). The bound fraction was resuspended a second time in 12 ml of Buffer 1 and recaptured on a magnet. The remaining unbound cells were combined with the original unbound fraction and spun (400 × g, 5 min, 25°C). The cell pellet, consisting of CRC/epithelial enriched cells, was

washed twice with cold PBS in preparation for cell lysis. The $CD45^+$ cell fractions were stored at -80°C for future analysis.

2.4.3 Protein lysate clean-up and quantification

A small volume of cell lysis buffer was added to CRC/epithelial enriched cells (approximately 100 µl per 10^7 cells). The cells were incubated with a small amount of benzonase nuclease (1-2 µl) on ice in a water bath sonicator for 1 h. The mixture was centrifuged (20,000 × g, 15 min, 4°C) and the clear protein supernatant collected.

The 2D Quant Kit (Bio-Rad) was used to determine protein concentrations prior to use of the 2D Clean-up Kit. This method was carried out according to the manufacturer's instructions. A standard curve was prepared with 2 mg/ml BSA (0 – 50 µg protein). The sample (1– 50 µg) was assayed in duplicate. In summary, 500 µl of precipitation buffer was added to each tube, the mixture was vortexed briefly and incubated for 3 min at room temperature. Co-precipitation buffer (500 µl) was added and mixed until precipitation became visible, the mixture was centrifuged (20,000 × g, 5 min, 4°C). The supernatant was carefully decanted without disturbing the pellet. The tubes were repositioned and pulse centrifuged before the remaining supernatant was pipetted out. Copper sulphate solution (100 µl) and 400 µl milli-Q water were added to the pellet and vortexed. Finally 1 ml working colour reagent (100 parts of colour reagent A to 1 part colour reagent B) was introduced rapidly by pipette. The solution was incubated at room temperature for 20 min, and the absorbance measured using a spectrophotometer at 480 nm. A standard curve was generated by plotting the absorbance of the standards against 5 – 50 µg of protein and used to determine the protein concentrations of the samples.

The 2D Clean-up Kit (BioRad) was used to remove salts and other contaminants that may affect isoelectric focusing (IEF). The method was carried out according to the manufacturer's instructions. In summary, a maximum of 100 µl (1 – 500 µg) protein solution was added to 300 µl of 'precipitating agent 1' and vortexed for 30 s. The solution was incubated on ice for 15 min before 300 µl of 'precipitating agent 2' was added and vortexed for 30 s. The solution was centrifuged (20,000 × g, 5 min, 4°C) to remove the supernatant, followed by a pulse spin to remove any residual liquids. Wash reagent 1 (40 µl) was added to the pellet and vortexed to resuspend the pellet. The sample was centrifuged (20,000 × g 5 min, 4°C) to remove wash reagent 1, followed by addition of 25 µl of milliQ water and vortexing until the pellet was redissolved. Wash reagent 2 (1 ml) and Wash additive (5 µl) were added and the mixture and vortexed for 1 min. This was incubated at -20°C for 30 min, with 30 s vortexing at 10 min intervals and centrifuged (20,000 × g , 5 min, 4°C) to remove the supernatant, followed by a pulse spin to remove residual liquids. The pellet was air dried for 5 min, changing from white to translucent. It was then resuspended in 75 µl of cell lysis buffer and vortexed until proteins were fully dissolved. The samples were stored at -80°C for up to 12 months. Protein quantification was repeated with the 2D Quant Kit prior to saturation-DIGE labelling.

2.4.4 Saturation-DIGE (labelling and gel electrophoresis)

CyDye DIGE Fluor Labeling Kit for scarce samples (GE Healthcare) was used for saturation-DIGE; the method was carried out according to the manufacturer's instructions for analytical gels. Optimisation of this technique was performed with the whole cell lysates of 3 CRC cell-lines (CaCo, LIM1215 and HT29) and 6 patient samples (ACPS B tumours and controls). Saturation-DIGE and data analysis were performed on 16 CRC patient samples (4 tumours and controls from each ACP stage). Cy3 and Cy5 dye powder was reconstituted in

dimethylformamide (DMF) to give a 2 mM working solution. That was vortexed, centrifuged, and stored for up to 8 weeks at -20°C. The global standard was generated by pooling the lysates of all tumours and controls. The protein concentration was quantified using the 2D Quant Kit. For each Saturation-DIGE gel, 10 µg of the protein sample and 10 µg of global standard were made up to 9 µl with cell lysis buffer in separate tubes. Reducing solution, TCEP (1 µl), was added to each of the protein lysates and mixed by pipetting. The tubes were incubated at 37°C in the dark for 1 h. Cy Dye solution (2 µl) was added to each tube (Cy3 to global standards and Cy5 to a sample) and mixed by pipetting. The tubes were incubated for 30 min at 37°C. The reaction was quenched with an equal amount of stop mixture and the two tubes combined. The final volume was made up to 300 µl with isoelectric focusing (IEF) rehydration buffer. This solution was pipetted along the well of a rehydration tray and a 17 cm pH 3-10 non-linear IEF strip placed gel side down over the solution, to allow for overnight in-gel rehydration. The gel strips were transferred to an IEF tray and covered with mineral oil to prevent drying. IEF focusing was conducted with a six-step process (3 h at 100 V, 2 h at 300 V, 2 h at 1 kV, 2 h at 2.5 kV, 99,999 Vh at 5 kV and a hold step for 24 h at 100 V). After focusing, the IPG strips were equilibrated for 20 min in equilibration buffer, then transferred into a second dimension polyacrylamide gel (8 – 18% linear gradient) and sealed with overlay solution. Second dimensional electrophoresis was carried out using a Protean Plus Dodeca cell (Bio-Rad) at 10^{o}C following a three-step program, 50 V for 30 min, followed by 100 V for 16 h then 200 V for 1 – 1.5 h for the dye to run off the bottom of the gel. The analytical gels were scanned with a Typhoon FLA 9000 Biomolecular Imager (GE Healthcare) using the Cy3 and Cy5 filters. Image quantification and statistical analysis (student's t-test and ANOVA) were conducted with Progenesis SameSpot version 4.1.3884.12788.

Parallel preparative gels were run for spot cutting and peptide digestion. CyDye DIGE Fluor Labelling Kit for scarce samples (GE Healthcare) was used for the preparative gel. The method was carried out according to the manufacturer protocols for preparative gel. The 16 CRC patient samples were pooled into tumour or normal lysate. Nine preparative gels were created, 6 to optimise the method and 3 were used for spot cutting, each gel contained 500 µg of protein made up to 250 µl with cell lysis buffer. Reducing solution TCEP (1 µl) was added and mixed by pipetting. The tubes were incubated at 37°C in the dark for 1 h. Cy5 dye solution (20 µl) was added to each tube then mixed by pipetting. The tubes were incubated for 30 min at 37°C for labelling. Ampholytes (2% (v/v)) and DTT (13 mM) were added to quench the reaction. The final solution was made up to 300 µl with rehydration buffer. The solution was pipetted along the well of a rehydration tray and a 17 cm pH 3-10 non-linear isoelectric focusing strip placed gel side down over the solution, covered with 1 – 2 ml mineral oil and left at room temperature to rehydrate overnight. The IEF and gel electrophoresis protocol for preparative gels was identical to that of analytical gels.

A double staining procedure was used for spot visualisation on preparative gels. Gels were left in fix/wash solution for 2 h, then stained with Sypro Ruby overnight. Gels were briefly washed in fix/wash for 1 h before being scanned on a Typhoon FLA 9000 Biomolecular Imager using Sypro Ruby filter (filter: LPB 510LP, wavelength: 510 nm). Gels were transferred to Coomassie blue working solution (4 parts Coomassie stock solution and 1 part methanol), covered with cling wrap and left on a shaker overnight. Gels were immersed in Coomassie destain for 1 h before being scanned using GS-800 calibrated densitometer (fluorescent white, 12-bit pixel density). Gels could then be kept in sealed plastic bags with 10 ml of Coomassie destain for up to 6 months.

2.4.5 Peptide digestion and MS identification

Differential spots were cut out using a Harris Uni-core (2 mm) spot cutter. Each gel plug was transferred to a LoBind tube and washed with destain until all Coomassie stain was removed. The gel plugs were washed with 100% (v/v) acetonitrile, at which point the gel plug changed from translucent to solid white. A vacuum centrifuge (30 min, 40°C) was used to completely dry the plugs. Plugs were immersed in trypsin solution (10 µl), then incubated for 1 h at 4°C, after which they became translucent. Following the incubation, trypsin residues were removed and 15 µl of ammonium bicarbonate (20 mM) was added prior to overnight incubation at 37°C. The gel plug solution was adjusted to pH 2 with formic acid prior to C18 ZipTip purification. To purify peptides, C18 ZipTips were rehydrated in 2 washes with wetting solution, C18 columns were activated with 2 aliquots of wash solution, samples were pipetted slowly 10–15 times to allow peptide binding, peptides were washed twice with wash solution, and eluted with elution solution into LoBind tubes. The peptides were vacuum centrifuged (30 min, 40°C) to dry, before adding 45 µl of HPLC solution and transferring to a LoBind plate for HPLC.

Prior to MS analysis, peptides from each gel plug fraction were fractionated using a strong cation exchange column (ZORBAX Bio-SCX series II, 3.5 mm, 50 x 0.8 mm) on an Agilent 1100 HPLC system in off-line mode. The peptides (30 µg) were loaded onto the column with SCX buffer A (25% (v/v) acetonitrile, 0.05 % (v/v) formic acid, pH 2.5). The peptides were eluted from the column with SCX buffer B (25% (v/v)) acetonitrile, 0.5 M ammonium formate, 2% (v/v) formic acid, pH 2.5 using a gradient of 0 - 20% over 42 min, 20 – 100% SCX buffer B over 14 min and 100% SCX buffer B for 5 min. Fractions (30) were collected for each sub-cellular fraction at 2 min intervals, using a Probot micro-fraction collector.

Prior to loading the samples, a LC-MS standard was run to test the performance and dynamic range of the instrument (0.1 µM BSA, 20 nM fetuin, 0.1 µM GluFib and 10 nM renin in 0.5% (v/v) acetonitrile with 0.01% (v/v) formic acid). The gel plug peptides were analysed using a Agilent 1100 HPLC system interfaced with a QSTAR Elite mass spectrometer. Peptides were diluted with wash/HPLC solution and loaded onto a C18 trap column (ZORBAX 300SB-C18, 300 µm × 5 mm, 5 µm) at 10 µl/min and washed for 7 min before switching the trap column in line with the C18 separation nanocolumn (ZORBAX 300SB C18, 3.5 µm, 150 × 0.1 mm). The peptides were eluted directly into the ionisation source of the mass spectrometer at 0.3 µl/min with the following gradient: 0 min, 5% solvent B; 8 min, 5% B; 10 min, 15% B; 90 min, 30% B; 105 min, 60% B; 115 min, 5% B; 120 min, 5% B.

The nano-LC-ESI-MS/MS system was set to perform data acquisition in the positive ion mode, with a selected mass range of 350-1750 m/z. Peptides with +2 to +4 charge states were selected for tandem mass spectrometry, and the time of summation of MS/MS events was set to 2 s. The three most abundantly charged peptides above a count threshold >30 were selected for MS/MS and dynamically excluded for 30 s with (50 milli-mass units mass tolerance). The instrument acquired data in information dependent acquisition (IDA) mode, using Analyst QS 2.0 software. Automatic collision energy and automatic MS/MS accumulation modes were used in the advanced IDA settings.

The data files from each 2D gel experiment were analysed using ProteinPilot 3.0 software, which uses the Paragon^{TM} algorithm to perform protein identification. All MS/MS spectra were searched against a combined Swiss-Prot protein database, version uni_sprot_20070123. Parameters set in ProteinPilot 3.0 were set to: Fixed modifications (oxidation (m), propionamide (c)), Enzyme digestion (trypsin), Species (*Homo sapiens*), Peptide tolerance (0.2), MS/MS tolerance (0.2), Peptide charge (+2 and +3) and Instrument (ESI-QUAD-TOF). The following processing options were used: quantitative, bias correction, background

correction, biological modifications and thorough identification search. A concatenated target-decoy database search strategy was also employed to estimate the rate of false positives. Only proteins identified with at least 95% confidence and ProtScore of >300 were reported.

2.4.6 Explorer antibody microarrays

Technique optimisation was performed on 2 CRC patient samples. The subsequent analysis was performed on whole cell lysate from 12 patient samples (3 tumours and controls from each ACP stage). The protein extraction and purification procedures were carried out with the Explorer Micorarray Protein Extraction Kit (FullMoon). In summary, the buffer exchange spin column was prepared by adding 650 µl labelling buffer, vortexed for 20 s to remove all air bubbles and left at room temperature to hydrate for 1 h. Once hydrated, the spin columns were centrifuged (750 × g, 2 min, 25°C) to remove excess fluid. The single cell suspension was thawed quickly from cryostorage in a 37°C water bath and washed with PBS. The cell pellet was lysed down with extraction buffer (100 µl for 2.5×10^6 cells) and lysis beads. The mixture was incubated on ice for 1 h and vortexed for 60 s at 10 min intervals. The mixture was centrifuged (20,000 × g, 15 min, 4°C) and the clear supernatant collected. Protein extract (100 µl) was transferred to the spin column. Care was taken not to disturb the gel layer. The columns were placed into collection tubes and spun at 750 × g for 2 min to collect the purified protein fraction. The concentration and purity of protein was quantified using a Nanodrop 3300. Samples were blanked with labelling buffer, and absorbance recorded at 260 nm and 280 nm. Purified protein solutions were stored at -80°C for up to 12 months.

Protein (100 µg) was made up to a final volume of 75 µl with labelling buffer. Biotin working solution (3 µl, 10 µg/µl biotin reconstituted in dimethylformamide) was added to the

protein solution and incubated at room temperature for 2 h with occasional mixing. Left-over biotin working solution was stored at -20°C. Following incubation, 35 µl of stop reagent was added and the biotinylated protein was incubated at room temperature for 30 min with occasional mixing.

The Explorer antibody microarray (FullMoon) can be stored at 4°C for up to 6 months. Before use, each microarray was left at room temperature in the packaging for 45 min before opening to air dry for 15 min. The microarray slide was submerged, antibody side up, in blocking solution (30 mg/ml skim milk powder in blocking reagent) and placed on an orbital shaker at 55 rpm for 45 min at room temperature. Following blocking, the slide was placed in a 50 ml tube filled with milli-Q water and inverted for 20 s. The water was replaced and the washing process repeated at least 10 times, or until residual water was uniform on the slide surface. The slide was placed into a well of the coupling chamber. Care was taken not to let the slide dry out.

The biotin labelled protein solution was added to 6 ml of coupling solution (30 mg/ml skim milk powder in blocking reagent) and vortexed; the whole mixture was poured onto the slide contained within a coupling chamber. After 2 h incubation at room temperature on an orbital shaker at 35 rpm, the slide was transferred to a petri dish and submerged in 30 ml of 1× wash solution and shaken on an orbital shaker at 55 rpm for 10 min at room temperature. The 1 × wash solution was replaced and the wash procedure repeated twice. The microarray was placed into a 50 ml tube filled with milliQ water and inverted for 20 s. The water was removed and the washing process repeated at least 10 times, or until residual water was uniform on the slide surface.

Detection solution was prepared by adding Cy3-streptavidin to detection buffer to a final concentration of 0.5 mg/ml. The microarray was submerged in detection solution (30 ml) in a

petri dish and incubated in the dark on an orbital shaker at 55 rpm for 20 min at room temperature. Following fluorescence labelling, the slide was transferred to another petri dish and submerged in 30 ml of 1× wash solution and shaken on an orbital shaker at 55 rpm for 10 min at room temperature. The 1× wash solution was replaced and the wash procedure repeated twice. The microarray was placed into a 50 ml tube filled with milli-Q water and inverted for 20 s. The water was replaced and the washing process repeated at least 10 times or until residual water was uniform on the slide surface. The slide was placed in an empty 50 ml tube and quickly dried by centrifugation at 600 × g. Microarrays were scanned with a Typhoon FLA 9000 Biomolecular Imager and fluorescence quantified using ImageQuant TL. The quantified results were exported to MultiExperiment Viewer and statistical analysis (two tailed student t-test, ANOVA) was performed.

2.4.7 DotScan antibody microarrays

The optimisation of DotScan to analysis CD antigesns on solid CRC tumour cells has been discussed in detail (Zhou, 2008, Zhou et al., 2010). Disaggregated cells were brought out of cryostorage (-80°C) in a 37°C water bath and washed with HBSS to remove DMSO. Cell pellets were treated with DNAse solution to remove any nucleic acid released during thawing. The cell pellet was resuspended to a final volume of 10 ml with HBSS and the Trypan blue exclusion method was conducted with 10 µl of the cell mixture and equal parts of Trypan blue. An optimal count of 6×10^6 viable epithelial cells was required for cell capture on DotScan microarray. The appropriate number of cells was pelleted and resuspended in 200 µl of RPMI 1640, pH 7.3.

DotScan microarrays (MedSaic) were stored at 4°C with desiccant for up to 1 year. Before use, microarrays were allowed to warm up at room temperature (10 - 20 min). Microarrays

were pre-moistened in PBS for 30 s and placed in the incubation chamber. The cell suspension was added to the moist nitrocellulose section, introducing drops to each corner to ensure an even spread of cells. The microarrays were incubated at 37°C for 1 h. Following incubation, unbound cells were washed off by 5 gentle vertical dips in PBS. DotScan fixative solution was added to cover the whole microarray. After fixation for 20 min at room temperature, the fixative was washed off with 5 vertical dips in PBS and cell binding was recorded by optical scanning using the DotScan scanner to provide the antigen expression pattern of a mixed cell population, mainly CRC cells, leukocytes and stromal cells. Microarrays were not allowed to dry before the next step.

Microarrays were blocked in 200 µl blocking buffer for 20 min at room temperature, to prepare for fluorescence multiplexing. Excess blocking buffer was poured off and 150 µl multiplexing solution (phycoerythrin-anti-CD3, Alexa Fluor 647-anti-EpCAM) was added and incubated in the dark at room temperature. Unbound antibodies were washed off with 5 vertical dips in PBS. The microarrays were left to dry in the dark. These could be stored at 4°C in the dark for up to 3 months without significant loss of fluorescence. Dried microarrays were scanned for PE and Alexa Fluor 647 with a Typhoon FLA 9000 scanner (Phycoerythrin with 532 nm excitation laser and 580 BP30 emission filter; Alexa Fluor 647 with 633 nm excitation laser and 670 BP30 emission filter) with resolution set to 50 µm. Images (.png) were adjusted to 17 × 25 cm and resolution 72 pixels/inch and uploaded on to DotScan analysis software for quantification. The DotReader (MedSaic) captures a digital image of the dot binding pattern and quantifies the density of cell binding on each antibody dot on an 8 bit greyness scale (1-256 U). Occasional non-specific isotype control binding occurred and was subtracted from binding values for antibodies of corresponding immunoglobulin isotypes. The MultiExperiment Viewer (MeV) software suite was used for data normalisation (log2

median centring), cluster generation (hierarchical clustering, Euclidean distance, complete linkage) and data analysis (2-tailed student's t-test).

Chapter 3

Proteomic alterations during colorectal cancer progression

3.1 Introduction

The first published accounts of CRC evolution were by Morson (Morson, 1974) and Muto *et al*. (Muto et al., 1975). They described the histopathological evolution of CRC based on tumour size, differential grade and histological type. In the following year, Peter Nowell (Nowell, 1976), published a landmark perspective on cancer as an evolutionary process that is driven by step-wise, somatic cell mutations with sequential, sub-clonal selection. Since then, studies have implicated mutational and epigenetic changes for the phenotypic traits

acquired by CRC and firmly established CRC progression as one of the best-characterised models of this multistep process (Fearon and Jones, 1992, Kinzler and Vogelstein, 1996). Modern cancer biology is taking the next logical step towards understanding cancer evolution through the emerging field of proteomics.

Cancer is a complex and dynamic disease and a prime target for proteomic research. Proteomic analysis can define and characterise regulatory and functional networks, identify molecular defects in diseased tissue, and identify biomarkers to diagnose a particular disease or stage of a disease. In the past few years, there has been substantial interest in applying proteomic methods to the discovery of therapeutic targets and biomarkers for the early diagnosis of CRC (Friedman et al., 2004, Alfonso et al., 2005, Uhlen et al., 2005, Bi et al., 2006). The majority of these proteomic studies have focused on finding differential proteins between tumour and normal colorectal tissue. Currently, very little information is available on changes in protein expression at different stages of CRC progression. Research into modulation of the CRC proteome during tumour development would provide critical insight into the dynamic states of the cancer ecosystem and the changing phenotype. Such proteomic analysis of CRC would also contribute a novel protein perspective to the well-established genetic model of cancer evolution (Greaves and Maley, 2012).

This PhD project investigates the modulation of the CRC proteome at each Australian ClinicoPathological Stage (ACPS) of CRC development (ACPS A-D). To obtain accurate protein profiles, we have used fresh CRC and normal colon tissue, disaggregated into viable single cells, and depleted of CD45 positive leukocytes. The fractionated tumour and normal cells were analysed by two complementary protein discovery techniques: saturation DIGE and antibody microarrays. Building on knowledge from past research, we have shown that

several tumour-associated pathways, such as proliferative self-renewal, aerobic glycolysis, angiogenesis and the ER stress response, were altered in tumours compared to normal tissue, and modulated at specific stages of tumourigenesis. Pathway analysis revealed that the proteomic phenotype reflected the intra- and extra-cellular selection driving CRC progression (Figure 3.1).

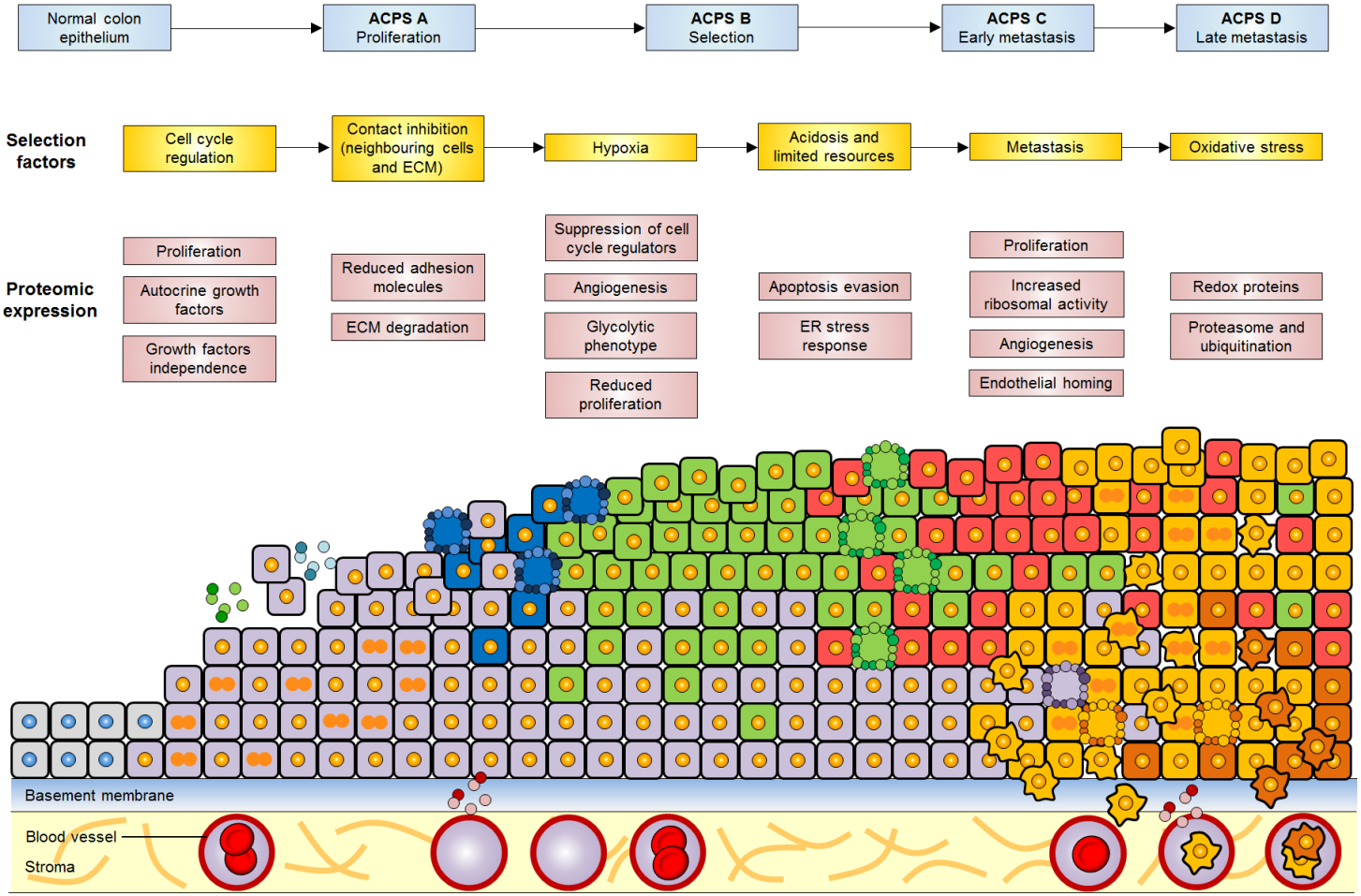

Figure 3.1 Model for proteome-environment interactions in CRC (adapted from Figure in Gatenby and Gillies, 2004, Nature Reviews). The stages of CRC growth and their associated proteomic phenotypes are diagrammed, showing that progression from one stage to the next is governed by several selection factors. Normal epithelial cells (grey cells) become hyperproliferative (dividing nucleus) following oncogenic induction (nuclei shown as blue in normal cells and orange for tumorigenic mutation). Over-expression of proliferation pathways and the deregulation of growth factors (green circles) initiate the first stage of tumour development (purple cells). Cancer cells also reduce adhesion molecules and produce proteases (blue circle) to escape contact inhibition imposed by neighbouring cells and the ECM. As cancer cells reach the oxygen diffusion limit, they become hypoxic (blue cells), which can lead to cell death (apoptotic cells shown with blebbing), increased angiogenesis (red circles) and emergence of the glycolytic phenotype (green cells). As a consequence of increased glycolysis, tumours become acidotic, which selects for apoptosis- and stress-resistant cells (red cells). Eventually, the combination of acidosis and limited substrates leads to motile cells with metastatic phenotypes (yellow cells) and breach of the basement membrane. Interaction between cancer cells and blood cells exposes them to increased oxidative stress, cancer cells respond by increased expression of redox and ubiquitin-proteasome associated proteins.

3.2 Results

Extensive proteomic profiles were obtained from fresh CRC cells depleted for $CD45^+$ leukocytes. Tumour and adjacent normal intestinal mucosa were collected from 28 CRC patients (Table 3.1). Protein profiles were compared between tumour and healthy mucosal tissue, ACP stages, and presence of metastasis. Additional factors were considered when relevant to the protein of interest.

Table 3.1. Clinico-pathological characteristics of the 28 patients

		Saturation-DIGE (n=16)	**Explorer microarray (n=12)**
Gender		No. patients (%)	No. patients (%)
	Male	7 (44%)	8 (67%)
	Female	9 (56%)	4 (33%)
Age			
	≤65	3 (19%)	6 (50%)
	>65	13 (81%)	6 (50%)
ACPS			
	A	4 (25%)	3 (25%)
	B	4 (25%)	3 (25%)
	C	4 (25%)	3 (25%)
	D	4 (25%)	3 (25%)
Differentiation			
	Well	0 (0%)	0 (0%)
	Moderate	13 (81%)	12 (100%)
	Poor	3 (19%)	0 (0%)
TIL			
	Present	5 (31%)	3 (25%)
	Absent	11 (69%)	9 (75%)
Inflammation[†]			
	Present	7 (44%)	7 (58%)
	Absent	9 (56%)	5 (42%)
Mucin*			
	Prominent	5 (31%)	3 (25%)
	Scant	11 (69%)	9 (75%)

ACPS (Australian clinico-pathological staging), TIL (Tumour infiltrating lymphocytes); *mucinous tumours (over 30% mucin) [†]Presence of peri-tumoural inflammation

A total of 16 CRC patient samples were analysed by saturation-DIGE and differentially abundant spots were excised from three replicate preparative gels and identified by HPLC coupled with tandem MS/MS. A reference 2D map of CRC proteins was established (Figure 3.2); 1159 spots were clearly detected; of these 72 differentially abundant spots were excised and 45 unique proteins were identified (Table 3.2). Most of the identified proteins were glycolytic enzymes and mitochondrial proteins, involved in the tricarboxylic acid cycle and ATP energy metabolism, and metabolite carriers. After statistical analysis of the normalised quantities of matched spots, 7 up-regulated and 11 down-regulated proteins were identified in CRC tissue compared to controls (Table 3.2a); one-way ANOVA identified 30 spots altered between the CRC stages (Table 3.2b). The one-way ANOVA analysis indicated that the greatest variation was between tumours with lymph node metastases and those without. Comparative analysis between these two groups showed 18 up-regulated and 5 down-regulated proteins in metastatic CRC, compared to non-metastatic CRC (Table 3.2c).

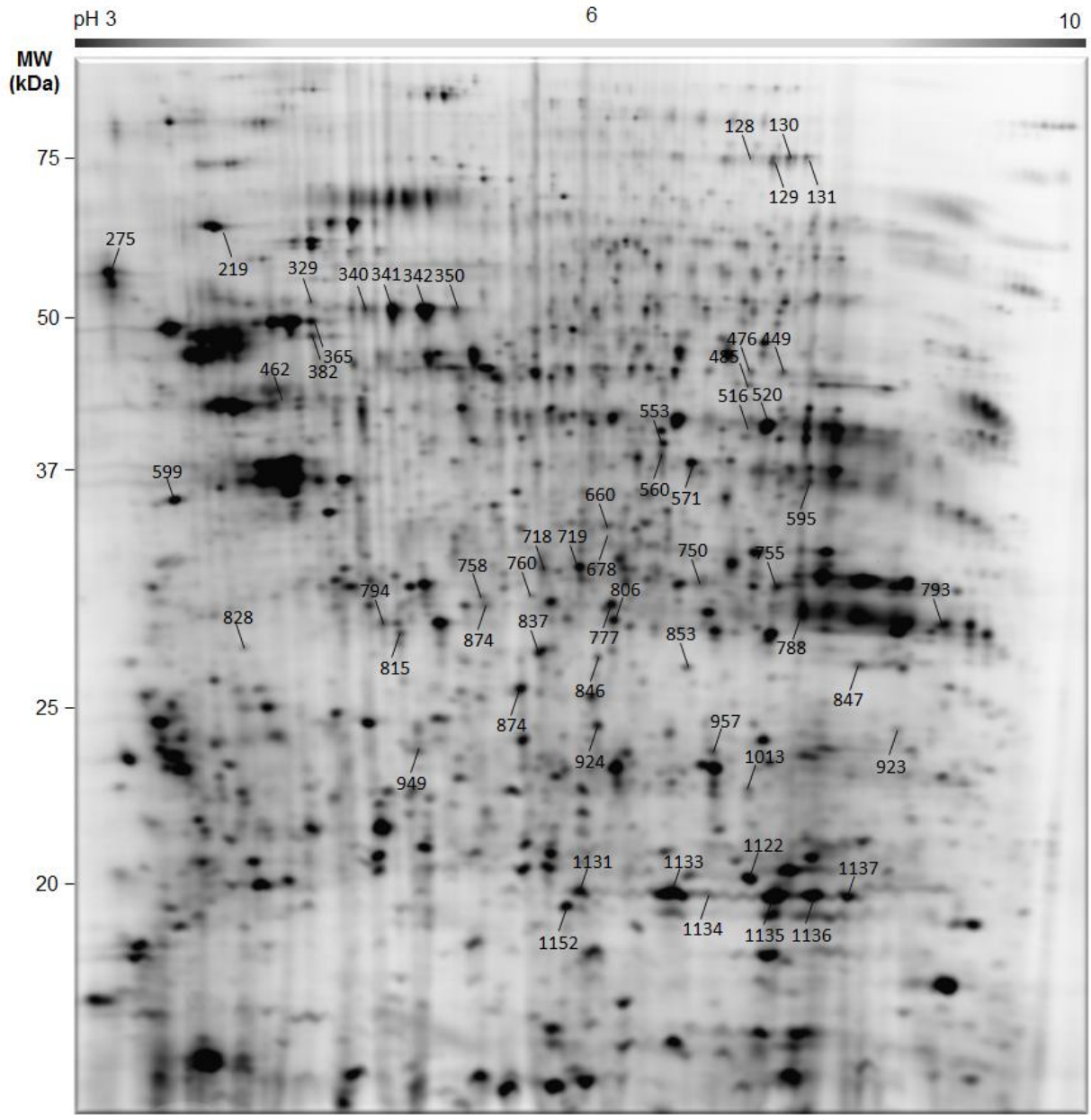

Figure 3.2 A representative 2D map of proteins from CRC. Proteins (5 µg) from 16 tumour samples (4 per ACP stage) and their corresponding controls (total 32 gels) were separated on a pH 3-10 NL IPG strip in the first dimension and by 8-18% acrymlamide SDS-PAGE in the second dimension. Differential spots were excised from three preparative gels and identified by RP-LC and tandem MS/MS analyses. Spots are labelled numerically and identified proteins are listed in Table 3.2.

Table 3.2 Significantly altered proteins in CRC cells identified by saturation-DIGE and RP-LC MS/MS. Only proteins with 95% confidence interval were selected.

a) Altered proteins between tumour and normal tissue									
Spot	Protein	Access #[a]	Score	Seq. (%)	Function	Mass (Da)	pI	Fold	p-value[b,c]
Elevated in CRC cells									
365	60 kDa heat shock protein (Hsp60)	P10809	3133	68	Protein folding	61,016	5.70	1.7	9.81E-04
382	60 kDa heat shock protein (Hsp60)	P10809	2935	73	Protein folding	61,016	5.70	2.6	7.49E-07
1122	Peroxiredoxin-1 (prdx-1)	Q06830	636	50	Redox balance	22,096	8.27	1.6	2.13E-04
1133	Manganese superoxide dimutase (MnSOD)	P04179	518	63	Redox balance	22,176	8.35	1.5	3.03E-04
1135	MnSOD mutant Q143n	P04179	1510	58	Redox balance	22,176	8.35	1.5	4.81E-05
1136	Peroxiredoxin-1 (Predx-1)	Q06830	2020	51	Redox balance	22,096	8.27	1.6	2.74E-06
1137	Peroxiredoxin-1 (Predx-1)	Q06830	310	53	Redox balance	22,096	8.27	1.8	5.45E-07
Reduced in CRC cells									
128	Aconitate hydratase	Q99798	1388	51	Krebs cycle	85,372	7.36	2.1	1.11E-05
129	Aconitate hydratase	Q99798	1344	45	Krebs cycle	85,372	7.36	1.9	2.92E-05
130	Aconitate hydratase	Q99798	1618	50	Krebs cycle	85,372	7.36	2.2	7.23E-05
131	Aconitate hydratase	Q99798	1527	55	Krebs cycle	85,372	7.36	2	2.00E-03
476	Glutamate dehydrogenase	P00367	789	30	Nitrogen metabolism	61398	7.66	3.5	3.75E-10
485	ATP synthase subunit alpha	P25705	1393	51	ATP synthesis	59,714	9.16	3.4	3.87E-09
660	Acyl-CoA dehydrogenase	P16219	1326	47	Lipid metabolism	43,615	7.01	2	1.03E-05
678	Acyl-CoA dehydrogenase	P16219	1326	38	Lipid metabolism	43,615	7.01	2.1	1.11E-05
793	Malate dehydrogenase precursor	P40925	548	31	Krebs cycle	35,509	8.92	1.6	7.48E-05
837	Delta (3,5)-delta (2,4)-dienoyl-CoA isomerase	Q13011	1346	54	Lipid metabolism	35,793	8.16	1.9	4.44E-06
957	Proteasome subunit alpha type 2	P25787	573	51	Proteolysis	25,899	7.29	2	4.70E-07

b) One-way ANOVA analysis between all CRC stages

Spot	Protein	Access #[a]	Score	Seq. (%)	Function	Mass (Da)	pI	Elevated stage(s)	Fold	p-value[b,c]
219	Glucose-regulated protein (GRP78)	P11021	1480	41	Protein folding	72431	5.07	Stage B	2.3	0.004
275	Calreticulin	P27797	1090	49	Protein folding	48297	4.29	Stage C	1.6	0.032
329	Heat shock protein (Hsp60)	P10809	1541	60	Protein folding	61016	5.70	Stage C, Stage D	1.8	0.002
340	Vimentin	P08670	1265	59	Structural	56747	5.98	Stage B	1.7	0.006
341	Protein disulfide-isomerase A3 (PDI)	P30101	1411	62	Protein folding	56747	5.98	Stage A, Stage B	1.5	0.048
342	Protein disulfide-isomerase A3 (PDI)	P30101	1678	64	Protein folding	56747	5.98	Stage B, Stage C	1.6	0.043
449	Adenylyl cyclase-associated protein	Q01518	770	48	Structural	51869	8.24	Stage B	1.9	0.048
516	Alpha-enolase isoform 1	P06733	1391	72	Glycolysis	47139	7.01	Stage B	1.6	0.030
520	Alpha-enolase isoform 1	P06733	1291	74	Glycolysis	47139	7.01	Stage B	2.1	0.025
553	Elongation factor Tu (EF-1α)	P49411	1053	49	Translation	49509	7.70	Stage C, Stage D	2	0.032
560	Elongation factor Tu (EF-1α)	P49411	2001	52	Translation	49509	7.70	Stage B	1.7	0.025
571	Isocitrate dehydrogenase (IDH)	O75874	1894	57	Redox balance	46630	6.53	Stage C, Stage D	2	0.046
595	Annexin A2	P07355	1027	33	Protein degradation	38618	7.10	Stage B	2.3	0.020
718	Phosphoglycerate kinase 1	P00558	1621	51	Glycolysis	44586	8.30	Stage C	1.4	0.026
719	28S ribosomal protein S22 (MRPS22)*	P82650	1307	68	Translation	41254	7.70	Stage C	1.5	0.004
750	Alcohol dehydrogenase (ADH)*	P14550	885	61	Ethanol oxidation	36550	6.32	Stage C, Stage D	1.7	0.011
755	Glyceraldehyde-3-phosphate dehydrogenase (GAPDH)	P04406	906	55	Glycolysis	36030	8.57	Stage C, Stage D	1.7	0.046
758	L-lactate dehydrogenase B chain	P07195	713	54	Glycolysis	36615	5.71	Stage C	1.5	0.032
760	m7GpppX diphosphatase	Q96C86	383	29	mRNA regulation	38585	5.93	Stage C, Stage D	1.7	0.035
777	Heterogeneous nuclear Ribonucleoprotein H3 (hnRNP H3)	P31942	466	44	DNA repair	36903	6.37	Stage C	2.5	0.025

788	Heterogeneous nuclear Ribonucleoproteins A2/B1 (hnRNP A2/B1)	P22626	877	46	DNA repair	35984	8.67	Stage C	1.6	0.041
794	Inorganic pyrophosphatase	Q15181	927	59	Phosphate metabolism	32639	5.54	Stage C	3.3	0.0[illegible]
806	3-Mercaptopyruvate sulfur transferase isoform 1	P25325	4431	69	Sulfide metabolism	35228	6.14	Stage C, Stage D	1.5	0.011
828	WD repeat-containing protein 61 (WDR61)*	Q9ERF3	1021	57	Transcription	33560	5.16	Stage A	2.3	0.012
847	Porin 31HM*	P21796	2104	69	Apoptosis/ glycolysis	30623	8.63	Stage C	1.5	0.037
853	Carbonic anhydrase 1	P00915	1259	65	Hypoxia response	28852	6.59	Stage C, Stage D	2	0.033
924	Endoplasmic reticulum resident protein 29 isoform 1 precursor (ERp29)	P30040	639	47	Protein transport	28975	6.77	Stage C, Stage D	1.9	0.042
1013	ES1 protein homolog	P30042	476	57	Unknown	28153	5.80	Stage A, Stage B	1.7	0.027
1131	Manganese superoxide dismutase (MnSOD)	P04179	396	30	Redox balance	22176	8.35	Stage C, Stage D	2.1	0.024
1152	PEST proteolytic signal-containing nuclear protein (PCNP)*	Q6P8I4	468	46	Proteolysis	18913	6.86	Stage C, Stage D	2.6	0.013

c) Differential proteins between non-metastatic and metastatic tumours

Spot	Protein	Access #[a]	Score	Seq. (%)	Function	Mass (Da)	pI	Fold	P-value[b,c]
Elevated in metastatic CRC									
329	60kDa heat shock protein (mito)	P10809	1541	60	Protein folding	61016	5.7	1.3	0.031
571	Isocitrate dehydrogenase (NADP) Cyto	O75874	1894	57	Kreb cycle	46630	6.53	1.5	0.027
599	Reticulocalbin-1 precursor (RCN1)	Q15293	1141	53	$Ca2^{+}$ metabolism	38866	4.86	1.3	0.025
750	alcohol dehydrogenase*	P14550	885	61	Ethanol oxidation	36550	6.32	1.3	0.048
755	Glyceraldehyde-3-phosphate dehydrogenase	P04406	906	55	Glycolysis	36030	8.57	1.4	0.014

760	m7GpppX diphosphatase	Q96C86	383	29	mRNA regulation	38585	5.93	1.5	0.005
777	Heterogeneous nuclear ribonucleoprotein H3	P31942	466	44	DNA repair	36903	6.37	1.7	0.048
794	Inorganic pyrophosphatase	Q15181	927	59	Phosphate metabolism	32639	5.54	2.0	0.
806	3-Mercaptopyruvate sulfur transferase	P25325	4431	69	Sulfide metabolism	35228	6.14	1.3	0.
815	Proteasome activator hPA28 subunit beta	Q9UL46	228	24	Proteolysis	31821	5.42	1.4	0.040
846	Proteasome subunit alpha type-1 isoform 2*	P25786	503	57	Proteolysis	29537	6.15	1.5	0.011
853	Carbonic anhydrase 1	P00915	1259	65	Hypoxia response	28852	6.59	1.5	0.017
874	ER resident protein 29 isoform 1 (ERp29)	P30040	639	47	Protein folding	28975	6.77	1.6	0.038
924	ER resident protein 29 isoform 1 (ERp29)	P30040	639	47	Protein folding	28975	6.77	1.4	0.036
924	ER resident protein 29 isoform 1 (ERp29)	P30040	639	47	Protein folding	28975	6.77	1.4	0.036
1131	Manganese superoxide dismutase (MnSOD)	P04179	396	30	Redox balance	22176	8.35	1.5	0.038
1133	MnSOD mutant Q143n	P04179	518	63	Redox balance	22176	8.35	1.4	0.032
1134	Manganese superoxide dismutase (MnSOD)	P04179	890	45	Redox balance	22176	8.35	1.6	0.005
1152	PEST proteolytic signal-containing nuclear protein (PCNP)*	Q6P8I4	468	46	Proteolysis	18913	6.86	1.3	0.007
Reduced in metastatic tumours									
341	Protein disulfide-isomerase A3 (PDI)	P30101	1411	62	Protein folding	56747	5.98	1.5	0.032
342	Protein disulfide-isomerase A3 (PDI)	P30101	1678	64	Protein folding	56747	5.98	1.6	0.012
350	Protein disulfide-isomerase A3 (PDI)	P30101	1894	67	Protein folding	56747	5.98	1.5	0.019
949	Peroxiredoxin-4 precursor (prdx-4)	Q13162	1089	54	Redox balance	30521	5.86	1.5	0.044
923	Electron transfer flavoprotein subunit beta isoform 1	P38117	27826	51	Electron transport	27826	8.24	1.6	0.040
949	Peroxiredoxin-4 precursor (prdx-4)	Q13162	1089	54	Redox balance	30521	5.86	1.5	0.044
923	Electron transfer flavoprotein subunit beta	P38117	27826	51	Electron transport	27826	8.24	1.7	0.040
1013	ES1 protein homolog	P30042	476	57	Unknown	28153	5.8	1.5	0.003

[a]Reference for protein identification using SWISS-Prot database
[b]Saturation-DIGE and preparative gels were scanned on a Typhoon scanner
[c]Data analysis was conducted with Progenesis SameSpot
*Novel protein and/or expression pattern associated with CRC development
Abbreviations: ECM (extracellular matrix), ER (endoplasmic reticulum

A total of 12 patient samples were analysed with Explorer microarrays. Each microarray contains a duplicate panel of 657 antibodies, of which up to 375 antibodies showed protein binding (Figure 3.3) and 42 differential proteins were identified. Most of these proteins were of nuclear origin, involved in DNA regulation and repair, transcription, and stress response. After statistical analysis of the normalised results identified 20 up-regulated and 2 down-regulated spots in CRC cells compared to control mucosa (Table 3.3a); one-way ANOVA identified 21 spots significantly altered between stages (Table 3.3b). The one-way ANOVA analysis indicated that the greatest amount of variation was between individual stages of CRC progression. T-test between different stages (ACPS A versus B, ACPS B versus C, and ACPS C versus D) identified a further 27 differentially abundant proteins not present in the ANOVA results (Figure 3.3c-e).

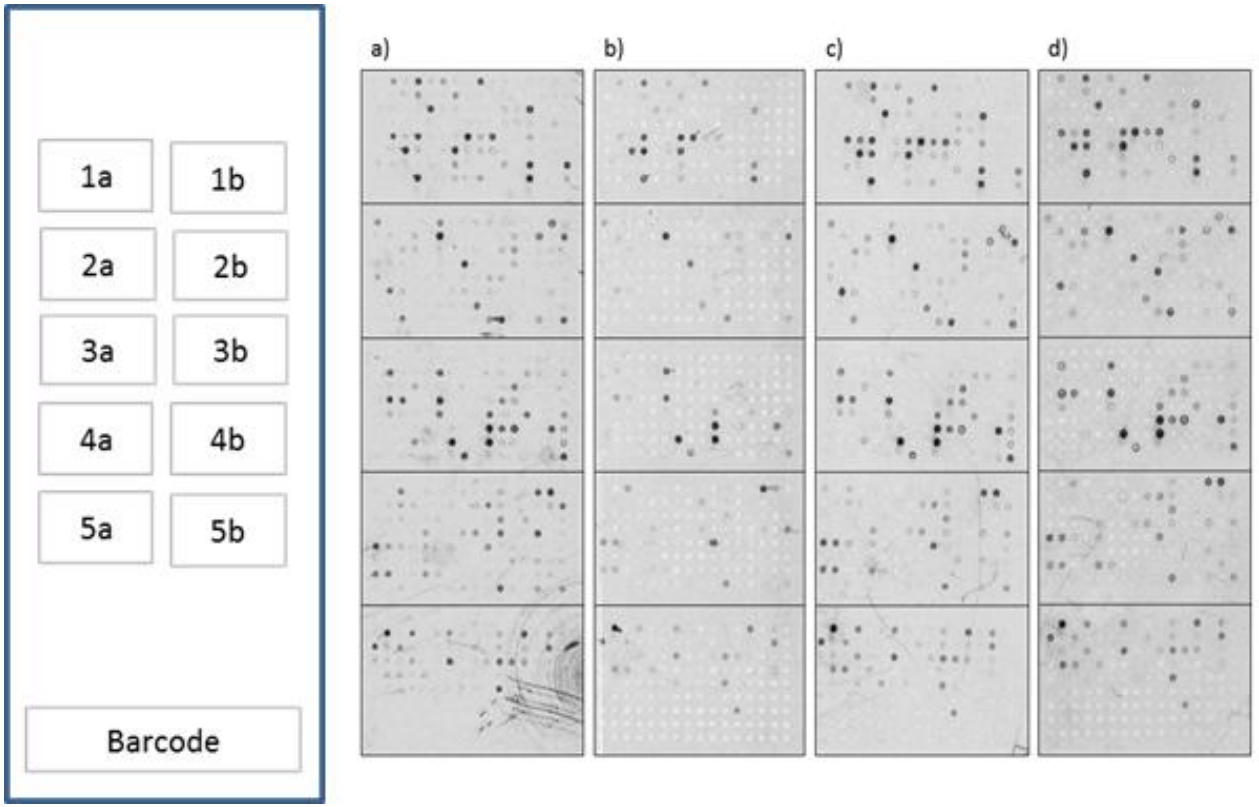

Figure 3.3 A single panel from each antibody microarray showing an example of the protein binding profiles from four CRC samples at different ACP stages a) ACPS A, b) ACPS B, c) ACPS C and d) ACPS D. The antibody layout for Explorer microarray is in Appendix Figure 6.1. Proteins (100 µg) from 12 samples (3 per ACP stage) and their corresponding controls (total 24 microarrays) were analysed.

Table 3.3 Significantly altered proteins in CRC samples identified with Explorer microarrays. Only proteins with over 1.5 fold change and 95% confidence interval were selected.

a) Differential proteins between tumour and normal mucosa tissue					
Protein	Uniprot IDa	Function	Location	Fold	p-value[b,c]
Elevated in CRC cells					
Granulocyte	White blood cell	Immune response	Extracellular	4.6	0.004
Alpha-1-antitrypsin (A1-AT)	P01009	Protease inhibitor	Extracellular	2.7	0.004
Keratin 5/6/18	Multiple protein	Cytoskeleton organisation	Cytoplasm	3.2	0.005
Keratin 8	P05787	Cytoskeleton organisation	Cytoplasm	1.6	0.006
CD171	P32004	Development	Membrane	6.7	0.006
Keratin 18	P05783	Cytoskeleton organisation	Cytoplasm	4.0	0.009
Prolactin Receptor	P16471	Transmembrane receptor	Membrane	4.0	0.009
Keratin 5/8	P13647	Cytoskeleton organisation	Cytoplasm	2.3	0.010
Mitochondria	Organelle	Energy production	Mitochondrial	3.5	0.014
Keratin 8/18	Multiple protein	Cytoskeleton organisation	Cytoplasm	1.5	0.014
Keratin, Multi	Multiple protein	Cytoskeleton organisation	Cytoplasm	2.0	0.015
Proteinase 3 (PR3)*	P24158	Serine-type peptidase activity	Lysosome	10.7	0.015
Milk Fat Globule Membrane Protein	Q08431	Cell adhesion molecule	Membrane	4.3	0.024
CREB-Binding Protein (CBP)	Q92793	Transcription regulator	Nucleus	3.1	0.030
Alpha-1-antichymotrypsin (A1-Achy)	P01011	Protease inhibitor	Extracellular	2.5	0.030
Epithelial Membrane Antigen (Muc1)	P15941	DNA damage repair	Membrane	3.4	0.033
CEA / CD66e	P06731	Cell adhesion	Membrane	3.2	0.034
Carbohydrate antigen 19-9 (CA19-9)	P78552	Transmembrane receptor	Membrane	10.9	0.043
Reduced in CRC cells					
CDC47	P33993	Helicase activity	Nucleus	2.4	0.025
B-cell lymphoma/leukemia 10 (Bcl-10)	O95999	Apoptosis	Cytoplasm	1.7	0.033

b) One-way ANOVA analysis between all CRC stages

Protein	Uniprot ID[a]	Function	Location	Elevated stage(s)	P-value[b,c]
p57	P49918	Cell communication	Nucleus	Stage A, Stage C	5.31E-04
Vacular endothelial growth factor (VEGF)	P15692	Cell communication	Extracellular	Stage A, Stage C	8.62E-04
Gamma glutamyl transferase	P19440	Metabolism	Membrane	Stage A	0.002
CD40	P25942	Cell communication	Cytoplasm	Stage C	0.006
Caspase 3	P42574	Apoptosis	Cytoplasm	Stage A	0.007
Prostate Specific Antigen (PSA)	P07288	Proteolysis	Extracellular	Stage A, Stage C	0.011
Nucleophosmin (NPM)	P06748	Ribosome assembly	Cytoplasm	Stage C	0.011
CD16	P08637	Immune response	Membrane	Stage A, Stage C	0.011
Proliferating cell nuclear antigen (PCNA)	P12004	DNA repair	Nucleus	Stage A, Stage C	0.015
Mek6*	P52564	Regulation of cell cycle	Nucleus	Stage A, Stage C	0.019
Von Willebrand factor (vWF)	P04275	Protein metabolism	Extracellular	Stage A	0.023
Transglutaminase II (TGM2)	P21980	Metabolism	Cytoplasm	Stage C	0.031
DNA repair protein XRCC2*	O43543	DNA repair	Nucleus	Stage B	0.031
Axonal growth cones	Structural fibers	Nervous system	Extracellular	Stage C	0.033
Gab-1	Q13480	Cell communication	Cytoplasm	Stage A	0.039
Moesin	P26038	Cell adhesion	Cytoplasm	Stage A	0.047

Differential proteins between CRC stages

Protein	Uniprot[a]	Function	Location	Fold change	P-value[b,c]
c) ACPS A versus A					
Reduced in ACPS B					
Synaptophysin	P08247	Cellular response	Cytoplasm	15.0	0.006
Caspase 1	P29466	Apoptosis	Cytoplasm	6.0	0.017
Laminin B1/b1	P07942	Cell adhesion	ECM	3.0	0.021
NF kappa B/p65	Q04206	Transcription regulation	Nucleus	3.0	0.025
HDJ-2	Q9NXZ8	Protein folding	Cytoplasm	12.0	0.026
DNA fragmentation factor subunit alpha	O00273	Inhibitor	Cytoplasm	3.0	0.029
Raf kinase (Raf)	P04049	Kinase	Membrane	6.0	0.033
Cyclic AMP-responsive element-binding protein 1 (CREB)	P16220	Differentiation/Transcription	Nucleus	4.0	0.035
p130	Q8NE70	Regulation of cell cycle	Nucleus	19.0	0.038
Matrix metalloproteinase-16 (MMP-16)*	P51512	Protease	ECM	5.0	0.044
Cullin-3*	Q13618	Transport	Golgi apparatus	2.0	0.045
Ras	Protein family	Signal transduction	Intracellular	2.0	0.047
E-Cadherin	P12830	Cell adhesion	Membrane	>100	0.050
d) ACPS B versus C					
Elevated in ACPS C					
Transcription factor E2F-5*	Q15329	Transcription	Nucleus	>100	0.006
p73	O15350	Apoptosis	Cytoplasm	41.0	0.007
CD63	P08962	Vesicle localisation	Membrane	2.0	0.015
Rhodopsin	P08100	Sensory transduction	Membrane	5.0	0.016
Survivin	O15392	Apoptosis	Centromere	4.0	0.016
CXC chemokine receptor type 4 (CXCR4)	P61073	Signal transduction	Membrane	>100	0.029
DNA fragmentation factor subunit alpha	O00273	Inhibitor	Cytoplasm	3.0	0.047
Caldesmon	Q05682	Movement	Cytoplasm	21.0	0.049

e) ACPS C versus D

Protein	Uniprot[a]	Function	Location	Fold change	P-value[b,c]
Reduced in ACPS D					
Neuron Specific Enolase	P09104	Glycolysis	Membrane	3.0	0.014
CD63	P08962	Cellular protein localisation	Membrane	2.0	0.014
CD10	P08473	Metabolism	Membrane	6.0	0.038
CXC chemokine receptor type 4 (CXCR4)	P61073	Signal transduction	Membrane	14.0	0.042
Notch	P46531	Differentiation	Membrane	4.0	0.048

[a]Reference for protein identification using SWISS-Prot database
[b]Intensity of the microarray binding was measured with ImageQuant TL
[c]Data analysis was conducted with TM4 MultiExperimentViewer v4.8
*Novel protein and/or expression pattern in CRC
Abbreviations: CD (cluster of differentiation), CEA (carcinoembryonic antigen), ECM (extracellular matrix)

3.3 Discussion

Cancer is a disease of clonal evolution within the body (Merlo et al., 2006). The concept of an evolutionary problem is not new, but until recently most of the focus has been from a genetic or epigenetic perspective. Proteomics offers a fundamental perspective on cancer evolution. It allows researchers to observe through protein expression, the heterogeneity between cancer cells, selection-induced phenotypic changes, and the consequences of this selection. This is one of the first proteomic studies to determine alterations in the CRC proteome at different stages of primary tumour development. Fresh CRC samples were collected, disaggregated into viable single cells, and depleted of $CD45^+$ leukocytes. Two proteomic discovery techniques were used, saturation DIGE analysis and Explorer antibody microarrays, to obtain 'molecular snapshots' of the CRC proteome at the 4 ACP stages of development. These proteomic data have mapped out the progression of CRC, with selection for proliferation and subsequently, metastasis. Unrestricted proliferation of CRC is driven by activated proliferation pathways and reduced cell cycle regulators. This rapid growth consumes substrates, and waste accumulates, leading to apoptosis evasion, aerobic glycolysis, and the ER stress response. Prolonged stress then selects for motile cells and the metastatic phenotype. Increased proliferation and angiogenesis enables cancer cells to invade surrounding tissue and to colonise distant sites (Figure 3.1).

In total, 38 differential proteins have been identified between tumour and normal tissue, and 101 differential proteins between CRC stages. Interestingly, most proteins detected by saturation-DIGE were localised to mitochondria or the endoplasmic reticulum, while the majority of proteins identified by Explorer microarrays were of cytoplasmic or nuclear origin. These differences may be attributed to differences between the 2D gel-based and antibody microarray techniques. 2D gel electrophoresis does not resolve most membrane associated

proteins and is limited to detecting proteins of medium abundance, such as those involved in glycolysis and protein folding. Antibody microarrays are unhindered by high abundance proteins but are limited by antibody availability and specificity, and may not detect proteins with multiple isoforms.

The one-way ANOVA analysis of data from each technique revealed disparate protein expression patterns, and therefore branching statistical analysis was applied to the data. Most of the differentially expressed proteins identified by saturation-DIGE distinguished non-metastatic CRC from metastatic CRC. In contrast, the Explorer microarray was better at identifying proteins that were differential between the 4 stages of tumour progression. Whilst there was no specific protein overlap between the 2 techniques, a number of common biological pathways were implicated by the proteins identified by the two techniques. This discussion will follow the differential protein expression at each ACPS of CRC progression. The changes in protein composition will be discussed, along with their functional significance.

3.3.1 Proliferation

Normal cellular proliferation is controlled by the interactions of a cell with surrounding cells, the extracellular matrix (ECM), and levels of growth factors. Regulated cell growth occurs in close proximity to blood vessels and within the diffusion limits of oxygen and glucose, survival in normal tissue is not constrained by substrate availability (Gatenby and Gillies, 2004). Therefore, early stages of carcinogenesis require alterations in cellular sensitivity to normal growth constraints, rather than adaptations for limited resources. The genetic model of CRC progression involves mutations in genes controlling proliferation. Mutations in the *APC* and *K-ras* genes are early events, while survival gene mutations such as those on

chromosome *18q* (related to *DCC* and *SMAD4* genes) and mutations in *p53* are associated with late events in CRC (Fearon and Vogelstein, 1990).

3.3.1.1 Initiators of proliferation

In ACPS A we found over-expression of several proteins commonly associated with CRC proliferation, including the signalling proteins (Gab-1, Ras and Raf; Tables 3.3b and 3.3c), oncogene transcription factors (NF-κβ, cyclic AMP-responsive element-binding protein 1 (CREB), CREB-binding protein (CBP); Tables 3.3a, and 3.3c), DNA replication proteins (proliferating cell nuclear antigen (PCNA) and WD repeat-containing protein 61 (WDR61; Tables 3.2b and 3.3b).

Proliferation starts with activation of growth signalling cascades, for example, MAPK/ERK is deregulated in ~30% of cancers (Fang and Richardson, 2005), and is initiated by activation of the MET (mesenchymal-epithelial transition factor) signalling pathway. **Gab-1** is a docking adaptor protein, involved in MET activation, that plays a critical role in sustained signalling (Maroun et al., 1999) and activates most c-Met-dependent biological functions (Gu and Neel, 2003). Following MET activation, the **Ras**/**Raf**/MEK/ERK cascade is activated. That in turn activates transcription factors for several proto-oncogenes.

Another proliferation pathway involves the oncogenic transcription factor, **NF-κB**, regulates expression of several anti-apoptotic and tumourigenesis genes used by the cancer to mediate cell survival and proliferation (Baldwin, 2001). NF-κβ is activated by various carcinogens and tumour promoters (Inoue et al., 2007).

CREB and CBP are transcription factors only recently found to be involved in cancer development. The role of **CREB** in cancer was identified by Shankar *et al.* (Shankar et al.,

2005). Higher CREB was found in acute myeloid leukemia (AML), where it may enhance S-phase entry and promote growth-factor-independent proliferation. CREB, along with **CBP** and its homolog p300, coordinate a number of transcriptional pathways, including survival, proliferation and glucose metabolism (Conkright and Montminy, 2005). Elevated CBP and its homolog p300, have been found in CRC; however only p300 over-expression is an indicator of poor prognosis, while high CBP correlates with survival (Ishihama et al., 2007).

Activation of proto-oncogenes increases replication and mitosis. PCNA and WDR61 are both required for completion of DNA replication. **PCNA** accumulates in late G1 and early S-phase, it is rarely observed in quiescent cells, while WDR61 is a part of the RNA polymerase II-associated factor 1 (PAF1). We observed the highest levels of PCNA in ACPS A and C primary CRC tumours (Table 3.3b), consistent with rapid cellular proliferation during these stages of tumour development. Past research has shown PCNA-positive cells in CRC to be inversely related to survival times (Mayer et al., 1993). **WDR61** was found elevated in ACPS A tumours. Its over-expression has been reported in a poorly differentiated pancreatic cancer cell line (Chaudhary et al., 2007). Furthermore, the targeted over-expression of this gene in a mouse embryonic fibroblast cell line led to transformation of the cells (Takahasi et al., 2011). Quantification of PCNA and WDR61-positive cells may help to decide whether further treatment should be administered to patients with local disease, because chemotherapy affects mainly dividing cells and should, therefore, be most successful against rapidly proliferating tumours.

3.3.1.2 Growth factors

During early tumourigenesis, signalling pathways that mediate the normal functions of growth factors are commonly subverted. The loss of, or reduced requirement for, specific

growth factors may help cancer cells evade growth constraints. Mutational changes that increase the ability of cancer cells to produce, and respond to, their own autocrine growth factors would increase proliferation. We observed the over-expression of 2 serine proteases and a growth factor receptor: proteinase 3 (PR3), which confers growth factor-independent proliferation, and prostate specific antigen (PSA) and prolactin receptor, which may promote proliferation through autocrine, insulin-like growth factor-1 (IGF-1) (LeRoith and Roberts, 2003) and prolactin (Ben-Jonathan et al., 2002), respectively.

We observed higher **PR3** levels in all tumour cells compared to controls (Table 3.3a); this is the first report of elevated PR3 in CRC. The serine protease, PR3, can confer growth factor-independence on mouse haematopoietic cell lines, and PR3 transfection increases proliferation (Desmedt et al., 2006). When aberrantly expressed, PR3 is able to cleave several intracellular proteins involved in the cell cycle and differentiation (Lutz et al., 2000). Inhibition of the PR3 breast cancer cell line with WGM2 anti-PR3 monoclonal antibody induces the opposite effect: increased differentiation and blocked proliferation (Horman et al., 2000).

Another serine protease found at elevated levels in ACPS A and C was **PSA** (Table 3.3b). This protein was originally found in prostate cells, making it a viable marker for early detection of prostate cancer. However, PSA has been found in other cancers, including 30% of CRC (Levesque et al., 1995). In the tumour micro-environment, PSA has a proteolytic role in cleaving a number of proteins involved in tumour proliferation and invasion. PSA cleavage of insulin-like growth factor binding protein-3 (IGFBP-3), the major serum binding protein for insulin-like growth factor-1 (IGF-1), reduces IGFBP-3 binding to IGF-1 and in turn can increase proliferation in response to added IGF-1 (Cohen et al., 1994). PSA may also cleave extracellular matrix glycoproteins such as fibronectin and laminin, promoting cell migration and metastasis (Webber et al., 1995).

All CRC tumours from our study were **prolactin receptor** positive with 92% showing higher than control levels (Table 3.3a). The deregulated production of prolactin might act via autocrine mechanisms (Manni et al., 1990), that require prolactin receptor. Prolactin receptor over-expression induces mammary carcinoma in prolactin positive mice (Wennbo et al., 1997). Transcripts of prolactin and its receptor, have been observed during progression of CRC from adenomas to liver metastasis (Nagano et al., 1995).

3.3.1.3 Immune suppression

Elevated levels of **α-1-antitrypsin (A1-AT)** and **α-1-antichymotrypsin (A1-Achy)** were found in all CRC tissues but not in controls (Table 3.3a). These proteins inhibit several serine proteases involved in blood coagulation, fibrinolysis, and inflammatory and immunologic processes (Bernacka et al., 1988). Past studies reported increased A1-AT at the invasive CRC margin correlating with shorter patient survival times in non-metastatic CRC (Karashima et al., 1990). A1-AChy is elevated in the sera of CRC patients (Bradham and McClay, 2006) but not in cancer cells. Expression of the protease inhibitors A1-AT and A1-Achy may protect cancer cells from the immune response. Leukocytes are frequently found in tumours, recruited there as a physiological response to cancer-specific antigens, and tissue injury during tumour development. A1-AT can modulate immune responses to favour tumour cells, by neutralisation of the lytic signal passed between natural killer (NK) cells and target (Ades et al., 1982), and can act as an endothelial cell growth and survival factor (McKeehan et al., 1986).

3.3.1.4 Suppression of regulators

Following the initial stages tumour progression, many of proliferation-associated proteins elevated in ACPS A were reduced in ACPS B, most only returning in the later metastatic phase of tumour development (Table 3.2b and 3.3b). The similarities between early tumourigenesis and initial metastasis observed here involve a resurgence of several proliferation proteins and markers of aggressive cell division in ACPS C. We predict that the over-expression of proliferation-associated proteins confers a selective advantage to the cancer cells in their microenvironment. Expansion of pre-metastatic cancer would eventually be limited by availability of substrates, as cell proliferation carries the population further from its blood supply (Gatenby and Gawlinski, 1996) (Figure 3.1). It follows that aggressive proliferation would become self-limiting, at least while the basement membrane remains intact. At the same time, environmental pressures are selecting for new phenotypes in cancer cells to maintain cell division by reducing cell cycle regulators (e.g. E2F5, p130, p57 and MEK6 to avoid senescence or apoptosis.

We observed reduced expression of the cell cycle regulators, **p130** and **E2F5**, in ACPS B, followed by an increase in E2F5 in early metastasis (Table 3.3c and 3.3d). This is the first report of differentially abundant E2F5 in CRC. Past studies have reported high levels of E2F5 in early-stage ovarian cancer (Kothandaraman et al., 2010) due to an initial immune response to arrest proliferation during the initial stage of CRC. E2F5 binds to p130 during G_0 and G_1 phases and inhibits cell cycle progression. Coinciding with CRC progression, reduced E2F5 would enable proliferation. As the cell progress to late G_1 phase, p130 is phosphorylated by cyclin dependent kinases. Simultaneously, p130 is targeted for ubiquitin-mediated degradation, its levels fall, and E2F5 is shuttled from the nucleus to the cytoplasm (Tsantoulis and Gorgoulis, 2005). The fact that E2F5 is no longer bound to p130 may allow binding to the antibody microarray and account for the increase in detectable E2F5 proteins for later

stage of CRC. An alternative theory proposes that the *E2F5* gene that maps to *8q21*, is part of a region frequently amplified in cancers, that also contains the *c-myc* and *c-mos* proto-oncogenes. Amplification of the *E2F5* gene, followed by increased transcription has been reported in breast cancer (Polanowska et al., 2000).

p57, another inhibitor of cell cycle, is lower in ACPS B (Table 3.3b). p57 blocks the cyclin dependent kinase (CDK) transition from G1 through to S phase in the cell cycle. Clinical data suggest that p57 functions as a tumour suppressor; mutations in the p57 gene are found in sporadic cancers and Beckwith-Wiedemann syndrome, a familial cancer syndrome (Matsuoka et al., 1995). Noura *et al.* (Noura et al., 2001) showed that low levels of p57 in CRC correlated with large tumour size.

Mek6 is a stress-induced negative regulator of the cell cycle. The reduced expression of Mek6 observed in ACPS B tumours was followed by its resurgence in ACPS C (Table 3.3b). To date, no expression data for Mek6 in CRC have been published. Mek6 expression is common in oncogenic transformations and may reflect a futile attempt to compensate for loss of p53 in the later stages of tumourigenesis (Wong et al., 2001). Increased levels of Mek6 in neoplasms are associated with the activation of p38, MAPK and casein kinase 2 (CK2) stress response pathways. Up-regulation of Mek6, along with its downstream partner p38, has been reported to correlate with the development of ovarian cancer and transformed cell lines (Wong et al., 2001).

3.3.1.5 Breaking contact inhibition

Normal cell growth is restricted by contact inhibition imposed by surrounding cells and the ECM. Tumourigenesis relies on cells breaking contact with their neighbours, breaking down

surrounding ECM and migrating into the extracellular medium. Compared with normal epithelium, cancer cells usually show diminished inter-cellular adhesiveness (Cavallaro and Christofori, 2004). Our data show alterations in the levels of adhesion and cytoskelectal proteins during early CRC progression, down-regulation of E-cadherin, laminin B1/b1, moesin and caldesmon, and up-regulation of CD171, annexin A2 and cytoskeletal organisation keratin 5/6/8/18 and vimentin. Down-regulation of adhesion molecules often coincides with secretion of proteolytic enzymes, such as matrix metalloproteinases. Breakdown and penetration of the ECM provides space into which the cells can move and generates gradients in diffusible and fixed ECM proteins for direction of cells (Murphy and Gavrilovic, 1999).

The adhesion protein, **E-cadherin**, decreased in ACPS B (Table 3.3c). The loss of E-cadherin leads to the dissociation of cells from their tissue (Behrens et al., 1985). There is a strong correlation between lack of E-cadherin with progression and lymph node metastasis in CRC (Gupta and Massague, 2006). In contrast, the adhesion protein **CD171,** was more abundant in tumour cells than control (Table 3.3a). CD171, a neural cell adhesion molecule, is expressed at the invasive front of CRC and is associated with tumour progression (Boo et al., 2007, Kaifi et al., 2007). CD171 can be cleaved by metalloproteinases at the tumour cell surface and in soluble form may aid micro-metastasis (Kaifi et al., 2007).

Reduced expression of the structural proteins, laminin B1/b1 and moesin in ACPS B (Tables 3.3b and 3.3c) also indicates reduced cell adhesion. Decreased expression of **laminin** has been implicated in abnormal behaviour of malignant cells (Christensen et al., 1988). Reduced extracellular laminin binding to corresponding cell surface receptors, including various integrins, decreases the redistribution of cytoskeletal and focal adhesion proteins (Huang and Chakrabarty, 1994). **Moesin** serves as a general cross-linker between plasma membranes and actin filaments. Moesin has been detected at low levels in CRC cell lines and in cancer cells

in vivo, but found at higher levels in surrounding stromal cells (Nishizuka et al., 2003). A decrease in moesin may result from increased cancer cell to stroma ratio.

The lowest level of **Caldesmon** was found in ACPS B CRC (Table 3.3d). The actin-binding protein caldesmon, negatively regulates the formation and dynamics of podosomes and invadopodia in smooth muscle cells, which are mediators of cancer cell invasion, forming highly dynamic cell-adhesion structures that degrade the ECM by secreting matrix metalloproteases. Evidence suggests that actin and its associated proteins facilitate podosomes/invadopodia formation (Albiges-Rizo et al., 2009) and the actin-binding protein caldesmon, negatively regulates podosome formation (Yoshio et al., 2007). Yoshio *et al.* (Yoshio et al., 2007), found more invadopodia and increased invasion in caldesmon depleted rat fibroblasts (3Y1/BY1), human colon carcinoma (HCA7) and breast cancer cell lines (B16F10).

In contrast, **Annexin A2** peaked during ACPS B, followed by a gradual reduction as tumours became metastatic (Table 3.2b). A similar trend in annexin A2 levels was observed between the metastatic CRC cell line, SW620, and its non-metastatic counterpart, SW480 (Katayama et al., 2006). There are several possible mechanisms by which annexin A2 may be involved in early tumour cell detachment and invasion. Annexin A2 interacts with tissue-type plasminogen activator to facilitate fibrinolysis. In addition, it forms a complex with cathepsin B that can initiate proteolytic cascades and degrade ECM proteins (Duncan et al., 2008).

Matrix metalloproteinases are the best known family of endopeptidases, collectively capable of degrading essentially all components of ECM. We observed elevated levels of matrix metalloproteinases-16 **(MMP-16)** in ACPS A CRC (Table 3.3c). This novel finding may relate more to the role of MMP-16 as a MMP-2 activator rather than its ECM degradation

properties because MMP-2, unlike MMP-16, can degrade type IV collagen in the basement membrane enabling accelerated tumour growth and metastasis (Papathoma et al., 2000).

3.3.2 Selection

Pre-metastatic tumours are often highly vascular as metastatic tumours, but only macroscopically. Although a pre-metastatic tumour may have a vascularised stroma, the cancer cells are separated from their blood supply by a basement membrane (Figure 3.1). Blood vessels are confined to the stromal compartment and, therefore, early development of the malignant phenotype occurs in an avascular environment. As a result, substrates, such as oxygen and glucose, must diffuse from the vessels across the basement membrane and through layers of tumour cells. Models for this diffusion and consumption show near-zero partial pressures of oxygen (pO_2), only 100 µm from a capillary (Helmlinger et al., 1997). Pre-metastatic tumours, with an intact basement membrane, will develop hypoxic regions near the oxygen diffusion limit. Persistent proliferation leads to thickening of the epithelial layer, pushing cells away from their blood supply. Hypoxia in pre-metastatic tumours has not been measured directly, but is consistent with the frequent observation of necrosis in CRC tumours, exceeding 20 mm, and the expression of hypoxia-inducible enzyme, carbonic anhydrase, in late stage CRC (Tables 3.2b and 3.2c).

3.3.2.1 Molecular response to hypoxia

The characteristics of hypoxic tumours can be explained, in part, by the up-regulation of a number of hypoxia-inducible genes mediated by the activation of the transcription factor, hypoxic inducible factor-1α (HIF-1α) (Semenza, 2002). Recently, the tumour-associated

carbonic anhydrase was reported to be a new class of HIF-1 responsive gene (Wykoff et al., 2000). Studies have shown an important causal link between hypoxia, extracellular acidification, and the enhanced expression of carbonic anhydrase in human tumours (Ivanov et al., 2001). Expression of hypoxia-inducible carbonic anhydrase-9 is linked to expression of proteins involved in angiogenesis, apoptosis inhibition, and cell-cell adhesion disruption in small cell lung cancer (Giatromanolaki et al., 2001). In our study, carbonic anhydrase expression correlated with metastatic CRC tumours. Similar reported expression of carbonic anhydrases I and II have been linked to biological aggressiveness and synchronous distant metastasis in CRC (Bekku et al., 2000).

3.3.2.2 Angiogenesis

Angiogenesis was the first response by CRC cells under hypoxic stress. Vascular endothelial growth factor (VEGF), and endothelial marker, Von Willebrand factor (vWF), were both elevated during ACPS A (Table 3.3b).

VEGF is a signalling protein for stimulation of vasculogenesis and angiogenesis. VEGF is strongly expressed in several human solid tumours and correlates with the density of microvessels in CRC (Takahashi et al., 1995). vWF, a glycoprotein produced uniquely by endothelial cells and megakaryocytes, is routinely used to identify vessels in tissue sections. VEGF alone can up-regulate vWF mRNA and protein in human endothelial cells (Zanetta et al., 2000). We observed significantly higher VEGF and vWF expression in ACPS A and stage C tumours compared to all other stages (Table 3.3b). Apart from its role as an angiogenesis marker, vWF has been implicated as a promoter of metastasis. There is a direct interaction between vWF and cancer cells, through the expression of adhesive ligands for vWF (Nierodzik et al., 1992). These interactions promote the binding of malignant cells to

platelets, creating heterotypic aggregates that can slip past the immune system undetected and are capable of adhering to endothelial surfaces (Floyd et al., 1992).

Despite the increased angiogenesis, these new capillaries are separated from the tumour cells by the basement membrane, which means the diffusion of substrates to cancer cells remains largely unaltered. For early cancers, angiogenesis may not relieve hypoxia because of the separation between vessels and the cells they feed. Angiogenesis-associated proteins decrease following ACPS A, and glycolysis-associated proteins increase for ACPS B. The resurgence of angiogenesis, in ACPS C, only occurs following breach of the basement membrane. Only then can vascularisation of the tumour be achieved by co-opting pre-existing vessels within the stroma and promoting new capillary growth directly into the tumour mass (Gatenby and Gillies, 2004).

3.3.2.3 Emergence of the glycolytic phenotype

Most cancer cells produce ATP by a high rate of glycolysis, with lactic acid produced in the cytosol. Comparatively, normal cells have a lower rate of glycolysis, with oxidation of pyruvate in mitochondria (Warburg, 1956). Most normal cells prefer to completely oxidise glucose to CO_2 and H_2O under aerobic conditions, but in cancer cells there is a shift toward lactate production, even in the presence oxygen. This phenomenon is termed the “Warburg effect” or aerobic glycolysis (Warburg, 1956). Persistent or cyclical hypoxia subsequently exerts selective pressure that leads to up-regulation of glycolysis. This constitutive up-regulation might occur through mutations or epigenetic changes such as alteration in the methylation patterns of promoters (Gatenby and Gillies, 2004).

Evidence for aerobic glycolysis in this study was the increased abundance of several key enzymes involved in glycolysis, **alpha-enolase**, **glyceraldehyde-3-phosphate dehydrogenase (GAPDH)** and **phosphoglycerate kinase 1**, as well as the over-expression of lactic acid fermentation protein, **L-lactate dehydrogenase**. These enzymes were significantly higher in ACPS B and ACPS C (Table 3.2b).

A novel protein yet to be associated with CRC glycolysis is **porin 31HM**, found in the mitochondrial outer membrane (Lawen et al., 2005). Traditionally, porin 31HM has been associated with the pro-apoptotic proteins Bax and Bak, and the release of cytochrome C (Shimizu et al., 1999). Porin 31HM is known to be up-regulated in malignant liver cancer (Shinohara et al., 2000), but the increased expression of porin 31HM during CRC development (Table 3.2b) has not been reported. In spite of porin's role in regulation of cell death, the differential expression of porin may be more related to glycolysis. Expression of porin 31HM is known to coincide with hexokinase I and II (HKI and HKII) expression in tumour cells (Shinohara et al., 2000). To enable rapid growth, tumour cells increase the activities of enzymes involved in glycolysis. Tumour mitochondria have a higher HK binding capability than normal cells, which is facilitated by up-regulation of porin 31HM.

Consistent with the Warburg effect, there was an impaired aerobic citric acid cycle in CRC as evidenced by reduced expression of **aconitate hydratase** and **malate dehydrogenase** (Table 3.2a). **Glutamate dehydrogenase**, involved in the production of α-ketoglutarate, was also reduced in tumour cells (Table 3.2a). These proteins are known to be down-regulated in CRC tissue compared to normal mucosa (Bi et al., 2006).

Mutations in mitochondrial DNA may impair oxidative phosphorylation in cancer (Polyak et al., 1998). Data from several studies, including our own, show reduced expression of key mitochondrial proteins required for synthesis of ATP. The down-regulation of ATP synthase

subunits, β-F1-ATPase (Willers et al., 2010) and reduced **α-F1F0-ATPase** (Table 3.2a) supports the Warburg efftect hypothesis with reduction of oxidative phosphorylation in most cancer cells. Decrease of ATPase in our CRC samples is accompanied by reduction of proteins involved in mitochondrial energy transduction, **electron transfer flavoprotein**, **delta(3,5)-delta(2,4)-dienoyl-CoA isomerase** and **acyl-CoA dehydrogenase** (Tables 3.2a and 3.3c).

3.3.2.4 Surviving acidosis

Up-regulation of glycolysis is a successful adaptation to hypoxia but increases acid production. Prolonged exposure to acid stress typically results in necrosis or apoptosis through p53- and caspase-3-dependent mechanisms (Park et al., 1999). Therefore, constitutive up-regulation of glycolysis requires additional adaptations against the negative effects of extracellular acidosis, through resistance to apoptosis or up-regulation of membrane transporters to maintain normal intracellular pH. In support of this theory we observed the down-regulation of several caspase-associated apoptotic proteins (B-cell lymphoma/leukaemia 10 (Bcl-10), caspase 1, caspase 3 and DNA fragmentation factor), coinciding with glycolysis in ACPS B CRC (Table 3.3a, b, c).

Bcl-10 is a caspase-recruitment domain protein involved in the induction of apoptosis and activation of the NF-κB complex. Activation of NF-κB complex is connected to pro-proliferation roles in oncogenesis (Baldwin, 2001) and may be the result of deregulation due to Bcl-10 gene mutation, rare in CRC (Stone et al., 1999). We observed a decrease in Bcl-10 in CRC compared to normal mucosa (Table 3.3a), the decrease in Bcl-10 expression may be attributed to its pro-apoptotic role. Previous studies support the pro-apoptotic role of Bcl-10;

its over-expression in human embryonic kidney cells (Willis et al., 1999) and in transformed cell-lines (Srinivasula et al., 1999) correlates with increased apoptosis.

Caspase 1, caspase 3 and DNA fragmentation factor were all reduced in ACPS B compared to ACPS A (Table 3.3b and 3.3c). Caspases are part of the cysteine-aspartic acid protease family and are essential activators in the caspase cascade involved in apoptosis. **Caspase 1** is an initiator caspase that cleaves inactive pro-interleukin 1β to generate the pro-inflammatory cytokine interleukin 1β (Thornberry et al., 1992). **Caspase 3** is the ultimate executioner caspase that is essential for the nuclear changes associated with apoptosis (Woo et al., 1998). Downstream of Caspase 3, **DNA fragmentation factor** induces DNA fragmentation and chromatin condensation during apoptosis (Wolf et al., 1999).

The combination of acidosis and uncontrolled proliferation of cancers increases the probability of DNA damage during cell replication; consequently, there may be over-expression of DNA repair proteins. One form of DNA repair is through homologous recombination; the central protein involved in this pathway is RAD51. This protein ensures high fidelity DNA repair by facilitating strand exchange between damaged and undamaged homologous DNA segments. Several RAD51-like proteins, including **XRCC2**, facilitate this process (Tambini et al., 2010). Overexpression of XRCC2 is most prevalent in ACPS B (Table 3.3b). Variations in the *XRCC2* gene may be associated with increased risk of CRC (Curtin et al., 2009). The associated protein, RAD51, is constitutively over-expressed in several cancer cell lines, and may protect tumour cells from undergoing apoptosis in response to DNA damage.

3.3.2.5 Endoplasmic reticulum response

The tumour microenvironment can perturb endoplasmic reticulum (ER) functions. Stress factors, in particular, hypoxia, nutrient limitation, and low pH promote activation of signalling pathways, from the ER, that are activated by accumulation of misfolded/unfolded proteins in the ER (Schroder and Kaufman, 2005). The ER responds to these stresses by activating signal transduction pathways that protect against stress-induced apoptosis. Alterations in ER protein levels, post-translational modifications, or abnormal secretion of ER-resident proteins, are hallmarks of ER deregulation. Levels of the ER chaperone **glucose-regulated protein (GRP) 78**, are increased in at least 10 cancers (Moenner et al., 2007). GRP78 is the chaperone for Hsp70 and facilitates protein folding and assembly in response to extracellular stresses (Brown and Giaccia, 1998). Our results show that GRP78 levels peaked during ACPS B (Table 3.2b), and may confer resistance to pro-apoptotic changes (e.g, protein denaturation).

Another Hsp70 chaperone, **HDJ-2**, was reduced in ACPS B (Table 3.3c). Consistent with previous findings that HDJ-2 is absent or reduced in CRC tissue (Kanazawa et al., 2003). GRP78 chaperone may confer greater benefits to the tumour during development.

Disulfide-isomerase A3 (PDI) and endoplasmic reticulum protein 29 (ERp29) are closely related proteins involved in secretory protein production (Shnyder and Hubbard, 2002). **PDI** was elevated in non-metastatic CRC tumours (Tables 3.2b and 3.2c). Stierum *et al.* (Stierum et al., 2003) observed a similar increase of PDI levels at the beginning of the differentiation process in CaCo-2, a CRC cell-line. Caco-2 in post-confluent phase differentiates into a cell type with remarkable small intestinal enterocyte-like features. The association of PDI and differentiated cancer cells may explain its reduced expression in metastatic tumours. PDI is also involved in peptide binding to major histocompatibility complex (MHC) class I

molecules in the ER (Lammert et al., 1997). Reduced expression of PDI in late stage CRC could indicate a possible mechanism to avoid immune detection.

Some ER proteins were over-expressed during late tumourigenesis, coinciding with metastatic transformation and are discussed below. Previous studies suggest they possess secondary functions as adhesion protein regulators and may contribute to the metastatic phenotype.

Elevated levels of endoplasmic reticulum protein **ERp29** were observed in metastatic CRC (Table 3.2b), indicating an ER stress response. Similar ERp29 levels have been reported in skin basal-cell carcinoma (Cheretis et al., 2006) and CRC serum (Kim et al., 2009).

Elevated levels of **calreticulin** were observed in ACPS C tumours (Table 3.2b), consistent with previous reports of elevated calreticulin in CRC (Brunagel et al., 2003). Calreticulin is a multifunctional protein, that acts as a chaperone for protein folding. Studies have correlated elevated ER specific calreticulin in various cancer models with enhanced resistance to stress (Delom et al., 2007). Additionally, calreticulin modulates steroid hormone receptors and retinoic acid receptors. It is also involved in the regulation of cell adhesion via interaction with the α-subunits of integrins (Brunagel et al., 2003).

Up-regulation of **Reticuloclabin-1 (RCN1)** was observed in metastatic CRC (Table 3.2c), consistent with the report of RCN1 levels correlating with metastasis and reduced expression of Ca^{2+}-dependent cadherin in breast cancer and CRC cell lines (Nimmrich et al., 2000). RNC1 is a protein reported to reside in the ER lumen and has a classic ER retention signal, C-terminal Lys-Asp-Glu-Leu sequence. The function of RCN1 is unknown, but it may play a role in Ca^{2+} dependent cell adhesion and intracellular Ca^{2+} metabolism (Nimmrich et al., 2000).

3.3.3 Metastasis

Hypoxia and acidification are strong selection forces affecting evolution of the metastatic phenotype. Most solid tumours eventually metastasise. Fidler (Fidler, 1970) attempted to quantify metastasis by tracking cancer cells with ^{125}I-iodo-deoxyguanidine. His study showed that within 24 of entry into the circulation, fewer than 0.1% of tumour cells were still viable, and of those cells, fewer than 0.01% survived to produce metastases. The inefficiency of the metastatic process implies that healthy tissues display a marked hostility towards invading tumour cells. To achieve metastasis, cancer cells must therefore evade or co-opt multiple barriers that have been refined over hundreds of millions of years of organismal evolution. Therefore, several studies, including our own, have found metastasis to be a highly selective process; actively selecting for cancer cells with metastatic phenotype to increase metastatic success.

3.3.3.1 Metastatic proliferation

We observed an interesting expression profile during early metastasis (ACPS C), reminiscent of early tumourigenesis (ACPS A). The resurgence of proliferation-associated proteins observed in ACPS A (including PCNA and PSA; Table 3.3b), along with the up-regulation of other pro-proliferation/anti-apoptosis proteins (survivin, 60 kDa heat shock protein (Hsp60), transglutaminase II (TGM2) and notch; Tables 3.2b, c, d, e) indicate return to aggressive proliferation. This characteristic of ACPS C tumours may address the metastatic paradox, that in theory metastatic tumours should have a fitness disadvantage relative to non-metastatic tumours, owing to the loss of constituent cells that emigrate (Merlo et al., 2006). We predict, in response to this loss of cells, metastatic tumours increase proliferation to ensure successful colonisation of distant sites and to maintain heterogeneity within the primary population.

Survivin is a known inhibitor of apoptosis; in CRC it is a predictive indicator of poor prognosis and shorter survival rates (Kawasaki et al., 1998). Another pro-survival protein is mitochondrial **Hsp60**. Several studies show Hsp60 up-regulation in colonic polyps (Melis and White, 1999) and during colorectal carcinogenesis (Cappello et al., 2003). Both proteins were significantly higher in metastatic tumours compared to non-metastatic tumours.

TGM2 levels were increased in ACPS C tumours (Table 3.3b). Several studies have reported that increased expression of TGM2 indicates prolonged cell survival and prevention of apoptosis in various cancers (Boehm et al., 2002). It is suggested that the induction of these signalling pathways is a result of TGM2 promoted interaction with ECM protein components in association with members of the integrin family of proteins (Herman et al., 2006). Other reports suggest that TGM2 regulates activation of NF-kB by forming a ternary complex with NF-kB/IkBa and inhibition of apoptosis through transamination and GTP-binding activity (Mann et al., 2006). A recent study by Miyoshi *et al.* (Miyoshi et al., 2010) found a correlation between high TGM2 mRNA in CRC and lymph node metastasis, tumour invasion and poorer post-operative survival rate.

Notch signalling has also been shown to contribute to CRC development through the maintenance and self-renewal of cancer stem cells (CSC) (Sikandar et al., 2010). Notch signalling, along with associated notch proteins was reported to show 10- to 30-fold increase in CSCs compared to CRC cell lines (Sikandar et al., 2010). We found elevated notch expression in ACPS C cancer cells, followed by a reduction in ACPS D (Table 3.3e). The role of CSC in cancer metastasis has only recently been explored. The inherent characteristics of CSCs make them more adept at survival in a foreign environment. Tumour-initiating capacity and increased genetic instability in metastatic CSCs are likely to provide a selective advantage in adapting to foreign sites (Li et al., 2007a). Production of CSC with metastatic

potential may increase during ACPS C, followed by a reduction of these CSC in ACPS D, a result of metastatic CSCs migrating away from the primary tumour site.

Surprisingly, some transcription regulators, that were reduced in ACPS B, are elevated in ACPS C (Mek6, E2F5 and p57 (Table 3.3b, d), along with the first appearance of p73 (Table 3.3d). This may reflect a futile attempt of the transformed cell lines to compensate for a loss of p53 function or may possess beneficial functions during metastasis.

p73 protein is homologous to p53, sharing common functions such as activating transcription of genes, inhibiting cell growth, and inducing apoptosis (Jost et al., 1997). However, activation of the p73 allele may also support tumour progression, as increased levels of p73 mRNA transcripts are found in many tumour cells compared to their normal counterpart (Sunahara et al., 1998). In support of our results, the over-expression of p73 has been correlated with CRC metastasis and poorer survival (Sun, 2002).

3.3.3.2 Ribosomes

Further evidence of accelerated growth was observed through the up-regulation of translation- and ribosome-associated proteins. The ribosome assembly protein, nucleophosmin (NPM), was most abundant in metastatic stage C CRC (Table 3.3b), along with ribosome proteins, (elongation factor Tu (EF-1α) and 28S ribosomal protein S22 (MRPS22); Table 3.2b) and translation regulators (M7GpppX diphosphatase, heterogeneous nuclear ribonucleoprotein (hnRNP) H3 and hnRNP A2/B1; Table 3.2b). Each of these is discussed below.

NPM was found to peak in ACPS C tumours (Table 3.3b); similar NPM over-expression were found in bladder and breast cancer, where the increased NPM mRNA correlated with

tumour progression (Tsui et al., 2004, Skaar et al., 1998). Nozawa *et al.* (Nozawa et al., 1996), showed that NPM, and its mRNA, increased in CRC adenomas when compared to normal mucosa; however its expression in tumours varied widely, with no direct correlation to proliferation. **NPM** has proven to be a multifunctional protein that is involved in many cellular activities, including ribosome assembly and transport; it is related to both proliferative and growth-suppressive roles in cells. Due to these properties, NPM falls into a new category as a proto-oncogene and a tumour-suppressor. Depending on expression levels and gene dosage, either a partial functional loss of NPM or aberrant overexpression can lead to neoplastic transformation through distinct mechanisms (Grisendi et al., 2006).

EF-1α expression was observed to increase with tumour progression (Table 3.2b). Its function supports our result, as EF-1α is a GTP-binding protein that catalyses the binding of aminoacyl-transfer RNAs to the ribosome, an essential step in translation (Moldave, 1985). It is likely that EF-1α functions as a tumour promoter by making cells competent for growth (Tatsuka et al., 1992). Previous research found higher EF-1α levels in CRC compared with normal tissue (Kuramitsu and Nakamura, 2006). Over-expression of EF-1α mRNA has been correlated with increased metastatic potential in mammary adenocarcinoma (Edmonds et al., 1996). EF-1α from metastatic cells has reduced affinity for actin, the distribution of EF-1α and filamentous actin in the cytoskeletal structure is thought to be important for supporting the cellular motility required for metastasis.

MRPS22 was found at the highest level in ACPS C tumours (Table 3.2b). Recent studies have correlated MRPS22 expression with Tiam1 (T-cell lymphoma invasion and metastasis-inducing protein 1) up-regulation (Liu et al., 2008). They also found Tiam1 to promote tumour progression and increase metastatic potential in CRC cell lines (Liu et al., 2008). The down-stream expression of MRPS22, following Tiam1 over-expression, may contribute to

one or several of the pro-metastatic pathways, including inhibition of apoptosis, reduction of cellular adhesion (Minard et al., 2006) and increase in cell migration (Bassi et al., 2008).

M7GpppX diphosphatase is a decapping scavenger enzyme that catalyses the cleavage of a residual cap structure following the degradation of mRNA by the exosome-mediated mRNA decay pathway (Gu et al., 2004). M7GpppX diphosphatase was more abundant in metastatic CRC compared to non-metastatic CRC (Table 3.2b, c). The 5'-cap structure (m7GppN, where m7G is 7-methylguanosine and N is the first nucleotide of the mRNA) plays a critical role in the life cycle of mRNA and is necessary for efficient gene expression and cell viability (Topisirovic et al., 2011).

HnRNP is a family of proteins that bind RNA polymerase II transcripts to form hnRNP particles. To our knowledge, there have been no previous reports of the differential expression of **hnRNP H3** and **hnRNP A2/B1** in cancer (Table 3.2b). HnRNP H3 and hnRNP A2/B1, along with similar hnRNPs (H, H', and F), are involved in pre-mRNA processing and in cellular differentiation. HnRNP H/H' and F are up-regulated in gastric carcinomas (Honore et al., 2004) and play fundamental roles in controlling gene expression. Model studies have shown that they participate in alternative splicing of the c-*src* gene (Min et al., 1995), the β-tropomyosin gene (Chen et al., 1999) and the thyroid hormone receptor gene (Hastings et al., 2001). Furthermore, changes in their expression levels are important for various cellular differentiation processes (Liu et al., 2001). HnRNP 2H9 is the most recently identified member of this family, and little is known about its functions except for a role in the splicing arrest induced by heat shock (Mahe et al., 2000). Mahe *et al.* have also observed hnRNP M and H3 intervention in the functional flexibility of the splicing machinery in mouse embryonic development. HnRNP H3, like its epitopes hnRNP H/H' and F, could participate in tissue-specific and developmental regulation of gene expression.

3.3.3.3 Metastatic angiogenesis

In order to metastasise, cancer cells must invade tumour associated vasculature to gain access to distant sites in the body. This is facilitated partly through induced outgrowth of the pre-existing vasculature and partly through *de novo* recruitment of vascular cell precursors from the circulation. The observed re-emergence of VEGF and vWF (Table 3.3b), along with metastatic-specific expression of the endothelial homing receptors, carbohydrate antigen 19-9 (CA19-9), epithelial membrane antigen (Muc1) and CXC chemokine receptor type 4 (CXCR4) in ACPS C and D cancer cells are evidence of this event.

Cancer cells expressing **CA19-9** bind to the endothelial cell-surface receptors E-selectin and P-selectin (Berg et al., 1992); this attachment is important in the development of tumour metastasis. CA19-9 is a tumour marker for CRC (Nakayama et al., 1997b). **Muc1** apomucin is the glycoprotein that carries the CA19-9 antigen (Baeckstrom et al., 1993) and is itself a predictor of tumour progression. Our results confirm the over-expression of Muc1 and CA19-9 in all CRC samples. The highest CA19-9 level was found for metastatic tumours (Table 3.3a), but the CA19-9 levels were variable for metastatic and non-metastatic. A reason for this could be that CA19-9 is expressed as a mono-sialo-ganglioside in cancer tissue, whereas in serum CA19-9 is found on mucin-type glycolipids (Magnani et al., 1982). Nakayama *et al.* (Nakayama et al., 1997a) showed that CA19-9 serum levels were better predictors of recurrence than tissue CA19-9.

Recent evidence indicates an important role for CVCL21 (CXC chemokine) and its receptor **CXCR4** in the metastatic homing of tumour cells (Murphy, 2001). Ottaiano et al. (Ottaiano et al., 2006) showed concurrent expression of CXCR4 and VEGF in >50% of Duke's stage B and C CRCs. Increased CXCR4/CXCL12 contributes to the attachment of CRC cells to the endothelium leading to cancer metastases. We found elevated levels of CXCR4 in ACPS C

that was reduced in ACPS D (Tables 3.3d, e), suggesting the possibility that CXCR4-positive cells were better adapted to escape from the primary tumour, the highest CXCR4 levels are found on liver metastases of CRC patients (Scala et al., 2005).

3.3.3.4 Oxidative stress

Once malignant CRC cells have broken through the basal membrane and invaded the circulatory compartment, they attain ready access to virtually all organs of the body. However, these cells must survive extracellular stresses such as increased reactive oxygen species (ROS), exacerbated as a result of metastases. We found progressively increased expression of redox proteins (e.g. peroxiredoxin, manganese superoxide dimutase) in early metastatic tumour compared with normal mucosa.

Numerous studies have shown that the level of oxidants and peroxides are higher in tumours than in the surrounding tissue (Dreher and Junod, 1996). Transformed cells have an increased growth rate, and produce higher levels of reactive oxidative species from accelerated cellular respiration (Toyokuni et al., 1995). Some cancer cells also produce higher levels of pro-inflammatory cytokines that stimulate tumour growth (Dreher and Junod, 1996), that places additional oxidative stress upon cancer cells. We have found that different redox regulation proteins were expressed at different stages of CRC development. Constitutive expression of peroxiredoxin-1 (Prdx-1) was found in all tumours (Table 3.2a), while peroxiredoxin-4 (Prdx-4) was only expressed in non-metastatic CRC (Table 3.2c). Metastasis correlated with the over-expression of manganese superoxide dismutase (MnSOD) and isocitrate dehydrogenase (IDH) (Table 3.2c), possibly as a response to oxygen from blood cells, once the tumour has penetrated the basement membrane (Nishikawa, 2008).

Prdx-1 and **Prdx-4** are members of a highly conserved 2-Cys peroxiredoxin family that regulates the cellular redox state by breaking down H_2O_2 (Rhee et al., 2005). Studies, including this one, have shown that Prdx-1 is elevated in CRC (Rho et al., 2008) (Table 3.2a), while Prdx-4 has been found reduced in CRC (Jang et al., 2004) (Table 3.2c). High levels of Prdx in cancers are associated with increased resistance to radiation (Park et al., 2000) and resistance to some anti-cancer drugs (Chung et al., 2001), whereas Prdx deficiency can sensitize cells to apoptosis (Pak et al., 2002). Residing in the ER, Prdx4 serves as a regulatory factor for NF-κB, an oxidative stress activated transcriptional factor (Park et al., 2009). The exact reason for down-regulation of Prdx4 in CRC remains unknown.

MnSOD is an antioxidant enzyme that suppresses cell growth of a variety of cancer cell lines (Liu et al., 1997). The MnSOD growth-retarding effects are at least partially due to triggering of a p53-dependent cellular senescence program (Behrend et al., 2005). Despite its general tumour suppressor activity, there are conflicting reports with regard to MnSOD level in CRC tumours. MnSOD level positively correlates with tumour grade in colorectal carcinoma (Nozoe et al., 2003) and with invasion and metastatic phenotype (Cullen et al., 2003). The discrepancy between growth inhibition and association with malignancy can be explained with the tumour progression model for CRC suggested by Kinzler and Vogelstein (Kinzler and Vogelstein, 1996). In low-grade CRC with predominantly functional p53, MnSOD levels are low, since high levels of MnSOD would result in p53 induced growth arrest. As tumour progression proceeds, p53 becomes inactivated, leading to accumulation of mutations and an increasing loss of growth control. At this point, high levels of MnSOD, no longer able to induce senescence and growth control due to the lack of p53, can activate matrix metalloproteases, that might drive the invasive phenotype of high-grade tumours.

IDH1 and **IDH2** are found in the cytoplasm and mitochondria, respectively, producing NADPH by converting isocitrate to α-ketoglutarate (αKG). However, with ROS IDH activity

is increasing, while the activities of other tricarboxylic acid cycle enzymes decrease (Mailloux et al., 2007), IDH may play a role in the cellular response to ROS, in addition to the normal role in cellular metabolism. Mutations of IDH1 and IDH2 have been found in liver metastasis of a CRC patient (Sjoblom et al., 2006), acute myeloid leukaemia, and gliomas (Cairns et al., 2011). These specific mutations cause IDH1 and IDH2 to acquire a novel enzyme activity that converts α-ketoglutarate to 2-hydroxyglutarate in a NADPH-dependent manner (Reitman and Yan, 2010). The function of this novel metabolite is not known and further investigation is required to determine if these IDH mutations occur as part of metastatic transformation in CRC.

3.3.3.5 Proteasome and protein degradation pathways

Increased proteasome activity is a survival response for cancers under oxidative stress. Prolonged exposure to ROS causes accumulation of abnormal proteins in cells, impeding cellular functions and initiating apoptosis. The up-regulation of the ubiquitin-proteasome pathway degrades any damaged proteins formed during oxidative stress, promoting cell survival (Kwak et al., 2003). Inhibition of proteasome function has been shown to induce apoptosis in cancer cells (Almond and Cohen, 2002).

Proteasome sub-units alpha type-1, proteasome activator hPA28 subunit beta, ubiquitin-associated protein and PEST proteolytic signal containing nuclear protein (PCNP), are elevated in metastatic CRC (ACPS C and D; Table 3.2c). Their expression could be a defensive response to increased oxidative stress as a result of metastasis; degradation of the basement membrane and increased angiogenesis. Evidence for the expression of the proteasome in late stage CRC has suggested survival and growth advantages for tumours. (Osburn and Kensler, 2008). The pro-cancer properties of proteasome activity may be limited

to advanced CRC, proteasome subunit alpha type-2 was found reduced in tumour tissue compared to normal tissue (Table 3.2a). The expression of the proteasome in normal colon tissue provides protection from potential mutagenic attack and down-regulation leads to the accumulation of abnormal proteins and tissue damage, potential promoters of tumourigenesis (Hayes and McMahon, 2009). It has also been proposed that reduced expression of proteasome subunits leads to the loss of HLA class I expression and may assist in immune evasion by cancer cells (Miyagi et al., 2003). Following metastasis, proteasome activity may re-emerge to promote tumour survival and growth advantages (Osburn and Kensler, 2008).

We also found elevated levels of **PCNP**, a part of the ubiquitin-proteasome pathway, in metastatic CRC tumours (Table 3.2c). The PEST hypothesis predicts that the proteins with 'PEST sequences' are degraded rapidly, often via the ubiquitin-proteasome pathway (Rechsteiner and Rogers, 1996). Mori *et al.* (Mori et al., 2004) suggest that PCNP and its ubiquitin ligase (Np95/ICBO90-like RING finger protein) may constitute a novel signalling pathway with some relation to cell proliferation. Recent studies have found PCNP to be involved in monkey embryonic stem cell proliferation (Nasrabadi et al., 2009), and Np95 to have an oncogenic role in CRC (Wang et al., 2012), but to our knowledge, our study is the first to correlate PCNP over-expression with CRC metastasis.

Cullin-3, another ubiquitin-associated protein, was reduced at later stages from the level in ACPS A (Table 3.3c). The human cullin protein family consists of seven members that function as scaffold proteins in the E3 ligases. Little is known about the physiological function of **cullin-3**, but it has a role in controlling cell proliferation (Du et al., 1998), and may be required for efficient TOP1 (DNA topoisomerase I) degradation by the ubiquitin-proteasome system (Zhang et al., 2004). Additional studies, especially identification of Cul3-containing E3 ligase complexes, will be needed to establish the molecular roles of Cul3 in TOP1 ubiquitylation and CRC metastasis.

3.3.3.6 Novel cancer-related protein

Alcohol dehydrogenases (ADH) are enzymes that oxidise ethanol to acetaldehyde. Subsequent oxidation of acetaldehyde to acetate is catalysed by aldehyde dehydrogenases (ALDH). There is sufficient evidence that, in the colon, acetaldehyde is involved in alcohol-induced colorectal carcinogenesis (Seitz et al., 1990). Acetaldehyde can be produced by colonic bacteria and, to a much lower degree, by intestinal mucosal ADH. This study was not the first to observe increased expression of ADH in CRC (Jelski et al., 2004) relative to normal mucosa, but we are the first to show significantly elevated ADH in metastatic CRC compared to levels in non-metastatic CRC (Table 3.2b). Jalski *et al.* (Jelski et al., 2004) found a much higher ADH:ALDH ratio in CRC than in normal mucosa, suggesting that the cancer cells have a high capability to oxidise exogenous ethanol to acetaldehyde, but a low capacity to remove acetaldehyde. The build-up of acetaldehyde derived from systemic blood or from luminal microbial fermentation can have direct mutagenic and carcinogenic effects. Acetaldehyde interferes at many sites with DNA synthesis and repair (Jelski et al., 2004). Moreover, Homann (Homann, 2001) showed that high acetaldehyde correlated with low local folate concentrations in the colon and may increase susceptibility to CRC. Further studies are required to investigate the role of ADH in metastatic tumours and to establish whether elevated levels of acetaldehyde contribute to disease progression and promote metastasis in CRC.

3.3.4 Future work and conclusions

This study focused on the expression patterns of intracellular proteins during the development and progression of primary CRC tumours. However, we note that local lymphatic and secondary distant organ metastases are also of great importance to the understanding of

cancer progression. Our work on primary tumours restricts our understanding of CRC metastasis to the selection for cancer cells bearing metastatic phenotype during early metastasis followed by their release into the blood vessels, evidenced by an increase in metastasis-associated proteins in stage C tumours followed by their reduction in stage D tumours (notch proteins, CXCR4; Table 3.3e). In future studies we wish to isolate and profile CRC-derived cancer cells from blood vessels, lymph nodes and secondary tumours. A review by Gupta and Massague (Gupta and Massague, 2006) highlights the evolving framework for metastasis and the selection factors influencing malignant cells to overcome diverse environmental defences. Defining protein expression profiles of cancer cells at different stages and locations of metastasis will contribute to our understanding of CRC and help predict CRC metastatic behaviour.

Proteomics has been used to identify processes that direct CRC progression, including interactions between cancer cells and their surroundings. Multiple mutations lead to development of cancerous tissue, allowing for aggressive growth, unrestricted by normal cellular constrains. Inevitably, uncontrolled proliferation results in hypoxia. Faced with this challenge cancer cells respond with a range of adaptations, with glycolytic phenotype as one of the preferred solutions. By-products of glycolysis provide the next selection force, acidosis. Tumours respond by reducing apoptosis-associated proteins and increasing stress response proteins, but ultimately the combination of acidosis and limited resources result in the metastatic phenotype. Following the breach of the basement membrane, direct exposure of cancer cells to blood vessels sees them respond to the oxidative stress and utilise endothelial homing proteins to begin metastasis. The metastatic transformation leads to migration of cancer cells towards secondary sites.

Our proteomic data have contributed towards an understanding of the processes involved in CRC progression at different stages of development. We have established protein expression profiles that provide markers of physiological events within cancer cells. These protein profiles provide a novel approach to CRC stratification and may improve patient outcome prediction and tailored therapy.

Chapter 4

Immunophenotyping of colorectal cancer cells and infiltrating T-lymphocytes for improved stratification

4.1 Introduction

Treatment for CRC is determined from the disease stage. Surgery may be curative with optional adjuvant therapy. Currently, chemotherapy is offered to all Australian Clinico-pathological Stage (ACPS) C and D patients. Although the majority of ACPS A and B patients will be cured by surgery alone, ~35% of stage B patients would benefit from further therapy (Morris et al., 2007). At least one third of ACPS C patients are cured by surgery and,

undergo unnecessary and debilitating further cytotoxic treatment (Durrant et al., 2003). This problem arises because of the heterogeneous nature of CRC (Li et al., 2007b) and the complexity of its development and spread. As a result, the clinical course for individuals remains difficult to predict even for same stage tumours. Additional discriminatory markers could enable prediction of cancer behaviour and selection of the best course of treatment.

The progression of CRC from adenomatous polyp to metastatic disease occurs due to progressive accumulation of mutations, epigenetic abnormalities (Moyret-Lalle et al., 2008), and complex interactions of different sub-populations of cells within the tumour microenvironment (cancer cells, normal stromal cells, infiltrating leukocytes and cytokines they produce) (McAllister and Weinberg, 2010). For the majority of CRC, cell dysfunction results from numerous mutations that modify proteins expressed and post-translational modifications (Steinert et al., 2002). A number of cell surface antigens, including cluster of differentiation (CD) antigens, have been identified as potential prognostic biomarkers in CRC (Belov et al., 2010). Levels of these antigens may change with tumour progression or interactions with other cell types, such as tumour-infiltrating lymphocytes (TIL).

Immunohistochemistry (IHC) for cancer stratification and prognostication is well established for some tumour types (Eifel et al., 2001, Swerdlow, 2008). Currently for CRC, the use of IHC is used to detect DNA microsatellite mismatch repair (MMR) protein to identify a subgroup of tumours (10 – 15%) that may be associated with a familial cancer syndrome, hereditary non-polyposis colorectal cancer, and development of metachronous tumours (Duffy et al., 2007, Greenson et al., 2009). Single markers do not provide prognostic significance greater than clinico-pathological staging and are not used for routine pathology of CRC.

A recent approach to stratify CRC phenotypes uses surface protein profiles of multiple markers. Proteomic techniques such as iTRAQ enable discovery of biomarkers (Xiao et al., 2008), but are too complex for routine use in diagnostic laboratories, and cannot distinguish different cell types in a mixed population. In addition, relatively large amounts of tumour tissue are required for profiling of membrane glycoproteins.

In this PhD project, we developed a method for surface proteome profiling of live cells from disaggregated CRC samples using DotScan^{TM} CRC antibody microarrays. The 122-antibody microarray consists of a standard 82-antibody region recognising a range of lineage-specific leukocyte markers, adhesion molecules, receptors and markers of inflammation and immune response (Belov et al., 2003), with additional antibodies for detection of 40 prognostic markers for CRC (Zhou et al., 2010). Whole cells are captured only on antibodies for which they express the corresponding antigens. We have profiled the surface antigen expression of EpCAM^{+} CRC cells and CD3^{+} T-cells within samples of primary CRC and normal mucosa from 50 patients. Hierarchical clustering of binding patterns for these two sub-populations of cells yielded clusters of patients that correlated with differentiation, ACP stage and inflammation. We found that the immunophenotypes of tumour cells correlated with the infiltrating T-cells, indicating a strong influence of the microenvironment on the surface proteomes of these cells. Disease signatures from surface protein markers may be more accurate than gene expression profile data. When applied with clinico-pathological features, immunophenotyping could further stratify intermediate stage CRC and improve prediction of patient outcomes.

4.2 Results

Surface antigen profiles of cell subtypes were obtained from 97 samples (adenoma, tumour and normal mucosa) from 50 patients. Clinicopathological and histological characteristics of the 50 patients are listed in Table 4.1. The tumours collected were predominantly intermediate stage (ACPS A3, B1, B2 and C1) tumours (78%). Clinico-pathology reports and haematology information were collected for each patient. No correlation was found between the ACPS and circulating lymphocyte levels ($p=0.87$) or ACPS and circulating neutrophil to lymphocyte ratio (NLR) ($p=0.45$).

Two cell types, $EpCAM^+$ cancer cells and $CD3^+$ T-cells, were profiled in each sample. Surface profiles (97) were obtained for CRC and normal mucosa cells, while 75 profiles were obtained for T-cells; 22 T-cell profiles were omitted due to low or zero cell binding. A total of 38 antibodies on the DotScan microarray showed positive cell binding in the $EpCAM^+$ cell profiles and 46 antibodies for $CD3^+$ T-cells.

Table 4.1 Clinico-pathological and haematological characteristics of the 50 CRC patients

	No. patients (%)
Gender	
Male	24 (48%)
Female	26 (52%)
Age	
≤ 65	33 (66%)
> 65	17 (34%)
Location	
Left (caecum, ascending colon, transverse)	26 (52%)
Right (descending colon, sigmoid, rectum)	24 (48%)
Australian clinico-pathological stage (ACPS)	
Adenoma	2 (4%)
A2	3 (6%)
A3	9 (18%)
B1	18 (36%)
B2	2 (4%)
C1	10 (20%)
C2	2 (4%)
D0	1 (2%)
D2	3 (6%)
Infiltration	
Submucosa	6 (12%)
Muscularis propria	12 (24%)
Subserosa	26 (32%)
Serosa	6 (12%)
Differentiation	
Adenoma	2 (4%)
Well	2 (4%)
Moderate	42 (80%)
Poor	6 (12%)
Peri-tumoural inflammation	
Present	21(42%)
Absent	29 (58%)
Tumour infiltrating lymphocytes (TIL)	
Present	5 (10%)
Absent	45 (90%)
Circulating lymphocyte count	
$< 1 \times 10^9$/L (low)	16 (32%)
$1.0\text{-}3.0 \times 10^9$/L (normal)	32 (64%)
Circulating neutrophil to lymphocyte ratio (NLR)	
≤ 5	23 (46%)
> 5	27 (54%)

4.2.1 Tumour versus normal

The Student's t-test was used to compare protein levels in CRC with normal mucosa. A total of 50 $EpCAM^+$ CRC cell profiles were compared with 47 $EpCAM^+$ normal mucosa profiles. A total of 38 surface antigens showed positive cell binding; of these, 4 antigens were significantly elevated, while 20 antigens were significantly reduced on CRC cells compared with the matching normal mucosa counterpart (Table 4.2a). Hierarchical clustering was performed on the antigen profiles (38 positive proteins) (Figure 4.1) to sub-classify samples on the basis of their $EpCAM^+$ cell profiles.

A total of 42 $CD3^+$ tumour-associated T-cell profiles were compared to 33 $CD3^+$ normal mucosa-associated T-cell profiles. A total of 46 surface antigens showed positive cell binding; of these 6 antigens were significantly elevated while 18 antigens were significantly reduced on tumour-infiltrating T-cells compared to T-cells from normal mucosa (Table 4.3a). Hierarchical clustering was performed with the antigen profiles (46 positive proteins) (Figure 4.2) to stratify samples on the basis of their cancer infiltrating T-cells and intra-epithelial T-cells.

Differential analysis between metastatic (ACPS C and D) and non-metastatic (ACPS A and B) $EpCAM^+$ cell profiles showed altered expression of 4 surface antigens (Table 4.2b). Comparison of T-cell profiles from metastatic (ACPS C and D) and non-metastatic (ACPS A and B) tumours identified 4 differentially abundant surface antigens (Table 4.3b). Antigen levels for cancer cells and T-cells between normal and high NLR (NLR $\leq$5 and NLR >5).

Table 4.2 Significantly altered surface proteins on EpCAM$^+$ CRC cells compared to EpCAM$^+$ normal mucosal cells as identified by DotScan antibody microarray. Only proteins with 95% confidence interval and >1.5-fold change are shown.

a) Differentially expressed proteins on tumour and normal mucosa cells

Protein	Uniprot ID[a]	Protein family	Function	p-value[b,c]	Fold
Elevated on CRC cells					
CD66c	P40199	Immunoglobulin superfamily	Adhesion	9.29E-07	4.3
HLA-DR	P01903	MHC class II receptor	Immune response	0.025	1.6
CD55	P08174	Receptors of complement activation	Complement regulation	0.049	1.4
CD98	Q01650	L-type amino acid transporter	Amino acid transporter	0.028	1.6
Reduced on CRC cells					
CD9	P21926	Tetraspanin family	Adhesion	6.32E-07	2.8
CD13	P15144	Peptidase M1 family	Aminopeptidase	1.39E-04	2.1
CD15	Carbohydrate	Carbohydrate adhesion molecule	Phagocytosis regulation	0.001	2.2
CD29	P05556	Integrin beta chain	Adhesion	2.50E-05	2.6
CD38	P28907	ADP-ribosyl cyclase	Cyclic ADP-ribose synthesis	1.52E-04	2.5
CD40	P25942	Tumour necrosis factor receptor	Signal transduction	0.039	1.5
CD43	P16150	Glycoprotein	Negative regulator of T-cell activation	0.014	1.5
CD49d	P12612	Integrin alpha chain	Adhesion	4.99E-05	2.0
CD95	P25445	Tumour necrosis factor receptor	Caspase recruiter	3.49E-08	5.3
CD47	Q08722	Immunoglobulin-like protein	Adhesion	1.59E-05	2.1
CD49f	P23229	Integrin alpha chain	Adhesion	3.99E-06	2.3
CD59	P13987	Glycoprotein	Complement inhibitor	0.015	1.6
CD63	P08962	Tetraspanin family	Cellular protein localisation	1.44E-08	2.6
CD66e (CEA)	P06731	Immunoglobulin superfamily	Adhesion	0.005	1.8
CD104	P16144	Integrin beta chain	Adhesion	9.03E-07	2.8
CD151	P48509	Tetraspanin family	Adhesion	5.07E-07	3.5
CD324	P12830	Cadherin family	Adhesion	0.045	1.5
CD326	P16422	Cadherin family	Adhesion	9.18E-07	2.6
Claudin-4	O14493	Claudin family	Structural	9.82E-04	2.0
HLA-ABC	Multiple proteins	MHC class I receptor	Immune response	3.74E-06	2.5

b) Differentially expressed proteins on non-metastatic and metastatic CRC cells

Protein	Uniprot ID[a]	Protein family	Function	p-value[b,c]	Fold
Elevated on metastatic CRC					
CD13	P15144	Peptidase M1 family	Aminopeptidase	0.03	1.8
CD66c	P40199	Immunoglobulin superfamily	Adhesion	0.02	2.2
CD26	P27487	Peptidase S9B family	T-cell activation	0.02	2.0
Reduced on metastatic CRC					
HLA-DR		MHC class II receptor	Immune response	0.002	2.3

CD Cluster of differentiation
HLA Human leukocyte antigen
CEA Carcinoembryonic antigen

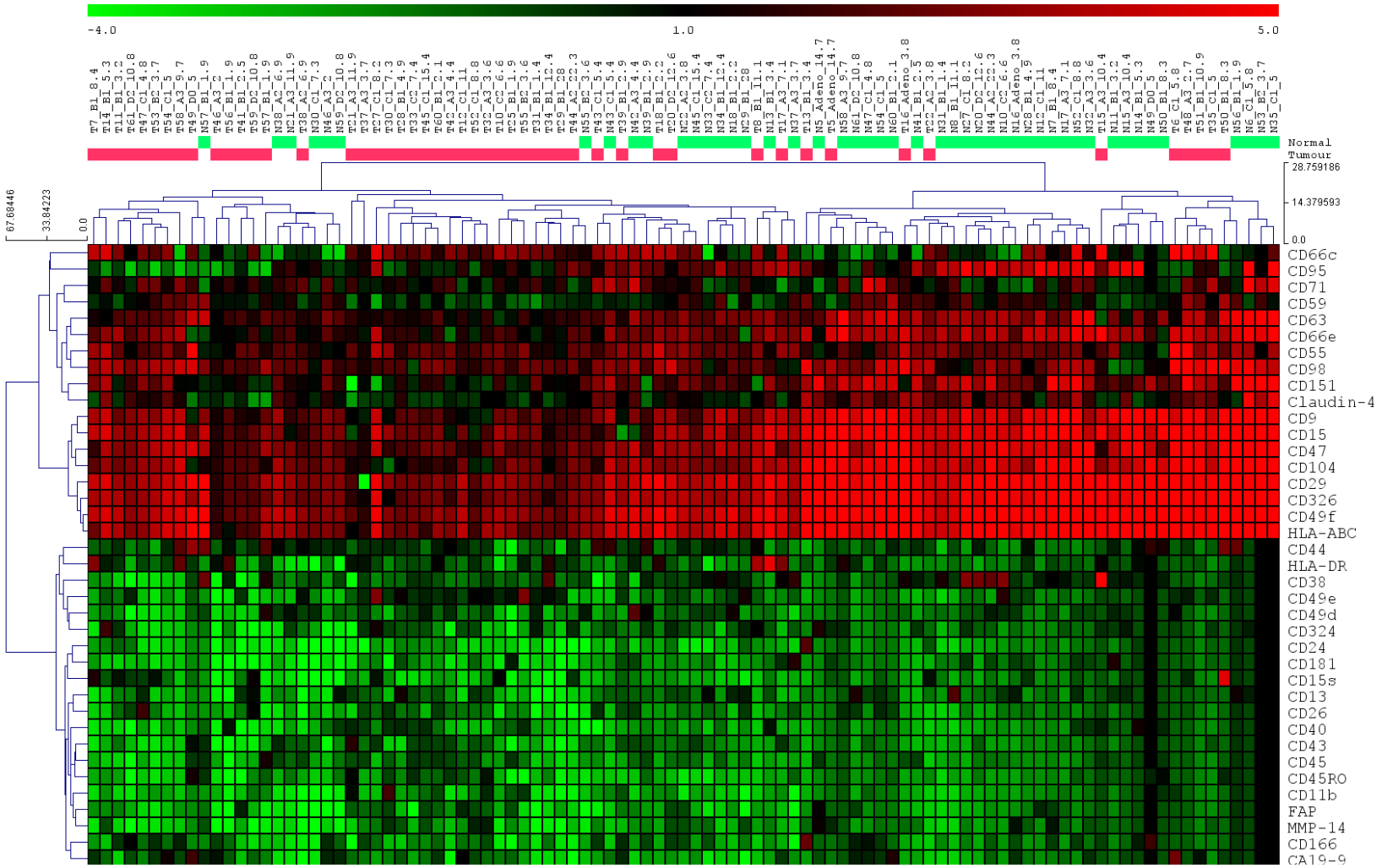

Figure 4.1 Hierarchical clustering of the EpCAM positive cell profiles from 97 CRC and normal samples. Each sample is identified with tumour (T) or normal (N), the Australian clinico-pathological stage (A – D) and the neutrophil to lymphocyte ratio (2 – 28). Hierarchical clustering (Euclidean distance, complete linkage) was conducted on the antigen profiles (38 positive proteins).

Table 4.3 Summary of significantly altered surface proteins on $CD3^+$ tumour infiltrating T-cells compared to normal intestinal intra-epithelial T-cells identified with DotScan antibody microarrays. Only proteins with 95% confidence interval and >1.5-fold change are listed.

a) Differential expressed proteins on T-cells from tumour and normal tissue					
Protein	Uniprot ID[a]	Protein family	Function	P-value[b,c]	Fold
Up-regulated on tumour infiltrating T-cells					
CD11c	P20702	Integrin alpha chain	Adhesion	0.023	1.8
CD49e	P08648	Integrin alpha chain	Adhesion	6.00E-05	2.5
CD66c	P40199	Immunoglobulin superfamily	Adhesion	0.004	2.2
CD71	P02786	Peptidase M28 family	Transferrin receptor activity	1.42E-09	5.4
CD86	P42081	Immunoglobulin-like protein	Stimulate T-cell proliferation	0.002	1.9
HLA-DR		MHC class II receptor	Immune response	6.98E-07	4.2
Down-regulated on tumour infiltrating T-cells					
CD2	P06729	Immunoglobulin-like protein	Adhesion	0.018	1.5
CD3	P09693	Immunoglobulin-like protein	Signal transduction	0.004	1.8
CD7	P09564	Immunoglobulin-like protein	T-cell activation	0.012	1.5
CD9	P21926	Tetraspanin family	Adhesion	5.93E-05	2.9
CD11a	P20701	Integrin alpha chain	Adhesion	0.001	1.5
CD29	P05556	Integrin beta chain	Adhesion	0.001	1.7
CD31	P16284	Immunoglobulin-like protein	Adhesion	0.006	1.8
CD38	P28907	ADP-ribosyl cyclase	Cyclic ADP-ribose synthesis	0.009	1.6
CD43	P16150	Glycoprotein	T-cell costimulation	1.06E-05	1.9
CD44	P16070	1 link domain protein	Adhesion	0.002	1.6
CD45	P08575	Protein-tyrosine phosphatase family	Leukocyte differentiation/proliferation	0.001	1.5
CD49d	P13612	Integrin alpha chain	Adhesion	0.004	1.5
CD103	P38570	Integrin alpha chain	Adhesion	3.58E-05	2.7
CD47	Q08722	Immunoglobulin-like protein	Adhesion	0.001	1.6
CD55	P08174	Receptors of complement activation	Complement regulation	0.006	1.5
CD63	P08962	Tetraspanin family	Cellular protein localisation	4.82E-04	1.9
CD151	P48509	Tetraspanin family	Adhesion	0.048	1.5
HLA-ABC		MHC class I receptor	Immune response	0.001	1.7

b) Differentially expressed proteins on T-cells from non-metastatic and metastatic CRC

Protein	Uniprot ID[a]	Protein family	Function	P-value[b,c]	Fold
Up-regulated in metastatic CRC					
CD26	P27487	Peptidase S9B family	T-cell activation	0.004	1.6
CD151	P48509	Tetraspanin family	Adhesion	3.45E-04	1.8
Down-regulated in metastatic CRC					
CD11c	P20702	Integrin alpha chain	Adhesion	0.029	1.9
CD31	P16284	Immunoglobulin-like protein	Adhesion	0.032	1.8

CD Cluster of differentiation
HLA Human leukocyte antigen
CEA Carcinoembryronic antigen

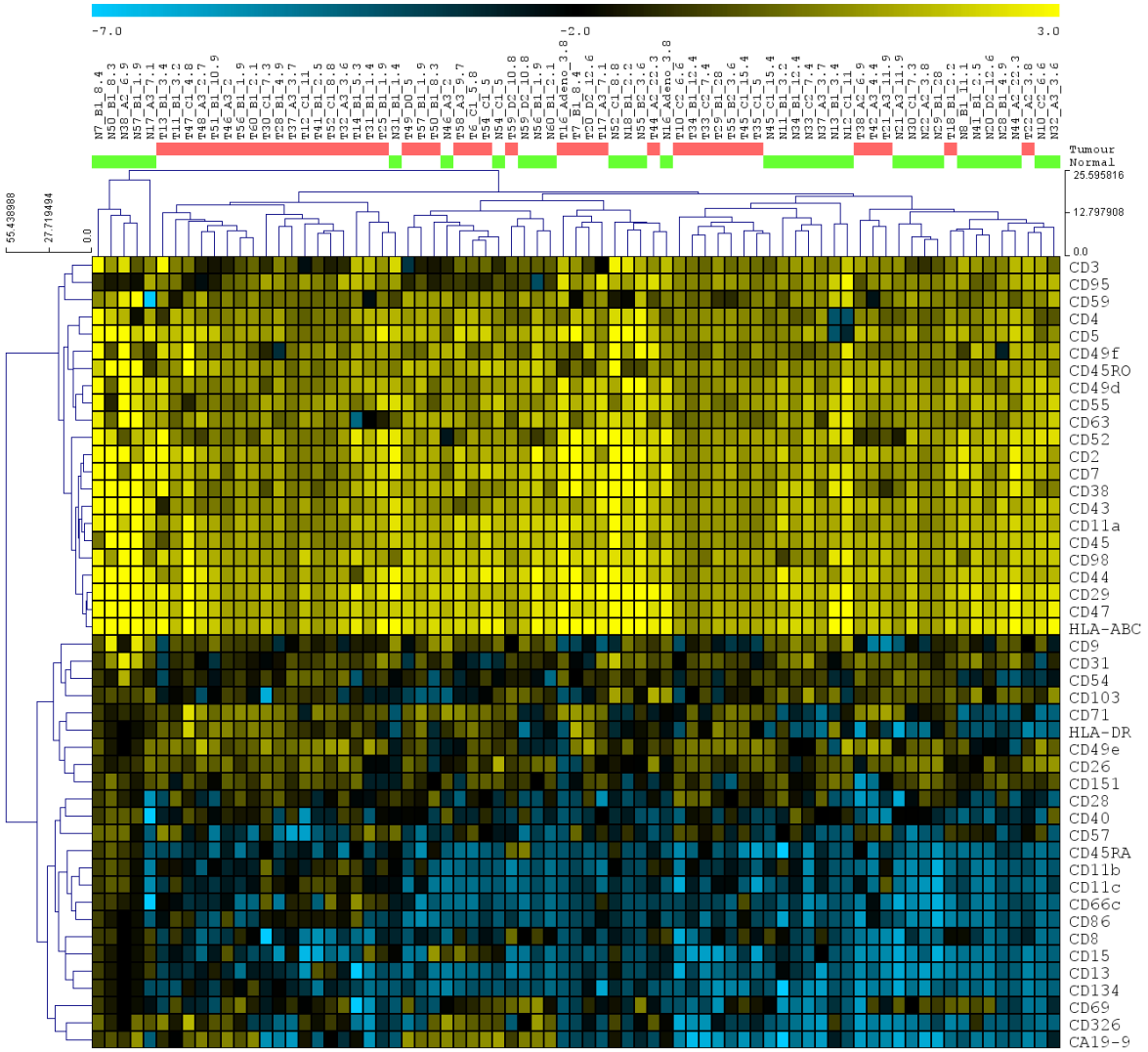

Figure 4.2 Hierarchical clustering of the CD3 positive cell profiles from 75 tumour and normal samples. Each sample is identified as tumour (T) or normal (N), the Australian clinico-pathological stage (A – D) and the neutrophil to lymphocyte ratio (2 – 28). Hierarchical clustering (Euclidean distance, complete linkage) was conducted on antigen profiles (46 positive proteins).

4.2.2 Hierarchical clustering

Hierarchical clustering (Euclidean distance, complete linkage) was used to identify pattern similarity. Unsupervised hierarchical clustering of the $EpCAM^+$ CRC profiles produced a dendrogram with 4 well-defined clusters (Figure 4.3). The clinico-pathological properties of each cluster is summarised in Table 4.4. Differentially expressed proteins were identified between related clusters generated from the split. The first split generated 2 clusters; cluster 1 (blue) and cluster 2 (green) consisted of 11 and 39 profiles, respectively. Proteins (15) were reduced in cluster 2 compared to cluster 1 (Table 4.5a). Further down the hierarchy, cluster 2 was split into clusters 3 (red) and 4 (yellow), consisting of 22 and 17 profiles, respectively. Comparison of cluster 3 with cluster 4 showed reduced binding levels for 13 proteins, and increased levels for 2 (Table 4.5b). The clinico-pathological information showed that CRC cluster 1 contained the lowest number of metastatic tumours (18%) compared with clusters 3 and 4 (32%, 35% respectively). Cluster 1 was associated with only well, and moderately, differentiated tumours, while clusters 2, 3 and 4 contained moderate and poorly differentiated tumours (Table 4.4).

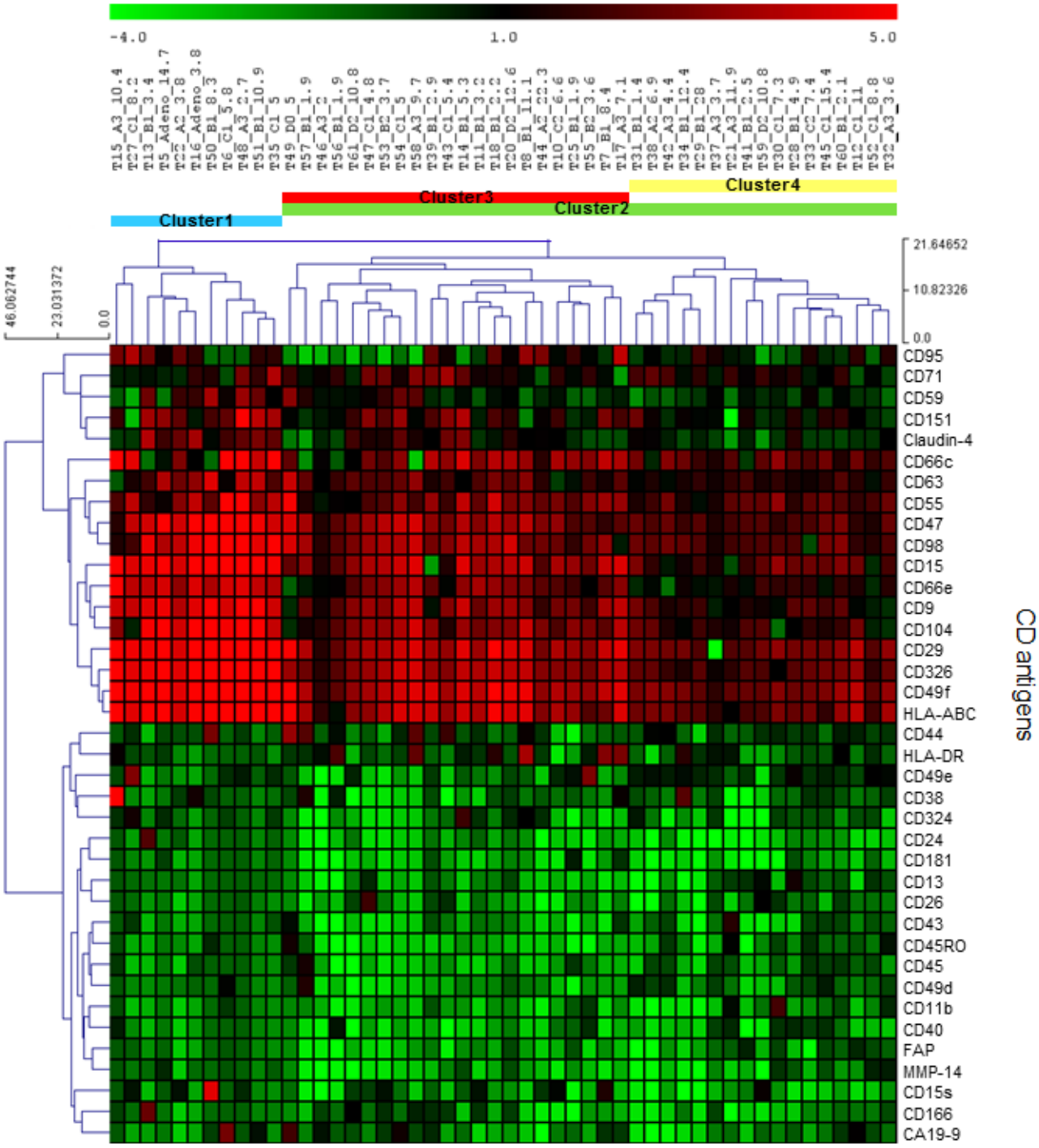

Figure 4.3 Hierarchical clustering of the EpCAM^{+} cell profiles from 50 CRC samples. Each sample is labelled with the Tumour ID (T#), Australian clinico-pathological stage (A – D) and the neutrophil to lymphocyte ratio (2 – 28). Hierarchical clustering (Euclidean distance, complete linkage) split the profiles into 4 clusters (Cluster groups 1 – 4).

Table 4.4 Patient clinico-pathological and haematological characteristics within $EpCAM^+$ CRC cell clusters.

	Cluster 1 (n=11)	Cluster 2 (n=39)	Cluster 3 (n=22)	Cluster 4 (n=17)
			No. patients (%)	
Gender				
Male	6 (55%)	18 (46%)	9 (41%)	9 (53%)
Female	5 (45%)	21 (54%)	13 (59%)	8 (47%)
Age				
≤ 65	3 (27%)	16 (41%)	8 (36%)	8 (47%)
> 65	8 (73%)	23 (59%)	14 (64%)	9 (53%)
Location				
Left (caecum, ascending colon, transverse)	5 (45%)	16 (41%)	10 (45%)	6 (35%)
Right (descending colon, sigmoid, rectum)	6 (55%)	23 (59%)	12 (55%)	11 (65%)
Australian clinico-pathological stage (ACPS)				
Adenoma	2 (19%)	0 (0%)	0 (0%)	0 (0%)
A	3 (27%)	9 (23%)	4 (18%)	5 (29%)
B	3 (27%)	17 (44%)	11 (50%)	6 (36%)
C	3 (27%)	9 (23%)	4 (18%)	5 (29%)
D	0 (0%)	4 (10%)	3 (14%)	1 (6%)
Infiltration				
Submucosa	3 (28%)	3 (8%)	2 (9%)	1 (6%)
Muscularis propria	4 (36%)	8 (21%)	4 (18%)	4 (24%)
Subserosa	4 (36%)	22 (56%)	13 (58%)	9 (53%)
Serosa	0 (0%)	6 (15%)	3 (14%)	3 (18%)
Differentiation				
Adenoma	2 (18%)	0 (0%)	0 (0%)	0 (0%)
Well	2 (18%)	0 (0%)	0 (0%)	0 (0%)
Moderate	7 (64%)	33 (85%)	20 (91%)	13 (76%)
Poor	0 (0%)	6 (15%)	2 (9%)	4 (24%)
Peri-tumoural inflammation				
Present	5 (45%)	16 (41%)	10 (45%)	6 (35%)
Absent	6 (55%)	23 (59%)	12 (55%)	11 (65%)
Tumour infiltrating lymphocytes (TIL)				
Present	1 (9%)	4 (10%)	2 (9%)	2 (12%)
Absent	10 (91%)	35 (90%)	20 (91%)	15 (88%)
Circulating lymphocytes count				
$< 1 \times 10^9$/L (low)	4 (36%)	12 (31%)	7 (32%)	5 (29%)
$1.0\text{-}3.0 \times 10^9$/L (normal)	7 (64%)	27 (69%)	15 (68%)	12 (71%)
Circulating neutrophil to lymphocyte ratio (NLR)				
≤ 5	4 (36%)	17 (44%)	10 (45%)	7 (41%)
> 5	7 (64%)	22 (56%)	12 (55%)	10 (59%)

Table 4.5 Significantly altered surface proteins between clusters of EpCAM$^+$ CRC cells. Only proteins with 95% confidence interval and over 1.5-fold change are listed.

a) Cluster 1 versus 2

Protein	Uniprot ID[a]	Protein family	Function	p-value[b,c]	Fold
Reduced on cluster 2 CRC cells					
CD9	P21926	Tetraspanin family	Adhesion	1.72E-11	5.1
CD13	P15144	Peptidase M1 family	Aminopeptidase	0.0074	1.7
CD15 (Lewis x)	Carbohydrate	Carbohydrate adhesion molecule	Adhesion	5.85E-10	6.8
CD24	P25063	CD24 family	Leukocyte signal transducer	3.12E-04	3.7
CD29	P05556	Integrin beta chain	Adhesion	2.31E-08	5.5
CD43	P16150	Glycoprotein	Negative regulator of T-cell activation	0.045	1.7
CD95	P25445	Tumour necrosis factor receptor	Caspase recruiter	0.045	2.4
CD181	P25024	G-protein coupled receptor 1	Neutrophil activator	7.34E-05	2.6
CD15s (Sialyl Lewis x)	Carbohydrate	Carbohydrate adhesion molecule	Adhesion	0.028	3.1
CD47	Q08722	Immunoglobulin-like protein	Adhesion	3.28E-04	3.4
CD49f	P23229	Integrin alpha chain	Adhesion	9.18E-08	4.8
CD66e (CEA)	P06731	Immunoglobulin superfamily	Adhesion	3.03E-10	5.5
CD104	P16144	Integrin beta chain	Adhesion	9.86E-04	4.4
CD324	P12830	Cadherin family	Adhesion	0.006	2.3
CD326 (EpCAM)	P16422	Cadherin family	Adhesion	2.15E-10	5.6
CD98	Q01650	L-type amino acid transporter	Amino acid transporter	0.004	3.3
Claudin-4	O14493	Claudin family	Structural	0.002	3.1
FAP	Q12884	Peptidase S9B family	Proteolysis	0.029	1.6
HLA-ABC	MHC family	MHC class I receptor	Immune response	1.07E-07	5.5
MMP-14	P50281	Peptidase M10A family	Endopeptidase	1.87E-04	2.6

b) Cluster 3 versus cluster 4					
Protein	Uniprot ID[a]	Protein family	Function	p-value[b,c]	Fold
Elevated on cluster 4 CRC cells					
CD49d	P12612	Integrin alpha chain	Adhesion	0.008534	2.1
CD49e	P08648	Integrin alpha chain	Adhesion	0.001013	3.0
Reduced on cluster 4 CRC cells					
CD9	P21926	Tetraspanin family	Adhesion	1.89E-04	2.4
CD15	Carbohydrate	Carbohydrate adhesion molecule	Phagocytosis regulation	0.006341	2.3
CD29	P05556	Integrin beta chain	Adhesion	0.017996	2.7
CD15s (Sialyl Lewis x)	Carbohydrate	Carbohydrate adhesion molecule	Adhesion	0.074097	2.1
CD47	Q08722	Immunoglobulin-like protein	Adhesion	4.25E-04	2.0
CD49f	P23229	Integrin alpha chain	Adhesion	4.77E-04	2.1
CD59	P13987	Glycoprotein	Complement inhibitor	0.033409	1.8
CD63	P08962	Tetraspanin family	Cellular protein localisation	0.049951	1.5
CD66e (CEA)	P06731	Immunoglobulin superfamily	Adhesion	0.004495	2.3
CD104	P16144	Integrin beta chain	Adhesion	0.00273	2.5
CD151	P48509	Tetraspanin family	Adhesion	0.101945	2.0
CD326 (EpCAM)	P16422	Cadherin family	Adhesion	1.07E-04	2.3
CD98	Q01650	L-type amino acid transporter	Amino acid transporter	0.00697	2.0
HLA-ABC	MHC family	MHC class I receptor	Immune response	0.005437	2.1

CD Cluster of differentiation
HLA Human leukocyte antigen
CEA Carcinoembryronic antigen
EpCAM Epithelial cell adhesion molecule

Unsupervised hierarchical clustering was applied to the tumour infiltrating T-cell profiles. This produced a dendrogram with 4 well-defined clusters (Figure 4.4). The clinico-pathological properties of each cluster are summarised in Table 4.6. Differentially expressed proteins were identified between related clusters generated from the split. The first split generated cluster 1 (blue) and cluster 2 (green) consisting of 14 and 28 profiles, respectively. Compared to cluster 1, cluster 2 showed elevated levels of 11 antigens and reduction of 6 antigens (Table 4.7a). Further down the hierarchy, cluster 2 was split into clusters 3 (red) and 4 (yellow), consisting of 15 and 13 profiles, respectively. Proteins (13) were reduced and 5 elevated in cluster 3 compared to cluster 4 (Table 4.7b). The clinico-pathological information showed that within each cluster the number of metastatic tumours inversely correlated with observable peri-tumoural inflammation (Table 4.6). T-cell cluster 3 contained the largest number of metastatic tumours but also the least number of CRCs with peri-tumoural inflammation (47% and 27%), followed by T-cell cluster 4 (31% and 54%) and cluster 1 (14% and 57%).

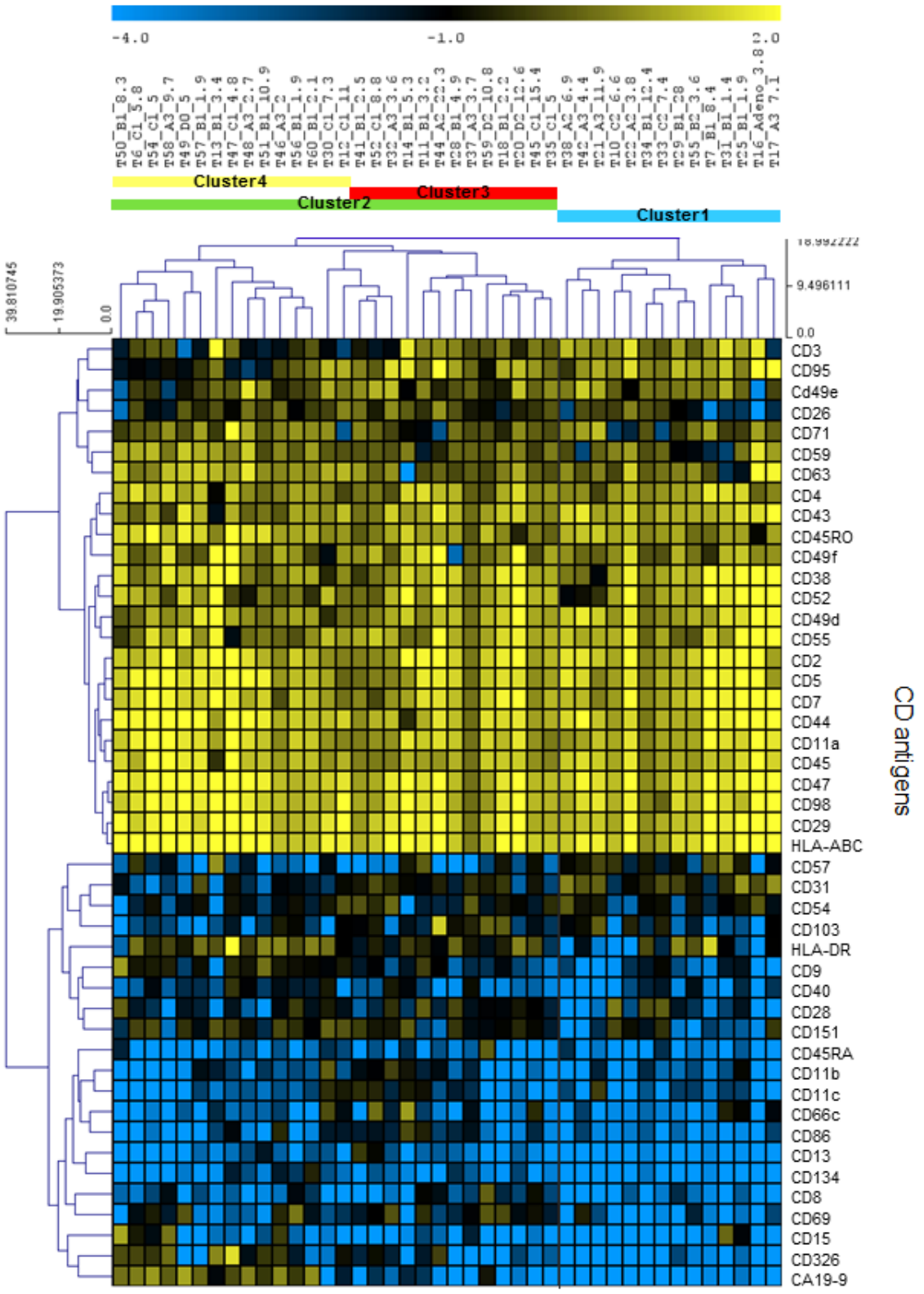

Figure 4.4 Hierarchical clustering of the $CD3^+$ cell profiles from 42 CRC samples. Each sample is labelled with the Tumour ID (T#), Australian clinico-pathological stage (A – D) and the neutrophil to lymphocyte ratio (2 – 28). Hierarchical clustering (Euclidean distance, complete linkage) split the profiles into 4 clusters (cluster groups 1 – 4).

Table 4.6 Patient clinico-pathological and haematological characteristics within $CD3^+$ T-cell clusters.

	Cluster 1 (n=14)	Cluster 2 (n=28)	Cluster 3 (n=15)	Cluster 4 (n=13)
			No. patients (%)	
Gender				
Male	5 (36%)	17 (61%)	11 (73%)	6 (46%)
Female	9 (64%)	11 (39%)	4 (27%)	7 (54%)
Age				
≤ 65	6 (43%)	10 (36%)	4 (27%)	6 (46%)
> 65	8 (57%)	18 (64%)	11 (73%)	7 (54%)
Location				
Left (caecum, ascending colon, transverse)	7 (50%)	11 (39%)	6 (40%)	5 (38%)
Right (descending colon, sigmoid, rectum)	7 (50%)	17 (61%)	9 (60%)	8 (62%)
Australian clinico-pathological stage (ACPS)				
Adenoma	1 (7%)	0 (0%)	0 (0%)	0 (0%)
A	5 (36%)	6 (21%)	3 (20%)	3 (23%)
B	6 (43%)	11 (39%)	5 (33%)	6 (46%)
C	2 (14%)	8 (29%)	5 (33%)	3 (23%)
D	0 (0%)	3 (11%)	2 (14%)	1 (8%)
Infiltration				
Submucosa	4 (29%)	1 (4%)	1 (7%)	0 (0%)
Muscularis propria	3 (21%)	7 (25%)	2 (13%)	5 (38%)
Subserosa	5 (36%)	16 (57%)	9 (60%)	7 (54%)
Serosa	2 (14%)	4 (14%)	3 (20%)	1 (8%)
Differentiation				
Adenoma	1 (7%)	0 (0%)	0 (0%)	0 (0%)
Well	0 (0%)	2 (7%)	0 (0%)	2 (15%)
Moderate	11 (79%)	22 (79%)	12 (80%)	10 (77%)
Poor	2 (14%)	4 (14%)	3 (20%)	1 (8%)
Peri-tumoural inflammation				
Present	8 (57%)	11 (39%)	4 (27%)	7 (54%)
Absent	6 (43%)	17 (61%)	11 (73%)	6 (46%)
Tumour infiltrating lymphocytes (TIL)				
Present	2 (14%)	3 (11%)	1 (7%)	2 (15%)
Absent	12 (86%)	25 (89%)	14 (93%)	11 (85%)
Circulating lymphocytes count				
$< 1 \times 10^9$/L (low)	4 (29%)	9 (32%)	6 (40%)	3 (23%)
$1.0\text{-}3.0 \times 10^9$/L (normal)	10 (71%)	19 (68%)	9 (60%)	10 (77%)
Circulating neutrophil to lymphocyte ratio (NLR)				
≤ 5	6 (43%)	13 (46%)	6 (40%)	7 (54%)
> 5	8 (57%)	15 (54%)	9 (60%)	6 (46%)

Table 4.7 Significantly altered surface proteins between clusters of $CD3^+$ tumour cells. Only proteins with 95% confidence interval and over 1.5-fold change are listed.

a) Cluster 1 versus 2

Protein	Uniprot ID[a]	Protein family	Function	p-value[b,c]	Fold
Elevated on cluster 2 CRC cells					
CD8	P10966	Immunoglobulin-like protein	Cytoxic/ immune suppressor	0.017	2.2
CD9	P21926	Tretraspanin family	Adhesion	0.001	3.1
CD13	P15144	Peptidase M1 family	Aminopeptidase	0.008	2.0
CD86	P42081	Immunoglobulin-like protein	T-lymphocyte activation	0.028	1.9
CD134	P43489	Tumour necrosis factor receptor	Lymphocyte proliferation and immune response	1.37E-05	2.9
HLA-DR	P01903	MHC class II receptor	Immune response	0.018	3.2
CD26	P27487	Peptidase S9B family	T-cell activation	0.037	1.9
CD69	Q07108	C-type lectin domain	Lymphocyte proliferation	9.30E-04	3.9
CD151	P48509	Tretraspanin family	Adhesion	0.006	3.0
CD326 (EpCAM)	P16422	Cadherin family	Adhesion	4.32E-06	6.1
CA19-9 (Siglylated Lewis a)	Carbohydrate	Carbohydrate adhesion molecule	Adhesion	1.49E-07	9.5
Reduced on cluster 2 CRC cells					
CD3	P09693	Immunoglobulin-like protein	Signal transduction	0.004681	2.1
CD31	P16284	Immunoglobulin-like protein	Adhesion	7.83E-04	2.3
CD43	P16150	Glycoprotein	T-cell costimulation	0.002468	1.5
CD49d	P13612	Integrin alpha chain	Adhesion	0.031068	1.5
CD57	Q9P2W7	Glycosyltransferase 43 family	Carbohydrate metabolism	7.81E-04	3.3
CD95	P25445	Tumour necrosis factor receptor	Caspase recruiter	0.002533	2.0

b) Cluster 3 versus 4

Protein	Uniprot ID[a]	Protein family	Function	p-value[b,c]	Fold change
Elevated on cluster 4 CRC cells					
CD5				9.86E-04	1.7
CD9	P21926	Tetraspanin family	Adhesion	0.037	1.9
CD11a	P20701	Integrin alpha chain	Adhesion	0.007	1.5
CD15	Carbohydrate	Carbohydrate adhesion molecule	Phagocytosis regulation	0.007	4.0
CD44	P16070	1 link domain protein	Adhesion	0.002	1.8
CD45	P08575	Protein-tyrosine phosphatase family	Leukocyte differentiation	0.026	1.5
CD45RO	P08575	Protein-tyrosine phosphatase	T-cell activation	3.82E-04	1.8
CD71	P02786	Peptidase M28 family	Transferrin receptor activity	0.013	1.9
CD47	Q08722	Immunoglobulin-like protein	Adhesion	0.023	1.5
CD59	P13987	Glycoprotein	Complement inhibitor	3.79E-04	1.7
CD63	P08962	Tetraspanin family	Cellular protein localisation	0.023	1.9
CD326 (EpCAM)	P16422	Cadherin family	Adhesion	0.019	3.3
CA19-9 (Siglylated Lewis a)	Carbohydrate	Carbohydrate adhesion molecule	Adhesion	2.09E-07	14.0
Reduced on cluster 4 CRC cells					
CD11c	P20702	Integrin alpha chain	Adhesion	0.024	2.5
CD31	P16284	Immunoglobulin-like protein	Adhesion	0.018	2.0
CD66c	P40199	Immunoglobulin superfamily	Adhesion	0.036	2.6
CD86	P42081	Immunoglobulin-like protein	Stimulate T-cell proliferation	0.009	2.9
CD95	P25445	Tumour necrosis factor receptor	Caspase recruiter	1.68E-05	3.2

CD Cluster of differentiation
HLA Human leukocyte antigen
CEA Carcinoembryonic antigen
EpCAM Epithelial cell adhesion molecule

4.2.3 Correlation between CRC cell profiles and T-cell profiles

There was an association between the EpCAM^{+} CRC profiles and those for the CD3^{+} T-cells from the same samples (Figure 4.5). T-cells in cluster 1 tended to associate with cancer cells from clusters 3 and 4 (29% and 41%); T-cells with the profile of cluster 3 were associated with CRC cells from clusters 3 and 4 (29% and 53%); T-cells of cluster 4 were predominantly associated with cancer cells from clusters 1 and 3 (63% and 41%).

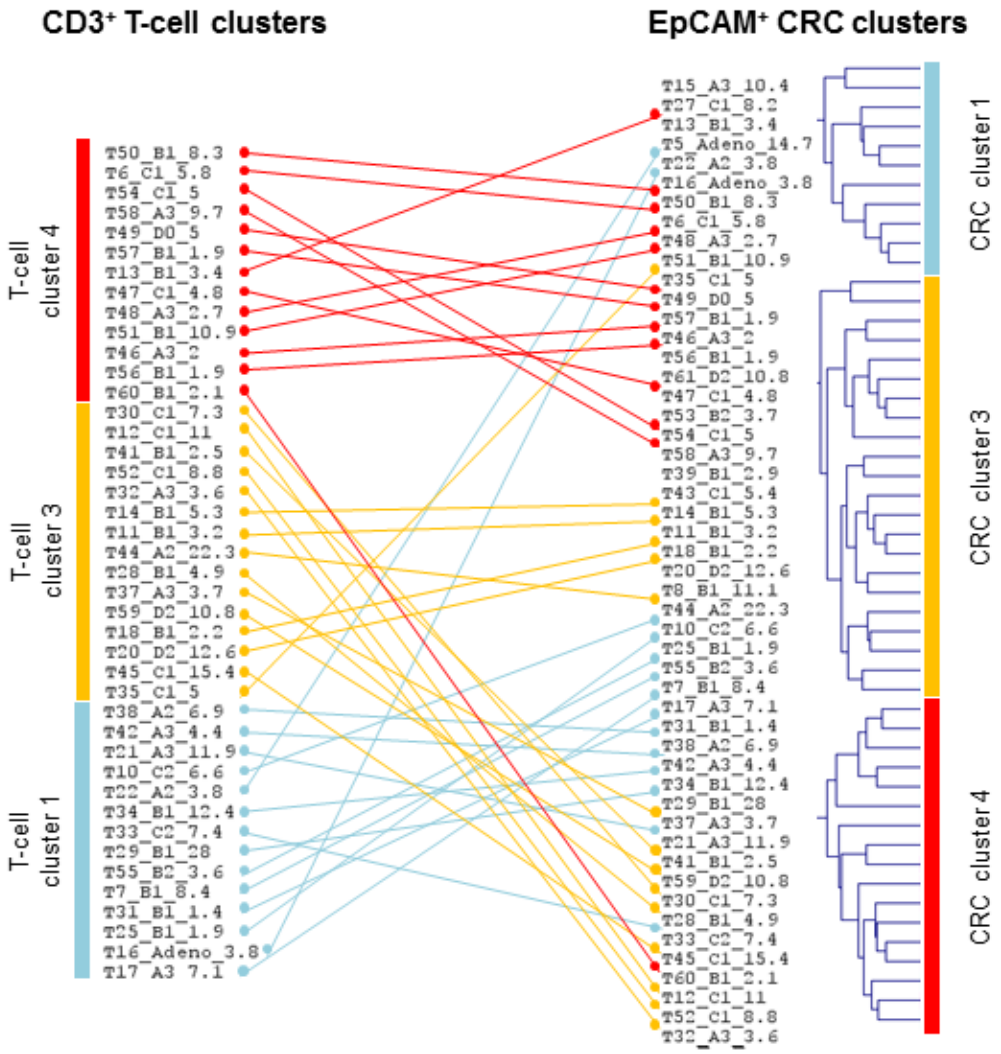

Figure 4.5 Association between CD3^{+} tumour-associated T-cell profiles and EpCAM^{+} cancer cell profiles. The coloured bars represent individual clusters of each cell type. The coloured lines connect clustering positions for each patient on the basis of CD3^{+} and EpCAM^{+} binding patterns. The line colour is based on the colour of the corresponding CD3^{+} clusters.

4.3 Discussion

We used a cell capture microarray (DotScan) in conjunction with fluorescence multiplexing (Zhou et al., 2010), to simultaneously profile surface antigen expression on $EpCAM^+$ CRC cells and $CD3^+$ T-cells from 97 CRC tumours and normal intestinal mucosa samples resected from 50 patients. The original DotScan microarray was designed to allow for the investigation of surface markers on leukocytes (Belov et al., 2003) and included markers which distinguish between various types of leukocytes (T-cells, B-cells, myeloid cells) as well as receptors and adhesion molecules. An additional 40 CRC markers were identified and selected through literature searches for CRC cell profiling on the DotScan antibody microarray (Zhou et al., 2010, Belov et al., 2010). The antibody selection on DotScan allowed us to profile the tumour associated leukocyte population along with the CRC cells. The $CD3^+$ T-cell population was found to be the most consistently detectable leukocyte population in our CRC samples.

To maintain the optimal number of viable cells (>70%) and the most accurate representation of surface antigen levels, the clinical samples were collected and immunophenotyped within 24 hours of surgical resection. As a result of this narrow time frame, we were only able to obtain the corresponding clinico-pathological information a week after the tumours were profiled. Hence the sample selection was unbiased and reflected the most frequently diagnosed stages of CRC (80% of the samples were moderately differentiated ACPS A3, B1 or C1). Patients with these intermediate stage CRCs benefit the least from traditional clinico-pathological staging, largely due to molecular heterogeneity within these tumours. Modern clinico-pathological is proficient for predicting the outcomes for very good and very poor prognosis patients (ACPS A and D), but not for predicting the long-term outcomes of intermediate prognosis patients (ACPS B and C) (Eschrich et al., 2005). There are limited

clinico-pathological discriminatory factors for intermediate stage CRCs, where the tumour has infiltrated the muscularis propria, but is restricted to local lymph node metastasis, making it difficult to determine which patients would benefit from further therapy. It is current practice to offer chemotherapy to all ACPS C patients but not all B stage patients. Although the majority of ACPS A and B patient will be cured by surgery alone, some patients would benefit from further therapy. In addition, at least one third of ACPS C patients are cured by surgery and, therefore, undergo unnecessary, and potentially debilitating, further treatment (Durrant et al., 2003).

Molecular profiling of cell surface antigens may provide a more accurate representation of cancer progression in intermediate stage tumours hence providing additional information for improved post-operative treatment and outcomes. Antibodies against 122 cells surface markers have been included on the antibody microarray to immunophenotype two sub-populations of cells derived from primary CRC patients. We were first able to cluster groups of cell profiles derived from CRC and normal mucosal tissue (Figures 4.1 and 4.2), validating the selection of $EpCAM^+$ and $CD3^+$ profiles. Subsequently, an unsupervised hierarchical clustering of $EpCAM^+$ CRC cell profiles identified 3 immunophenotypically distinct groups of CRC cells within clinico-pathologically indistinguishable tumours (Figure 4.3).

We also observed similarly distinct immunophenotypes in the tumour-infiltrating T-cells population (Figure 4.4). A strong correlation was observed between the cancer cell profiles and the surface profiles of tumour infiltrating T-cells found around them (Figure 4.5), suggesting strong mutual influences between tumour cells and immune cells within the microenvironment. T-cells with high levels of activation (e.g. HLA-DR and CD71) and proliferation markers (e.g. CD5, CD47 and CD59) were found in tumours with CRC cell

immunophenotypes associated with reduced invasiveness and well differentiated cells. T-cells exhibiting low levels of activation markers were indicating tumours with immunophenotypes associated with poorer prognosis and higher metastatic potential. The immunophenotyping of CRC cells and tumour infiltrating T-lymphocytes was highly effective in stratifying clinico-pathologically similar CRCs. Our results for the sub-stratification of intermediate stage CRC patients on the basis of their cancer cell and T-cell surface expression profiles indicated that the DotScan antibody microarray approach may provide important additional prognostic and predictive information for this group of patients, enabling the identification of patients requiring further therapy after surgery. However, this application cannot be validated until the 5-year patient outcome information becomes available for analysis against the DotScan profiles.

4.3.1 $EpCAM^+$ CRC cell profile

Twenty-four proteins showed altered expression between CRC and normal mucosa (Table 4.2a). The largest group of tumour markers showing reduced expression on CRC cells belonged to the adhesion molecule family. Down-regulation of these antigens confers upon CRC cells the ability to evade contact inhibition mediated through tight adhesion to neighbouring cells and promotes proliferation through loss of cell-cell and cell-matrix adhesion (Nigam et al., 1993).

Adhesion molecules are classified into 4 groups according to their biochemical structures: integrins, immunoglobulin-like proteins, cadherins and selectins (Menger and Vollmar, 1996). Three of these groups showed reduced expression on CRC cells compared to normal intestinal mucosa cells (Table 4.2a): integrin subunits (CD49d, CD49f, CD29 and CD104), cadherin, (CD324) and immunoglobulin-like proteins (CD66e, CD47 and HLA-ABC). In

addition CD15, a member of the group of cell adhesion molecules that bind to selectin, was also reduced. Another family of proteins essential to the regulation of cell-cell interactions is the claudin family. Claudins play a key role in the construction of tight junctions, and reduced claudin-4 expression has been observed in many human malignancies (Ueda et al., 2007), including the CRC cell surface observed here.

The integrin family of cell adhesion proteins controls cell attachment to the ECM (Jin and Varner, 2004). Decreased CD29, CD49f and CD104 has been reported in CRC (Jin and Varner, 2004). Although reduced CD49d has been associated with invasion and metastasis in endometrial cancer and melanoma (Lessey et al., 1995, Qian et al., 1994), it has not previously been reported for CRC.

Cadherins are responsible for cell-cell adhesion in epithelial tissues (Dorudi et al., 1993). Loss of CD324 (E-cadherin) has been associated with poorly differentiated CRC (Nigam et al., 1993), and CD324 is also reported to exhibit a gradual loss during CRC progression from adenoma to high grade carcinoma (van der Wurff et al., 1992).

The immunoglobulin family protein CD66e (CEA) was found reduced on the surface of CRC cells (Table 4.2). In contrast, analysis of CRC whole cell lysates revealed elevated levels of cytoplasmic CD66e (Chapter 3: Table 3.2). This has been previously reported by in poorly differentiated CRC (Goldstein and Mitchell, 2005). The low surface expression of CEA may result from shedding of antigen from the cell surface into the circulation, which has been associated with higher vascular invasion in late stage CRC patients (Ng et al., 1993). Although found in the same family as CD66e, CD66c was found to be over-expressed on all tumour samples, and increased with CRC progression (Table 4.2a and 4.2b). In a previous study, CD66c up-regulation in colon carcinomas was also found to correlate inversely with

the degree of cellular differentiation and overall survival (Jantscheff et al., 2003). Well differentiated cancers are associated with better patient prognosis (Jass et al., 1986).

Another immunoglobulin protein, CD47, was found at lower levels in CRC cells compared to normal mucosa. CD47 functions as a "don't eat me" signal that ensures autologous cells are not inappropriately phagocytosed. Tumour cells often display signs of cellular "damage" and/or glycosidic variations on their cell surface, and these markers of "stressed self" may induce a reduction in CD47 expression and consequent recognition by natural killer (NK) cells. Although not observed in this study, some tumour cells have been reported to over-express CD47 as a general mechanism to evade phagocytosis (Willingham et al., 2012). The cause of decreased CD47 expression on tumour cells is unknown, but may be an attempt to initiate phagocytosis of neoplastic cells.

Several members of the immunoglobulin superfamily are involved in T-cell mediated responses that are antigen presenting molecules: the MHC class I receptor (including HLA-ABC) and MHC class II receptor (including HLA-DR). The expression of HLA-ABC on tumour cells is essential for cytotoxic T-cell mediated responses and important for constraining tumour growth (Zinkernagel and Doherty, 1979). Consistent with its function, we found HLA-ABC was lower on tumour cells than normal cells. Down-regulated HLA-ABC has been correlated with worse clinical outcomes and lower grade of differentiation in CRC (Cordon-Cardo et al., 1991, Garrido et al., 1993).

We found HLA-DR to be elevated on CRC cells compared to normal cells, a trend consistent with previous studies (Diederichsen et al., 2003, Matsushita et al., 2006). In addition we found HLA-DR to be elevated on early stage CRC (Table 4.2b). The prognostic significance of HLA-DR levels remains debatable, as antigen-presenting cells found in CRC often lack

co-stimulatory signals, CD80 and CD86 (Schwartz, 1990), thus the interaction between HLA-DR positive tumour cells and lymphocytes would give rise to anergy.

In addition to adhesion molecules, several other surface molecules were found differentially expressed on $EpCAM^+$ tumour and normal cells as discussed below. Epithelial cells express a variety of surface proteins that regulate cell fate. Two mediators of cell death, CD40 and CD95, were reduced on CRC cells, and the complement cofactor protein CD59 was also decreased, while the decay accelerating factor CD55 increased (Table 4.2a). The down-regulation of CD40 and CD95, both members of the tumour necrosis factor family, has been documented in CRC (Georgopoulos et al., 2007, Moller et al., 1994). CD40 and CD95 mediate growth inhibition or apoptosis through immune response and caspase activation, respectively.

CD59 and CD55 protect cells from autologous lysis by complement (Durrant et al., 2003, Watson et al., 2006). The current study found that CD59 was reduced on cancer cells, while CD55 was elevated. Although elevated CD55 has been consistently observed in CRC (Durrant et al., 2003), reports of CD59 levels have been variable. Koretz *et al.* and Schmitt *et al.* described high CD59 levels in early stage and moderately to well differentiated CRC tumours (Koretz et al., 1993, Schmitt et al., 1999), whereas Watson *et al.* found reduced CD59 (Watson et al., 2006) and a correlation between the loss of CD59 and increased CD55 in low-grade tumours. The differential expression of complement regulatory membrane proteins suggests that the over-expression of one or more regulator proteins compensates for the absence of others (Koretz et al., 1993).

CD98, an L-type amino acid transporter, was elevated on CRC cells (Table 4.2a) as well as other cancers (Kaira et al., 2008). CD98 provides a consistent supply of essential amino acids with consequent increased CRC tumour size (Ohkame et al., 2001).

CD38 was reduced on CRC compared to normal cells (Table 4.2a). CD38 may be used as a cell differential marker (Mehta et al., 1996). Recently, CD38 negative CRC cells have been identified as cancer stem cells (Dalerba et al., 2007a).

CD13 and CD26 are ectopeptidases that process bioactive peptides. We found CD13 to be reduced on CRC cells compared to normal $EpCAM^+$ intestinal mucosal cells (Table 4.2a), but both were increased in late stage CRC (Table 4.2b). CD13 and CD26 positive cells have been associated in CRC with late stage processes, angiogenesis and metastasis (Hashida et al., 2002, Pang et al., 2010).

4.3.2 Hierarchical clustering of $EpCAM^+$ CRC cells

Unsupervised hierarchical clustering of $EpCAM^+$ CRC profiles generated 4 distinct clusters (Figure 4.3). Cluster 1 contained slightly more early stage CRC with low levels of tumour invasion, while cluster 2 contained most of the metastatic tumours, with tumour infiltration beyond the serosa. Despite these differences, most of samples in each cluster were moderately differentiated stage B and C tumours (Table 4.4). There were, however, significant differences in antigen expression between these clusters (Table 4.5).

The first split in the dendrogram generated cluster 1, a small group of 11 CRC patients distinct from the main group. The clinico-pathological properties of cluster 1 included several benign adenomas, several well differentiated tumours (Table 4.4) and no poorly differentiated

tumours. Cluster 1 had 20 differentially expressed proteins compared to cluster 2 (Table 4.5a), 14 of which were previously observed reduced on CRC cells compared with normal mucosal cells (discussed in the previous section). Cluster 1 profiles were relatively similar to normal mucosal profile, as only 6 differential proteins were observed between them. Cluster 1 CRC showed higher CD15, CD55, CD66c, CD66e (CEA), and CD98, while the death receptor CD95, was reduced. Of particular interest, the levels of CD15, CD66e and CD98 were highest on cluster 1 samples, compared with samples from the other 3 cluster groups.

CD15 belongs to a family of cell adhesion molecules that bind to selectin and are involved in leukocyte-endothelial adhesion. Elevated expression of CD15 on CRC may indicate adhesion to endothelium during metastasis. Elevated CD15 has been associated with poor prognosis in metastatic CRC (Hoff et al., 1990); however the majority of cluster 1 tumours were early to mid ACPS with metastatic tumours confined to local lymph node infiltration. For low-grade CRC (cluster 1) CD15 expression is restricted to cells at the invading front and the periphery of the primary tumour mass (Marcial et al., 1993). At these sites, CD15 appears to be involved in homotypic aggregation of CRC cells, and in heterotypic aggregation with other CD15-positive cells, such as T-cells (Brooks and Leathem, 1995). High CD15 may promote tumour invasion, but also encourage interactions with immune cells.

High levels of surface CD66e have been reported on adenomas and differentiated CRC (O'Brien et al., 1981, Denk et al., 1972), consistent with the phenotype of cluster 1 tumours. CD66e is lower in moderately differentiated tumours, while poorly differentiated tumours may not express surface CD66e (Denk et al., 1972). Up-regulation of CD66e (CEA) on tumour cells may contribute to disruption of normal inter-cellular and cell-collagen bonds, contributing to disordered histological architecture and facilitating cellular migration (Goldstein and Mitchell, 2005).

Elevated CD98 on colonic cells has been reported to aggravate intestinal inflammation in a mouse model of chronic dextran sulphate sodium (DSS)-induced colitis, with greatly increased pro-inflammatory cytokines and chemokines (Nguyen et al., 2011). Therefore, within cluster 1, elevated CD98 over-expression may not be limited to CRC cells, but maybe also present on normal cells under the influence of inflammation. The link between chronic inflammation and tumourigenesis is well established (Mantovani et al., 2008); elevated CD98 may occur at sites of inflammation before formation of malignant tumours. This proposal is supported by the elevated CD98 we observed on benign adenomas and CRC.

Cluster 2 contains a large group of CRC patients (39), these CRC cells have reduced levels of antigens (20) compared with cluster 1 (Table 4.5a). Low levels of these antigens are characteristic of cancer cells, and many of them were previously found to be differentially abundant between CRC and normal mucosa. The immunophenotypes in cluster 2 can be further sub-divided into clusters 3 and 4 (Figure 4.3). Cluster 4 showed reduction expression of 13 surface antigens compared to cluster 3, while 2 antigens, CD49d and CD49e, were elevated. Cluster 4 showed the lowest levels of CD9, CD15, CD29, CD47, CD49f, CD59, CD63, CD66e, CD98, CD104, CD151, CD326 and HLA-ABC (Table 4.4b) and was the most immunophenotypically distinct from normal mucosa. The reductions in antigen levels in cluster 4 correlated with more poorly differentiated tumours (24%) than clusters 1 (0%) or 3 (9%).

Although clusters 3 and 4 shared similar numbers of metastatic CRC (32% and 35%, respectively) their immunophenotypes, suggested that cluster 4 may have higher metastatic potential and a worse prognosis, supported by over-expression of CD49d and CD49e, which correlate with enhanced metastatic activity (Okazaki et al., 1998). The reduced levels of HLA-ABC, CD66e and CD326 on CRC cells are associated with lower T-cell activation that may assist in CRC escape from the immune system (Nagorsen et al., 2000).

Tetraspanin proteins have recently been linked to cancer prognosis and metastasis (Le Naour et al., 2006). Although the tetraspanin proteins CD9, CD63 and CD151 were down-regulated on all CRC cells in our study, lowest expression was observed in cluster 4 (Table 4.2a,c). CD9 and CD63 both function as suppressors of metastasis (Le Naour et al., 2006, Sordat et al., 2002), while CD151 in solid tumours is inhibited by elevated hypoxia inducible factor 1 alpha (HIF-1α) (Chien et al., 2008), a common response to limited oxygen within solid tumours.

The ACPS differentiation grade and immunophenotypic differences between clusters, were consistent with other clinico-pathological observations. The proportion of patients over the age of 65 decreased as the clusters contained an increasing number of poorly differentiated tumours (Table 4.4). Tumour histological features, such as the occurrence of poorly differentiated and mucinous/signet ring cell tumours have been associated with CRC of young patients (Chung et al., 1998). However, the proposal that CRC in younger patients may correlate with poorer prognosis remains controversial (Molnar et al., 1994, Chung et al., 1998). Cluster 4, that had the most patients with poorly differentiated CRC also contained more tumours from the right colon (descending colon, sigmoid and rectum), with a majority showing evidence of peri-tumoural inflammation (Table 4.4). Both of these factors have been reported to correlate with worse patient outcome (Wolmark et al., 1983, Coussens and Werb, 2002).

4.3.3 $CD3^+$ tumour-associated T-cell profiles

For the surface profiling of tumour-infiltrating T-cells, we used the standard 82-antibody region of the original DotScan microarray, that recognises a range of lineage-specific leukocyte markers, adhesion molecules, receptors and markers of inflammation and immune

response (Belov et al., 2003). Previous studies have shown that the presence of tumour-infiltrating lymphocytes (TIL) in CRC is associated with reduced signs of metastatic invasion and prolonged survival (Pages et al., 2005). In this study we have profiled the antigen expression of $CD3^+$ T-cells within CRC and normal intestinal mucosa to determine differences in their immunophenotypes and the possible use of T-cell profiling for CRC stratification.

$CD3^+$ profiles were normalised (Log2 transformed, median centre) to allow direct comparison between surface protein levels on T-cells in different samples. CD antigens levels were compared between $CD3^+$ T-cells isolated around and within tumour tissue compared to T-cells on normal mucosa: 18 were reduced on tumour-infiltrating T-cells, the majority were adhesion molecules (Table 4.3a) and 6 antigens were elevated on tumour-associated T-cells: CD11c, CD49e, CD66c, CD71, CD86 and HLA-DR (Table 4.3a). CD71 and HLA-DR are associated with late-activated T-cells (Caruso et al., 1997), while CD86 on T-cells is found only after T-cell activation (Azuma et al., 1993). The adhesion molecule CD66c has previously been reported on T-cells (Singer et al., 2002) but no satisfactory function has yet been assigned to this protein.

CD3 was found reduced on tumour-infiltrating $CD3^+$ T-cells compared to T-cells in normal mucosa. T-cell signal deregulation in tumours was first described by Mizoguchi *et al.* and Nakagomi *et al.*, where significantly less CD3 was found on T-cells isolated from CRC compared with those in the peripheral blood of those patients (Mizoguchi et al., 1992, Nakagomi et al., 1993). It was speculated that this reduction in CD3 resulted from local production of suppressor factors by CRC cells, deletion of some tumour-specific clones, and diminished production of lymphokines. Later studies identified tumour associated macrophages (TAM) as one of the factors responsible for the down-regulation of CD3 (Otsuji et al., 1996). TAMs induce immune-suppression through oxidative stress induced reduction

of CD3 on T lymphocytes, at the same time producing inflammatory cytokines and chemokines that contribute to tumour survival and proliferation (Sica et al., 2008). In spite of the reduced levels of the costimulation antigen CD3, we found that tumour-infiltrating T-cells exhibit higher levels of activation and proliferation markers than T-cells in normal tissue. These results suggest that tumour-associated T-cells may be activated through CD3-independent pathways such as by interleukin-2 induced activation (Clevers et al., 1988).

CD2, CD7, CD31 and CD44 all have fundamental roles in the regulation of T-cell adhesion (Shimizu et al., 1990, Tanaka et al., 1992) and were all reduced on the surface of tumour-infiltrating T-cells (Table 4.3a). Adhesion molecules function in two essential aspects of T-cell physiology: migration and recognition. We found the integrin subunits, CD11c and CD49e, to be elevated on tumour-infiltrating T-cells while four others were reduced, CD11a, CD29, CD49d and CD103 (Table 4.3a). Integrin alpha subunits CD11a and CD11c can form a heterodimeric receptor with CD18 (antibody not on microarray), which is responsible for T-cell adhesion to the vascular endothelium as well as T-cell activation and proliferation (Shelley et al., 2002, Krensky et al., 1983). Similarly, integrin alpha subunits CD49d and CD49e, bind to beta subunit CD29 to form very late activation antigen-4 (VLA4) and -5 (VLA5), respectively. Both VLA4 and VLA5 promote proliferation of naïve and memory T-cells through binding to fibronectin in the ECM (Davis et al., 1990). In addition, VLA4 and VLA5 are responsible for a rapid increase in adhesion to thrombospondin upon T-cell activation (Yabkowitz et al., 1993). Thrombospondin is an ECM protein that is transiently expressed at high concentrations in damaged and inflamed tissue. Hence the increased expression of CD49e on tumour-associated T-cells may reflect this homing potential. Further investigation is required to understand the reasons behind the differential expression of integrins in tumour-associated T-cells and their roles in tumourigenesis.

The reduced levels of CD103 (Integrin αE) on tumour-infiltrating T-cells suggest a decrease in the sub-population of intestinal intraepithelial regulatory T-cells. CD103 was reported to be necessary for efficient migration of T-cells into inflammatory sites where these cells are involved in suppression of peripheral inflammation (Huehn et al., 2004).

Three tetraspanin proteins, CD9, CD63 and CD151, were reduced on tumour-associated T-cells (Table 4.3a). CD9 is responsible for CD28-independent T-cell activation and proliferation (Tai et al., 1996). Similarly, CD63 is a T-cell activation-induced trans-membrane protein involved in sustaining and amplifying the ongoing activation (Pfistershammer et al., 2004). CD151 directly interacts with integrin α3β1 and facilitates T-cell migration (Chien et al., 2008). The expression of tetraspanins is not essential to normal T-cell function, since CD9- and CD151-deficient mice have normal immune function (Levy and Shoham, 2005).

4.3.4 Hierarchical clustering of $CD3^+$ tumour-infiltrating T-cells

The hierarchical clustering of tumour-associated T-cells generated 3 clusters with different T-cell characteristics. The first split in the dendrogram generated cluster 1, a small group of 14 T-cell profiles distinct from the larger cluster 2 (Figure 4.4). Another division in the hierarchy, separated cluster 2 into clusters 3 and 4. We found T-cells in cluster 1 to be characteristic of T-cell exhaustion, consisting of well differentiated T-cells in the late stages of an immune response. Reduced T-cell activation and proliferation suggest prolonged exposure to chronic inflammation, which correlates with the relatively high levels of inflammation (57%) found around their corresponding tumours (Table 4.6). Cluster 3 T-cells exhibited intermediate levels of activation makers but reduced CD3 expression. The reduced levels of T-cell markers may reflect a lack of T-cells, as the clinico-pathological and

haematological information suggests cluster 3 contains lower than average levels of circulating and peri-tumoural lymphocytes (Table 4.6). Cluster 4 T-cells also have reduced CD3 but, unlike cluster 3, the members of this group contain much higher levels of activated lymphocytes in the circulation and around the tumour.

The T-cell population of cluster 1 is characterised by well differentiated T-cells with low levels of activation and proliferation markers. The clinico-pathology data on this cluster indicate a high number of tumours with peri-tumoural inflammation (Table 4.6). Similar to viral infections, cancers induce functional tumour-specific T-cells; however, they gradually lose their function during the course of the cancer and, as a result, show signs of reduced activation and proliferation (Wherry, 2011). Evidence for this was observed in the reduction in $CD8^+$ T-cells and the down-regulation of early- and late-activation markers (CD69 and HLA-DR, respectively) (Table 4.3). Several antigens associated with activated T-cells were also down-regulated: CD86 (Azuma et al., 1993), CD134 (Taylor and Schwarz, 2001) and CD151 (Hasegawa et al., 1996), along with two enzymes (CD13 and CD26) with regulatory functions in T-cell activation. Previous studies have shown that the mitogenic activation of human peripheral T-cells correlates with a large increase in CD13 mRNA content and the presence of CD13 on the surface of these cells (Lendeckel et al., 1996). Similarly, CD26 molecule is able to transmit an activating signal to the T-cell and is associated with T-cell activation and proliferation (Fleischer, 1994).

CD3, CD31 and CD43 are regulators of T-cell adhesion-induced signalling and were found to be over-expressed in cluster 1. They are mediators of integrin dependent-adhesion of T-cells to other cells and to the ECM. While integrins are expressed on circulating (“resting”) T-cells, they do not mediate effective adhesion without induction from specific regulators

(Tanaka et al., 1992). CD3 is the critical adhesion inducer in antigen-specific recognition. CD3 induces the beta 2 integrin, particularly lymphocyte function-associated antigen 1 (LFA-1). In turn, LFA-1 mediates binding to ICAM-1 on antigen-presenting cells, and such regulated adhesion accounts for many of the adhesive events that accompany antigen-specific T-cell recognition (Dustin and Springer, 1989).

The adhesion-amplifying role for CD3 is analogous to the adhesion-amplifying role played by CD31 in T-cell-endothelium interaction. CD31 expression on T-cells induces the function of beta 1 integrin (CD29), particularly very late antigen-4 (VLA-4 integrin) (Tanaka et al., 1992). Evidence for the "adhesion cascade" generated by CD31 is the observed high levels of CD49d, the alpha subunit of VLA-4, in cluster 1 (Figure 4.7). Past studies indicate that CD31 is an amplifier of T-cell-endothelial cell interactions, as a result of the role of VLA-4 (Tanaka et al., 1992). In vivo studies in the rat model indicate the contribution of VLA-4 on T-cell movement into the gut (Issekutz, 1991). CD49d, may also have a role in gut-homing T-cells, as there is another CD49d-containing integrin ($\alpha 4\beta 7$) that interacts with ligands on gut endothelium (Holzmann and Weissman, 1989).

CD43 diminishes T-cell adhesion, irrespective of the adhesion pathway responsible (e.g. CD4, $\beta 1$, or $\beta 2$ integrins), and provides a general anti-adhesive barrier on cell surfaces, impeding the function of several types of receptors (Stockton et al., 1998, Onami et al., 2002). The over-expression of CD43 by cluster 1 T-cells may prevent promiscuous adhesion in vascular beds, where ligand density is too low to override its anti-adhesive effect.

The net result of increased CD31, CD43 and CD49d could be the enhanced selectivity of T-cell migration to the gut or tumour site that displays the highest concentrations of homing receptor ligands.

Evidence of reduced T-cell proliferation in cluster 1 was indicated by the over-expression of CD57 and CD95. D'Angeac *et al* proposed that CD57 expression is a T-cell differentiation event during the late immune response on $CD3^+$ T-cells (d'Angeac et al., 1994), while a similar study reported that $CD57^+$ T-cells exert a suppressive effect on other T-cells (Brenchley et al., 2003). Although $CD57^+$ T-cells could no longer be induced to proliferate, they remained efficient producers of cytokines. $CD3^+$ $CD57^+$ natural killer T-cells produced high levels of IFN-γ, that induces HLA-DR expression on a wide variety of cells, including tumour-derived cell lines (Trinchieri and Perussia, 1985). IFN-γ may influence HLA-DR over-expression on CRC. Similarly, over-expression of CD95 (Fas) helps terminate an ongoing immune response by inducing death of activation-mediated T-cells (Ju et al., 1995). Naïve T-cells express little or no Fas, whereas activated and memory T-cells show increased Fas in both $CD4^+$ and $CD8^+$ sub-populations (Aggarwal and Gupta, 1998). Some malignant tumours express CD95 ligand as a mechanism of inducing apoptosis of T-cells and to mediate immune escape (Hahne et al., 1996). Interestingly, both CD57 and CD95 increase on T-cells of aging humans (d'Angeac et al., 1994, Aggarwal and Gupta, 1998) but there was no correlation between cluster 1 patients and age (Table 4.6).

This information suggests that cluster 1 T-cells may have been recruited to the tumour as part of an immune response. However, most of the T lymphocytes in this cluster also showed reduced activation/proliferation markers, correlating with T-cell exhaustion, and a lower capability of fighting the cancer compared with those in cluster 2. Clinico-pathologically, cluster 1 contains predominantly early stage tumours (86%) with a majority showing signs of peri-tumour inflammation (Table 4.6). This supports the proposal that inflammation plays an important role in early tumourigenesis, either as an initiator of CRC development or as a mediator of tumourigenesis once the tumour has formed (Hofseth and Ying, 2006).

Further down the hierarchy, the next division separated cluster 2 into two distinct groups (Figure 4.4). The phenotypic differences between clusters 3 and 4 showed increases in CD11c, CD31, CD66c, CD86 and CD95 in cluster 3, while cluster 4 had elevated CD5, CD9, CD11a, CD15, CD44, CD45, CD45RO, CD47, CD59, CD63, CD71, CD326 and CA19-9.

Cluster 3 is characterised by intermediate levels of antigens. It shows higher levels of activation markers than cluster 1, but lower levels than cluster 4 (CD69, CD71 and HLA-DR). T-cells in cluster 3 contain the highest levels of CD11c, CD66c and CD86, but the lowest levels of CD44 and CD45. CD11c and CD66c are endothelial adhesion markers, while CD86 expression has been associated with activated T-cells (Azuma et al., 1993). The reduced levels of CD44 and CD45 suggest a larger population of naïve T-cells within cluster 3. Clinico-pathological information indicates that cluster 3 contains the largest number of metastatic tumours (47%) but the lowest levels of peri-tumour inflammation (27%), and lowest levels of circulating- and tumour infiltrating- lymphocytes, at 60% and 7% respectively (Table 4.6). These factors may contribute towards fewer T-lymphocytes in cluster 3 patients and the below average CD3 levels.

The T-cell population in cluster 4 is characterised by elevated expression of the memory T-cell markers, CD11a, CD44 and CD45RO (Sanders et al., 1988, Lee and Vitetta, 1991, Clement, 1992), and “classic” markers of T-cell activation and proliferation, CD44, CD45 and CD71 (DeGrendele et al., 1997, Janeway, 1992, Brekelmans et al., 1994). CD15, increased in cluster 4 T-cells, may also be associated with T-cell activation (Chadburn et al., 1992) and has been found elevated on tumour TILs isolated from various human cancers (Roussel et al., 1996).

Cluster 4 T-cells show low levels of CD3, despite having relatively high levels of both circulating T-cells and TILs (Table 4.6). The presence of peri-tumoural inflammation may

reduce CD3 levels on T-cells, resulting from TAM mediated immune-suppression. However, activation markers are present on these T-cells, suggesting that alternative signalling pathways are involved. T-cells in cluster 4 also show elevation of the tetraspanin proteins CD9 and CD63, both associated with T-cell stimulation and activation. CD9 can induce stimulation of naïve T-cells independently of the co-stimulatory molecules CD28 and, CD80 and CD86 on the surface of antigen presenting cells, which are generally considered to be the primary co-stimulatory pathway of T-cells (Tai et al., 1996). Similarly, the CD63 can induce T-cell activation independent of CD28, but relies on antigen presenting cells. Following antigen presenting cell co-stimulatory signal to T-cells, CD63 further sustains and amplifies the ongoing activation, resulting in efficiently stimulated T-cells (Pfistershammer et al., 2004).

The antigens CD5, CD47 and CD59, up-regulated on T-cells in cluster 4, have roles in T-cell survival. Recent reports have suggested CD47 to function in T-cell co-stimulation (Reinhold et al., 1997, Seiffert et al., 2001) and the active protection of T-cells from phagocytosis (Blazar et al., 2001). Elevated CD47 has been observed on haematopoietic stem cells as protection during migration to the periphery after a strong mobilisation or inflammatory stimulus (Jaiswal et al., 2009), and could also apply to migrating T-cells seeking out tumour targets. CD59 has also been implicated in T-cell activation (Korty et al., 1991) and the inhibition of complement-mediated lysis (Davies et al., 1989). CD59-mediated T-cell activation induces internalisation of the molecule and results in diminished surface CD59. As a result, active T-cells with decreased CD59 expression are susceptible to *in vitro* apoptosis by autologous complement as a means to control hyper-reactivity of T-cells (Tsunoda et al., 2000). The up-regulation of CD59 may prolong the immune response by avoiding activation-induced cell death. CD5 is expressed on the surface of all mature T-cells (Van de Velde et al., 1991) and is elevated on TILs isolated from various human tumours (Dalloul, 2009). Over-

expression of CD5 protects TILs from apoptosis mediated by uncontrolled over-reactivity to self-antigens (Friedlein et al., 2007).

The immunophenotype of cluster 4 suggests these T-cells to be highly active and proliferative. T-cell activation is induced via a variety of stimulation pathways and sustained through the expression of multiple antigens (CD9 and CD63). In contrast to cluster 1 T-cells, cluster 4 T-cells show no sign of activation-induced apoptosis, with several antigens over-expressed to ensure T-cell survival (CD5, CD47 and CD59).

An interesting finding was the cell binding on antibody dots for CD326 (EpCAM) and CA19-9 by cluster 4 T-cells. Both of these antigens are CRC markers (Nakayama et al., 1997a, Munz et al., 2009) and found on CRC cells, microvesicles and in serum. We speculate that the positive results for CD326 and CA19-9 may be due to the capture of T-cells on these antibody dots by virtue of adhering membrane fragments from damaged CRC cells on their surface. This is supported by the finding that positive CD326 and CA19-9 results were limited to the profiles of highly activated T-cells expressing high levels of adhesion molecules found within cluster group 4. While the large cancer cells were easily damaged during tumour disaggregation, T-cells remained intact, and no T-cell markers were detected in the $EpCAM^+$ CRC profiles.

4.3.5 Correlation between CRC cells profiles and T-cell profiles

Tumour progression is a complex process that depends on interactions between CRC and normal cells (Hart and Saini, 1992). One aspect of the host response, the presence of infiltrating T-lymphocytes, is of particular interest, because signs of an immune response within CRC are associated with reduced tumour invasion and prolonged survival (Pages et

al., 2005). We found this to be the case, as T-cells with elevated activation and proliferation markers (T-cell cluster 4) were associated with well differentiated tumours with low metastatic potential (CRC cluster 1). The immunophenotype of the CRC cells within these tumours was similar to that of normal mucosa. This group of cancer cells, unlike those of clusters 3 and 4, retained the expression of several antigens that make them susceptible to an immune response, e.g., normal levels of HLA-ABC and CD95. HLA-A and B are essential for the presentation of antigens from within the cancer cell to T-cells (Zinkernagel and Doherty, 1979), while CD95 acts as a receptor for CD95 ligand on cytotoxic T-cells expressing CD95 (Moller et al., 1994).

CRC cells in cluster 3 are characterised by moderate expression of tumour associated antigens and consist of infiltrating T-cells from all immune-phenotypic clusters (Figure 4.5). Within cluster 3, subsequent hierarchical divisions further stratify the CRC samples into sub-groups that correlate with the distribution of T-cell cluster profiles. Metastatic tumours in cluster 3 are more likely to be associated with the activated T-cells from cluster 4, while non-metastatic tumours are found with less activated T-cells from clusters 1 and 3. Interactions between CRC and associated T-cells may be responsible for the clustering of surface profiles and may provide additional information for the sub-classification of clinico-pathologically similar CRC. Further investigation is required to determine if the similarities in immunophenotype translates to similar patient outcomes.

The immunophenotype of CRC cells in cluster 4 is associated with more aggressive tumours, with high metastatic potential. Subsequent divisions further down the hierarchy consist of samples corresponding to clusters 1 and 3 of the tumour-infiltrating T-cells. T-cell cluster 3, with low levels of moderately activated T-cells, contains samples corresponding to the metastatic tumours in cluster 4, while T-cell cluster 1, characteristic of T-cell exhaustion, corresponds to the non-metastatic tumours in cluster 3 (Figure 4.5). The immunophenotype of

this CRC cluster represents cells associated with a diminished or low level immune response. The down-regulation of HLA-ABC and the tumour-associated antigens, CD66e and CD326, on CRC cells in cluster 4 correlates with the reduction in activation markers on tumour-infiltrating T-cells. In addition, these T-cells show high levels of surface CD95, while the corresponding CRC has reduced CD95. Previous studies reported that melanoma cells express CD95 ligand in order to escape immune surveillance by inducing apoptosis in $CD95^+$ T-cells, while also down-regulating their own CD95 (Hahne et al., 1996).

This strong interrelationship between the immunophenotypes of CRC cells and T-cells from the same tumour illustrate the mutual influences between cancer cells and the various cells within their microenvironment. We have shown that surface profiling of CRC cells and tumour-infiltrating T-cells provides more discrimination between intermediate stage CRC than traditional clinico-pathological staging by ACPS.

4.3.6 Conclusions and future studies

The next logical step for this project would be to correlate the immunophenotypes with 5-year patient survival data. The surface profiles for CRC and tumour infiltrating T-cells have clustered with good and poor prognosis. When information on 5-year patient outcome becomes available, these findings can be confirmed, and surface antigen profiles can be validated with a larger group of patients as a prognostic assay. In addition, we wish to correlate these profiles with cancer recurrence and response to therapy. The use of a training data set as established here coupled with an independent validation cohort is required to determine clinical utility.

Gene expression profiles and individual tumour markers (e.g., CEA or CD66e) have shown promise in predicting long-term outcomes in CRC patients, especially for intermediate ACPS B and C, where prognosis is problematic (Durrant et al., 2003, Eschrich et al., 2005). It has been suggested that multiple markers will be required to enable reliable sub-classification of cancers (Simpson and Dorow, 2001). The results presented here support this hypothesis, the profiling of CRC and infiltrating T-cells using DotScan microarrays may produce "disease signatures" that would provide a more accurate measurement of tumour progression and enable better prediction of patient survival. Hierarchical clustering generated clusters with surface profiles of CD antigens associated with good or poor prognosis. Clinico-pathological data from the extreme stages of CRC (early stage/ ACPS A versus metastatic/ stage D) and histological assessment (differentiation, tumour location, inflammation) supported the patient survival prediction for each cluster. Intermediate stage CRCs (ACPS B and C) were distributed within all cluster groups and showed various immunophenotypes. Surface profiles may enable distinction between intermediate-stage CRC patients that would benefit from adjuvant therapy, and those that would be cured from surgery alone. In addition, surface profiling enabled correlation between cancer cells and infiltrating T-lymphocytes. The correlation between activated T-cells and a favourable CRC immunophenotype shows that strong mutual influences shape the surface proteomes of CRC and T-cells within the microenvironment. Surface profiling detects molecular heterogeneity within ACPS B and C CRC with similar histology. DotScan analysis, in conjunction with clinico-pathological data, should enhance prognosis and enable more effective personalised treatment of CRC patients.

Chapter 5

General discussion

5.1 Proteomic techniques

The proteomic techniques, saturation-DIGE and antibody microarrays, were used to identify differentially abundant proteins between whole cell lysates of CRC and matching normal intestinal mucosal cells. Although each technique yielded a substantial number of differentially abundant proteins (58 by Saturation-DIGE and 64 by antibody microarrays), there was no overlap between them. These results suggest that each method may only capture a specific subset of the proteomic changes. Interestingly, many of the differential protein changes between tumour stages were observed between Stage A and Stage C, but not for Stage B (e.g. proliferation markers, growth factors, suppressors of regulators). These results

may be the result of technical artefacts. However, precautions were taken in the experiment design to avoid data bias, such as running samples in random.

Saturation-DIGE improves upon normal DIGE by significantly reducing the amount of protein required (5 µg per gel) because of label saturation on cysteine residues, and increased reproducibility with an internal control. However, the major limitation associated with 2D gel based techniques remains that low abundance proteins are not easily detected by 2D electrophoresis/MS proteomics (Gygi et al., 1999), because high abundance proteins often mask their detection. This was evident from our results; the majority of differential proteins detected by saturation-DIGE were relatively high abundance and involved in glycolysis (e.g., enolase, ATP synthase, aconitate hydratase) or stress response (e.g. Hsp60, peroxiredoxin, superoxide dismutase). This is unfortunate, since it is often the less abundant proteins that respond in interesting ways to various stimuli (Gygi et al., 2000).

Antibody microarrays have been applied to cancer research for protein identification. Microarrays can simultaneously measure hundreds of proteins in a rapid, low volume assay. The major challenge with antibody microarrays is acquiring the desired set of antibodies. Consequently, many microarrays are limited to specific pathways or diseases (Huang et al., 2001, Paweletz et al., 2001). Even a large-scale discovery focused microarray, such as the Explorer microarray, has only 656 antibodies. Selection bias can be inadvertently introduced as a result of antibody availability. Although many monoclonal and polyclonal antibodies are commercially available, it may not be financially feasible to incorporate multiple antibodies with redundant antigen specificities in an array. Several attempts have been made to replace expensive antibody production in hybridomas with scFvs or Fabs by phage display (Hallborn and Carlsson, 2002) or ribosomal display (Hanes et al., 2000), but this approach has not yet been widely used for microarray analysis.

In this study, the Explorer antibody microarray was able to detect changes in some relatively low abundance proteins (e.g., p73, chemokine receptor type 4), but displayed only weak binding for some of the proteins identified by saturation-DIGE/MS analysis (Hsp60, superoxide dismutase and glyceraldehyde-3-phosphate dehydrogenase). We speculate that the relatively low binding density of manganese superoxide dismutase (MnSOD) on the microarray may be due to reduced affinity of the corresponding antibody with the mutant form of the protein (MnSOD Q143N mutant) identified by saturation-DIGE/MS (Table 3.2). This mutant contains a replacement of 143Gln→Asn, resulting in a slight conformational change (Hsieh et al., 1998). This mutation may alter the antibody binding site (antibody clone 30F11 recognises MnSOD epitope N-terminal domains I-V), resulting in reduced detection by antibody microarrays. For GAPDH and Hsp60, no mutants were identified by MS but we did observe multiple charged isoforms of these proteins on the gel, some of which may lack the epitope recognised by the antibody clone used on the microarray. Proteins often undergo numerous post-translational modifications that may be crucial to their functions, but some of these modifications may render the protein undetectable by an antibody that recognises a specific isoform of the protein.

Another source of inconsistencies in antibody microarray data is the variation in affinity and performance of different antibodies on the array, due to conformational changes after application on the solid phase. Heterogeneity in antibody affinity can span orders of magnitude. The performance of each individual antibody can depend on the chemistry of the solid surface to which it is applied, the buffer, the storage conditions and storage time. The shelf-lives of different antibodies vary in solution, and in the solid phase.

The DotScan antibody microarray screens for known CD markers to classify CRC cells and infiltrating T-cells. Live cells are captured on the microarray via their surface antigens, recognised by antibodies of corresponding specificity on the microarray. This procedure

provides a profile of the cell surface proteome, with minimal chemical/physical alterations to protein integrity. The main challenge associated with this method is to profile cells under consistent conditions for all microarrays. The pairs of CRC tumour and mucosa samples contain a variety of cell types, of variable relative abundance. While we aim to use 6×10^6 total cells per microarray, the final number of cells profiled may vary with a heterogeneous cell population. Subtraction of background and normalisation of DotScan microarray data is critical for the comparison of different samples.

Median normalisation was selected as the global normalisation technique, in preference to LOESS normalisation or normalisation relative to housekeeping proteins. Median normalisation is the simplest and most widely used global normalization technique for antibody microarray data. In cases where a large number of outliers in the sample data may provide an inaccurate estimate of the true centre of distribution, median centring can be employed. The advantage of median normalisation is its mathematical simplicity, enabling quick and easy implementation. Median centring, and its variations, have proven to be a reliable method of minimising technical variance for large-scale high-throughput data (Mestdagh et al., 2009, Wylie et al., 2011). The main issue with this normalisation method is that it implicitly assumes that differences between arrays and/or samples are of a linear nature. Despite these short-comings, median centring remains the preferred normalisation approach for antibody microarray analysis. It is hoped that a normalisation method capable of handling non-linear signals may be developed in the future, enabling the standardisation of antibody microarray normalisation.

Direct implementation of LOESS normalisation to antibody microarray data has been shown to lower reproducibility and reduces correlation between data (Hamelinck et al., 2005). The main reason for this is that the LOESS method was developed for DNA microarray data and relies on having a large number of data points to produce an accurate measure of intensity-

based differences between two samples. Generally antibody microarrays have fewer data points, often less than a thousand different antibodies, compared to 5,000 genes on DNA microarrays. Therefore, without compensation for fewer data points, direct translation of this normalisation method may add noise to the data and reduce the detection of true biological variation.

Sets of housekeeping genes are often used to normalise DNA microarray data, but corresponding "house-keeping" proteins are more difficult to find for antibody microarrays, due to the dynamic nature of protein expression. Currently, there are no known proteins expressed at consistent levels on the surface of CRC cells and normal mucosa.

5.2 Cancer markers: intracellular versus surface proteomics

Alterations in the intracellular and surface proteomes of CRC cells, compared to normal intestinal mucosa, were investigated. The expression profiles of intracellular and surface proteins differentiated between cancer cells and normal mucosa (Table 3.2a, 3.3a and 4.2). Changes in the intracellular proteome reflected functional changes found in most cancer cells (e.g., elevation of glycolysis, proliferation signalling and stress-response proteins). These changes correlated with tumour progression and the availability of resources (such as space, oxygen and nutrient; Table 3.2b and 3.3b). Many of the changes in intracellular proteins correlated with disease stage and showed little variation between patients with histologically similar tumours. By contrast, the surface proteome showed greater diversity between same-stage tumours, often correlating with external factors such as inflammation, circulating lymphocyte counts and the expression profiles of non-cancerous cells, such as tumour-infiltrating T-cells (Table 4.2b and 4.4).

The differences in expression between intracellular and surface proteins may provide a guide to their application in CRC treatment. The characteristics of intracellular markers make them better anti-cancer drug targets; many are essential in tumourigenesis and remain relatively consistent within clinico-pathological stages. Our results also show that the CRC proteome is highly dynamic during CRC progression. These fluctuations in protein levels could be used to guide selection of the most effective drugs for a particular stage of CRC. Many of the proteins whose levels change are potential therapeutic targets, such as proteins involved in the Ras signalling pathway (Downward, 2003), glycolytic metabolism (Gatenby and Gillies, 2007) and redox regulation (Trachootham et al., 2009). The effectiveness of these therapeutic interventions may be increased if they are tailored for the appropriate protein, for example Ras and its downstream Raf kinase are elevated in early CRC stage A patients (Table 3.3c). The proteins driving glycolysis (alpha-enolase, GAPDH, phosphoglycerate kinase 1 and L-lactate dehydrogenase) were most abundant during intermediate CRC stage B and C (Table 3.2b), or redox proteins (MnSOD and peroxiredoxins) elevated only in late metastatic C and D CRC (Table 3.2b and c).

The immuno-phenotypes of cancer cells were highly variable within same-stage CRC (Figure 4.3). Differences in surface antigen expression are dependent on the patient's immune response, the microenvironment and on tumour progression. This variation between patients may enable sub-classification of CRC and indicate the patient-specific immune response to CRC. For example, the presence of the one or all HLA-A,B and C antigens on the surface of tumour cells indicate the presence of antigen presentation machinery able to initiate an immune response (Romero et al., 2005). Our data confirm that, CRC cells with high levels of HLA-ABC were more likely to be associated with activated TILs (Figure 4.5). There was a correlation between the immuno-phenotypes of CRC cells and their tumour-infiltrating T-cells. This relationship shows that interactions between CRC cells and immune cells are

variable within CRC stages, especially for intermediate B and C CRC. Histologically similar CRC can be sub-classified by the level of local tumour infiltrating T-cells. An assay that could determine the positive or negative influences of these interactions with TILs could be used to determine the course of treatment and overall survival.

5.3 Future research

The direction of this study is to apply the DotScan™ CRC microarray as a rapid approach (workflow 3 hr) to antigen profiling of cells isolated from clinical samples. It can be adapted to contain small number of antibodies that detect only the signature antigens, to reduce costs. While the current results obtained are promising, the survival data and validation with a larger independent cohort is required to confirm the surface signatures. There is implicit bias in the results presented here as, due to the small sample size, no validation could be performed. These limitations are part of the inherent challenges associated with using fresh clinical CRC: the limited availability of samples and the 3-year waiting period for outcome data. Surface profiling may focus attention on the association between tumor spread and patient survival, and the influence of the host immune response on patient outcome. Application of prognostic antigen signatures may aid in the identification of interactions between cancer cells and T-cells, and together with traditional clinico-pathologic staging, may improve the selection of high-risk CRC patients who could benefit most from adjuvant therapy.

5.4 Conclusions

Expression patterns of biomarkers have enormous potential to improve diagnosis, guide molecularly targeted therapy and monitor proliferative activity and therapeutic response of CRC. As cancer therapies become increasingly patient specific, biomarkers play greater roles in cancer staging and treatment. The evolution of powerful proteomic methods for high throughput analysis has facilitated biomarker discovery. In this project, saturation-DIGE and Explorer antibody microarrays have provided extensive profiles of proteins that are modulated during CRC progression. These protein changes offer a proteomic approach to CRC stratification and insight into the tumour microenvironment. Essential processes in CRC progression, such as glycolysis, ER stress response, angiogenesis and the redox response, offer molecular landmarks for CRC progression and novel targets for therapy. The sequential nature in which these protein changes occur may also allow clinicians to predict physiological events occurring within the cancer cells and tailor treatments accordingly.

The cancer surface proteome offers a unique perspective of the interactions between cancer cells and normal cells in the microenvironment. The DotScan antibody microarray enables the profiling of surface antigens on viable cells and utilises cell specific panels of antibodies to profile the immunophenotype of CRC cells and tumour-infiltrating T-cells. We have identified distinct groups of cancer cells and infiltrating T-cells from histologically similar tumours. These differences in antigen expression correlate with CRC cell differentiation, peri-tumoural inflammation and T-cell stimulation. The application of surface profiling enables more accurate prediction of survival in same stage tumours. We have also found that CRC cell profiles correlate with the pattern of surface proteins of their tumour-infiltrating T-cells. This finding proves that cancer antigens are actively influencing the surface protein expression of neighbouring cells and *vice versa*. This degree of mutual influence suggests

that patient survival is dependent on cancer progression permitted by surrounding microenvironment.

References

ADES, E. W., HINSON, A., CHAPUIS-CELLIER, C. & ARNAUD, P. 1982. Modulation of the immune response by plasma protease inhibitors. I. Alpha 2-macroglobulin and alpha 1-antitrypsin inhibit natural killing and antibody-dependent cell-mediated cytotoxicity. *Scand J Immunol,* 15**,** 109-13.

AGGARWAL, S. & GUPTA, S. 1998. Increased apoptosis of T cell subsets in aging humans: altered expression of Fas (CD95), Fas ligand, Bcl-2, and Bax. *J Immunol,* 160**,** 1627-37.

AHN, Y. H., LEE, J. Y., KIM, Y. S., KO, J. H. & YOO, J. S. 2009. Quantitative analysis of an aberrant glycoform of TIMP1 from colon cancer serum by L-PHA-enrichment and SISCAPA with MRM mass spectrometry. *J Proteome Res,* 8**,** 4216-24.

ALBIGES-RIZO, C., DESTAING, O., FOURCADE, B., PLANUS, E. & BLOCK, M. R. 2009. Actin machinery and mechanosensitivity in invadopodia, podosomes and focal adhesions. *J Cell Sci,* 122**,** 3037-49.

ALFONSO, P., CANAMERO, M., FERNANDEZ-CARBONIE, F., NUNEZ, A. & CASAL, J. I. 2008. Proteome analysis of membrane fractions in colorectal carcinomas by using 2D-DIGE saturation labeling. *J Proteome Res,* 7**,** 4247-55.

ALFONSO, P., NUNEZ, A., MADOZ-GURPIDE, J., LOMBARDIA, L., SANCHEZ, L. & CASAL, J. I. 2005. Proteomic expression analysis of colorectal cancer by two-dimensional differential gel electrophoresis. *Proteomics,* 5**,** 2602-11.

ALMOND, J. B. & COHEN, G. M. 2002. The proteasome: a novel target for cancer chemotherapy. *Leukemia,* 16**,** 433-43.

ANDRE, M., LE CAER, J. P., GRECO, C., PLANCHON, S., EL NEMER, W., BOUCHEIX, C., RUBINSTEIN, E., CHAMOT-ROOKE, J. & LE NAOUR, F. 2006. Proteomic analysis of the tetraspanin web using LC-ESI-MS/MS and MALDI-FTICR-MS. *Proteomics,* 6**,** 1437-49.

AZUMA, M., ITO, D., YAGITA, H., OKUMURA, K., PHILLIPS, J. H., LANIER, L. L. & SOMOZA, C. 1993. B70 antigen is a second ligand for CTLA-4 and CD28. *Nature,* 366**,** 76-9.

BAECKSTROM, D., NILSSON, O., PRICE, M. R., LINDHOLM, L. & HANSSON, G. C. 1993. Discrimination of MUC1 mucins from other sialyl-Le(a)-carrying glycoproteins produced by colon carcinoma cells using a novel monoclonal antibody. *Cancer Res,* 53**,** 755-61.

BALDWIN, A. S., JR. 2001. Series introduction: the transcription factor NF-kappaB and human disease. *J Clin Invest,* 107**,** 3-6.

BANTSCHEFF, M., SCHIRLE, M., SWEETMAN, G., RICK, J. & KUSTER, B. 2007. Quantitative mass spectrometry in proteomics: a critical review. *Anal Bioanal Chem,* 389**,** 1017-31.

BARDERAS, R., BABEL, I. & CASAL, J. I. 2010. Colorectal cancer proteomics, molecular characterization and biomarker discovery. *Proteomics Clin Appl,* 4**,** 159-78.

BASSI, R., GIUSSANI, P., ANELLI, V., COLLEONI, T., PEDRAZZI, M., PATRONE, M., VIANI, P., SPARATORE, B., MELLONI, E. & RIBONI, L. 2008. HMGB1 as an autocrine stimulus in human T98G glioblastoma cells: role in cell growth and migration. *J Neurooncol,* 87**,** 23-33.

BEHREND, L., MOHR, A., DICK, T. & ZWACKA, R. M. 2005. Manganese superoxide dismutase induces p53-dependent senescence in colorectal cancer cells. *Mol Cell Biol,* 25**,** 7758-69.

BEHRENS, J., BIRCHMEIER, W., GOODMAN, S. L. & IMHOF, B. A. 1985. Dissociation of Madin-Darby canine kidney epithelial cells by the monoclonal antibody anti-arc-1: mechanistic aspects and identification of the antigen as a component related to uvomorulin. *J Cell Biol,* 101**,** 1307-15.

BEKKU, S., MOCHIZUKI, H., YAMAMOTO, T., UENO, H., TAKAYAMA, E. & TADAKUMA, T. 2000. Expression of carbonic anhydrase I or II and correlation to clinical aspects of colorectal cancer. *Hepatogastroenterology,* 47**,** 998-1001.

BELOV, L., HUANG, P., BARBER, N., MULLIGAN, S. P. & CHRISTOPHERSON, R. I. 2003. Identification of repertoires of surface antigens on leukemias using an antibody microarray. *Proteomics,* 3**,** 2147-54.

BELOV, L., ZHOU, J. & CHRISTOPHERSON, R. I. 2010. Cell surface markers in colorectal cancer prognosis. *Int J Mol Sci,* 12**,** 78-113.

BEN-JONATHAN, N., LIBY, K., MCFARLAND, M. & ZINGER, M. 2002. Prolactin as an autocrine/paracrine growth factor in human cancer. *Trends Endocrinol Metab,* 13**,** 245-50.

BERG, E. L., MAGNANI, J., WARNOCK, R. A., ROBINSON, M. K. & BUTCHER, E. C. 1992. Comparison of L-selectin and E-selectin ligand specificities: the L-selectin can bind the E-selectin ligands sialyl Le(x) and sialyl Le(a). *Biochem Biophys Res Commun,* 184**,** 1048-55.

BERNACKA, K., KURYLISZYN-MOSKAL, A. & SIERAKOWSKI, S. 1988. The levels of alpha 1-antitrypsin and alpha 1-antichymotrypsin in the sera of patients with gastrointestinal cancers during diagnosis. *Cancer,* 62**,** 1188-93.

BI, X., LIN, Q., FOO, T. W., JOSHI, S., YOU, T., SHEN, H. M., ONG, C. N., CHEAH, P. Y., EU, K. W. & HEW, C. L. 2006. Proteomic analysis of colorectal cancer reveals alterations in metabolic pathways: mechanism of tumorigenesis. *Mol Cell Proteomics,* 5**,** 1119-30.

BLAZAR, B. R., LINDBERG, F. P., INGULLI, E., PANOSKALTSIS-MORTARI, A., OLDENBORG, P. A., IIZUKA, K., YOKOYAMA, W. M. & TAYLOR, P. A. 2001. CD47 (integrin-associated protein) engagement of dendritic cell and macrophage counterreceptors is required to prevent the clearance of donor lymphohematopoietic cells. *J Exp Med,* 194**,** 541-9.

BOEHM, J. E., SINGH, U., COMBS, C., ANTONYAK, M. A. & CERIONE, R. A. 2002. Tissue transglutaminase protects against apoptosis by modifying the tumor suppressor protein p110 Rb. *J Biol Chem,* 277**,** 20127-30.

BOO, Y. J., PARK, J. M., KIM, J., CHAE, Y. S., MIN, B. W., UM, J. W. & MOON, H. Y. 2007. L1 expression as a marker for poor prognosis, tumor progression, and short survival in patients with colorectal cancer. *Ann Surg Oncol,* 14**,** 1703-11.

BRADHAM, C. & MCCLAY, D. R. 2006. p38 MAPK in development and cancer. *Cell Cycle,* 5**,** 824-8.

BREKELMANS, P., VAN SOEST, P., VOERMAN, J., PLATENBURG, P. P., LEENEN, P. J. & VAN EWIJK, W. 1994. Transferrin receptor expression as a marker of immature cycling thymocytes in the mouse. *Cell Immunol,* 159**,** 331-9.

BRENCHLEY, J. M., KARANDIKAR, N. J., BETTS, M. R., AMBROZAK, D. R., HILL, B. J., CROTTY, L. E., CASAZZA, J. P., KURUPPU, J., MIGUELES, S. A., CONNORS, M., ROEDERER, M., DOUEK, D. C. & KOUP, R. A. 2003. Expression of CD57 defines replicative senescence and antigen-induced apoptotic death of CD8+ T cells. *Blood,* 101**,** 2711-20.

BROOKS, S. A. & LEATHEM, A. J. 1995. Expression of the CD15 antigen (Lewis x) in breast cancer. *Histochem J,* 27**,** 689-93.

BROWN, J. M. & GIACCIA, A. J. 1998. The unique physiology of solid tumors: opportunities (and problems) for cancer therapy. *Cancer Res,* 58**,** 1408-16.

BRUNAGEL, G., SHAH, U., SCHOEN, R. E. & GETZENBERG, R. H. 2003. Identification of calreticulin as a nuclear matrix protein associated with human colon cancer. *J Cell Biochem,* 89**,** 238-43.

CAIRNS, R. A., HARRIS, I. S. & MAK, T. W. 2011. Regulation of cancer cell metabolism. *Nat Rev Cancer,* 11**,** 85-95.

CAPPELLO, F., BELLAFIORE, M., PALMA, A., DAVID, S., MARCIANO, V., BARTOLOTTA, T., SCIUME, C., MODICA, G., FARINA, F., ZUMMO, G. & BUCCHIERI, F. 2003. 60KDa chaperonin (HSP60) is over-expressed during colorectal carcinogenesis. *Eur J Histochem,* 47**,** 105-10.

CARUSO, A., LICENZIATI, S., CORULLI, M., CANARIS, A. D., DE FRANCESCO, M. A., FIORENTINI, S., PERONI, L., FALLACARA, F., DIMA, F., BALSARI, A. & TURANO, A. 1997. Flow cytometric analysis of activation markers on stimulated T cells and their correlation with cell proliferation. *Cytometry,* 27**,** 71-6.

CAVALLARO, U. & CHRISTOFORI, G. 2004. Multitasking in tumor progression: signaling functions of cell adhesion molecules. *Ann N Y Acad Sci,* 1014**,** 58-66.

CELIS, J. E., KRUHOFFER, M., GROMOVA, I., FREDERIKSEN, C., OSTERGAARD, M., THYKJAER, T., GROMOV, P., YU, J., PALSDOTTIR, H., MAGNUSSON, N. & ORNTOFT, T. F. 2000. Gene expression profiling: monitoring transcription and translation products using DNA microarrays and proteomics. *FEBS Lett,* 480**,** 2-16.

CHADBURN, A., INGHIRAMI, G. & KNOWLES, D. M. 1992. The kinetics and temporal expression of T-cell activation-associated antigens CD15 (LeuM1), CD30 (Ki-1), EMA, and CD11c (LeuM5) by benign activated T cells. *Hematol Pathol,* 6**,** 193-202.

CHAUDHARY, K., DEB, S., MONIAUX, N., PONNUSAMY, M. P. & BATRA, S. K. 2007. Human RNA polymerase II-associated factor complex: dysregulation in cancer. *Oncogene,* 26**,** 7499-507.

CHEN, C. D., KOBAYASHI, R. & HELFMAN, D. M. 1999. Binding of hnRNP H to an exonic splicing silencer is involved in the regulation of alternative splicing of the rat beta-tropomyosin gene. *Genes Dev,* 13**,** 593-606.

CHERETIS, C., DIETRICH, F., CHATZISTAMOU, I., POLITI, K., ANGELIDOU, E., KIARIS, H., MKRTCHIAN, S. & KOUTSELINI, H. 2006. Expression of ERp29, an endoplasmic reticulum secretion factor in basal-cell carcinoma. *Am J Dermatopathol,* 28**,** 410-2.

CHIEN, C. W., LIN, S. C., LAI, Y. Y., LIN, B. W., LEE, J. C. & TSAI, S. J. 2008. Regulation of CD151 by hypoxia controls cell adhesion and metastasis in colorectal cancer. *Clin Cancer Res,* 14**,** 8043-51.

CHRISTENSEN, L., NIELSEN, M., ANDERSEN, J. & CLEMMENSEN, I. 1988. Stromal fibronectin staining pattern and metastasizing ability of human breast carcinoma. *Cancer Res,* 48**,** 6227-33.

CHUNG, Y. F., EU, K. W., MACHIN, D., HO, J. M., NYAM, D. C., LEONG, A. F., HO, Y. H. & SEOW-CHOEN, F. 1998. Young age is not a poor prognostic marker in colorectal cancer. *Br J Surg,* 85**,** 1255-9.

CHUNG, Y. M., YOO, Y. D., PARK, J. K., KIM, Y. T. & KIM, H. J. 2001. Increased expression of peroxiredoxin II confers resistance to cisplatin. *Anticancer Res,* 21**,** 1129-33.

CLEMENT, L. T. 1992. Isoforms of the CD45 common leukocyte antigen family: markers for human T-cell differentiation. *J Clin Immunol,* 12**,** 1-10.

CLEVERS, H., ALARCON, B., WILEMAN, T. & TERHORST, C. 1988. The T cell receptor/CD3 complex: a dynamic protein ensemble. *Annu Rev Immunol,* 6**,** 629-62.

COHEN, P., PEEHL, D. M., GRAVES, H. C. & ROSENFELD, R. G. 1994. Biological effects of prostate specific antigen as an insulin-like growth factor binding protein-3 protease. *J Endocrinol,* 142**,** 407-15.

COMPTON, C. C. 2003. Colorectal carcinoma: diagnostic, prognostic, and molecular features. *Mod Pathol,* 16**,** 376-88.

CONKRIGHT, M. D. & MONTMINY, M. 2005. CREB: the unindicted cancer co-conspirator. *Trends Cell Biol,* 15**,** 457-9.

CORDON-CARDO, C., FUKS, Z., DROBNJAK, M., MORENO, C., EISENBACH, L. & FELDMAN, M. 1991. Expression of HLA-A,B,C antigens on primary and metastatic tumor cell populations of human carcinomas. *Cancer Res,* 51**,** 6372-80.

COUSSENS, L. M. & WERB, Z. 2002. Inflammation and cancer. *Nature,* 420**,** 860-7.

CULLEN, J. J., WEYDERT, C., HINKHOUSE, M. M., RITCHIE, J., DOMANN, F. E., SPITZ, D. & OBERLEY, L. W. 2003. The role of manganese superoxide dismutase in the growth of pancreatic adenocarcinoma. *Cancer Res,* 63**,** 1297-303.

CURTIN, K., LIN, W. Y., GEORGE, R., KATORY, M., SHORTO, J., CANNON-ALBRIGHT, L. A., SMITH, G., BISHOP, D. T., COX, A. & CAMP, N. J. 2009. Genetic variants in XRCC2: new insights into colorectal cancer tumorigenesis. *Cancer Epidemiol Biomarkers Prev,* 18**,** 2476-84.

D'ANGEAC, A. D., MONIER, S., PILLING, D., TRAVAGLIO-ENCINOZA, A., REME, T. & SALMON, M. 1994. CD57+ T lymphocytes are derived from CD57- precursors by differentiation occurring in late immune responses. *Eur J Immunol,* 24**,** 1503-11.

DALERBA, P., CHO, R. W. & CLARKE, M. F. 2007a. Cancer stem cells: models and concepts. *Annu Rev Med,* 58**,** 267-84.

DALERBA, P., DYLLA, S. J., PARK, I. K., LIU, R., WANG, X., CHO, R. W., HOEY, T., GURNEY, A., HUANG, E. H., SIMEONE, D. M., SHELTON, A. A., PARMIANI, G., CASTELLI, C. & CLARKE, M. F. 2007b. Phenotypic characterization of human colorectal cancer stem cells. *Proc Natl Acad Sci U S A,* 104**,** 10158-63.

DALLOUL, A. 2009. CD5: a safeguard against autoimmunity and a shield for cancer cells. *Autoimmun Rev,* 8**,** 349-53.

DAVIES, A., SIMMONS, D. L., HALE, G., HARRISON, R. A., TIGHE, H., LACHMANN, P. J. & WALDMANN, H. 1989. CD59, an LY-6-like protein expressed in human lymphoid cells, regulates the action of the complement membrane attack complex on homologous cells. *J Exp Med,* 170**,** 637-54.

DAVIS, L. S., OPPENHEIMER-MARKS, N., BEDNARCZYK, J. L., MCINTYRE, B. W. & LIPSKY, P. E. 1990. Fibronectin promotes proliferation of naive and memory T cells by signaling through both the VLA-4 and VLA-5 integrin molecules. *J Immunol,* 145**,** 785-93.

DEGRENDELE, H. C., KOSFISZER, M., ESTESS, P. & SIEGELMAN, M. H. 1997. CD44 activation and associated primary adhesion is inducible via T cell receptor stimulation. *J Immunol,* 159**,** 2549-53.

DELOM, F., EMADALI, A., COCOLAKIS, E., LEBRUN, J. J., NANTEL, A. & CHEVET, E. 2007. Calnexin-dependent regulation of tunicamycin-induced apoptosis in breast carcinoma MCF-7 cells. *Cell Death Differ,* 14**,** 586-96.

DENK, H., TAPPEINER, G., ECKERSTORFER, R. & HOLZNER, J. H. 1972. Carcinoembryonic antigen (CEA) in gastrointestinal and extragastrointestinal tumors and its relationship to tumor-cell differentiation. *Int J Cancer,* 10**,** 262-72.

DESCHOOLMEESTER, V., BAAY, M., SPECENIER, P., LARDON, F. & VERMORKEN, J. B. 2010. A review of the most promising biomarkers in colorectal cancer: one step closer to targeted therapy. *Oncologist,* 15**,** 699-731.

DESMEDT, C., OURIAGHLI, F. E., DURBECQ, V., SOREE, A., COLOZZA, M. A., AZAMBUJA, E., PAESMANS, M., LARSIMONT, D., BUYSE, M., HARRIS, A., PICCART, M., MARTIAT, P. & SOTIRIOU, C. 2006. Impact of cyclins E, neutrophil elastase and proteinase 3 expression levels on clinical outcome in primary breast cancer patients. *Int J Cancer,* 119**,** 2539-45.

DIEDERICHSEN, A. C., HJELMBORG, J., CHRISTENSEN, P. B., ZEUTHEN, J. & FENGER, C. 2003. Prognostic value of the CD4+/CD8+ ratio of tumour infiltrating lymphocytes in colorectal cancer and HLA-DR expression on tumour cells. *Cancer Immunol Immunother,* 52**,** 423-8.

DORUDI, S., SHEFFIELD, J. P., POULSOM, R., NORTHOVER, J. M. & HART, I. R. 1993. E-cadherin expression in colorectal cancer. An immunocytochemical and in situ hybridization study. *Am J Pathol,* 142**,** 981-6.

DOWNWARD, J. 2003. Cell biology: metabolism meets death. *Nature,* 424**,** 896-7.

DREHER, D. & JUNOD, A. F. 1996. Role of oxygen free radicals in cancer development. *Eur J Cancer,* 32A**,** 30-8.

DU, M., SANSORES-GARCIA, L., ZU, Z. & WU, K. K. 1998. Cloning and expression analysis of a novel salicylate suppressible gene, Hs-CUL-3, a member of cullin/Cdc53 family. *J Biol Chem,* 273**,** 24289-92.

DUFFY, M. J., VAN DALEN, A., HAGLUND, C., HANSSON, L., HOLINSKI-FEDER, E., KLAPDOR, R., LAMERZ, R., PELTOMAKI, P., STURGEON, C. & TOPOLCAN, O. 2007. Tumour markers in colorectal cancer: European Group on Tumour Markers (EGTM) guidelines for clinical use. *Eur J Cancer,* 43**,** 1348-60.

DUNCAN, R., CARPENTER, B., MAIN, L. C., TELFER, C. & MURRAY, G. I. 2008. Characterisation and protein expression profiling of annexins in colorectal cancer. *Br J Cancer,* 98**,** 426-33.

DURRANT, L. G., CHAPMAN, M. A., BUCKLEY, D. J., SPENDLOVE, I., ROBINS, R. A. & ARMITAGE, N. C. 2003. Enhanced expression of the complement regulatory protein CD55 predicts a poor prognosis in colorectal cancer patients. *Cancer Immunol Immunother,* 52**,** 638-42.

DUSTIN, M. L. & SPRINGER, T. A. 1989. T-cell receptor cross-linking transiently stimulates adhesiveness through LFA-1. *Nature,* 341**,** 619-24.

DWEK, M. V., ROSS, H. A. & LEATHEM, A. J. 2001. Proteome and glycosylation mapping identifies post-translational modifications associated with aggressive breast cancer. *Proteomics,* 1**,** 756-62.

EDMONDS, B. T., WYCKOFF, J., YEUNG, Y. G., WANG, Y., STANLEY, E. R., JONES, J., SEGALL, J. & CONDEELIS, J. 1996. Elongation factor-1 alpha is an overexpressed actin binding protein in metastatic rat mammary adenocarcinoma. *J Cell Sci,* 109 (Pt 11)**,** 2705-14.

EIFEL, P., AXELSON, J. A., COSTA, J., CROWLEY, J., CURRAN, W. J., JR., DESHLER, A., FULTON, S., HENDRICKS, C. B., KEMENY, M., KORNBLITH, A. B., LOUIS, T. A., MARKMAN, M., MAYER, R. & ROTER, D. 2001. National Institutes of Health Consensus Development Conference Statement: adjuvant therapy for breast cancer, November 1-3, 2000. *J Natl Cancer Inst,* 93**,** 979-89.

ESCHRICH, S., YANG, I., BLOOM, G., KWONG, K. Y., BOULWARE, D., CANTOR, A., COPPOLA, D., KRUHOFFER, M., AALTONEN, L., ORNTOFT, T. F., QUACKENBUSH, J. & YEATMAN, T. J. 2005. Molecular staging for survival prediction of colorectal cancer patients. *J Clin Oncol,* 23**,** 3526-35.

FANG, J. Y. & RICHARDSON, B. C. 2005. The MAPK signalling pathways and colorectal cancer. *Lancet Oncol,* 6**,** 322-7.

FEARON, E. R. & JONES, P. A. 1992. Progressing toward a molecular description of colorectal cancer development. *FASEB J,* 6**,** 2783-90.

FEARON, E. R. & VOGELSTEIN, B. 1990. A genetic model for colorectal tumorigenesis. *Cell,* 61**,** 759-67.

FERNEBRO, E., BENDAHL, P. O., DICTOR, M., PERSSON, A., FERNO, M. & NILBERT, M. 2004. Immunohistochemical patterns in rectal cancer: application of tissue microarray with prognostic correlations. *Int J Cancer,* 111**,** 921-8.

FIDLER, I. J. 1970. Metastasis: guantitative analysis of distribution and fate of tumor embolilabeled with 125 I-5-iodo-2'-deoxyuridine. *J Natl Cancer Inst,* 45**,** 773-82.

FIELDING, L. P., ARSENAULT, P. A., CHAPUIS, P. H., DENT, O., GATHRIGHT, B., HARDCASTLE, J. D., HERMANEK, P., JASS, J. R. & NEWLAND, R. C. 1991. Clinicopathological staging for colorectal cancer: an International Documentation System (IDS) and an International Comprehensive Anatomical Terminology (ICAT). *J Gastroenterol Hepatol,* 6**,** 325-44.

FLEISCHER, B. 1994. CD26: a surface protease involved in T-cell activation. *Immunol Today,* 15**,** 180-4.

FLOYD, C. M., IRANI, K., KIND, P. D. & KESSLER, C. M. 1992. von Willebrand factor interacts with malignant hematopoietic cell lines: evidence for the presence of specific binding sites and modification of von Willebrand factor structure and function. *J Lab Clin Med,* 119**,** 467-76.

FODDE, R., KUIPERS, J., ROSENBERG, C., SMITS, R., KIELMAN, M., GASPAR, C., VAN ES, J. H., BREUKEL, C., WIEGANT, J., GILES, R. H. & CLEVERS, H. 2001. Mutations in the APC tumour suppressor gene cause chromosomal instability. *Nat Cell Biol,* 3**,** 433-8.

FORSSELL, J., OBERG, A., HENRIKSSON, M. L., STENLING, R., JUNG, A. & PALMQVIST, R. 2007. High macrophage infiltration along the tumor front correlates with improved survival in colon cancer. *Clin Cancer Res,* 13**,** 1472-9.

FRIEDLEIN, G., EL HAGE, F., VERGNON, I., RICHON, C., SAULNIER, P., LECLUSE, Y., CAIGNARD, A., BOUMSELL, L., BISMUTH, G., CHOUAIB, S. & MAMI-CHOUAIB, F. 2007. Human CD5 protects circulating tumor antigen-specific CTL from tumor-mediated activation-induced cell death. *J Immunol,* 178**,** 6821-7.

FRIEDMAN, D. B., HILL, S., KELLER, J. W., MERCHANT, N. B., LEVY, S. E., COFFEY, R. J. & CAPRIOLI, R. M. 2004. Proteome analysis of human colon cancer by two-dimensional difference gel electrophoresis and mass spectrometry. *Proteomics,* 4**,** 793-811.

GARRIDO, F., CABRERA, T., CONCHA, A., GLEW, S., RUIZ-CABELLO, F. & STERN, P. L. 1993. Natural history of HLA expression during tumour development. *Immunol Today,* 14**,** 491-9.

GATENBY, R. A. & GAWLINSKI, E. T. 1996. A reaction-diffusion model of cancer invasion. *Cancer Res,* 56**,** 5745-53.

GATENBY, R. A. & GILLIES, R. J. 2004. Why do cancers have high aerobic glycolysis? *Nat Rev Cancer,* 4**,** 891-9.

GATENBY, R. A. & GILLIES, R. J. 2007. Glycolysis in cancer: a potential target for therapy. *Int J Biochem Cell Biol,* 39**,** 1358-66.

GEORGOPOULOS, N. T., MERRICK, A., SCOTT, N., SELBY, P. J., MELCHER, A. & TREJDOSIEWICZ, L. K. 2007. CD40-mediated death and cytokine secretion in colorectal cancer: a potential target for inflammatory tumour cell killing. *Int J Cancer,* 121**,** 1373-81.

GIATROMANOLAKI, A., KOUKOURAKIS, M. I., SIVRIDIS, E., PASTOREK, J., WYKOFF, C. C., GATTER, K. C. & HARRIS, A. L. 2001. Expression of hypoxia-inducible carbonic anhydrase-9 relates to angiogenic pathways and independently to poor outcome in non-small cell lung cancer. *Cancer Res,* 61**,** 7992-8.

GIL-BAZO, I. 2007. Novel translational strategies in colorectal cancer research. *World J Gastroenterol,* 13**,** 5902-10.

GOLDSTEIN, M. J. & MITCHELL, E. P. 2005. Carcinoembryonic antigen in the staging and follow-up of patients with colorectal cancer. *Cancer Invest,* 23**,** 338-51.

GREAVES, M. & MALEY, C. C. 2012. Clonal evolution in cancer. *Nature,* 481**,** 306-13.

GREENSON, J. K., HUANG, S. C., HERRON, C., MORENO, V., BONNER, J. D., TOMSHO, L. P., BEN-IZHAK, O., COHEN, H. I., TROUGOUBOFF, P., BEJHAR, J., SOVA, Y., PINCHEV, M., RENNERT, G. & GRUBER, S. B. 2009. Pathologic predictors of microsatellite instability in colorectal cancer. *Am J Surg Pathol,* 33**,** 126-33.

GRISENDI, S., MECUCCI, C., FALINI, B. & PANDOLFI, P. P. 2006. Nucleophosmin and cancer. *Nat Rev Cancer,* 6**,** 493-505.

GU, H. & NEEL, B. G. 2003. The "Gab" in signal transduction. *Trends Cell Biol,* 13**,** 122-30.

GU, M., FABREGA, C., LIU, S. W., LIU, H., KILEDJIAN, M. & LIMA, C. D. 2004. Insights into the structure, mechanism, and regulation of scavenger mRNA decapping activity. *Mol Cell,* 14**,** 67-80.

GUPTA, G. P. & MASSAGUE, J. 2006. Cancer metastasis: building a framework. *Cell,* 127**,** 679-95.

GYGI, S. P., CORTHALS, G. L., ZHANG, Y., ROCHON, Y. & AEBERSOLD, R. 2000. Evaluation of two-dimensional gel electrophoresis-based proteome analysis technology. *Proc Natl Acad Sci U S A,* 97**,** 9390-5.

GYGI, S. P., ROCHON, Y., FRANZA, B. R. & AEBERSOLD, R. 1999. Correlation between protein and mRNA abundance in yeast. *Mol Cell Biol,* 19**,** 1720-30.

HAAB, B. B. 2005. Antibody arrays in cancer research. *Mol Cell Proteomics,* 4**,** 377-83.

HABERMANN, J. K., BADER, F. G., FRANKE, C., ZIMMERMANN, K., GEMOLL, T., FRITZSCHE, B., RIED, T., AUER, G., BRUCH, H. P. & ROBLICK, U. J. 2008. From the genome to the proteome--biomarkers in colorectal cancer. *Langenbecks Arch Surg,* 393**,** 93-104.

HAHNE, M., RIMOLDI, D., SCHROTER, M., ROMERO, P., SCHREIER, M., FRENCH, L. E., SCHNEIDER, P., BORNAND, T., FONTANA, A., LIENARD, D., CEROTTINI, J. & TSCHOPP, J. 1996. Melanoma cell expression of Fas(Apo-1/CD95) ligand: implications for tumor immune escape. *Science,* 274**,** 1363-6.

HALAMA, N., MICHEL, S., KLOOR, M., ZOERNIG, I., POMMERENCKE, T., VON KNEBEL DOEBERITZ, M., SCHIRMACHER, P., WEITZ, J., GRABE, N. & JAGER, D. 2009. The localization and density of immune cells in primary tumors of human metastatic colorectal cancer shows an association with response to chemotherapy. *Cancer Immun,* 9**,** 1.

HALLBORN, J. & CARLSSON, R. 2002. Automated screening procedure for high-throughput generation of antibody fragments. *Biotechniques,* Suppl**,** 30-7.

HAMELINCK, D., ZHOU, H., LI, L., VERWEIJ, C., DILLON, D., FENG, Z., COSTA, J. & HAAB, B. B. 2005. Optimized normalization for antibody microarrays and application to serum-protein profiling. *Mol Cell Proteomics,* 4**,** 773-84.

HANASH, S. 2003. Disease proteomics. *Nature,* 422**,** 226-32.

HANES, J., SCHAFFITZEL, C., KNAPPIK, A. & PLUCKTHUN, A. 2000. Picomolar affinity antibodies from a fully synthetic naive library selected and evolved by ribosome display. *Nat Biotechnol,* 18**,** 1287-92.

HART, I. R. & SAINI, A. 1992. Biology of tumour metastasis. *Lancet,* 339**,** 1453-7.

HASEGAWA, H., UTSUNOMIYA, Y., KISHIMOTO, K., YANAGISAWA, K. & FUJITA, S. 1996. SFA-1, a novel cellular gene induced by human T-cell leukemia virus type 1, is a member of the transmembrane 4 superfamily. *J Virol,* 70**,** 3258-63.

HASHIDA, H., TAKABAYASHI, A., KANAI, M., ADACHI, M., KONDO, K., KOHNO, N., YAMAOKA, Y. & MIYAKE, M. 2002. Aminopeptidase N is involved in cell motility and angiogenesis: its clinical significance in human colon cancer. *Gastroenterology,* 122**,** 376-86.

HASTINGS, M. L., WILSON, C. M. & MUNROE, S. H. 2001. A purine-rich intronic element enhances alternative splicing of thyroid hormone receptor mRNA. *RNA,* 7**,** 859-74.

HAVENITH, M. G., ARENDS, J. W., SIMON, R., VOLOVICS, A., WIGGERS, T. & BOSMAN, F. T. 1988. Type IV collagen immunoreactivity in colorectal cancer. Prognostic value of basement membrane deposition. *Cancer,* 62**,** 2207-11.

HAYES, J. D. & MCMAHON, M. 2009. NRF2 and KEAP1 mutations: permanent activation of an adaptive response in cancer. *Trends Biochem Sci,* 34**,** 176-88.

HELMLINGER, G., YUAN, F., DELLIAN, M. & JAIN, R. K. 1997. Interstitial pH and pO2 gradients in solid tumors in vivo: high-resolution measurements reveal a lack of correlation. *Nat Med,* 3**,** 177-82.

HERMAN, J. F., MANGALA, L. S. & MEHTA, K. 2006. Implications of increased tissue transglutaminase (TG2) expression in drug-resistant breast cancer (MCF-7) cells. *Oncogene,* 25**,** 3049-58.

HLUBEK, F., BRABLETZ, T., BUDCZIES, J., PFEIFFER, S., JUNG, A. & KIRCHNER, T. 2007. Heterogeneous expression of Wnt/beta-catenin target genes within colorectal cancer. *Int J Cancer,* 121**,** 1941-8.

HOFF, S. D., IRIMURA, T., MATSUSHITA, Y., OTA, D. M., CLEARY, K. R. & HAKOMORI, S. 1990. Metastatic potential of colon carcinoma. Expression of ABO/Lewis-related antigens. *Arch Surg,* 125**,** 206-9.

HOFSETH, L. J. & YING, L. 2006. Identifying and defusing weapons of mass inflammation in carcinogenesis. *Biochim Biophys Acta,* 1765**,** 74-84.

HOLZMANN, B. & WEISSMAN, I. L. 1989. Peyer's patch-specific lymphocyte homing receptors consist of a VLA-4-like alpha chain associated with either of two integrin beta chains, one of which is novel. *EMBO J,* 8**,** 1735-41.

HOMANN, N. 2001. Alcohol and upper gastrointestinal tract cancer: the role of local acetaldehyde production. *Addict Biol,* 6**,** 309-323.

HONORE, B., BAANDRUP, U. & VORUM, H. 2004. Heterogeneous nuclear ribonucleoproteins F and H/H' show differential expression in normal and selected cancer tissues. *Exp Cell Res,* 294**,** 199-209.

HORMAN, S., FOKAN, D. & GALAND, P. 2000. MCF-7 mammary tumour cells express the myeloid cell differentiation controlling factor, serine protease 3/myeloblastin. *Cell Prolif,* 33**,** 331-40.

HSIEH, Y., GUAN, Y., TU, C., BRATT, P. J., ANGERHOFER, A., LEPOCK, J. R., HICKEY, M. J., TAINER, J. A., NICK, H. S. & SILVERMAN, D. N. 1998. Probing the active site of human manganese superoxide dismutase: the role of glutamine 143. *Biochemistry,* 37**,** 4731-9.

HUANG, R. P., HUANG, R., FAN, Y. & LIN, Y. 2001. Simultaneous detection of multiple cytokines from conditioned media and patient's sera by an antibody-based protein array system. *Anal Biochem,* 294**,** 55-62.

HUANG, S. & CHAKRABARTY, S. 1994. Regulation of fibronectin and laminin receptor expression, fibronectin and laminin secretion in human colon cancer cells by transforming growth factor-beta 1. *Int J Cancer,* 57**,** 742-6.

HUEHN, J., SIEGMUND, K., LEHMANN, J. C., SIEWERT, C., HAUBOLD, U., FEUERER, M., DEBES, G. F., LAUBER, J., FREY, O., PRZYBYLSKI, G. K., NIESNER, U., DE LA ROSA, M., SCHMIDT, C. A., BRAUER, R., BUER, J., SCHEFFOLD, A. & HAMANN, A. 2004. Developmental stage, phenotype, and migration distinguish naive- and effector/memory-like CD4+ regulatory T cells. *J Exp Med,* 199**,** 303-13.

INOUE, J., GOHDA, J., AKIYAMA, T. & SEMBA, K. 2007. NF-kappaB activation in development and progression of cancer. *Cancer Sci,* 98**,** 268-74.

ISHIHAMA, K., YAMAKAWA, M., SEMBA, S., TAKEDA, H., KAWATA, S., KIMURA, S. & KIMURA, W. 2007. Expression of HDAC1 and CBP/p300 in human colorectal carcinomas. *J Clin Pathol,* 60**,** 1205-10.

ISSEKUTZ, T. B. 1991. Inhibition of in vivo lymphocyte migration to inflammation and homing to lymphoid tissues by the TA-2 monoclonal antibody. A likely role for VLA-4 in vivo. *J Immunol,* 147**,** 4178-84.

IVANOV, S., LIAO, S. Y., IVANOVA, A., DANILKOVITCH-MIAGKOVA, A., TARASOVA, N., WEIRICH, G., MERRILL, M. J., PROESCHOLDT, M. A., OLDFIELD, E. H., LEE, J., ZAVADA, J., WAHEED, A., SLY, W., LERMAN, M. I. & STANBRIDGE, E. J. 2001. Expression of hypoxia-inducible cell-surface transmembrane carbonic anhydrases in human cancer. *Am J Pathol,* 158**,** 905-19.

JAISWAL, S., JAMIESON, C. H., PANG, W. W., PARK, C. Y., CHAO, M. P., MAJETI, R., TRAVER, D., VAN ROOIJEN, N. & WEISSMAN, I. L. 2009. CD47 is upregulated on circulating hematopoietic stem cells and leukemia cells to avoid phagocytosis. *Cell,* 138**,** 271-85.

JANEWAY, C. A., JR. 1992. The T cell receptor as a multicomponent signalling machine: CD4/CD8 coreceptors and CD45 in T cell activation. *Annu Rev Immunol,* 10**,** 645-74.

JANG, J. S., CHO, H. Y., LEE, Y. J., HA, W. S. & KIM, H. W. 2004. The differential proteome profile of stomach cancer: identification of the biomarker candidates. *Oncol Res,* 14**,** 491-9.

JANTSCHEFF, P., TERRACCIANO, L., LOWY, A., GLATZ-KRIEGER, K., GRUNERT, F., MICHEEL, B., BRUMMER, J., LAFFER, U., METZGER, U., HERRMANN, R. & ROCHLITZ, C. 2003. Expression of CEACAM6 in resectable colorectal cancer: a factor of independent prognostic significance. *J Clin Oncol,* 21**,** 3638-46.

JASS, J. R., ATKIN, W. S., CUZICK, J., BUSSEY, H. J., MORSON, B. C., NORTHOVER, J. M. & TODD, I. P. 1986. The grading of rectal cancer: historical perspectives and a multivariate analysis of 447 cases. *Histopathology,* 10**,** 437-59.

JEDINAK, A., DUDHGAONKAR, S. & SLIVA, D. 2010. Activated macrophages induce metastatic behavior of colon cancer cells. *Immunobiology,* 215**,** 242-9.

JELSKI, W., ZALEWSKI, B., CHROSTEK, L. & SZMITKOWSKI, M. 2004. The activity of class I, II, III, and IV alcohol dehydrogenase isoenzymes and aldehyde dehydrogenase in colorectal cancer. *Dig Dis Sci,* 49**,** 977-81.

JIMENEZ, C. R., KNOL, J. C., MEIJER, G. A. & FIJNEMAN, R. J. 2010. Proteomics of colorectal cancer: overview of discovery studies and identification of commonly identified cancer-associated proteins and candidate CRC serum markers. *J Proteomics,* 73**,** 1873-95.

JIN, H. & VARNER, J. 2004. Integrins: roles in cancer development and as treatment targets. *Br J Cancer,* 90**,** 561-5.

JOST, C. A., MARIN, M. C. & KAELIN, W. G., JR. 1997. p73 is a simian [correction of human] p53-related protein that can induce apoptosis. *Nature,* 389**,** 191-4.

JU, S. T., PANKA, D. J., CUI, H., ETTINGER, R., EL-KHATIB, M., SHERR, D. H., STANGER, B. Z. & MARSHAK-ROTHSTEIN, A. 1995. Fas(CD95)/FasL interactions required for programmed cell death after T-cell activation. *Nature,* 373**,** 444-8.

KAIFI, J. T., REICHELT, U., QUAAS, A., SCHURR, P. G., WACHOWIAK, R., YEKEBAS, E. F., STRATE, T., SCHNEIDER, C., PANTEL, K., SCHACHNER, M., SAUTER, G. & IZBICKI, J. R. 2007. L1 is associated with micrometastatic spread and poor outcome in colorectal cancer. *Mod Pathol,* 20**,** 1183-90.

KAIRA, K., ORIUCHI, N., IMAI, H., SHIMIZU, K., YANAGITANI, N., SUNAGA, N., HISADA, T., TANAKA, S., ISHIZUKA, T., KANAI, Y., ENDOU, H., NAKAJIMA, T. & MORI, M. 2008. l-type amino acid transporter 1 and CD98 expression in primary and metastatic sites of human neoplasms. *Cancer Sci,* 99**,** 2380-6.

KALER, P., GALEA, V., AUGENLICHT, L. & KLAMPFER, L. 2010. Tumor associated macrophages protect colon cancer cells from TRAIL-induced apoptosis through IL-1beta-dependent stabilization of Snail in tumor cells. *PLoS One,* 5**,** e11700.

KALLURI, R. & ZEISBERG, M. 2006. Fibroblasts in cancer. *Nat Rev Cancer,* 6**,** 392-401.

KANAZAWA, T., WATANABE, T. & NAGAWA, H. 2003. Does early polypoid colorectal cancer with depression have a pathway other than adenoma-carcinoma sequence? *Tumori,* 89**,** 408-11.

KARASHIMA, S., KATAOKA, H., ITOH, H., MARUYAMA, R. & KOONO, M. 1990. Prognostic significance of alpha-1-antitrypsin in early stage of colorectal carcinomas. *Int J Cancer,* 45**,** 244-50.

KATAYAMA, M., NAKANO, H., ISHIUCHI, A., WU, W., OSHIMA, R., SAKURAI, J., NISHIKAWA, H., YAMAGUCHI, S. & OTSUBO, T. 2006. Protein pattern difference in the colon cancer cell lines examined by two-dimensional differential in-gel electrophoresis and mass spectrometry. *Surg Today,* 36**,** 1085-93.

KATZ, S. C., PILLARISETTY, V., BAMBOAT, Z. M., SHIA, J., HEDVAT, C., GONEN, M., JARNAGIN, W., FONG, Y., BLUMGART, L., D'ANGELICA, M. & DEMATTEO, R. P. 2009. T cell infiltrate predicts long-term survival following resection of colorectal cancer liver metastases. *Ann Surg Oncol,* 16**,** 2524-30.

KAUFMAN, K. L., BELOV, L., HUANG, P., MACTIER, S., SCOLYER, R. A., MANN, G. J. & CHRISTOPHERSON, R. I. 2010. An extended antibody microarray for surface profiling metastatic melanoma. *J Immunol Methods,* 358**,** 23-34.

KAWASAKI, H., ALTIERI, D. C., LU, C. D., TOYODA, M., TENJO, T. & TANIGAWA, N. 1998. Inhibition of apoptosis by survivin predicts shorter survival rates in colorectal cancer. *Cancer Res,* 58**,** 5071-4.

KIM, H. J., KANG, H. J., LEE, H., LEE, S. T., YU, M. H., KIM, H. & LEE, C. 2009. Identification of S100A8 and S100A9 as serological markers for colorectal cancer. *J Proteome Res,* 8**,** 1368-79.

KINZLER, K. W. & VOGELSTEIN, B. 1996. Lessons from hereditary colorectal cancer. *Cell,* 87**,** 159-70.

KLINTRUP, K., MAKINEN, J. M., KAUPPILA, S., VARE, P. O., MELKKO, J., TUOMINEN, H., TUPPURAINEN, K., MAKELA, J., KARTTUNEN, T. J. & MAKINEN, M. J. 2005. Inflammation and prognosis in colorectal cancer. *Eur J Cancer,* 41**,** 2645-54.

KNEZEVIC, V., LEETHANAKUL, C., BICHSEL, V. E., WORTH, J. M., PRABHU, V. V., GUTKIND, J. S., LIOTTA, L. A., MUNSON, P. J., PETRICOIN, E. F., 3RD & KRIZMAN, D. B. 2001. Proteomic profiling of the cancer microenvironment by antibody arrays. *Proteomics,* 1**,** 1271-8.

KOPETZ, S., FREITAS, D., CALABRICH, A. F. & HOFF, P. M. 2008. Adjuvant chemotherapy for stage II colon cancer. *Oncology (Williston Park),* 22**,** 260-70; discussion 270, 273, 275.

KORETZ, K., BRUDERLEIN, S., HENNE, C. & MOLLER, P. 1993. Expression of CD59, a complement regulator protein and a second ligand of the CD2 molecule, and CD46 in normal and neoplastic colorectal epithelium. *Br J Cancer,* 68**,** 926-31.

KORTY, P. E., BRANDO, C. & SHEVACH, E. M. 1991. CD59 functions as a signal-transducing molecule for human T cell activation. *J Immunol,* 146**,** 4092-8.

KOTHANDARAMAN, N., BAJIC, V. B., BRENDAN, P. N., HUAK, C. Y., KEOW, P. B., RAZVI, K., SALTO-TELLEZ, M. & CHOOLANI, M. 2010. E2F5 status significantly improves malignancy diagnosis of epithelial ovarian cancer. *BMC Cancer,* 10**,** 64.

KRENSKY, A. M., SANCHEZ-MADRID, F., ROBBINS, E., NAGY, J. A., SPRINGER, T. A. & BURAKOFF, S. J. 1983. The functional significance, distribution, and structure of LFA-1, LFA-2, and LFA-3: cell surface antigens associated with CTL-target interactions. *J Immunol,* 131**,** 611-6.

KURAMITSU, Y. & NAKAMURA, K. 2006. Proteomic analysis of cancer tissues: shedding light on carcinogenesis and possible biomarkers. *Proteomics,* 6**,** 5650-61.

KWAK, M. K., WAKABAYASHI, N., GREENLAW, J. L., YAMAMOTO, M. & KENSLER, T. W. 2003. Antioxidants enhance mammalian proteasome expression through the Keap1-Nrf2 signaling pathway. *Mol Cell Biol,* 23**,** 8786-94.

LAMMERT, E., STEVANOVIC, S., BRUNNER, J., RAMMENSEE, H. G. & SCHILD, H. 1997. Protein disulfide isomerase is the dominant acceptor for peptides translocated into the endoplasmic reticulum. *Eur J Immunol,* 27**,** 1685-90.

LAWEN, A., LY, J. D., LANE, D. J., ZARSCHLER, K., MESSINA, A. & DE PINTO, V. 2005. Voltage-dependent anion-selective channel 1 (VDAC1)--a mitochondrial protein, rediscovered as a novel enzyme in the plasma membrane. *Int J Biochem Cell Biol,* 37**,** 277-82.

LAWRIE, L. C. & CURRAN, S. 2005. Laser capture microdissection and colorectal cancer proteomics. *Methods Mol Biol,* 293**,** 245-53.

LE NAOUR, F., ANDRE, M., GRECO, C., BILLARD, M., SORDAT, B., EMILE, J. F., LANZA, F., BOUCHEIX, C. & RUBINSTEIN, E. 2006. Profiling of the tetraspanin web of human colon cancer cells. *Mol Cell Proteomics,* 5**,** 845-57.

LEE, W. S., PARK, S., LEE, W. Y., YUN, S. H. & CHUN, H. K. 2010. Clinical impact of tumor-infiltrating lymphocytes for survival in stage II colon cancer. *Cancer,* 116**,** 5188-99.

LEE, W. T. & VITETTA, E. S. 1991. The differential expression of homing and adhesion molecules on virgin and memory T cells in the mouse. *Cell Immunol,* 132**,** 215-22.

LEHNINGER, A. L. 1972. *Biochemistry: The molecular basis of cell structure and function,* New York, Worth publishers.

LENDECKEL, U., WEX, T., REINHOLD, D., KAHNE, T., FRANK, K., FAUST, J., NEUBERT, K. & ANSORGE, S. 1996. Induction of the membrane alanyl aminopeptidase gene and surface expression in human T-cells by mitogenic activation. *Biochem J,* 319 (Pt 3)**,** 817-21.

LEROITH, D. & ROBERTS, C. T., JR. 2003. The insulin-like growth factor system and cancer. *Cancer Lett,* 195**,** 127-37.

LESSEY, B. A., ALBELDA, S., BUCK, C. A., CASTELBAUM, A. J., YEH, I., KOHLER, M. & BERCHUCK, A. 1995. Distribution of integrin cell adhesion molecules in endometrial cancer. *Am J Pathol,* 146**,** 717-26.

LEVESQUE, M., HU, H., D'COSTA, M. & DIAMANDIS, E. P. 1995. Prostate-specific antigen expression by various tumors. *J Clin Lab Anal,* 9**,** 123-8.

LEVY, S. & SHOHAM, T. 2005. The tetraspanin web modulates immune-signalling complexes. *Nat Rev Immunol,* 5**,** 136-48.

LI, F., TIEDE, B., MASSAGUE, J. & KANG, Y. 2007a. Beyond tumorigenesis: cancer stem cells in metastasis. *Cell Res,* 17**,** 3-14.

LI, J. Q., XU, B. J., SHAKHTOUR, B., DEANE, N., MERCHANT, N., HESLIN, M. J., WASHINGTON, K., COFFEY, R. J., BEAUCHAMP, R. D., SHYR, Y. & BILLHEIMER, D. 2007b. Variability of in situ proteomic profiling and implications for study design in colorectal tumors. *Int J Oncol,* 31**,** 103-11.

LIU, J., BEQAJ, S., YANG, Y., HONORE, B. & SCHUGER, L. 2001. Heterogeneous nuclear ribonucleoprotein-H plays a suppressive role in visceral myogenesis. *Mech Dev,* 104**,** 79-87.

LIU, L., WANG, S., ZHANG, Q. & DING, Y. 2008. Identification of potential genes/proteins regulated by Tiam1 in colorectal cancer by microarray analysis and proteome analysis. *Cell Biol Int,* 32**,** 1215-22.

LIU, R., OBERLEY, T. D. & OBERLEY, L. W. 1997. Transfection and expression of MnSOD cDNA decreases tumor malignancy of human oral squamous carcinoma SCC-25 cells. *Hum Gene Ther,* 8**,** 585-95.

LUQUE-GARCIA, J. L., MARTINEZ-TORRECUADRADA, J. L., EPIFANO, C., CANAMERO, M., BABEL, I. & CASAL, J. I. 2010. Differential protein expression on the cell surface of colorectal cancer cells associated to tumor metastasis. *Proteomics,* 10**,** 940-52.

LUTZ, P. G., MOOG-LUTZ, C., COUMAU-GATBOIS, E., KOBARI, L., DI GIOIA, Y. & CAYRE, Y. E. 2000. Myeloblastin is a granulocyte colony-stimulating factor-responsive gene conferring factor-independent growth to hematopoietic cells. *Proc Natl Acad Sci U S A,* 97**,** 1601-6.

LYALL, M. S., DUNDAS, S. R., CURRAN, S. & MURRAY, G. I. 2006. Profiling markers of prognosis in colorectal cancer. *Clin Cancer Res,* 12**,** 1184-91.

MAGNANI, J. L., NILSSON, B., BROCKHAUS, M., ZOPF, D., STEPLEWSKI, Z., KOPROWSKI, H. & GINSBURG, V. 1982. A monoclonal antibody-defined antigen associated with gastrointestinal cancer is a ganglioside containing sialylated lacto-N-fucopentaose II. *J Biol Chem,* 257**,** 14365-9.

MAHE, D., FISCHER, N., DECIMO, D. & FUCHS, J. P. 2000. Spatiotemporal regulation of hnRNP M and 2H9 gene expression during mouse embryonic development. *Biochim Biophys Acta,* 1492**,** 414-24.

MAILLOUX, R. J., BERIAULT, R., LEMIRE, J., SINGH, R., CHENIER, D. R., HAMEL, R. D. & APPANNA, V. D. 2007. The tricarboxylic acid cycle, an ancient metabolic network with a novel twist. *PLoS One,* 2**,** e690.

MANN, A. P., VERMA, A., SETHI, G., MANAVATHI, B., WANG, H., FOK, J. Y., KUNNUMAKKARA, A. B., KUMAR, R., AGGARWAL, B. B. & MEHTA, K. 2006. Overexpression of tissue transglutaminase leads to constitutive activation of nuclear factor-kappaB in cancer cells: delineation of a novel pathway. *Cancer Res,* 66**,** 8788-95.

MANN, M. 2006. Functional and quantitative proteomics using SILAC. *Nat Rev Mol Cell Biol,* 7**,** 952-8.

MANNI, A., WRIGHT, C., BADGER, B., BARTHOLOMEW, M., HERLYN, M., MENDELSOHN, J., MASUI, H. & DEMERS, L. 1990. Role of transforming growth factor-alpha-related peptides in the autocrine/paracrine control of experimental breast cancer growth in vitro by estradiol, prolactin, and progesterone. *Breast Cancer Res Treat,* 15**,** 73-83.

MANTOVANI, A., ALLAVENA, P., SICA, A. & BALKWILL, F. 2008. Cancer-related inflammation. *Nature,* 454**,** 436-44.

MARCIAL, M. A., GONZALEZ, A. & RAMOS RUIZ, E. 1993. Colorectal carcinoma: a pathologic and immunopathologic study. *P R Health Sci J,* 12**,** 183-7.

MAROUN, C. R., HOLGADO-MADRUGA, M., ROYAL, I., NAUJOKAS, M. A., FOURNIER, T. M., WONG, A. J. & PARK, M. 1999. The Gab1 PH domain is required for localization of Gab1 at sites of cell-cell contact and epithelial morphogenesis downstream from the met receptor tyrosine kinase. *Mol Cell Biol,* 19**,** 1784-99.

MATSUOKA, S., EDWARDS, M. C., BAI, C., PARKER, S., ZHANG, P., BALDINI, A., HARPER, J. W. & ELLEDGE, S. J. 1995. p57KIP2, a structurally distinct member of the p21CIP1 Cdk inhibitor family, is a candidate tumor suppressor gene. *Genes Dev,* 9**,** 650-62.

MATSUSHITA, K., TAKENOUCHI, T., SHIMADA, H., TOMONAGA, T., HAYASHI, H., SHIOYA, A., KOMATSU, A., MATSUBARA, H. & OCHIAI, T. 2006. Strong HLA-DR antigen expression on cancer cells relates to better prognosis of colorectal cancer patients: Possible involvement of c-myc suppression by interferon-gamma in situ. *Cancer Sci,* 97**,** 57-63.

MAYER, A., TAKIMOTO, M., FRITZ, E., SCHELLANDER, G., KOFLER, K. & LUDWIG, H. 1993. The prognostic significance of proliferating cell nuclear antigen, epidermal growth factor receptor, and mdr gene expression in colorectal cancer. *Cancer,* 71**,** 2454-60.

MCALLISTER, S. S. & WEINBERG, R. A. 2010. Tumor-host interactions: a far-reaching relationship. *J Clin Oncol,* 28**,** 4022-8.

MCKEEHAN, W. L., SAKAGAMI, Y., HOSHI, H. & MCKEEHAN, K. A. 1986. Two apparent human endothelial cell growth factors from human hepatoma cells are tumor-associated proteinase inhibitors. *J Biol Chem,* 261**,** 5378-83.

MEHTA, K., SHAHID, U. & MALAVASI, F. 1996. Human CD38, a cell-surface protein with multiple functions. *FASEB J,* 10**,** 1408-17.

MELIS, R. & WHITE, R. 1999. Characterization of colonic polyps by two-dimensional gel electrophoresis. *Electrophoresis,* 20**,** 1055-64.

MENGER, M. D. & VOLLMAR, B. 1996. Adhesion molecules as determinants of disease: from molecular biology to surgical research. *Br J Surg,* 83**,** 588-601.

MERLO, L. M., PEPPER, J. W., REID, B. J. & MALEY, C. C. 2006. Cancer as an evolutionary and ecological process. *Nat Rev Cancer,* 6**,** 924-35.

MESTDAGH, P., VAN VLIERBERGHE, P., DE WEER, A., MUTH, D., WESTERMANN, F., SPELEMAN, F. & VANDESOMPELE, J. 2009. A novel and universal method for microRNA RT-qPCR data normalization. *Genome Biol,* 10**,** R64.

MIN, H., CHAN, R. C. & BLACK, D. L. 1995. The generally expressed hnRNP F is involved in a neural-specific pre-mRNA splicing event. *Genes Dev,* 9**,** 2659-71.

MINARD, M. E., ELLIS, L. M. & GALLICK, G. E. 2006. Tiam1 regulates cell adhesion, migration and apoptosis in colon tumor cells. *Clin Exp Metastasis,* 23**,** 301-13.

MIYAGI, T., TATSUMI, T., TAKEHARA, T., KANTO, T., KUZUSHITA, N., SUGIMOTO, Y., JINUSHI, M., KASAHARA, A., SASAKI, Y., HORI, M. & HAYASHI, N. 2003. Impaired expression of proteasome subunits and human leukocyte antigens class I in human colon cancer cells. *J Gastroenterol Hepatol,* 18**,** 32-40.

MIYOSHI, N., ISHII, H., MIMORI, K., TANAKA, F., HITORA, T., TEI, M., SEKIMOTO, M., DOKI, Y. & MORI, M. 2010. TGM2 is a novel marker for prognosis and therapeutic target in colorectal cancer. *Ann Surg Oncol,* 17**,** 967-72.

MIZOGUCHI, H., O'SHEA, J. J., LONGO, D. L., LOEFFLER, C. M., MCVICAR, D. W. & OCHOA, A. C. 1992. Alterations in signal transduction molecules in T lymphocytes from tumor-bearing mice. *Science,* 258**,** 1795-8.

MOENNER, M., PLUQUET, O., BOUCHECAREILH, M. & CHEVET, E. 2007. Integrated endoplasmic reticulum stress responses in cancer. *Cancer Res,* 67**,** 10631-4.

MOLDAVE, K. 1985. Eukaryotic protein synthesis. *Annu Rev Biochem,* 54**,** 1109-49.

MOLLER, P., KORETZ, K., LEITHAUSER, F., BRUDERLEIN, S., HENNE, C., QUENTMEIER, A. & KRAMMER, P. H. 1994. Expression of APO-1 (CD95), a member of the NGF/TNF receptor superfamily, in normal and neoplastic colon epithelium. *Int J Cancer,* 57**,** 371-7.

MOLNAR, L., KOVES, I. & BESZNYAK, I. 1994. Malignant colorectal tumours in young adults. *Acta Chir Hung,* 34**,** 133-8.

MOOK, O. R., FREDERIKS, W. M. & VAN NOORDEN, C. J. 2004. The role of gelatinases in colorectal cancer progression and metastasis. *Biochim Biophys Acta,* 1705**,** 69-89.

MORI, T., LI, Y., HATA, H. & KOCHI, H. 2004. NIRF is a ubiquitin ligase that is capable of ubiquitinating PCNP, a PEST-containing nuclear protein. *FEBS Lett,* 557**,** 209-14.

MORRIS, E. J., MAUGHAN, N. J., FORMAN, D. & QUIRKE, P. 2007. Who to treat with adjuvant therapy in Dukes B/stage II colorectal cancer? The need for high quality pathology. *Gut,* 56**,** 1419-25.

MORSON, B. C. 1974. Evolution of cancer of the colon and rectum. *Cancer,* 34**,** suppl:845-9.

MOYRET-LALLE, C., FALETTE, N., GRELIER, G. & PUISIEUX, A. 2008. [Tumour genomics: an unstable landscape]. *Bull Cancer,* 95**,** 923-30.

MUNZ, M., BAEUERLE, P. A. & GIRES, O. 2009. The emerging role of EpCAM in cancer and stem cell signaling. *Cancer Res,* 69**,** 5627-9.

MURPHY, G. & GAVRILOVIC, J. 1999. Proteolysis and cell migration: creating a path? *Curr Opin Cell Biol,* 11**,** 614-21.

MURPHY, P. M. 2001. Chemokines and the molecular basis of cancer metastasis. *N Engl J Med,* 345**,** 833-5.

MUTO, T., BUSSEY, H. J. & MORSON, B. C. 1975. The evolution of cancer of the colon and rectum. *Cancer,* 36**,** 2251-70.

NAGANO, M., CHASTRE, E., CHOQUET, A., BARA, J., GESPACH, C. & KELLY, P. A. 1995. Expression of prolactin and growth hormone receptor genes and their isoforms in the gastrointestinal tract. *Am J Physiol,* 268**,** G431-42.

NAGORSEN, D., KEILHOLZ, U., RIVOLTINI, L., SCHMITTEL, A., LETSCH, A., ASEMISSEN, A. M., BERGER, G., BUHR, H. J., THIEL, E. & SCHEIBENBOGEN, C. 2000. Natural T-cell response against MHC

class I epitopes of epithelial cell adhesion molecule, her-2/neu, and carcinoembryonic antigen in patients with colorectal cancer. *Cancer Res,* 60**,** 4850-4.

NAKAGOMI, H., PETERSSON, M., MAGNUSSON, I., JUHLIN, C., MATSUDA, M., MELLSTEDT, H., TAUPIN, J. L., VIVIER, E., ANDERSON, P. & KIESSLING, R. 1993. Decreased expression of the signal-transducing zeta chains in tumor-infiltrating T-cells and NK cells of patients with colorectal carcinoma. *Cancer Res,* 53**,** 5610-2.

NAKAYAMA, T., WATANABE, M., TERAMOTO, T. & KITAJIMA, M. 1997a. CA19-9 as a predictor of recurrence in patients with colorectal cancer. *J Surg Oncol,* 66**,** 238-43.

NAKAYAMA, T., WATANABE, M., TERAMOTO, T. & KITAJIMA, M. 1997b. Slope analysis of CA19-9 and CEA for predicting recurrence in colorectal cancer patients. *Anticancer Res,* 17**,** 1379-82.

NASRABADI, D., REZAEI LARIJANI, M., PIRHAJI, L., GOURABI, H., SHAHVERDI, A., BAHARVAND, H. & SALEKDEH, G. H. 2009. Proteomic analysis of monkey embryonic stem cell during differentiation. *J Proteome Res,* 8**,** 1527-39.

NEWLAND, R. C., CHAPUIS, P. H., PHEILS, M. T. & MACPHERSON, J. G. 1981. The relationship of survival to staging and grading of colorectal carcinoma: a prospective study of 503 cases. *Cancer,* 47**,** 1424-9.

NG, I. O., HO, J., PRITCHETT, C. J., CHAN, E. Y. & HO, F. C. 1993. CEA tissue staining in colorectal cancer patients--correlation with plasma CEA, histology and staging. *Pathology,* 25**,** 219-22.

NGUYEN, H. T., DALMASSO, G., TORKVIST, L., HALFVARSON, J., YAN, Y., LAROUI, H., SHMERLING, D., TALLONE, T., D'AMATO, M., SITARAMAN, S. V. & MERLIN, D. 2011. CD98 expression modulates intestinal homeostasis, inflammation, and colitis-associated cancer in mice. *J Clin Invest,* 121**,** 1733-47.

NIERODZIK, M. L., KAJUMO, F. & KARPATKIN, S. 1992. Effect of thrombin treatment of tumor cells on adhesion of tumor cells to platelets in vitro and tumor metastasis in vivo. *Cancer Res,* 52**,** 3267-72.

NIGAM, A. K., SAVAGE, F. J., BOULOS, P. B., STAMP, G. W., LIU, D. & PIGNATELLI, M. 1993. Loss of cell-cell and cell-matrix adhesion molecules in colorectal cancer. *Br J Cancer,* 68**,** 507-14.

NIMMRICH, I., ERDMANN, S., MELCHERS, U., FINKE, U., HENTSCH, S., MOYER, M. P., HOFFMANN, I. & MULLER, O. 2000. Seven genes that are differentially transcribed in colorectal tumor cell lines. *Cancer Lett,* 160**,** 37-43.

NISHIKAWA, M. 2008. Reactive oxygen species in tumor metastasis. *Cancer Lett,* 266**,** 53-9.

NISHIZUKA, S., CHEN, S. T., GWADRY, F. G., ALEXANDER, J., MAJOR, S. M., SCHERF, U., REINHOLD, W. C., WALTHAM, M., CHARBONEAU, L., YOUNG, L., BUSSEY, K. J., KIM, S., LABABIDI, S., LEE, J. K., PITTALUGA, S., SCUDIERO, D. A., SAUSVILLE, E. A., MUNSON, P. J., PETRICOIN, E. F., 3RD, LIOTTA, L. A., HEWITT, S. M., RAFFELD, M. & WEINSTEIN, J. N. 2003. Diagnostic markers that distinguish colon and ovarian adenocarcinomas: identification by genomic, proteomic, and tissue array profiling. *Cancer Res,* 63**,** 5243-50.

NOURA, S., YAMAMOTO, H., SEKIMOTO, M., TAKEMASA, I., MIYAKE, Y., IKENAGA, M., MATSUURA, N. & MONDEN, M. 2001. Expression of second class of KIP protein p57KIP2 in human colorectal carcinoma. *Int J Oncol,* 19**,** 39-47.

NOWELL, P. C. 1976. The clonal evolution of tumor cell populations. *Science,* 194**,** 23-8.

NOZAWA, Y., VAN BELZEN, N., VAN DER MADE, A. C., DINJENS, W. N. & BOSMAN, F. T. 1996. Expression of nucleophosmin/B23 in normal and neoplastic colorectal mucosa. *J Pathol,* 178**,** 48-52.

NOZOE, T., HONDA, M., INUTSUKA, S., YASUDA, M. & KORENAGA, D. 2003. Significance of immunohistochemical expression of manganese superoxide dismutase as a marker of malignant potential in colorectal carcinoma. *Oncol Rep,* 10**,** 39-43.

O'BRIEN, M. J., ZAMCHECK, N., BURKE, B., KIRKHAM, S. E., SARAVIS, C. A. & GOTTLIEB, L. S. 1981. Immunocytochemical localization of carcinoembryonic antigen in benign and malignant colorectal tissues. Assessment of diagnostic value. *Am J Clin Pathol,* 75**,** 283-90.

O'CONNELL, J. B., MAGGARD, M. A. & KO, C. Y. 2004. Colon cancer survival rates with the new American Joint Committee on Cancer sixth edition staging. *J Natl Cancer Inst,* 96**,** 1420-5.

OHKAME, H., MASUDA, H., ISHII, Y. & KANAI, Y. 2001. Expression of L-type amino acid transporter 1 (LAT1) and 4F2 heavy chain (4F2hc) in liver tumor lesions of rat models. *J Surg Oncol,* 78**,** 265-71; discussion 271-2.

OKAZAKI, K., NAKAYAMA, Y., SHIBAO, K., HIRATA, K., NAGATA, N. & ITOH, H. 1998. Enhancement of metastatic activity of colon cancer as influenced by expression of cell surface antigens. *J Surg Res,* 78**,** 78-84.

OLD, W. M., MEYER-ARENDT, K., AVELINE-WOLF, L., PIERCE, K. G., MENDOZA, A., SEVINSKY, J. R., RESING, K. A. & AHN, N. G. 2005. Comparison of label-free methods for quantifying human proteins by shotgun proteomics. *Mol Cell Proteomics,* 4**,** 1487-502.

ONAMI, T. M., HARRINGTON, L. E., WILLIAMS, M. A., GALVAN, M., LARSEN, C. P., PEARSON, T. C., MANJUNATH, N., BAUM, L. G., PEARCE, B. D. & AHMED, R. 2002. Dynamic regulation of T cell immunity by CD43. *J Immunol,* 168**,** 6022-31.

ONG, S. E. & MANN, M. 2005. Mass spectrometry-based proteomics turns quantitative. *Nat Chem Biol,* 1**,** 252-62.

OSBURN, W. O. & KENSLER, T. W. 2008. Nrf2 signaling: an adaptive response pathway for protection against environmental toxic insults. *Mutat Res,* 659**,** 31-9.

OTSUJI, M., KIMURA, Y., AOE, T., OKAMOTO, Y. & SAITO, T. 1996. Oxidative stress by tumor-derived macrophages suppresses the expression of CD3 zeta chain of T-cell receptor complex and antigen-specific T-cell responses. *Proc Natl Acad Sci U S A,* 93**,** 13119-24.

OTTAIANO, A., FRANCO, R., AIELLO TALAMANCA, A., LIGUORI, G., TATANGELO, F., DELRIO, P., NASTI, G., BARLETTA, E., FACCHINI, G., DANIELE, B., DI BLASI, A., NAPOLITANO, M., IERANO, C., CALEMMA, R., LEONARDI, E., ALBINO, V., DE ANGELIS, V., FALANGA, M., BOCCIA, V., CAPUOZZO, M., PARISI, V., BOTTI, G., CASTELLO, G., VINCENZO IAFFAIOLI, R. & SCALA, S. 2006. Overexpression of both CXC chemokine receptor 4 and vascular endothelial growth factor proteins predicts early distant relapse in stage II-III colorectal cancer patients. *Clin Cancer Res,* 12**,** 2795-803.

PAGES, F., BERGER, A., CAMUS, M., SANCHEZ-CABO, F., COSTES, A., MOLIDOR, R., MLECNIK, B., KIRILOVSKY, A., NILSSON, M., DAMOTTE, D., MEATCHI, T., BRUNEVAL, P., CUGNENC, P. H., TRAJANOSKI, Z., FRIDMAN, W. H. & GALON, J. 2005. Effector memory T cells, early metastasis, and survival in colorectal cancer. *N Engl J Med,* 353**,** 2654-66.

PAGES, F., GALON, J. & FRIDMAN, W. H. 2008. The essential role of the in situ immune reaction in human colorectal cancer. *J Leukoc Biol,* 84**,** 981-7.

PAK, J. H., MANEVICH, Y., KIM, H. S., FEINSTEIN, S. I. & FISHER, A. B. 2002. An antisense oligonucleotide to 1-cys peroxiredoxin causes lipid peroxidation and apoptosis in lung epithelial cells. *J Biol Chem,* 277**,** 49927-34.

PANG, R., LAW, W. L., CHU, A. C., POON, J. T., LAM, C. S., CHOW, A. K., NG, L., CHEUNG, L. W., LAN, X. R., LAN, H. Y., TAN, V. P., YAU, T. C., POON, R. T. & WONG, B. C. 2010. A subpopulation of CD26+ cancer stem cells with metastatic capacity in human colorectal cancer. *Cell Stem Cell,* 6**,** 603-15.

PAPATHOMA, A. S., PETRAKI, C., GRIGORAKIS, A., PAPAKONSTANTINOU, H., KARAVANA, V., STEFANAKIS, S., SOTSIOU, F. & PINTZAS, A. 2000. Prognostic significance of matrix metalloproteinases 2 and 9 in bladder cancer. *Anticancer Res,* 20**,** 2009-13.

PARK, H. J., LYONS, J. C., OHTSUBO, T. & SONG, C. W. 1999. Acidic environment causes apoptosis by increasing caspase activity. *Br J Cancer,* 80**,** 1892-7.

PARK, J. J., CHANG, H. W., JEONG, E. J., ROH, J. L., CHOI, S. H., JEON, S. Y., KO, G. H. & KIM, S. Y. 2009. Peroxiredoxin IV protects cells from radiation-induced apoptosis in head-and-neck squamous cell carcinoma. *Int J Radiat Oncol Biol Phys,* 73**,** 1196-202.

PARK, S. H., CHUNG, Y. M., LEE, Y. S., KIM, H. J., KIM, J. S., CHAE, H. Z. & YOO, Y. D. 2000. Antisense of human peroxiredoxin II enhances radiation-induced cell death. *Clin Cancer Res,* 6**,** 4915-20.

PAWELETZ, C. P., CHARBONEAU, L., BICHSEL, V. E., SIMONE, N. L., CHEN, T., GILLESPIE, J. W., EMMERT-BUCK, M. R., ROTH, M. J., PETRICOIN, I. E. & LIOTTA, L. A. 2001. Reverse phase protein microarrays which capture disease progression show activation of pro-survival pathways at the cancer invasion front. *Oncogene,* 20**,** 1981-9.

PETRAK, J., IVANEK, R., TOMAN, O., CMEJLA, R., CMEJLOVA, J., VYORAL, D., ZIVNY, J. & VULPE, C. D. 2008. Deja vu in proteomics. A hit parade of repeatedly identified differentially expressed proteins. *Proteomics,* 8**,** 1744-9.

PFISTERSHAMMER, K., MAJDIC, O., STOCKL, J., ZLABINGER, G., KIRCHBERGER, S., STEINBERGER, P. & KNAPP, W. 2004. CD63 as an activation-linked T cell costimulatory element. *J Immunol,* 173**,** 6000-8.

POETZ, O., SCHWENK, J. M., KRAMER, S., STOLL, D., TEMPLIN, M. F. & JOOS, T. O. 2005. Protein microarrays: catching the proteome. *Mech Ageing Dev,* 126**,** 161-70.

POLANOWSKA, J., LE CAM, L., ORSETTI, B., VALLES, H., FABBRIZIO, E., FAJAS, L., TAVIAUX, S., THEILLET, C. & SARDET, C. 2000. Human E2F5 gene is oncogenic in primary rodent cells and is amplified in human breast tumors. *Genes Chromosomes Cancer,* 28**,** 126-30.

POLYAK, K., LI, Y., ZHU, H., LENGAUER, C., WILLSON, J. K., MARKOWITZ, S. D., TRUSH, M. A., KINZLER, K. W. & VOGELSTEIN, B. 1998. Somatic mutations of the mitochondrial genome in human colorectal tumours. *Nat Genet,* 20**,** 291-3.

QIAN, F., VAUX, D. L. & WEISSMAN, I. L. 1994. Expression of the integrin alpha 4 beta 1 on melanoma cells can inhibit the invasive stage of metastasis formation. *Cell,* 77**,** 335-47.

RECHSTEINER, M. & ROGERS, S. W. 1996. PEST sequences and regulation by proteolysis. *Trends Biochem Sci,* 21**,** 267-71.

REINHOLD, M. I., LINDBERG, F. P., KERSH, G. J., ALLEN, P. M. & BROWN, E. J. 1997. Costimulation of T cell activation by integrin-associated protein (CD47) is an adhesion-dependent, CD28-independent signaling pathway. *J Exp Med,* 185**,** 1-11.

REITMAN, Z. J. & YAN, H. 2010. Isocitrate dehydrogenase 1 and 2 mutations in cancer: alterations at a crossroads of cellular metabolism. *J Natl Cancer Inst,* 102**,** 932-41.

RHEE, S. G., CHAE, H. Z. & KIM, K. 2005. Peroxiredoxins: a historical overview and speculative preview of novel mechanisms and emerging concepts in cell signaling. *Free Radic Biol Med,* 38**,** 1543-52.

RHO, J. H., QIN, S., WANG, J. Y. & ROEHRL, M. H. 2008. Proteomic expression analysis of surgical human colorectal cancer tissues: up-regulation of PSB7, PRDX1, and SRP9 and hypoxic adaptation in cancer. *J Proteome Res,* 7**,** 2959-72.

ROMERO, J. M., JIMENEZ, P., CABRERA, T., COZAR, J. M., PEDRINACI, S., TALLADA, M., GARRIDO, F. & RUIZ-CABELLO, F. 2005. Coordinated downregulation of the antigen presentation machinery and HLA class I/beta2-microglobulin complex is responsible for HLA-ABC loss in bladder cancer. *Int J Cancer,* 113**,** 605-10.

ROSS, D. T., SCHERF, U., EISEN, M. B., PEROU, C. M., REES, C., SPELLMAN, P., IYER, V., JEFFREY, S. S., VAN DE RIJN, M., WALTHAM, M., PERGAMENSCHIKOV, A., LEE, J. C., LASHKARI, D., SHALON, D., MYERS, T. G., WEINSTEIN, J. N., BOTSTEIN, D. & BROWN, P. O. 2000. Systematic variation in gene expression patterns in human cancer cell lines. *Nat Genet,* 24**,** 227-35.

ROUSSEL, E., GINGRAS, M. C., GRIMM, E. A., BRUNER, J. M. & MOSER, R. P. 1996. Predominance of a type 2 intratumoural immune response in fresh tumour-infiltrating lymphocytes from human gliomas. *Clin Exp Immunol,* 105**,** 344-52.

RUSH, J., MORITZ, A., LEE, K. A., GUO, A., GOSS, V. L., SPEK, E. J., ZHANG, H., ZHA, X. M., POLAKIEWICZ, R. D. & COMB, M. J. 2005. Immunoaffinity profiling of tyrosine phosphorylation in cancer cells. *Nat Biotechnol,* 23**,** 94-101.

SANDERS, M. E., MAKGOBA, M. W., SHARROW, S. O., STEPHANY, D., SPRINGER, T. A., YOUNG, H. A. & SHAW, S. 1988. Human memory T lymphocytes express increased levels of three cell adhesion molecules (LFA-3, CD2, and LFA-1) and three other molecules (UCHL1, CDw29, and Pgp-1) and have enhanced IFN-gamma production. *J Immunol,* 140**,** 1401-7.

SCALA, S., OTTAIANO, A., ASCIERTO, P. A., CAVALLI, M., SIMEONE, E., GIULIANO, P., NAPOLITANO, M., FRANCO, R., BOTTI, G. & CASTELLO, G. 2005. Expression of CXCR4 predicts poor prognosis in patients with malignant melanoma. *Clin Cancer Res,* 11**,** 1835-41.

SCHERF, U., ROSS, D. T., WALTHAM, M., SMITH, L. H., LEE, J. K., TANABE, L., KOHN, K. W., REINHOLD, W. C., MYERS, T. G., ANDREWS, D. T., SCUDIERO, D. A., EISEN, M. B., SAUSVILLE, E. A., POMMIER, Y., BOTSTEIN, D., BROWN, P. O. & WEINSTEIN, J. N. 2000. A gene expression database for the molecular pharmacology of cancer. *Nat Genet,* 24**,** 236-44.

SCHMITT, C. A., SCHWAEBLE, W., WITTIG, B. M., MEYER ZUM BUSCHENFELDE, K. H. & DIPPOLD, W. G. 1999. Expression and regulation by interferon-gamma of the membrane-bound complement regulators CD46 (MCP), CD55 (DAF) and CD59 in gastrointestinal tumours. *Eur J Cancer,* 35**,** 117-24.

SCHRODER, M. & KAUFMAN, R. J. 2005. The mammalian unfolded protein response. *Annu Rev Biochem,* 74**,** 739-89.

SCHWARTZ, R. H. 1990. A cell culture model for T lymphocyte clonal anergy. *Science,* 248**,** 1349-56.

SEIFFERT, M., BROSSART, P., CANT, C., CELLA, M., COLONNA, M., BRUGGER, W., KANZ, L., ULLRICH, A. & BUHRING, H. J. 2001. Signal-regulatory protein alpha (SIRPalpha) but not SIRPbeta is involved in T-cell activation, binds to CD47 with high affinity, and is expressed on immature CD34(+)CD38(-) hematopoietic cells. *Blood,* 97**,** 2741-9.

SEITZ, H. K., SIMANOWSKI, U. A., GARZON, F. T., RIDEOUT, J. M., PETERS, T. J., KOCH, A., BERGER, M. R., EINECKE, H. & MAIWALD, M. 1990. Possible role of acetaldehyde in ethanol-related rectal cocarcinogenesis in the rat. *Gastroenterology,* 98**,** 406-13.

SEMENZA, G. L. 2002. HIF-1 and tumor progression: pathophysiology and therapeutics. *Trends Mol Med,* 8**,** S62-7.

SHANKAR, D. B., CHENG, J. C., KINJO, K., FEDERMAN, N., MOORE, T. B., GILL, A., RAO, N. P., LANDAW, E. M. & SAKAMOTO, K. M. 2005. The role of CREB as a proto-oncogene in hematopoiesis and in acute myeloid leukemia. *Cancer Cell,* 7**,** 351-62.

SHAW, J., ROWLINSON, R., NICKSON, J., STONE, T., SWEET, A., WILLIAMS, K. & TONGE, R. 2003. Evaluation of saturation labelling two-dimensional difference gel electrophoresis fluorescent dyes. *Proteomics,* 3**,** 1181-95.

SHEEHAN, K. M., GULMANN, C., EICHLER, G. S., WEINSTEIN, J. N., BARRETT, H. L., KAY, E. W., CONROY, R. M., LIOTTA, L. A. & PETRICOIN, E. F., 3RD 2008. Signal pathway profiling of epithelial and stromal compartments of colonic carcinoma reveals epithelial-mesenchymal transition. *Oncogene,* 27**,** 323-31.

SHELLEY, C. S., TEODORIDIS, J. M., PARK, H., FAROKHZAD, O. C., BOTTINGER, E. P. & ARNAOUT, M. A. 2002. During differentiation of the monocytic cell line U937, Pur alpha mediates induction of the CD11c beta 2 integrin gene promoter. *J Immunol,* 168**,** 3887-93.

SHIMIZU, S., NARITA, M. & TSUJIMOTO, Y. 1999. Bcl-2 family proteins regulate the release of apoptogenic cytochrome c by the mitochondrial channel VDAC. *Nature,* 399**,** 483-7.

SHIMIZU, Y., VAN SEVENTER, G. A., HORGAN, K. J. & SHAW, S. 1990. Roles of adhesion molecules in T-cell recognition: fundamental similarities between four integrins on resting human T cells (LFA-1, VLA-4, VLA-5, VLA-6) in expression, binding, and costimulation. *Immunol Rev,* 114**,** 109-43.

SHINOHARA, Y., ISHIDA, T., HINO, M., YAMAZAKI, N., BABA, Y. & TERADA, H. 2000. Characterization of porin isoforms expressed in tumor cells. *Eur J Biochem,* 267**,** 6067-73.

SHNYDER, S. D. & HUBBARD, M. J. 2002. ERp29 is a ubiquitous resident of the endoplasmic reticulum with a distinct role in secretory protein production. *J Histochem Cytochem,* 50**,** 557-66.

SICA, A., ALLAVENA, P. & MANTOVANI, A. 2008. Cancer related inflammation: the macrophage connection. *Cancer Lett,* 267**,** 204-15.

SIKANDAR, S. S., PATE, K. T., ANDERSON, S., DIZON, D., EDWARDS, R. A., WATERMAN, M. L. & LIPKIN, S. M. 2010. NOTCH signaling is required for formation and self-renewal of tumor-initiating

cells and for repression of secretory cell differentiation in colon cancer. *Cancer Res,* 70**,** 1469-78.

SIMPSON, R. J. & DOROW, D. S. 2001. Cancer proteomics: from signaling networks to tumor markers. *Trends Biotechnol,* 19**,** S40-8.

SINGER, B. B., SCHEFFRAHN, I., HEYMANN, R., SIGMUNDSSON, K., KAMMERER, R. & OBRINK, B. 2002. Carcinoembryonic antigen-related cell adhesion molecule 1 expression and signaling in human, mouse, and rat leukocytes: evidence for replacement of the short cytoplasmic domain isoform by glycosylphosphatidylinositol-linked proteins in human leukocytes. *J Immunol,* 168**,** 5139-46.

SJOBLOM, T., JONES, S., WOOD, L. D., PARSONS, D. W., LIN, J., BARBER, T. D., MANDELKER, D., LEARY, R. J., PTAK, J., SILLIMAN, N., SZABO, S., BUCKHAULTS, P., FARRELL, C., MEEH, P., MARKOWITZ, S. D., WILLIS, J., DAWSON, D., WILLSON, J. K., GAZDAR, A. F., HARTIGAN, J., WU, L., LIU, C., PARMIGIANI, G., PARK, B. H., BACHMAN, K. E., PAPADOPOULOS, N., VOGELSTEIN, B., KINZLER, K. W. & VELCULESCU, V. E. 2006. The consensus coding sequences of human breast and colorectal cancers. *Science,* 314**,** 268-74.

SKAAR, T. C., PRASAD, S. C., SHARAREH, S., LIPPMAN, M. E., BRUNNER, N. & CLARKE, R. 1998. Two-dimensional gel electrophoresis analyses identify nucleophosmin as an estrogen regulated protein associated with acquired estrogen-independence in human breast cancer cells. *J Steroid Biochem Mol Biol,* 67**,** 391-402.

SORAVIA, C., BERK, T., MADLENSKY, L., MITRI, A., CHENG, H., GALLINGER, S., COHEN, Z. & BAPAT, B. 1998. Genotype-phenotype correlations in attenuated adenomatous polyposis coli. *Am J Hum Genet,* 62**,** 1290-301.

SORDAT, I., BOSMAN, F. T., DORTA, G., ROUSSELLE, P., ABERDAM, D., BLUM, A. L. & SORDAT, B. 1998. Differential expression of laminin-5 subunits and integrin receptors in human colorectal neoplasia. *J Pathol,* 185**,** 44-52.

SORDAT, I., DECRAENE, C., SILVESTRE, T., PETERMANN, O., AUFFRAY, C., PIETU, G. & SORDAT, B. 2002. Complementary DNA arrays identify CD63 tetraspanin and alpha3 integrin chain as differentially expressed in low and high metastatic human colon carcinoma cells. *Lab Invest,* 82**,** 1715-24.

SRINIVASULA, S. M., AHMAD, M., LIN, J. H., POYET, J. L., FERNANDES-ALNEMRI, T., TSICHLIS, P. N. & ALNEMRI, E. S. 1999. CLAP, a novel caspase recruitment domain-containing protein in the tumor necrosis factor receptor pathway, regulates NF-kappaB activation and apoptosis. *J Biol Chem,* 274**,** 17946-54.

STEINER, S. & WITZMANN, F. A. 2000. Proteomics: applications and opportunities in preclinical drug development. *Electrophoresis,* 21**,** 2099-104.

STEINERT, R., BUSCHMANN, T., VAN DER LINDEN, M., FELS, L. M., LIPPERT, H. & REYMOND, M. A. 2002. The role of proteomics in the diagnosis and outcome prediction in colorectal cancer. *Technol Cancer Res Treat,* 1**,** 297-304.

STIERUM, R., GASPARI, M., DOMMELS, Y., OUATAS, T., PLUK, H., JESPERSEN, S., VOGELS, J., VERHOECKX, K., GROTEN, J. & VAN OMMEN, B. 2003. Proteome analysis reveals novel proteins associated with proliferation and differentiation of the colorectal cancer cell line Caco-2. *Biochim Biophys Acta,* 1650**,** 73-91.

STOCKTON, B. M., CHENG, G., MANJUNATH, N., ARDMAN, B. & VON ANDRIAN, U. H. 1998. Negative regulation of T cell homing by CD43. *Immunity,* 8**,** 373-81.

STONE, J. G., ROWAN, A. J., TOMLINSON, I. P. & HOULSTON, R. S. 1999. Mutations in Bcl10 are very rare in colorectal cancer. *Br J Cancer,* 80**,** 1569-70.

SUN, X. F. 2002. p73 overexpression is a prognostic factor in patients with colorectal adenocarcinoma. *Clin Cancer Res,* 8**,** 165-70.

SUNAHARA, M., ICHIMIYA, S., NIMURA, Y., TAKADA, N., SAKIYAMA, S., SATO, Y., TODO, S., ADACHI, W., AMANO, J. & NAKAGAWARA, A. 1998. Mutational analysis of the p73 gene localized at chromosome 1p36.3 in colorectal carcinomas. *Int J Oncol,* 13**,** 319-23.

SUTANDY, F. X., QIAN, J., CHEN, C. S. & ZHU, H. 2013. Overview of protein microarrays. *Curr Protoc Protein Sci,* Chapter 27**,** Unit 27 1.

SWERDLOW, S. H., CAMPO, E., HARRIS, N.L., JAFFE, E.S., PILERI, S.A., STEIN, H., THIELE, J., VARDIMAN, J.W. 2008. WHO Classification of Tumours of Haematopoietic and Lymphoid Tissues. *IARC WHO Classification of Tumours.* 4 ed.

TAI, X. G., YASHIRO, Y., ABE, R., TOYOOKA, K., WOOD, C. R., MORRIS, J., LONG, A., ONO, S., KOBAYASHI, M., HAMAOKA, T., NEBEN, S. & FUJIWARA, H. 1996. A role for CD9 molecules in T cell activation. *J Exp Med,* 184**,** 753-8.

TAKAHASHI, Y., KITADAI, Y., BUCANA, C. D., CLEARY, K. R. & ELLIS, L. M. 1995. Expression of vascular endothelial growth factor and its receptor, KDR, correlates with vascularity, metastasis, and proliferation of human colon cancer. *Cancer Res,* 55**,** 3964-8.

TAKAHASI, K. R., MATSUO, T. & TAKANO-SHIMIZU-KOUNO, T. 2011. Two types of cis-trans compensation in the evolution of transcriptional regulation. *Proc Natl Acad Sci U S A,* 108**,** 15276-81.

TAMBINI, C. E., SPINK, K. G., ROSS, C. J., HILL, M. A. & THACKER, J. 2010. The importance of XRCC2 in RAD51-related DNA damage repair. *DNA Repair (Amst),* 9**,** 517-25.

TANAKA, Y., ALBELDA, S. M., HORGAN, K. J., VAN SEVENTER, G. A., SHIMIZU, Y., NEWMAN, W., HALLAM, J., NEWMAN, P. J., BUCK, C. A. & SHAW, S. 1992. CD31 expressed on distinctive T cell subsets is a preferential amplifier of beta 1 integrin-mediated adhesion. *J Exp Med,* 176**,** 245-53.

TATSUKA, M., MITSUI, H., WADA, M., NAGATA, A., NOJIMA, H. & OKAYAMA, H. 1992. Elongation factor-1 alpha gene determines susceptibility to transformation. *Nature,* 359**,** 333-6.

TAYLOR, L. & SCHWARZ, H. 2001. Identification of a soluble OX40 isoform: development of a specific and quantitative immunoassay. *J Immunol Methods,* 255**,** 67-72.

THORNBERRY, N. A., BULL, H. G., CALAYCAY, J. R., CHAPMAN, K. T., HOWARD, A. D., KOSTURA, M. J., MILLER, D. K., MOLINEAUX, S. M., WEIDNER, J. R., AUNINS, J. & ET AL. 1992. A novel heterodimeric cysteine protease is required for interleukin-1 beta processing in monocytes. *Nature,* 356**,** 768-74.

TOPISIROVIC, I., SVITKIN, Y. V., SONENBERG, N. & SHATKIN, A. J. 2011. Cap and cap-binding proteins in the control of gene expression. *Wiley Interdiscip Rev RNA,* 2**,** 277-98.

TOYOKUNI, S., OKAMOTO, K., YODOI, J. & HIAI, H. 1995. Persistent oxidative stress in cancer. *FEBS Lett,* 358**,** 1-3.

TRACHOOTHAM, D., ALEXANDRE, J. & HUANG, P. 2009. Targeting cancer cells by ROS-mediated mechanisms: a radical therapeutic approach? *Nat Rev Drug Discov,* 8**,** 579-91.

TRINCHIERI, G. & PERUSSIA, B. 1985. Immune interferon: a pleiotropic lymphokine with multiple effects. *Immunol Today,* 6**,** 131-136.

TSANTOULIS, P. K. & GORGOULIS, V. G. 2005. Involvement of E2F transcription factor family in cancer. *Eur J Cancer,* 41**,** 2403-14.

TSUI, K. H., CHENG, A. J., CHANG, P., PAN, T. L. & YUNG, B. Y. 2004. Association of nucleophosmin/B23 mRNA expression with clinical outcome in patients with bladder carcinoma. *Urology,* 64**,** 839-44.

TSUNODA, S., KAWANO, M., KONI, I., KASAHARA, Y., YACHIE, A., MIYAWAKI, T. & SEKI, H. 2000. Diminished expression of CD59 on activated CD8+ T cells undergoing apoptosis in systemic lupus erythematosus and Sjogren's syndrome. *Scand J Immunol,* 51**,** 293-9.

UEDA, J., SEMBA, S., CHIBA, H., SAWADA, N., SEO, Y., KASUGA, M. & YOKOZAKI, H. 2007. Heterogeneous expression of claudin-4 in human colorectal cancer: decreased claudin-4 expression at the invasive front correlates cancer invasion and metastasis. *Pathobiology,* 74**,** 32-41.

UHLEN, M., BJORLING, E., AGATON, C., SZIGYARTO, C. A., AMINI, B., ANDERSEN, E., ANDERSSON, A. C., ANGELIDOU, P., ASPLUND, A., ASPLUND, C., BERGLUND, L., BERGSTROM, K., BRUMER, H., CERJAN, D., EKSTROM, M., ELOBEID, A., ERIKSSON, C., FAGERBERG, L., FALK, R., FALL, J.,

FORSBERG, M., BJORKLUND, M. G., GUMBEL, K., HALIMI, A., HALLIN, I., HAMSTEN, C., HANSSON, M., HEDHAMMAR, M., HERCULES, G., KAMPF, C., LARSSON, K., LINDSKOG, M., LODEWYCKX, W., LUND, J., LUNDEBERG, J., MAGNUSSON, K., MALM, E., NILSSON, P., ODLING, J., OKSVOLD, P., OLSSON, I., OSTER, E., OTTOSSON, J., PAAVILAINEN, L., PERSSON, A., RIMINI, R., ROCKBERG, J., RUNESON, M., SIVERTSSON, A., SKOLLERMO, A., STEEN, J., STENVALL, M., STERKY, F., STROMBERG, S., SUNDBERG, M., TEGEL, H., TOURLE, S., WAHLUND, E., WALDEN, A., WAN, J., WERNERUS, H., WESTBERG, J., WESTER, K., WRETHAGEN, U., XU, L. L., HOBER, S. & PONTEN, F. 2005. A human protein atlas for normal and cancer tissues based on antibody proteomics. *Mol Cell Proteomics,* 4**,** 1920-32.

VAN DE VELDE, H., VON HOEGEN, I., LUO, W., PARNES, J. R. & THIELEMANS, K. 1991. The B-cell surface protein CD72/Lyb-2 is the ligand for CD5. *Nature,* 351**,** 662-5.

VAN DER WURFF, A. A., TEN KATE, J., VAN DER LINDEN, E. P., DINJENS, W. N., ARENDS, J. W. & BOSMAN, F. T. 1992. L-CAM expression in normal, premalignant, and malignant colon mucosa. *J Pathol,* 168**,** 287-91.

VOGELSTEIN, B., FEARON, E. R., HAMILTON, S. R., KERN, S. E., PREISINGER, A. C., LEPPERT, M., NAKAMURA, Y., WHITE, R., SMITS, A. M. & BOS, J. L. 1988. Genetic alterations during colorectal-tumor development. *N Engl J Med,* 319**,** 525-32.

WANG, F., ZHANG, P., MA, Y., YANG, J., MOYER, M. P., SHI, C., PENG, J. & QIN, H. 2012. NIRF is frequently upregulated in colorectal cancer and its oncogenicity can be suppressed by let-7a microRNA. *Cancer Lett,* 314**,** 223-31.

WANG, P., BOUWMAN, F. G. & MARIMAN, E. C. 2009. Generally detected proteins in comparative proteomics--a matter of cellular stress response? *Proteomics,* 9**,** 2955-66.

WARBURG, O. 1956. On respiratory impairment in cancer cells. *Science,* 124**,** 269-70.

WATSON, N. F., DURRANT, L. G., MADJD, Z., ELLIS, I. O., SCHOLEFIELD, J. H. & SPENDLOVE, I. 2006. Expression of the membrane complement regulatory protein CD59 (protectin) is associated with reduced survival in colorectal cancer patients. *Cancer Immunol Immunother,* 55**,** 973-80.

WEBBER, M. M., WAGHRAY, A. & BELLO, D. 1995. Prostate-specific antigen, a serine protease, facilitates human prostate cancer cell invasion. *Clin Cancer Res,* 1**,** 1089-94.

WENNBO, H., GEBRE-MEDHIN, M., GRITLI-LINDE, A., OHLSSON, C., ISAKSSON, O. G. & TORNELL, J. 1997. Activation of the prolactin receptor but not the growth hormone receptor is important for induction of mammary tumors in transgenic mice. *J Clin Invest,* 100**,** 2744-51.

WHERRY, E. J. 2011. T cell exhaustion. *Nat Immunol,* 12**,** 492-9.

WILLERS, I. M., ISIDORO, A., ORTEGA, A. D., FERNANDEZ, P. L. & CUEZVA, J. M. 2010. Selective inhibition of beta-F1-ATPase mRNA translation in human tumours. *Biochem J,* 426**,** 319-26.

WILLINGHAM, S. B., VOLKMER, J. P., GENTLES, A. J., SAHOO, D., DALERBA, P., MITRA, S. S., WANG, J., CONTRERAS-TRUJILLO, H., MARTIN, R., COHEN, J. D., LOVELACE, P., SCHEEREN, F. A., CHAO, M. P., WEISKOPF, K., TANG, C., VOLKMER, A. K., NAIK, T. J., STORM, T. A., MOSLEY, A. R., EDRIS, B., SCHMID, S. M., SUN, C. K., CHUA, M. S., MURILLO, O., RAJENDRAN, P., CHA, A. C., CHIN, R. K., KIM, D., ADORNO, M., RAVEH, T., TSENG, D., JAISWAL, S., ENGER, P. O., STEINBERG, G. K., LI, G., SO, S. K., MAJETI, R., HARSH, G. R., VAN DE RIJN, M., TENG, N. N., SUNWOO, J. B., ALIZADEH, A. A., CLARKE, M. F. & WEISSMAN, I. L. 2012. The CD47-signal regulatory protein alpha (SIRPa) interaction is a therapeutic target for human solid tumors. *Proc Natl Acad Sci U S A,* 109**,** 6662-7.

WILLIS, T. G., JADAYEL, D. M., DU, M. Q., PENG, H., PERRY, A. R., ABDUL-RAUF, M., PRICE, H., KARRAN, L., MAJEKODUNMI, O., WLODARSKA, I., PAN, L., CROOK, T., HAMOUDI, R., ISAACSON, P. G. & DYER, M. J. 1999. Bcl10 is involved in t(1;14)(p22;q32) of MALT B cell lymphoma and mutated in multiple tumor types. *Cell,* 96**,** 35-45.

WOLF, B. B., SCHULER, M., ECHEVERRI, F. & GREEN, D. R. 1999. Caspase-3 is the primary activator of apoptotic DNA fragmentation via DNA fragmentation factor-45/inhibitor of caspase-activated DNase inactivation. *J Biol Chem,* 274**,** 30651-6.

WOLMARK, N., WIEAND, H. S., ROCKETTE, H. E., FISHER, B., GLASS, A., LAWRENCE, W., LERNER, H., CRUZ, A. B., VOLK, H., SHIBATA, H. & ET AL. 1983. The prognostic significance of tumor location and bowel obstruction in Dukes B and C colorectal cancer. Findings from the NSABP clinical trials. *Ann Surg,* 198**,** 743-52.

WONG, A. S., KIM, S. O., LEUNG, P. C., AUERSPERG, N. & PELECH, S. L. 2001. Profiling of protein kinases in the neoplastic transformation of human ovarian surface epithelium. *Gynecol Oncol,* 82**,** 305-11.

WOO, M., HAKEM, R., SOENGAS, M. S., DUNCAN, G. S., SHAHINIAN, A., KAGI, D., HAKEM, A., MCCURRACH, M., KHOO, W., KAUFMAN, S. A., SENALDI, G., HOWARD, T., LOWE, S. W. & MAK, T. W. 1998. Essential contribution of caspase 3/CPP32 to apoptosis and its associated nuclear changes. *Genes Dev,* 12**,** 806-19.

WYKOFF, C. C., BEASLEY, N. J., WATSON, P. H., TURNER, K. J., PASTOREK, J., SIBTAIN, A., WILSON, G. D., TURLEY, H., TALKS, K. L., MAXWELL, P. H., PUGH, C. W., RATCLIFFE, P. J. & HARRIS, A. L. 2000. Hypoxia-inducible expression of tumor-associated carbonic anhydrases. *Cancer Res,* 60**,** 7075-83.

WYLIE, D., SHELTON, J., CHOUDHARY, A. & ADAI, A. T. 2011. A novel mean-centering method for normalizing microRNA expression from high-throughput RT-qPCR data. *BMC Res Notes,* 4**,** 555.

XIAO, G. G., RECKER, R. R. & DENG, H. W. 2008. Recent advances in proteomics and cancer biomarker discovery. *Clin Med Oncol,* 2**,** 63-72.

YABKOWITZ, R., DIXIT, V. M., GUO, N., ROBERTS, D. D. & SHIMIZU, Y. 1993. Activated T-cell adhesion to thrombospondin is mediated by the alpha 4 beta 1 (VLA-4) and alpha 5 beta 1 (VLA-5) integrins. *J Immunol,* 151**,** 149-58.

YAMASAKI, M., TAKEMASA, I., KOMORI, T., WATANABE, S., SEKIMOTO, M., DOKI, Y., MATSUBARA, K. & MONDEN, M. 2007. The gene expression profile represents the molecular nature of liver metastasis in colorectal cancer. *Int J Oncol,* 30**,** 129-38.

YOSHIO, T., MORITA, T., KIMURA, Y., TSUJII, M., HAYASHI, N. & SOBUE, K. 2007. Caldesmon suppresses cancer cell invasion by regulating podosome/invadopodium formation. *FEBS Lett,* 581**,** 3777-82.

ZANETTA, L., MARCUS, S. G., VASILE, J., DOBRYANSKY, M., COHEN, H., ENG, K., SHAMAMIAN, P. & MIGNATTI, P. 2000. Expression of Von Willebrand factor, an endothelial cell marker, is up-regulated by angiogenesis factors: a potential method for objective assessment of tumor angiogenesis. *Int J Cancer,* 85**,** 281-8.

ZHANG, H. F., TOMIDA, A., KOSHIMIZU, R., OGISO, Y., LEI, S. & TSURUO, T. 2004. Cullin 3 promotes proteasomal degradation of the topoisomerase I-DNA covalent complex. *Cancer Res,* 64**,** 1114-21.

ZHOU, J. 2008. *Fluorescence multiplexing of an extended DotScan antibody microarray for the sub-classification of colorectal cancer.* Bachelor of Science (Honours), University of Sydney.

ZHOU, J., BELOV, L., HUANG, P. Y., SHIN, J. S., SOLOMON, M. J., CHAPUIS, P. H., BOKEY, L., CHAN, C., CLARKE, C., CLARKE, S. J. & CHRISTOPHERSON, R. I. 2010. Surface antigen profiling of colorectal cancer using antibody microarrays with fluorescence multiplexing. *J Immunol Methods,* 355**,** 40-51.

ZHOU, J., BELOV, L., SOLOMON, M. J., CHAN, C., CLARKE, S. J. & CHRISTOPHERSON, R. I. 2011. Colorectal cancer cell surface protein profiling using an antibody microarray and fluorescence multiplexing. *J Vis Exp*.

ZINKERNAGEL, R. M. & DOHERTY, P. C. 1979. MHC-restricted cytotoxic T cells: studies on the biological role of polymorphic major transplantation antigens determining T-cell restriction-specificity, function, and responsiveness. *Adv Immunol,* 27**,** 51-177.

Appendix

6.1 Explorer antibody microarray

	1	2	3	4	5	6	7	8	9	10	11	12	13	14	15	16
A	1	2	3	4	5	6	7	8	9	10	11	12	13	14	15	16
B	17	18	19	20	21	22	23	24	25	26	27	28	29	30	31	32
C	33	34	35	36	37	38	39	40	41	42	43	44	45	46	47	48
D	49	50	51	52	53	54	55	56	57	58	59	60	61	62	63	64
E	65	66	67	68	69	70	71	72	73	74	75	76	77	78	79	80
F	81	82	83	84	85	86	87	88	89	90	91	92	93	94	95	96
G	97	98	99	100	101	102	103	104	105	106	107	108	109	110	111	112
H	113	114	115	116	117	118	119	120	121	122	123	124	125	126	127	128

	1	2	3	4	5	6	7	8	9	10	11	12	13	14	15	16
A	129	130	131	132	133	134	135	136	137	138	139	140	141	142	143	144
B	145	146	147	148	149	150	151	152	153	154	155	156	157	158	159	160
C	161	162	163	164	165	166	167	168	169	170	171	172	173	174	175	176
D	177	178	179	180	181	182	183	184	185	186	187	188	189	190	191	192
E	193	194	195	196	197	198	199	200	201	202	203	204	205	206	207	208
F	209	210	211	212	213	214	215	216	217	218	219	220	221	222	223	224
G	225	226	227	228	229	230	231	232	233	234	235	236	237	238	239	240
H	241	242	243	244	245	246	247	248	249	250	251	252	253	254	255	256

	1	2	3	4	5	6	7	8	9	10	11	12	13	14	15	16
A	257	258	259	260	261	262	263	264	265	266	267	268	269	270	271	272
B	273	274	275	276	277	278	279	280	281	282	283	284	285	286	287	288
C	289	290	291	292	293	294	295	296	297	298	299	300	301	302	303	304
D	305	306	307	308	309	310	311	312	313	314	315	316	317	318	319	320
E	321	322	323	324	325	326	327	328	329	330	331	332	333	334	335	336
F	337	338	339	340	341	342	343	344	345	346	347	348	349	350	351	352
G	353	354	355	356	357	358	359	360	361	362	363	364	365	366	367	368
H	369	370	371	372	373	374	375	376	377	378	379	380	381	382	383	384

	1	2	3	4	5	6	7	8	9	10	11	12	13	14	15	16
A	385	386	387	388	389	390	391	392	393	394	395	396	397	398	399	400
B	401	402	403	404	405	406	407	408	409	410	411	412	413	414	415	416
C	417	418	419	420	421	422	423	424	425	426	427	428	429	430	431	432
D	433	434	435	436	437	438	439	440	441	442	443	444	445	446	447	448
E	449	450	451	452	453	454	455	456	457	458	459	460	461	462	463	464
F	465	466	467	468	469	470	471	472	473	474	475	476	477	478	479	480
G	481	482	483	484	485	486	487	488	489	490	491	492	493	494	495	496
H	497	498	499	500	501	502	503	504	505	506	507	508	509	510	511	512

	1	2	3	4	5	6	7	8	9	10	11	12	13	14	15	16
A	513	514	515	516	517	518	519	520	521	522	523	524	525	526	527	528
B	529	530	531	532	533	534	535	536	537	538	539	540	541	542	543	544
C	545	546	547	548	549	550	551	552	553	554	555	556	557	558	559	560
D	561	562	563	564	565	566	567	568	569	570	571	572	573	574	575	576
E	577	578	579	580	581	582	583	584	585	586	587	588	589	590	591	592
F	593	594	595	596	597	598	599	600	601	602	603	604	605	606	607	608
G	609	610	611	612	613	614	615	616	617	618	619	620	621	622	623	624
H	625	626	627	628	629	630	631	632	633	634	635	636	637	638	639	640
I	641	642	643	644	645	646	647	648	649	650	651	652	653	654	655	656

Figure 6.1 The Explorer antibody microarray consisted of 656 antibodies arranged over 5 duplicate panels (1-5). Panels 1 – 4 consist of 128 antibodies while panel 5 contains 144 antibodies. The antibody are listed in table 6.1 below.

Table 6.1 Explorer microarray antibody list.

ID	*Antibody Name*	*Reactivity*	*IG Isotype*	*Epitope*	*Source*
1	**p18INK4c**	HM	N/A	aa 155-168	Rabbit
2	**Cyclin B1**	HMR	N/A	C-terminal	Rabbit
3	**Cyclin C**	HMRD	N/A	aa 290-303	Rabbit
4	**Cyclin E**	HMR	N/A	C-terminal	Rabbit
5	**Cdk3**	HMR		aa 290-305	Rabbit
6	**Cdk8**	HMR	N/A	aa 451-464	Rabbit
7	**BRCA2 (aa 1323-1346)**	H	N/A	aa1324-1347	Rabbit
8	**Nck**	HMR	N/A	Not determined	Rabbit
9	**CDC37**	HM	N/A	aa 369-379	Rabbit
10	**p19Skp1**	HM	N/A	aa 152-163	Rabbit
11	**CDC47**	HMRDX	IgG1 / κ	Not determined	Rabbit
12	**Cullin-1 (CUL-1)**	HM	N/A	aa 742-752	Rabbit
13	**CDC34**	H	N/A	aa285-298	Rabbit
14	**p14ARF**	H	N/A	aa 119-132	Rabbit
15	**Cullin-2 (CUL-2)**	HM	N/A	aa 733-745	Rabbit
16	**Cyclin E2**	H	N/A	aa 391-404	Rabbit
17	**GSTmu**	H	N/A	Not determined	Rabbit
18	**DNA Polymerase Gamma**	HM	N/A	aa714-1061	Rabbit
19	**Gab-1**	HMRY	N/A	aa 675-694	Rabbit
20	**SIRP a1**	HY	N/A	aa476-503	Rabbit
21	**DNA Primase (p49)**	HM	N/A	Not determined	Rabbit
22	**DNA Primase (p58)**	HM	N/A	Not determined	Rabbit
23	**APC11**	HM	N/A	aa 76-84	Rabbit
24	**APC2**	HM	N/A	aa 76-84	Rabbit
25	**ROC**	HM	N/A	aa 97-108	Rabbit
26	**Endostatin**	H	N/A	Not determined	Rabbit
27	**Caspase 5**	HMRSTWY	N/A	Middle region	Rabbit
28	**FGF-1**	H	N/A	Not determined	Rabbit
29	**Catenin alpha**	HM	N/A	Not determined	Rabbit
30	**Catenin beta**	HM	N/A	Not determined	Rabbit
31	**Stat-1**	H	N/A	C-terminal	Rabbit
32	**Stat3**	HMR	N/A	C-terminal	Rabbit
33	**Stat5a**	HMR	N/A	C-terminal	Rabbit
34	**Stat5b**	HMR	N/A	C-terminal	Rabbit
35	**Stat6**	HMR	N/A	C-terminal	Rabbit
36	**Negative Control for Rabbit IgG**	All	N/A	Not determined	Rabbit
37	**Heat Shock Protein 27/hsp27**	HY	IgG1	Not determined	Mouse
38	**Glucose-Regulated Protein 94**	HMRDEGpKPSTX	IgG2a	Not determined	Rat
39	**c-erbB-2/HER-2/neu Ab-1 (21N)**	HMRY	N/A	C-terminal	Rabbit
40	**p53**	H	IgG1	aa 212-217	Mouse
41	**PCNA**	HMR	IgG2a / κ	Not determined	Mouse
42	**Retinoblastoma**	H	IgG1	aa703-722	Mouse
43	**Cdk1/p34cdc2**	HMRGKX	IgG2a	aa220-227	Mouse
44	**pS2**	H	IgG1	Not determined	Mouse
45	**CD45RO**	HM	IgG2a / κ	Not determined	Mouse
46	**FGF-2**	H	N/A	Not determined	Rabbit
47	**CD54/ICAM-1**	H	IgG1 / κ	Extracellular (close to transmembrane domain)	Mouse

48	**Keratin 14**	HR	IgG3	C-terminal	Mouse
49	**nm23**	H	N/A	aa 86-102	Rabbit
50	**Topoisomerase IIa**	H	N/A	aa 1513-1530	Rabbit
51	**Heat Shock Protein 90b/hsp84**	HMR	N/A	aa 2-13	Rabbit
52	**claudin 11**	HMR	N/A	C-terminal	Rabbit
53	**Heat Shock Protein 60/hsp60**	HMRKS	IgG1	aa 383-447	Mouse
54	**DJ-1**	H	N/A	C-terminal	Rabbit
55	**bcl-2a**	H	IgG1 / κ	GAAPAPGIFSSQPG-Cys	Mouse
56	**Involucrin**	HRDP	IgG1	Codon 421-568	Mouse
57	**SIM Ag (SIMA-4D3)**	H	N/A	Not determined	Mouse
58	**Tenascin**	H	IgG1	Not determined	Mouse
59	**Vimentin**	HMRCDKSTY	IgG1 / κ	Not determined	Mouse
60	**CDw75**	H	IgM / κ	Not determined	Mouse
61	**E3-binding protein (ARM1)**	H	N/A	Not determined	Mouse
62	**Myeloid Specific Marker**	H	IgG1	Not determined	Mouse
63	**MHC II (HLA-DR) Ia**	H	IgG2b	Not determined	Mouse
64	**CD57**	H	IgM / κ	Not determined	Mouse
65	**TAG-72**	HRDSW	IgG1 / κ	Mucin-carried-sialylated-Tn epitope	Mouse
66	**Keratin 18**	H	IgG1	Not determined	Mouse
67	**Kappa Light Chain**	H	IgG1 / κ	Not determined	Mouse
68	**Epithelial Specific Antigen**	H	IgG1 / κ	Not determined	Mouse
69	**Mucin 5AC**	MRCPTK	IgG1 / κ	Destroyed by β-mercaptoethanol and proteases but not by periodate treatment	Mouse
70	**CD43**	H	IgG1	Not determined	Mouse
71	**Macrophage**	HMRCDGpY	IgG1	Not determined	Mouse
72	**Keratin, Multi**	HMRW	IgG1	Not determined	Mouse
73	**EMA/CA15-3/MUC-1**	H	IgG1 / κ	APDTR in tandem repeats	Mouse
74	**Keratin 5/8**	H	IgG1 / κ	Not determined	Mouse
75	**Keratin 10/13**	HRC	IgG2a	Not determined	Mouse
76	**MHC II (HLA-DP)**	H	IgG2b	Not determined	Mouse
77	**MHC II (HLA-DQ)**	HP	IgG2a	Not determined	Mouse
78	**Lck**	HMR	IgG2b / κ	aa 1-225	Mouse
79	**Fibronectin**	H	IgG1	Peptide core	Mouse
80	**Estrogen Receptor**	HMRTW	IgG1 / λ	aa 125-165	Mouse
81	**Inhibin alpha**	H	IgG2a / κ	aa 1-32	Mouse
82	**IL-8**	H	N/A	Not determined	Mouse
83	**Lambda Light Chain**	H	IgG2a / k	Not determined	Mouse
84	**Granulocyte**	H	IgG1	Not determined	Mouse
85	**p170 / MDR-1**	Ch	IgG1 / κ	Not determined	Mouse
86	**Progesterone Receptor**	HKTW	IgG1 / κ	N-terminal half of human progesterone	Mouse
87	**Keratin 19**	H	IgG2a / λ	aa 312-335	Mouse
88	**Helicobacter pylori**	Helicobacter pylori	N/A	Not determined	Rabbit
89	**CD25/IL-2 Receptor a**	H	IgG1 / κ	Not determined	Mouse
90	**CD56/NCAM-1**	H	IgG1 / κ	Extracellular (close to transmembrane domain)	Mouse
91	**FITC**	All	IgG1 / κ	Not determined	Mouse
92	**PLAP**	H	IgG2a / κ	Not determined	Mouse

93	**Cyclin D1**	HMR	N/A	C-terminus	Rabbit
94	**Integrin beta5**	HMRS	N/A	Not determined	Mouse
95	**Cyclin D3**	HMRY	IgG1 / κ	Not determined	Mouse
96	**p16INK4a**	H	IgG1	Not determined	Mouse
97	**Cdk7**	HR	IgG2b	221 amino acid fragment of C-terminus	Mouse
98	**Transglutaminase II**	HDT	IgG1 / κ	aa 447-478	Mouse
99	**HDJ-2/DNAJ**	HMRPSTY	IgG1	aa 1-179	Mouse
100	**Alpha Fetoprotein (AFP)**	HDP	IgG2a	Not determined	Mouse
101	**p21WAF1**	H	IgG2a	Not determined	Mouse
102	**Fibrillin-1**	HW	IgG1 / κ	aa 451-909	Mouse
103	**Collagen II**	HMRKW	IgG2a / κ	Carboxyl-terminal one quarter of the type	Mouse
104	**CD35/CR1**	H	IgG1	Not determined	Mouse
105	**CD4**	H	IgG1	Not determined	Mouse
106	**Mucin 2**	H	IgG1	Not determined	Mouse
107	**CD45/T200/LCA**	H	IgG1	Not determined	Mouse
108	**Ga0**	HRGpW	IgG1	Not determined	Mouse
109	**Gai1**	HMRGpW	IgG2b	Not determined	Mouse
110	**Myelin / Oligodendrocyte**	HMRCKY	IgM	Not determined	Mouse
111	**tau**	HMRW	IgG1	Middle of Tau	Mouse
112	**MAP1B**	HRW	IgG1	Not determined	Mouse
113	**MAP2a,b**	HMRKW	IgG1	aa 997-1332	Mouse
114	**IL-6**	H	N/A	Not determined	Rat
115	**Tubulin-b**	HMRW	IgM	Not determined	Mouse
116	**E2F-2**	HR	IgG1	aa 1-85	Mouse
117	**p27Kip1**	HMRD	IgG1 / κ	aa 83-197	Mouse
118	**Amphiregulin**	HM	N/A	aa 8-26	Rabbit
119	**Laminin Receptor**	H	IgM	Not determined	Mouse
120	**Prostate Specific Antigen**	H	IgG1 / κ	Not determined	Mouse
121	**Prohibitin**	HMRKP	IgG1	Not determined	Mouse
122	**E2F-3**	HR	IgG2b	aa 1-132	Mouse
123	**UCP3**	HRM	N/A	C-terminal	Rabbit
124	**Heregulin**	HMR	IgG2a	Not determined	Mouse
125	**MyoD1**	HMRK	IgG1 / κ	aa 180-189	Mouse
126	**GFAP**	HRKP	IgG1 / κ	Not determined	Mouse
127	**CLAUDIN 7**	HMR	N/A	C-terminal	Rabbit
128	**Ku (p80)**	HY	IgG1 / κ	aa 610-705	Mouse
129	**Ku (p70/p80)**	HMXY	IgG2a	A conformational epitope of p70/p80 dimer	Mouse
130	**MDM2**	HMR	IgG1 / κ	aa 154-167	Mouse
131	**MLH1**	H	N/A	aa 557-756	Rabbit
132	**Bcl-6**	H	N/A	aa 1-150	Rabbit
133	**S100**	HMRW	IgG2a	Not determined	Mouse
134	**Cdk4**	HMRP	IgG 1 / κ	aa 1-20	Mouse
135	**c-erbB-4/HER-4**	HMRW	IgG2a/κ	aa1295-1323	Mouse
136	**EGFR**	H	N/A	aa 985-996 (Cytoplasmic domain)	Mouse
137	**Prostate Specific Acid Phosphatase**	H	IgG1	Not determined	Mouse
138	**Syk**	H	N/A	aa 313-339	Mouse
139	**Caspase 6 (Mch 2)**	H	N/A	N-terminal	Rabbit
140	**Chromogranin A**	HRPTY	IgG1 / κ	Not determined	Mouse

141	**Mekk-1**	HMR	N/A	Near C-terminus	Rabbit
142	**ER beta**	HR	N/A	N-terminus	Rabbit
143	**Neuron Specific Enolase**	H	IgG1	Not determined	Mouse
144	**IL-2**	H	N/A	Not determined	Rat
145	**Fyn**	HMR	IgG1 / κ	aa 26-75	Mouse
146	**Keratin, LMW**	HMRKTW	IgG1	Not determined	Mouse
147	**GM-CSF**	H	N/A	Not determined	Rat
148	**Keratin, Pan**	HMRKTW	IgG1 + IgG1	Not determined	Mouse
149	**Collagen IX**	KQ	IgG1 / κ	Close to the C-terminus (COL2) of the HMW fragment, which is present in both the long- and short-form type IX collagens	Mouse
150	**CNPase**	HMRCDEGPTWY	IgG1	Not determined	Mouse
151	**CD79a mb-1**	HMRGpKPTWY	IgG1 / κ	GTYQDVGSLNIADVQ	Mouse
152	**Neurofilament**	HMRCT	IgG1 / κ	Not determined	Mouse
153	**TNF alpha**	H	N/A	Not determined	Rat
154	**DNA-PKcs**	HR	IgG1	aa 1-2713	Mouse
155	**Myeloperoxidase**	HMR	N/A	Not determined	Mouse
156	**CA19-9**	H	IgM	Not determined	Mouse
157	**CD45RB**	H	IgG1	Not determined	Mouse
158	**Keratin 5/6/18**	HRW	IgG1 / κ	Not determined	Mouse
159	**NGF-Receptor (p75NGFR)**	HCT	IgG1 / κ	aa 1-160	Mouse
160	**Streptavidin**	Bacterium Streptomyces avidinii	N/A	Not determined	Rabbit
161	**CD68**	HRCY	IgG1 / κ	Not determined	Mouse
162	**IL-1 alpha**	H	N/A	Not determined	Rabbit
163	**Paxillin**	HR	IgG1 / κ	Not determined	Mouse
164	**Heat Shock Factor 1**	HMR	IgG1	aa 425-439 of mouse HSF1	Rat
165	**Heat Shock Factor 2**	HMK	IgG1	Not determined	Rat
166	**Renal Cell Carcinoma**	HR	IgG1 / κ	Carbohydrate domain	Mouse
167	**TNFa**	H	IgG1	Not determined	Mouse
168	**p95VAV**	HM	IgG1	Not determined	Mouse
169	**Thrombospondin**	HMRWDP	IgG1	Calcium-binding domain of TSP (Cterminal 50kDa piece of the 120kDa fragment)	Mouse
170	**IL-1 beta**	H	IgG1	Not determined	Mouse
171	**Retinol Binding Protein**	HMRGTY	IgG1 / κ	aa 74-182	Mouse
172	**CD6**	H	IgG1 / κ	Not determined	Mouse
173	**CD15**	H	IgM	Not determined	Mouse
174	**CD20**	H	IgG2a / κ	Extracellular domain	Mouse
175	**XRCC1**	HR	IgG2b	Not determined	Mouse
176	**Interferon-g**	H	IgG1 / κ	Not determined	Mouse
177	**DFF45 / ICAD**	H	N/A	Not determined	Rabbit
178	**b-2-Microglobulin**	H	IgG2a / κ	Not determined	Mouse
179	**Erk1**	HMR	N/A	N-terminal	Rabbit
180	**Androgen Receptor**	HD	IgG1	aa 299-315	Mouse

181	**Collagen VII**	HEGpGtPWY	IgG1 / κ	On non-helical (non-collagenous) Cterminal region of collagen VII and is resistant to collagenase, trypsin, pronase, neuraminidase, chondroitinase, and hyaluronidase. However, it is lost by digestion of collagen VII with pepsin.	Mouse
182	**Phosphotyrosine**	All	IgG2b	Not determined	Mouse
183	**Filaggrin**	H	IgG1 / κ	Not determined	Mouse
184	**sm**	HRPT	IgG3 / κ	Not determined	Mouse
185	**Adrenocorticotrophic Hormone**	H	IgG1	aa 1-24	Mouse
186	**Thomsen-Friedenreich Antigen**	HR	IgM / κ	Galβ1-3GalNAc	Mouse
187	**Cdk2**	HMR	IgG2b	Not determined	Mouse
188	**Ornithine Decarboxylase**	HMR	IgG1	aa 355-360 (-IWGPTC-)	Mouse
189	**CD155/PVR (Polio Virus Receptor)**	HY	IgG1	aa 35-50	Mouse
190	**CD36GPIIIb/GPIV**	H	N/A	Not determined	Mouse
191	**GAD65**	HR	N/A	C-terminal	Rabbit
192	**MGMT**	H	IgG1	aa 8-221	Mouse
193	**Thymidylate Synthase**	H	IgG1 / κ	Not determined	Mouse
194	**Xanthine Oxidase**	HMRT	IgG1	C-terminal 358 amino acids	Mouse
195	**Golgi Complex**	N/A	N/A	Not determined	Mouse
196	**Perforin**	H	IgG2b / κ	Not determined	Mouse
197	**Keratin 10**	HRP	IgG1 / κ	Not determined	Mouse
198	**Heat Shock Protein 70/hsp70**	HKW	IgG2a	Not determined	Mouse
199	**Dystrophin**	HMRKX	IgG1	Not determined	Mouse
200	**Plasma Cell Marker**	H	IgG2a	Not determined	Mouse
201	**GnRH Receptor**	H	IgG1	aa 1-29	Mouse
202	**LewisA**	H	IgG1 / κ	Gal β1-3(Fuc α1-4) GlcNAc	Mouse
203	**NuMA**	H	IgM / κ	Not determined	Mouse
204	**Thymidine Phosphorylase**	HMR	IgG1	Not determined	Mouse
205	**CD81/TAPA-1**	H	IgG1 / κ	Not determined	Mouse
206	**CD5**	H	IgG1	Not determined	Mouse
207	**CD59 / MACIF / MIRL / Protectin**	H	IgG1 / κ	Not determined	Mouse
208	**B-cell Linker Protein (BLNK)**	H	IgG1	aa 4-205	Mouse
209	**mGluR5**	HRT	N/A	C-terminal	Rabbit
210	**Milk Fat Globule Membrane Protein**	H	IgG1 / κ	Not determined	Mouse
211	**CD1**	H	IgG2a / κ	Not determined	Mouse
212	**CD2**	H	N/A	Not determined	Rabbit
213	**CD1b**	H	IgM / κ	Not determined	Mouse
214	**GABA a Receptor 1**	HMR	N/A	N-terminal	Rabbit
215	**CD14**	H	IgG1 / κ	Not determined	Mouse
216	**CD16**	H	IgG2a / κ	Not determined	Mouse
217	**CDw17**	H	IgM / κ	Not determined	Mouse
218	**CD26/DPP IV**	HR	IgG2b / κ	Not determined	Mouse
219	**CD32/Fcg Receptor II**	H	IgG1 / κ	Second Ig-like domain (D2γ)	Mouse
220	**mGluR1**	HMRKY	N/A	C-terminal	Rabbit

221	**CD8**	H	IgG1 / κ	Not determined	Mouse
222	**CD21**	H	IgG1 / κ	5-8 short consensus repeats	Mouse
223	**alpha-1-antichymotrypsin**	H	N/A	Not determined	Rabbit
224	**Cadherin-E**	H	N/A	600-707aa	Rabbit
225	**Oct-2/**	HMR	N/A	C-terminal	Rabbit
226	**CD53**	H	IgG1 / κ	Extracellular (close to transmembrane domain)	Mouse
227	**CDw78**	H	IgG1 / κ	Not determined	Mouse
228	**CD98**	H	IgM / κ	Not determined	Mouse
229	**CD100/Leukocyte Semaphorin**	H	N/A	Not determined	Mouse
230	**Rabies Virus**	H	IgG2a / κ	Not determined	Mouse
231	**MHC I (HLA-A,B,C)**	H+Primates	IgG2a / κ	Not determined	Mouse
232	**MHC II (HLA-DR)**	HP	IgG2a / κ	Not determined	Mouse
233	**MHC II (HLA-DP and DR)**	H	IgG3 / κ	Epitope common to human major histocompatibility (MHC) class II antigens, HLA-DR and DP	Mouse
234	**MMP-2 (72kDa Collagenase IV)**	HMR	IgG1	N-terminal (APSPIIKFPGD-VAPKTDK)	Mouse
235	**MMP-9 (92kDa Collagenase IV)**	H	IgG1	Not determined	Mouse
236	**TIMP-1**	HR	IgG1	Not determined	Mouse
237	**TIMP-2**	H	IgG1	aa 111-126	Mouse
238	**Bovine Serum Albumin**	W	IgG1 / κ	Not determined	Mouse
239	**Interferon-a(II)**	H	IgG1 / κ	aa 43-53	Mouse
240	**Tubulin-a**	HMRGpKPW	IgG1 / κ	aa 426-450	Mouse
241	**p300 / CBP**	HMRKY	IgG2b / κ	aa 2071-2091	Mouse
242	**Adenovirus Type 5 E1A**	A	IgG2a / κ	Not determined	Mouse
243	**Adenovirus Type 2 E1A**	A	IgG2a / κ	Not determined	Mouse
244	**CD29**	HP	IgG1 / κ	Not determined	Mouse
245	**CD115/c-fms/CSF-1R/M-CSFR**	H	IgG2b	Not determined	Rat
246	**MART-1/Melan-A**	H	IgG2b / κ	Not determined	Mouse
247	**Keratin 16**	H	IgG1	C-terminal	Mouse
248	**CD137 (4-1BB)**	H	IgG1/ κ	Ectodomain	Mouse
249	**Cryptococcus neoformans**	All strains of C. neoformans	IgG2b	Carbohydrate moiety occuring on one or two glycoproteins.	Mouse
250	**CD50/ICAM-3**	H	N/A	Not determined	Mouse
251	**Histone H1**	H	IgG2a	Not determined	Mouse
252	**Insulin Receptor Substrate-1**	HMR	IgG1	aa 1221-1235	Mouse
253	**Insulin Receptor**	H	IgG2a / κ	aa 469-592 (exon 7/8)	Mouse
254	**Actin beta**	HMRCDGpKPST	N/A	N-terminus	Rabbit
255	**IGF-1R**	H	IgG1	aa 283-440 (exon 4-6)	Mouse
256	**ERCC1**	H	IgG2a / κ	Not determined	Mouse
257	**XPA**	H	IgG2a / k	Not determined	Mouse
258	**Hepatocyte Growth Factor**	H	IgG2b	Not determined	Mouse
259	**IL-10**	H	N/A	Not determined	Rat
260	**CD18**	H	IgG2a	Not determined	Mouse
261	**Ruv A**	E. Coli	IgG1 / κ	Not determined	Mouse
262	**Ruv B**	E. Coli	IgG1 / κ	Not determined	Mouse
263	**Ruv C**	E. Coli	IgG2b / κ	Not determined	Mouse

264	**Plasminogen**	H	IgG1 / κ	Not determined	Mouse
265	**Ezrin/p81/80K/Cytovillin**	HMRSTWY	IgG1	aa 362-585	Mouse
266	**LRP / MVP**	HR	IgG1 / κ	Not determined	Mouse
267	**6-Histidine**	All	IgG2a / κ	HHHHHHGS	Mouse
268	**Transforming Growth Factor a**	HMRW	IgG1 / κ	C-terminal	Mouse
269	**Maltose Binding Protein**	Bacteria	IgM	Not determined	Mouse
270	**XPG**	H	IgG2a / k	Not determined	Mouse
271	**IL-30**	H	N/A	Not determined	Rat
272	**Activin Receptor Type II**	H	IgG1	Tyrosine kinase domain	Mouse
273	**Mcl-1**	H	IgG1 / κ	aa 1-327	Mouse
274	**Melanoma (gp100)**	H	IgG2a	Not determined	Mouse
275	**von Hippel-Lindau Protein**	HM	IgG1 / κ	aa 1-54	Mouse
276	**RPA/p32**	H	IgG1 / κ	Not determined	Mouse
277	**RPA/p70**	H	IgG1 / κ	Not determined	Mouse
278	**CREB-Binding Protein**	HR	IgG1 / κ	Not determined	Mouse
279	**TTF-1**	HMR	IgG1 / κ	Not determined	Mouse
280	**HIF-1a**	H	IgG1 / κ	aa 530-826	Mouse
281	**Surfactant Protein A**	H	IgG2b / κ	Not determined	Mouse
282	**Surfactant Protein B (Pro)**	HR	IgG2a / κ	Not determined	Mouse
283	**DR3**	H	IgG2a	Not determined	Mouse
284	**GST**	All	IgG1	Not determined	Mouse
285	**TR2**	H	IgG1	Not determined	Mouse
286	**Bax**	H	IgG1 / k	aa 3-16	Mouse
287	**bcl-X**	HMPR	IgG2a	Cys-QSNRELVVDFLS	Mouse
288	**Tubulin**	H	N/A	Not determined	Mouse
289	**F.VIII/VWF**	H	IgG1 / κ	Not determined	Mouse
290	**Factor VIII Related Antigen**	H	N/A	Not determined	Rabbit
291	**IPO-38 Proliferation Marker**	HMR	IgM / κ	Not determined	Mouse
292	**Moesin**	HRW	IgG1 / κ	Not determined	Mouse
293	**Collagen IV**	H	IgG1+ IgG1	Not determined	Mouse
294	**Negative Control for Mouse IgG1**	All	IgG1 / κ	Not determined	Mouse
295	**CDC25C**	H	IgG1 / κ	aa 1-150	Mouse
296	**p73a**	HY	IgG1	aa380-637 (p73α)	Mouse
297	**p73a/b**	HY	IgG1 / κ	aa380-637 (p73α)	Mouse
298	**Ang-1**	HM	N/A	Not determined	Rabbit
299	**HPV 16-E7**	HPV-16	IgG2a / κ	Not determined	Mouse
300	**HPV 16**	HPV-16	IgG2a	Not determined	Mouse
301	**L1 Cell Adhesion Molecule**	H	IgG1 / κ	Not determined	Mouse
302	**Microphthalmia**	HMRD	IgG1 / κ	N-terminal	Mouse
303	**DNA Ligase I**	HW	IgG1	Not determined	Mouse
304	**Ang-2**	HM	N/A	Not determined	Rabbit
305	**CD46**	H	IgG2a / κ	Four immunogenic short consensus repeat (SCR) domains at N-terminus of the protein	Mouse
306	**B7-H2**	H	IgG2b / κ	Extracellular	Mouse
307	**CD84**	H	IgG1 / κ	Not determined	Mouse
308	**Heparan Sulfate Proteoglycan**	HMWP	IgG2a / κ	Not determined	Rat
309	**Laminin B2/g1**	HM	IgG2a / κ	Not determined	Rat
310	**Laminin B1/b1**	HMPS	IgG1 / κ	Not determined	Rat
311	**Tyrosinase**	HCD	IgG2a	aa 1-433	Mouse

312	**MMP-1 (Collagenase-I)**	H	IgG1 / κ	aa 1-81 of the pro-form of MMP-1	Mouse
313	**A-Raf**	HMR	N/A	C-terminal	Rabbit
314	**MMP-7 (Matrilysin)**	H	IgG2b / κ	Not determined	Mouse
315	**MMP-10 (Stromilysin-2)**	H	IgG2b	Not determined	Mouse
316	**MMP-13 (Collagenase-3)**	H	IgG1 / κ	Not determined	Mouse
317	**uPA**	H	IgG1 / κ	Not determined	Mouse
318	**BAG-1**	H	IgG1	Not determined	Mouse
319	**MAGE-1**	H	IgG2a	aa 37-44	Mouse
320	**S100A6**	HMRCD	N/A	Not determined	Rabbit
321	**Thymine Glycols**	All	IgM / κ	Not determined	Mouse
322	**p130cas**	HR	IgG1 / κ	Not determined	Mouse
323	**p130**	H	IgG1	aa 878-913	Mouse
324	**Claudin-1**	HMRDY	N/A	C-terminal	Rabbit
325	**CDC6**	H	IgG1	Not determined	Mouse
326	**E2F-1**	HMR	IgG2a / κ	aa1-89	Mouse
327	**p15INK4b**	HD	IgG1 / κ	Not determined	Mouse
328	**p35nck5a**	H	IgG2b / κ	Not determined	Mouse
329	**DFF40 (DNA Fragmentation Factor 40) / CAD**	H	N/A	N-terminal	Rabbit
330	**IRAK**	HMR	N/A	C-terminal	Rabbit
331	**PCTAIRE2**	H	N/A	Not determined	Mouse
332	**Cdk5**	HMR	IgG1	Not determined	Mouse
333	**p19ARF**	M	N/A	Middle of p19ARF	Rabbit
334	**CD106 / VCAM**	H	N/A	Not determined	Mouse
335	**MHC I (HLA-A)**	H	IgG1 / κ	aa65-to-aa80 of the α1 domain of the HLA-A	Mouse
336	**MHC I (HLA25 and HLA-Aw32)**	H	IgG2a / κ	Not determined	Mouse
337	**MHC I (HLA-B)**	H	IgG1 / κ	Intralocus determinant present on HLA-B locus-encoded gene products	Mouse
338	**Casein**	H	IgG1	Not determined	Mouse
339	**Alpha Lactalbumin**	H	IgM	Not determined	Mouse
340	**c-Abl**	HM	IgG1 / γ	SH2 domain	Mouse
341	**CD95 / Fas**	H	IgG1	Not determined	Mouse
342	**Parkin**	HMR	N/A	N-terminal	Rabbit
343	**CD10**	H	N/A	Not determined	Rabbit
344	**Rad51**	HMR	IgG1 / κ	Not determined	Mouse
345	**CD1a**	H	IgG1 / κ	Not determined	Mouse
346	**Keratin 8**	H	IgG1 / κ	aa 343-357	Mouse
347	**IgA**	H	IgG1 / κ	Third constant domain (CH3) of the alpha chain of IgA	Mouse
348	**Alkaline Phosphatase (AP)**	H	IgG1 / κ	Not determined	Mouse
349	**Presenillin**	H	N/A	N-terminal	Rabbit
350	**APC**	HMR	N/A	C-terminus	Rabbit
351	**LewisB**	H	IgG1 / κ	Not determined	Mouse
352	**Adenovirus Fiber**	A	IgG2a / κ	Not determined	Mouse
353	**Negative Control for Mouse IgM**	All	IgM	Not determined	Mouse
354	**MMP-11 (Stromelysin-3)**	H	IgG1 / κ	Not determined	Mouse
355	**Chorionic Gonadotropin beta (hCG-beta)**	H	IgG2b / κ	Not determined	Mouse

356	**Progesterone**	All	IgG1 / κ	Not determined	Mouse
357	**Testosterone**	All	IgG1	Not determined	Mouse
358	**FSH-b**	H	IgG1 / κ	Not determined	Mouse
359	**Estriol**	All	IgG1	Not determined	Rat
360	**Leukotriene (C4, D4, E4)**	H	IgG1	Not determined	Rat
361	**Medroxyprogesterone Acetate (MPA)**	H	IgG1	Not determined	Rat
362	**Biotin**	All	IgG1 / κ	Not determined	Mouse
363	**Estradiol**	All	IgG2a / κ	Not determined	Mouse
364	**Growth Hormone (hGH)**	H	IgG1 / κ	Not determined	Mouse
365	**IL-3**	H	N/A	Not determined	Rat
366	**E2F-4**	HR	IgG1	Not determined	Mouse
367	**BrdU**	All	IgG1	Not determined	Mouse
368	**Keratin 15**	HMRW	IgG2a / κ	C-terminal	Mouse
369	**Adenovirus**	A	IgG2a / κ + IgG2a / κ	Not determined	Mouse
370	**Glycophorin A**	H	IgM / κ	N-terminal	Mouse
371	**p63 (p53 Family Member)**	HMR	IgG2a / κ	aa 1-205	Mouse
372	**TdT**	H	IgG2a	N-terminal	Mouse
373	**Fascin**	HR	IgG1	Not determined	Mouse
374	**Myogenin**	HMRC	IgG1 / κ	aa 138-158	Mouse
375	**cdh1**	H	IgG1 / κ	Not determined	Mouse
376	**CD63**	H	IgG1 / κ	Not determined	Mouse
377	**Ret Oncoprotein**	H	IgG1	C-terminal	Mouse
378	**Caspase 3**	H	IgG2a	Not determined	Mouse
379	**SRC1 (Steroid Receptor Coactivator-1) Ab-1**	H	IgG1 / κ	Not	Mouse
380	**GRIP1**	H	IgG1 / κ	Not determined	Mouse
381	**Caspase 9**	HM	IgG1 / κ	Caspase 9 prodomain	Mouse
382	**CA125**	H	IgG1	Not determined	Mouse
383	**Heat Shock Protein 90a/hsp86**	HMR	N/A	aa 2-12	Rabbit
384	**Calponin**	HR	IgG1 / κ	Not determined	Mouse
385	**Caldesmon**	H	IgG1 / k	Not determined	Mouse
386	**GCDFP-15**	HR	IgG2a / k	Not determined	Mouse
387	**CD42b**	H	IgG1	Not determined	Mouse
388	**Myosin Smooth Muscle Heavy Chain**	H	IgG1 / κ	Not determined	Mouse
389	**ER Ca+2 ATPase2**	H	N/A	Not determined	Mouse
390	**IL-10R**	H	N/A	Not determined	Rat
391	**G-CSF**	H	N/A	Not determined	Rat
392	**SHP-1**	H	IgG2b / κ	Not determined	Mouse
393	**CD40**	H	IgG1 / κ	Not determined	Mouse
394	**ATM**	H	IgG1	C-terminal	Mouse
395	**Survivin**	HR	IgG1 / κ	aa 1-99	Mouse
396	**SREBP-1 (Sterol Regulatory Element Binding Protein-1)**	HS	IgG1 / κ	aa 301-407	Mouse
397	**Vinculin**	H	IgG1	Not determined	Mouse
398	**Filamin**	HRGpKT	IgG1	Not determined	Mouse
399	**Mast Cell Chymase**	H	IgG1	Not determined	Mouse
400	**Amyloid A**	H	IgG2a / κ	Not determined	Mouse
401	**CDw60**	H	IgM	Not determined	Mouse

402	**Synaptophysin**	H	IgG1	Near C-terminus	Mouse
403	**Axonal Growth Cones**	H	IgG1	Not determined	Mouse
404	**Neurofilament (68kDa)**	H	IgG1	Not determined	Mouse
405	**Neurofilament (160kDa)**	H	IgG1	Not determined	Mouse
406	**Neurofilament (200kDa)**	H	IgM	Not determined	Mouse
407	**Rhodopsin (Opsin)**	HMR	IgG1	Not determined	Mouse
408	**HRP**	Not determined	N/A	Not determined	Rabbit
409	**IgG**	H	IgG1 / κ	Not determined	Mouse
410	**Keratin 8 (phospho-specific Ser73)**	HM	IgG2a	LLpS/TPL	Mouse
411	**Ferritin**	H	IgG1	Not determined	Mouse
412	**Cystic Fibrosis Transmembrane Regulator**	H	IgG1a / κ	N-terminus	Mouse
413	**GAPDH**	HMRChKTY	IgM	Not determined	Mouse
414	**Tropomyosin**	HRK	IgG1 / κ	Not determined	Mouse
415	**Calmodulin**	HRKW	IgG1	Not determined	Mouse
416	**ADP-ribosylation Factor (ARF-6)**	H	IgG1 / κ	Not determined	Mouse
417	**Parathyroid Hormone Receptor Type 1**	H	IgG1 / κ	aa 146-169	Mouse
418	**SRF (Serum Response Factor)**	H	N/A	Not determined	Mouse
419	**Gamma Glutamyl Transferase (gGT)**	H	IgG1	Not determined	Mouse
420	**Cytochrome c**	HDW	IgG2a / κ	Not determined	Mouse
421	**CD9**	H	IgG1 / κ	Not determined	Mouse
422	**CD24**	H	IgG1 / κ	Not determined	Mouse
423	**CD79b**	H	IgG1 / κ	Extracellular domain	Mouse
424	**CD165**	H	IgG1 / κ	Not determined	Mouse
425	**CD231**	H	IgG1 / k	Not determined	Mouse
426	**Green Fluorescent Protein (GFP)**	All	IgG1 / κ	Not determined	Mouse
427	**CD3zeta**	HMR	IgG1	aa 36-54 of T Cell Receptor ζ Chain	Mouse
428	**CD105**	H	IgG1 / κ	Not determined	Mouse
429	**Clathrin**	HW	IgG2b / κ	aa23-44	Mouse
430	**PMP-22**	H	IgM / κ	aa 118-132	Mouse
431	**Luciferase**	All	IgG1 / κ	Not determined	Mouse
432	**Actin, Pan**	HMRDKPTW	IgG1 / κ	Not determined	Mouse
433	**Actin, Muscle Specific**	HMRDPW	IgG1 / κ	Not determined	Mouse
434	**Hepatocyte Factor Homologue-4**	HR	IgG1 / κ	Not determined	Mouse
435	**Hepatic Nuclear Factor-3B**	H	IgG2a / κ	Not determined	Mouse
436	**Surfactant Protein B**	H	IgG2a / κ	Not determined	Mouse
437	**Ras**	HMRW	N/A	aa 31-43	Rabbit
438	**Calcium Pump ATPase**	H	IgG1 / κ	aa 1156-1180	Mouse
439	**Heat Shock Protein 75/hsp75**	H	IgG	Not determined	Mouse
440	**B-Cell**	M	IgG2b / κ	Not determined	Rat
441	**Thyroid Hormone Receptor, Human**	HMRP	IgG2a / κ	aa 13-32	Mouse
442	**Thyroid Hormone Receptor beta, human**	HD	IgG1 / κ	aa31-50	Mouse
443	**Laminin-s**	HGpRKTW	IgG1	Not determined	Mouse
444	**L-Plastin**	H	IgG1	Headpiece region	Mouse
445	**b Galactosidase**	All	IgG1	Not determined	Mouse
446	**Progesterone Receptor (phospho-**	H	IgG1 / κ	aa184-196	Mouse

	specific) - Serine 190				
447	**Progesterone Receptor (phospho-specific) - Serine 294**	H	IgG1 / κ	aa 288-300	Mouse
448	**PR3 (Proteinase 3)**	H	IgG1 / κ	Not determined	Mouse
449	**bcl-XL**	HM	IgG2a	TEAPEETEAERETPSA	Mouse
450	**Prolactin Receptor**	H	IgG1	Not determined	Mouse
451	**Notch**	HM	IgG2b	Ligand binding region	Mouse
452	**Retinoic Acid Receptor (b)**	H	IgG1 / κ	aa 11-25	Mouse
453	**Retinoid X Receptor (hRXR)**	H	IgG2a / κ	aa 213-226 (Hinge region)	Mouse
454	**MCM2**	H	IgG1	Not determined	Mouse
455	**Negative Control for Mouse IgG3**	All	IgG3 / κ	Not determined	Mouse
456	**Prolactin**	H	IgG1 / κ	Not determined	Mouse
457	**Thyroglobulin**	HMRD	IgG1	Not determined	Mouse
458	**Mitochondria**	H	IgG1	Not determined	Mouse
459	**c-Src**	HMR	N/A	N-terminal	Rabbit
460	**Insulin**	HRPTW	IgG1 / κ	Not determined	Mouse
461	**XPF**	H	IgG2 / κ	Not determined	Mouse
462	**Negative Control for Mouse IgG2a**	All	IgG2a / κ	Not determined	Mouse
463	**MCM5**	H	IgG2b	Not determined	Mouse
464	**RAD1**	H	IgG2a / κ	Not determined	Mouse
465	**DNA Polymerase Beta**	H	IgG2a	Not determined	Mouse
466	**c-fos**	H	IgG2a	Extracellular domain	Mouse
467	**c-jun**	H	N/A	Not determined	Rabbit
468	**DP-2**	HMR	N/A	C-terminus	Rabbit
469	**E2F-5**	HMR	N/A	N-terminal	Rabbit
470	**Glucagon**	HMR	N/A	Not determined	Rabbit
471	**Pneumocystis jiroveci**	Pneumocystis jiroveci	IgM / κ	Not determined	Mouse
472	**Topo II beta**	H	N/A	C-terminal 300 aa	Rabbit
473	**Fli-1**	HMR	N/A	C-terminal	Rabbit
474	**ITK**	HM	IgG1 / κ	N-terminal	Mouse
475	**LH**	H	IgG1 / κ	Not determined	Mouse
476	**FSH**	HW	IgG1 / κ	Not determined	Mouse
477	**Thyroid Stimulating Hormone (TSH)**	H	IgG1 / κ	Not determined	Mouse
478	**Grb2**	HMRW	IgG1 / κ	aa 54-62	Mouse
479	**CXCR4 / Fusin**	H	IgG2a / κ	Not determined	Mouse
480	**Vacular Endothelial Growth Factor(VEGF)**	H	IgG1 / κ	Not determined	Mouse
481	**14.3.3 gamma**	H	IgG1 / κ	Not determined	Mouse
482	**14.3.3, Pan**	H	IgG1 / κ	Not determined	Mouse
483	**IL-4**	H	N/A	Not determined	Rat
484	**Ki67**	HR	N/A	Middle of Ki67 protein	Rabbit
485	**Pds1**	H	IgG2a / κ	Not determined	Mouse
486	**Chk1**	H	N/A	Not determined	Rabbit
487	**IL-5**	H	N/A	Not determined	Rat
488	**PARP**	HMR	N/A	N-terminal	Rabbit
489	**Calcitonin**	HMRDEPY	N/A	Not determined	Rabbit
490	**Bak**	HMS	N/A	N-terminal	Rabbit
491	**Cadherin, (Pan)**	HMRDKWXY	N/A	C-terminal	Rabbit
492	**Flk-1 / KDR / VEGFR2**	HMR	Synthetic	C-terminal	Rabbit

			peptide		
493	**Flt-1 / VEGFR1**	HMR	N/A	C-terminal	Rabbit
494	**TRADD**	H	N/A	C-terminal	Rabbit
495	**Exo1**	HM	IgG1 / κ	Not determined	Mouse
496	**MMP-23**	H	N/A	Not determined	Rabbit
497	**MMP-14 / MT1-MMP**	H	N/A	Second quarter of MMP-14	Rabbit
498	**MMP-15 / MT2-MMP**	HM	N/A	Catalytic domain of mouse MMP-15	Rabbit
499	**MMP-16 / MT3-MMP**	HMR	N/A	Catalytic domain	Rabbit
500	**I-FLICE / CASPER**	H	N/A	C-terminal	Rabbit
501	**TID-1**	HMR	IgG1 / κ	Not determined	Mouse
502	**Somatostatin Receptor-I**	HMR	N/A	C-terminal	Rabbit
503	**NOS-u**	HMRPW	N/A	C-terminal	Rabbit
504	**Fra2**	H	N/A	C-terminal	Rabbit
505	**Synuclein**	H	IgG2a / κ	Not determined	Mouse
506	**ERK2**	HMR	N/A	Not determined	Rabbit
507	**Cullin-3 (CUL-3)**	HM	N/A	N-terminal	Rabbit
508	**p73**	H	N/A	aa1-15	Rabbit
509	**RAIDD**	H	N/A	C-terminal	Rabbit
510	**MADD**	H	N/A	Second half of MADD protein	Rabbit
511	**XRCC2**	H	N/A	N-terminal	Rabbit
512	**Glycogen Synthase Kinase 3b (GSK3b)**	HMRW	N/A	Kinase subdomain XI region	Rabbit
513	**Granzyme B**	HR	N/A	aa 139-157	Rabbit
514	**Keratin 8/18**	H	IgG1 / κ + IgG1	Not determined	Mouse
515	**NOS-i**	HMR	N/A	C-terminal	Rabbit
516	**Caspase 1**	HMR	N/A	Second quarter of Caspase 1	Rabbit
517	**D4-GDI**	HW	N/A	N-terminal	Rabbit
518	**Bim (BOD)**	HMR	N/A	N-terminal	Rabbit
519	**PLC gamma 1**	HRW	N/A	C-terminal	Rabbit
520	**PHAS-I**	HMR	N/A	C-terminal	Rabbit
521	**TRP75 / gp75**	H	IgG2a	Not determined	Mouse
522	**$p57^{Kip2}$ Ab-7**	HMW	N/A	Near C-terminus	Rabbit
523	**NF kappa B / p65 (Rel A)**	HDMPRSTW	N/A	C-terminal	Mouse
524	**Amyloid A4 Protein Precursor**	HMR	N/A	Extreme C–terminus	Rabbit
525	**Amyloid Beta (APP)**	HMR	N/A	aa653-662 (DAEFRHDSGY)	Rabbit
526	**ARC**	H	N/A	C-terminal	Rabbit
527	**NF kappa B / p50**	H	N/A	aa44-61	Rabbit
528	**Lck (p56lck)**	H	N/A	Near the N-terminus	Rabbit
529	**AIF (Apoptosis Inducing Factor)**	H	N/A	N-terminal	Rabbit
530	**Human Sodium Iodide Symporter (hNIS)**	H	IgG1 / κ	aa625-643	Mouse
531	**Caspase 7 (Mch 3)**	H	N/A	Not determined	Rabbit
532	**Ask1 / MAPKKK5**	H	N/A	C-terminal	Rabbit
533	**TACE (TNF-alpha converting enzyme) / ADAM17**	HMR	N/A	C-terminal	Rabbit
534	**Zip kinase**	HMR	N/A	Not determined	Rabbit
535	**Mek1**	HMR	N/A	N-terminal	Rabbit

536	**Mek2**	HMR	N/A	N-terminal	Rabbit
537	**Mek6**	HMR	N/A	N-terminal	Rabbit
538	**I-Kappa-B Kinase b (IKKb)**	HMR	N/A	Near C-terminus	Rabbit
539	**JNK Activating kinase (JKK1)**	HMR	N/A	Near C-terminus	Rabbit
540	**FLIP**	HM	N/A	C-terminal	Rabbit
541	**Raf1**	HMRF	N/A	Middle of Raf1	Rabbit
542	**PARP (Poly ADP-Ribose Polymerase)**	HMRW	N/A	C-terminal	Rabbit
543	**Bonzo / STRL33 / TYMSTR**	H	N/A	Near the C-terminus	Rabbit
544	**FADD (FAS-Associated death domain-containing protein)**	HM	N/A	Middle of mouse FADD	Rabbit
545	**SODD (Silencer of Death Domain)**	H	N/A	C terminal	Rabbit
546	**Vitamin D Receptor (VDR)**	H	N/A	C-terminal	Rabbit
547	**PDGFR, alpha**	HMR	N/A	C-terminal	Rabbit
548	**PDGFR, beta**	HM	N/A	Near C-terminal	Rabbit
549	**Daxx**	HKM	N/A	C-terminal	Rabbit
550	**Caspase 8 (FLICE)**	HMRW	N/A	Not determined	Rabbit
551	**Gamma Glutamylcysteine Synthetase(GCS)/Glutamate-cysteine Ligase**	HMR	IgG1	aa 295-313 of rat GCLC	Rabbit
552	**DcR2 / TRAIL-R4 / TRUNDD**	H	N/A	Intracellular	Rabbit
553	**Caspase 2**	HMRK	N/A	C-terminal	Rabbit
554	**CREB**	HMR	N/A	Middle region	Rabbit
555	**Nitric Oxide Synthase, brain (bNOS)**	HR	N/A	Near N-terminal	Rabbit
556	**Acinus**	HM	N/A	Present in AcinusL, AcinusS' and AcinusS	Rabbit
557	**CIDE-A**	H	N/A	C-terminal	Rabbit
558	**CIDE-B**	M	N/A	C-terminal	Rabbit
559	**Bcl10 / CIPER / CLAP / mE10**	HMR	N/A	N-terminal	Rabbit
560	**Nitric Oxide Synthase, endothelial (eNOS)**	HMRDPW	N/A	C-terminal	Rabbit
561	**Int-2 Oncoprotein**	HM	IgG2a / κ	Not determined	Mouse
562	**CEA / CD66e**	H	IgG1	Not determined	Mouse
563	**Epithelial Membrane Antigen (EMA / CA15-3 / MUC-1)**	H	IgG1 / κ	Not determined	Mouse
564	**Raf-1 (Phospho-specific)**	H	IgG1	GQRDS*SYY*WEIEAS	Rat
565	**Mucin 3 (MUC3)**	H	IgG2a	Tandem repeats of the human MUC3	Mouse
566	**MyD88**	HM	N/A	Near C-terminus	Rabbit
567	**Cadherin-P**	H	IgG1	External domain	Mouse
568	**Glicentin**	HRP	N/A	Not determined	Rabbit
569	**Superoxide Dismutase**	H	IgG1	N-terminal domains I-V	Mouse
570	**TRAP**	H	IgG2b	N-terminal	Mouse
571	**p170**	H	IgG2a	C-terminal cytoplasmic	Mouse
572	**CD138**	H	IgG1	Not determined	Mouse
573	**Hepatocyte**	H	IgG1 / κ	Not determined	Mouse
574	**SV40 Large T Antigen**	SV40 virus	IgG2a	IgG2a	Mouse
575	**Apolipoprotein D**	HM	N/A	aa 810-822	Rabbit
576	**Neutrophil Elastase**	H	IgG1 / κ	Not determined	Mouse
577	**CD61 / Platelet Glycoprotein IIIA**	H	IgG1 / κ	Not determined	Mouse

578	**Bromodeoxyuridine (BrdU)**	All	IgG1 / κ	Not determined	Mouse
579	**Nucleophosmin (NPM)**	H	IgG / κ	N-terminal	Mouse
580	**Keratin 20**	H	IgG1	Not determined	Mouse
581	**Retinoblastoma (Rb) (Phospho-specific Serine608)**	HM	IgG1	Not determined	Mouse
582	**CDC14A Phosphatase**	H	IgG1	C-terminal	Mouse
583	**CD71 / Transferrin Receptor**	H	IgG1	Not determined	Mouse
584	**IgM (m-Heavy Chain)**	H	IgG1 / κ	Not determined	Mouse
585	**PHAS-II**	H	N/A	Amino acids 99-120 of human PHAS-II	Rabbit
586	**DcR1**	H	N/A	Amino acids 111-123 of human DcR1	Rabbit
587	**Rad18**	H	N/A	Amino acids 402-414 of human Rad18	Rabbit
588	**DR5**	HR	N/A	Amino acids 255-270 of rat DR5	Rabbit
589	**Stat5**	H	N/A	Amino acids 371-389 of human Stat5	Rabbit
590	**Calretinin**	HMR	N/A	Not determined	Rabbit
591	**Desmin**	HMR	N/A	Near C-terminus	Rabbit
592	**CD30 (Reed-Sternberg Cell Marker)**	H	IgG1	Extracellular domain	Mouse
593	**Dysferlin**	H	N/A	C-terminus	Rabbit
594	**Fas-ligand**	HMR	N/A	N-terminus	Rabbit
595	**Connexin 43**	HMR	N/A	3rd cytoplasmic	Mouse
596	**Synuclein beta**	HR	N/A	Near C-terminus	Rabbit
597	**Parathyroid Hormone**	HM	N/A	N-terminus	Rabbit
598	**Synuclein pan**	HR	N/A	Near C-terminus	Rabbit
599	**Cathepsin D**	H	N/A	Not determined	Rabbit
600	**GLUT-1**	HR	N/A	C-terminal	Rabbit
601	**GluR4**	HMRKY	N/A	C-terminal	Rabbit
602	**GSK-3**	HMRKY	N/A	C-terminal	Rabbit
603	**14-3-3 beta**	HMR	N/A	N-terminal	Rabbit
604	**GluR6/7**	HMRKY	N/A	C-terminal	Rabbit
605	**hPL**	H	N/A	Not determined	Rabbit
606	**Myoglobin**	H	N/A	Not determined	Rabbit
607	**GluR 2/3**	HMRY	N/A	C-terminal	Rabbit
608	**H.Pylori**	Helicobacter pylori	N/A	Not determined	Rabbit
609	**CD23**	H	N/A	48-248aa	Rabbit
610	**COX2**	HMR	N/A	C-terminus	Rabbit
611	**GluR1**	HR	N/A	C-terminal	Rabbit
612	**Phospho-Ser/Thr/Tyr**	All	IgG1	Not determined	Mouse
613	**GLUT-3**	H	N/A	C-terminal	Rabbit
614	**Osteopontin**	HDP	N/A	Internal domain	Rabbit
615	**PSCA**	H	N/A	Extracellular	Rabbit
616	**PGP9.5**	H	N/A	Not determined	Rabbit
617	**Ubiquitin**	H	N/A	Not determined	Rabbit
618	**Amylin Peptide**	H	N/A	N-terminal	Rabbit
619	**Prostate Apoptosis Response Protein-4**	HMR	N/A	C-terminus	Rabbit
620	**alpha-1-antitrypsin**	H	N/A	Not determined	Rabbit
621	**CITED1**	H	N/A	Not determined	Rabbit

622	**Muc-1**	HM	N/A	aa 239-255	Rabbit
623	**HDAC1**	HMR	N/A	C-terminus	Rabbit
624	**TrxR2**	HR	N/A	C-terminus	Rabbit
625	**FHIT**	H	N/A	Not determined	Rabbit
626	**Catenin gamma**	HMR	N/A	C-terminal	Rabbit
627	**IGF-I**	HMR	N/A	Not determined	Rabbit
628	**Claudin 5**	HM	N/A	C-terminal	Rabbit
629	**a-B-Crystallin**	H	N/A	Not determined	Rabbit
630	**TGF-beta 2**	HMR	N/A	C-terminal	Rabbit
631	**Claudin 3**	HMR	N/A	C-terminal	Rabbit
632	**O ct-1**	HMR	N/A	C-terminal	Rabbit
633	**Flt-4**	HMR	N/A	C-terminus	Rabbit
634	**Actin, skeletal muscle**	HREGpT	N/A	N-terminus	Rabbit
635	**PDGF**	HR	N/A	101-116aa	Rabbit
636	**Claudin 2**	HM	N/A	C-terminal	Rabbit
637	**TGF beta 3**	HMR	N/A	C-terminal	Rabbit
638	**Wnt-1**	HMR	N/A	N-terminal	Rabbit
639	**Claudin 4**	HM	N/A	C-terminal	Rabbit
640	**MMP-19**	H	N/A	Not determined	Rabbit
641	**TNR-R2**	HMR	N/A	C-terminal	Rabbit
642	**Pax-5**	HMR	N/A	C-terminal	Rabbit
643	**P504S**	H	N/A	Not determined	Rabbit
644	**S100A4**	H	N/A	Not determined	Rabbit
645	**Urocortin**	HR	N/A	Not determined	Rabbit
646	**Gastrin 1**	H	N/A	Not determined	Rabbit
647	**CCK-8**	H	N/A	Not determined	Rabbit
648	**IP10/CRG2**	H	N/A	Not determined	Mouse
649	**IL17**	H	N/A	Not determined	Mouse
650	**Toxoplasma Gondii**	H	N/A	Not determined	Rabbit
651	**IFN gamma**	H	IgG1	Not determined	Mouse
652	**mRANKL**	M	IgG1	Not determined	Rat
653	**CD94**	H	IgG1	Not determined	Mouse
654	**ZAP-70**	H	N/A	aa 1-254	Rabbit
655	**Oct-3/**	H	N/A	Not determined	Rabbit
656	**PPAR-gamma**	H	N/A	Not determined	Mouse

Reactivity: H human, A adenovirus, C cat, Ch Chinese hamster, D dog, E sheep, Gp guinea pig, Gt goat, K chicken, M mouse, P pig, Q quail, S hamster, T rabbit, W cow, X xenopus, Y monkey

6.2 Saturation-DIGE

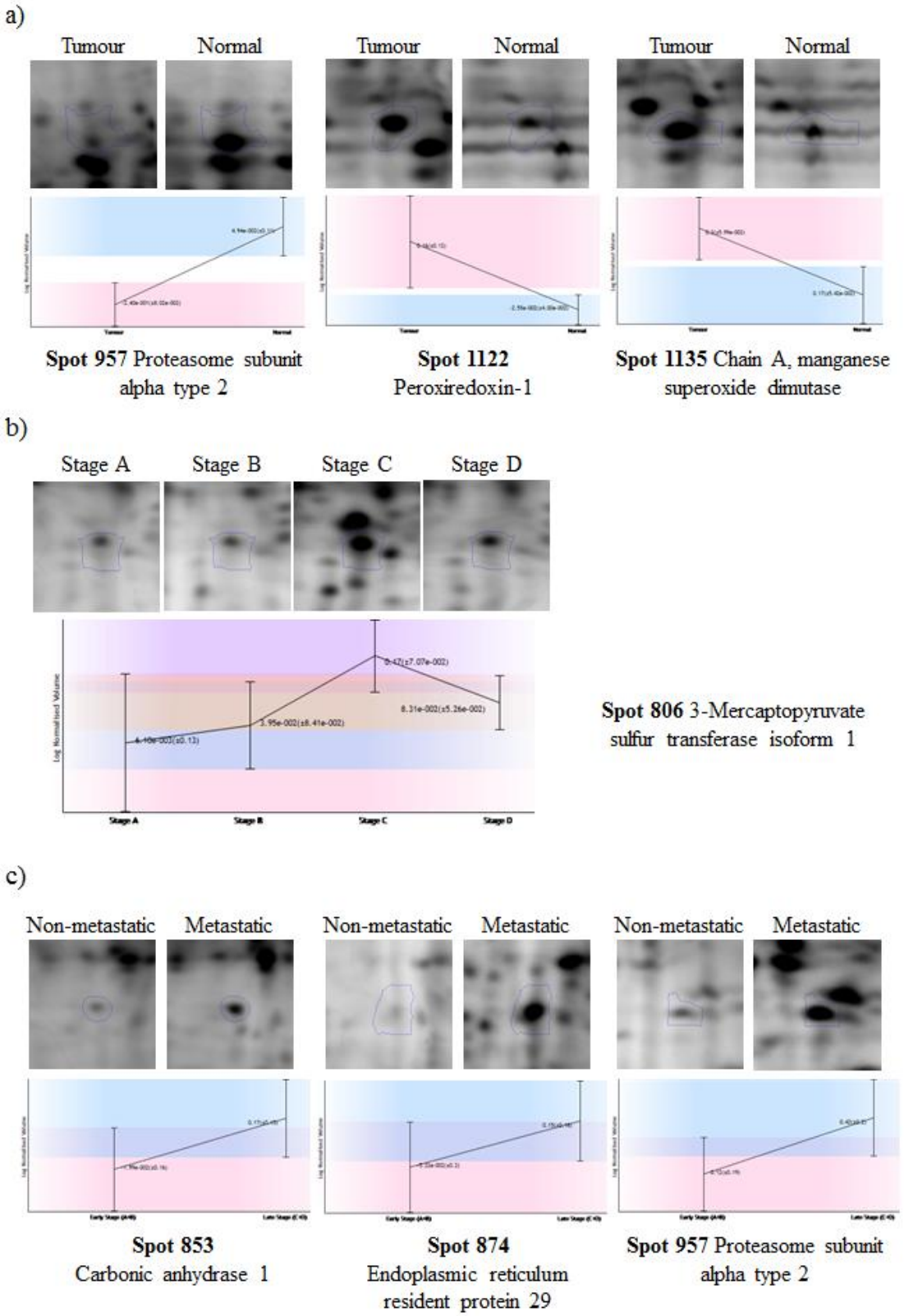

Figure 6.2 Examples of differential spots identified by Progenesis SameSpot a) tumour versus normal b) ANOVA CRC stages and c) non-metastatic versus metastatic CRC

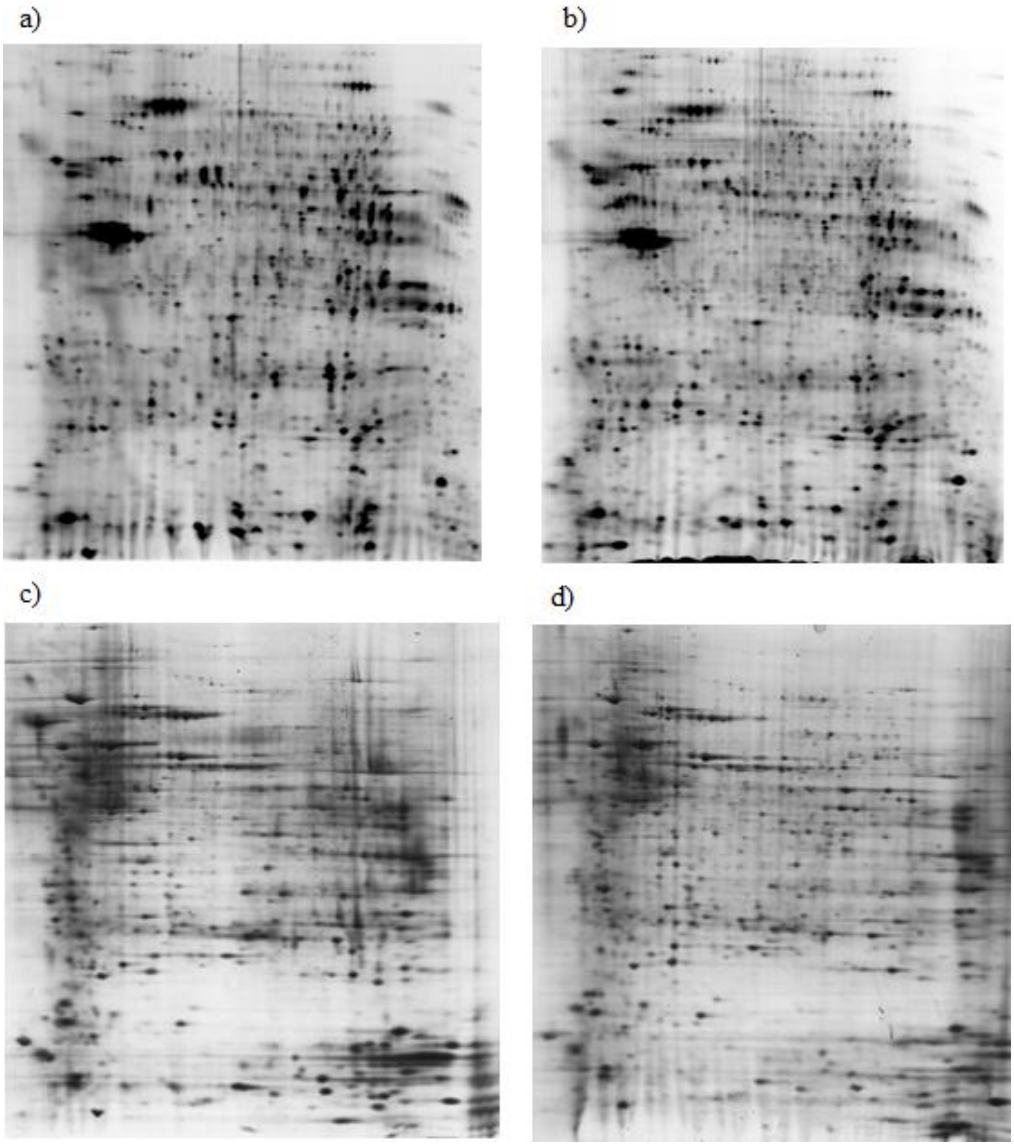

Figure 6.3 Analytical gel scans of a) tumour b) and control samples (saturation-DIGE labelled, patient ACPS B2, 5 µl protein) compared to preparative gel scans of c) pooled tumour and d) control (double stained: SybrRuby and Coomassie blue, pooled from 16 tumour or control samples, 500 µl protein).

6.3 DotScan antibody microarray

a)

Leukaemia array	TCR α/β	TCR γ/δ	CD1a	CD2	CD3	CD4	CD5
	CD7	CD8	CD9	CD10	CD11a	CD11b	CD11c
	CD13	CD14	CD15	CD16	CD19	CD20	CD21
	CD22	CD23	CD24	CD25	CD28	CD29	CD31
	CD32	CD33	CD34	CD36	CD37	CD38	CD40
	CD41	CD42a	CD43	CD44	CD45	CD45RA	CD45RO
	CD49d	CD49e	CD52	CD54	CD56	CD57	CD60
	CD61	CD62L	CD62E	CD62P	CD64	CD65	CD66c
	CD71	CD77	CD79a	CD79b	CD80	CD86	CD88
	CD95	CD102	CD103	CD117	CD120a	CD122	CD126
	CD128	CD130	CD134	CD135	CD138	CD154	CD235a
	HLA-DR	FMC7	κ	λ	sIg		
Colorectal cancer array	CD15s	CD26	CD44v6	CD47	CD49f	CD55	CD59
	CD63	CD69	CD66e	CD82	CD87	CD104	CD151
	CD166	CD175s	CD227	CD244	CD261	CD262	CD324
	CD326	CD340	CD98	β-catenin	Annexin II	CA-125	Claudin-4
	DCC	EGFR	FAP	Galectin-3	Galectin-4	Galectin-8	HLA-ABC
	MICA	MMP-14	PRGR	CA 19-9	TSP-1		
Isotype control	mIgG1 500	mIgG1 200	mIgG1 50	mIgG2a 500	mIgG2a 200	mIgG2a 50	mIgG2b 500
	mIgG2b 200	mIgG3 500	mIgM 500	mIgM 200	mIgM 50	Mabthera	

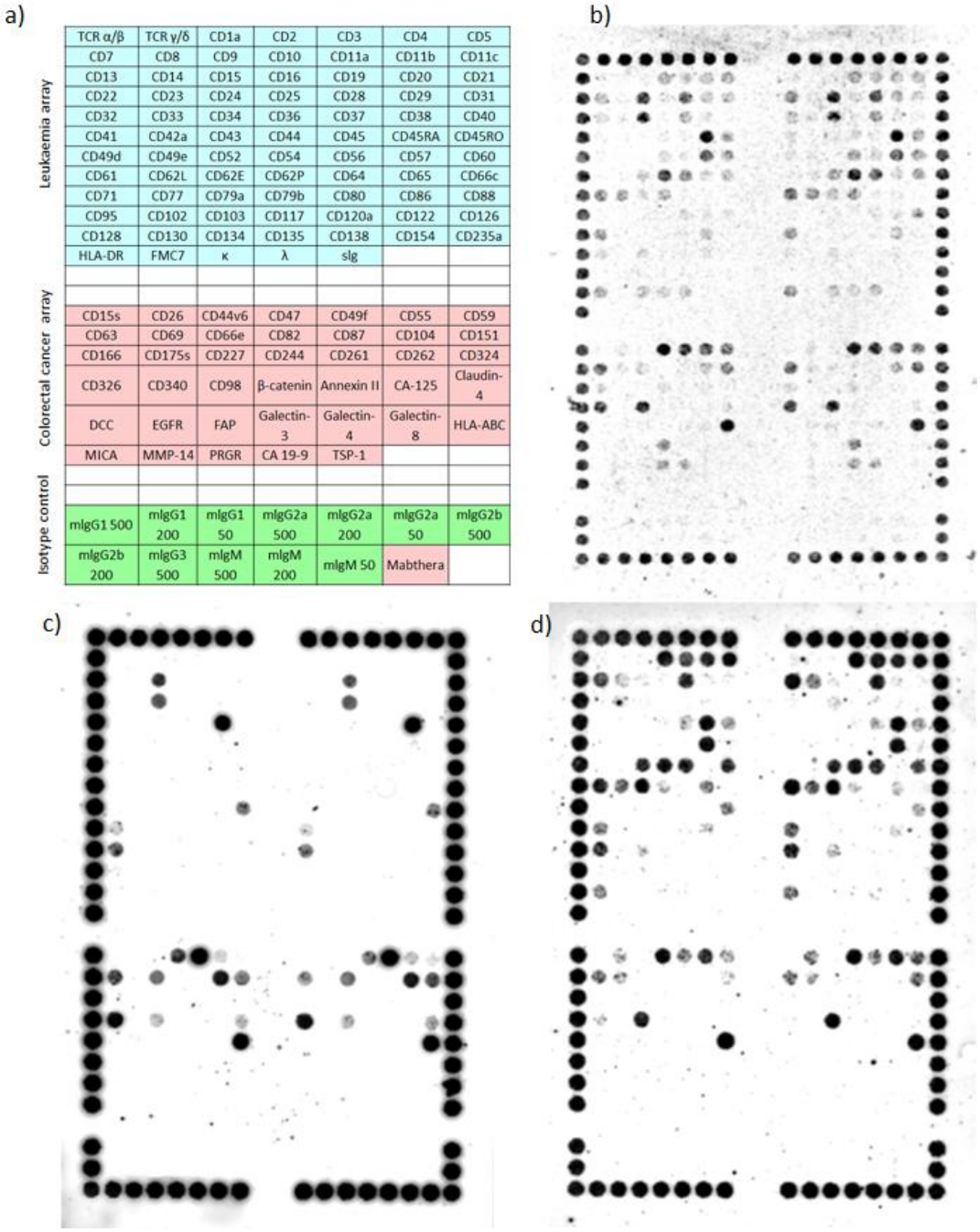

Figure 6.4 Example of the surface profiles obtained with the Dotscan antibody microarray. The antibody address a) shows the antibody ID within each leukocyte, CRC and isotype control panel. Viable cells from a stage B1 CRC tumour was captured on the DotScan microarray; the optical scan b) shows the surface profile of the mixture of cell types within the tumour, the EpCAM c) and CD3 d) profiles show the expression of surface proteins on epithelial/cancer and T-cells, respectively. TCR α/β T-cell receptor alpha/beta, TCR γ/δ T-cell receptor gamma/delta, κ kappa light chain, λ lambda light chain, sIg surface immunoglobulin, CA-125 cancer antigen 125, DCC deleted in colon cancer protein, FAP fibroblast activation protein, PRGR progesterone receptor, TSP-1 thrombospondin-1, Mabthera (rituximab) monoclonal antibody against CD20.

Table 6.2 DotScan microarray antibody list.

CD marker or antigen	Clone	Antibody Isotype	Antibody Source	Cat No	Stock Ab Conc (µg/ml)
TCR a/b	BMA031	IgG2b	Immunotech	IM1466	200
TCR g/d	Immu 510	IgG1	Immunotech	IM1349	100
CD1a	BL6	IgG1	Immunotech	IM0130	200
CD2	RPA-2.10	IgG1	Pharmingen	555324	500
CD3	SP34	IgG3	Pharmingen	556610	500
CD4	13B8.2	IgG1	Immunotech	IM0398	200
CD5	BL1a	IgG2a	BioDesign	P42116M	200
CD6	M-T605	IgG1	Pharmingen	555356	500
CD7	8H8.1	IgG2a	BioDesign	P42179M	200
CD8	B9.11	IgG1	Immunotech	IMBULK1	1480
CD9	ALB6	IgG1	Immunotech	IM0117	200
CD10	ALB2	IgG2a	Immunotech	IMBULK1	200
CD11a	25.3.1	IgG1	Immunotech	IM0157	200
CD11b	BEAR1	IgG1	Immunotech	190	200
CD11c	BU 15	IgG1	Immunotech	712	200
CD13	L138	IgG1	Pharmingen	347830	100 tests
CD14	RM052	IgG2a	Immunotech	IM0643	200
CD15	HI98	IgM	Pharmingen	555400	500
CD16	3G8	IgG1	Immunotech	IM0813	200
CD19	J4119	IgG1	Immunotech	IM1313	200
CD20	H299 (B1)	IgG2a	Coulter	6602140	250
CD21	BL13	IgG1	Immunotech	111	200
CD22	HIB 22	IgG1	Pharmingen	555423	200
CD23	9P.25	IgG1	Immunotech	419	200
CD24	ALB9	IgG1	Immunotech	IM0118	200
CD25	B1.49.9	IgG2a	Immunotech	119	200
CD28	CD28.8	IgG1	Immunotech	1376	200
CD29	K20	IgG2a	Beckman Coulter	IMBULK1	200
CD31	1F11	IgG1	Immunotech	2052	200
CD32	2E1	IgG2a	Immunotech	IM0417	200
CD33	P67.6	IgG1	Biolab	sc-19660	200
CD34	QBEND 10	IgG1	Immunotech	786	200
CD36	FA6-152	IgG1	Immunotech	765	200
CD37	BL 14	IgG1	Immunotech	110	200
CD38	T16	IgG1	Immunotech	IM 0366	200
CD40	MAB89	IgG1	Beckman Coulter	IM1374	200
CD41	P2	IgG1	Immunotech	IM0145	200
CD42a	SZ1	IgG2a	Beckman Coulter	IM0538	200
CD43	DFT1	IgG1	Immunotech	IM1843	200

CD44	J-173	IgG1	Immunotech	IM0845	200
CD45	69	IgG1	Pharmingen	610266	250
CD45RA	HI100	IgG2b	Pharmingen	555486	500
CD45RO	UCHL1	IgG2a	Pharmingen	555491	500
CD49d	HP2/1	IgG1	Immunotech	IM 0764	200
CD49e	SAM1	IgG2b	Beckman Coulter	IM0771	200
CD52	CF1D12	IgG3	Caltage Lab	MHCD5200	200
CD54	84H10	IgG1	Immunotech	544	200
CD56	N901(NKH-1)	IgG1	Immunotech	6602705	
CD57	NK-1	IgM	Pharmingen	555618	500
CD60	M-T6004	IgM	Serotec	MCA1314	200 test
CD61	SZ21	IgG1	Immunotech	0540	200
CD62L	Dreg56	IgG1	Pharmingen	555542	500
CD62E	1.2B6	IgG1	Immunotech	IM1243	200
CD62P	CLB-Thromb/6	IgG1	Immunotech	IM1315	200
CD64	32.2	IgG1	BioDesign	P20410M	
CD65	88H7	IgM	Sanquin	M1719	200
CD66c	KOR-SA3544	IgG1	MBL	D028-3	500
CD71	4DJ1.2.2	IgG1	Immunotech	IM2117	200
CD77	38-13	IgM	Immunotech	175	150
CD79a	HM47	IgG1	Pharmingen	555934	500
CD79b	CD3.1	IgG1	Pharmingen	555678	500
CD80	MAB 104	IgG1	Immunotech	1449	200
CD86	2331 (FUN-1)	IgG1	Pharmingen	555655	500
CD88	D53-1473	IgG1	Pharmingen	550493	500
CD95	UB2	IgG1	Immunotech	1505	1000
CD102	B-T1	IgG1	Serotec	MCA1140	1000
CD103	Ber-ACT8	IgG1	Pharmingen	550258	500
CD117	YB5.B8	IgG1	Pharmingen	555713	500
CD120a	H398	IgG2a	Serotec	MCA1340	1000
CD122	Mik-b2	IgG2a	Pharmingen	554520	500
CD126	M5	IgG1	Pharmingen	551462	500
CD128	5A12	IgG2b	Pharmingen	555937	500
CD130	A1/gp130	IgG1	Pharmingen	552426	500
CD134	ACT35	IgG1	Pharmingen	555836	500
CD135	SF1-340	IgG1	Immunotech	2036	200
CD138	DL-101	IgG1	Pharmingen	550804	500
CD138 (40C)	Mi15	IgG1	Pharmingen	551902	500
CD154	TRAP1	IgG1	Immunotech	1842	200
CD235a	11E4B7.6	IgG1	Immunotech	IM2210	200
HLA-DR	L243	IgG2a	Immunotech	347360	100 tests
FMC7	FMC7	IgM	Millipore	MAB1217	500
Kappa	6E1	IgG1	Immunotech	IM0173	200

Lambda	C4	IgG1	Immunotech	IM0174	200
sIg	polyclonal	IgG	Sigma	I-8758	N/A
CD15s	CSLEX1	IgM	Pharmingen	551344	500
CD26	M-A261	IgG1	Pharmingen	555435	500
CD44v6	2F10	IgG1	R&D	BBA13	1000
CD47	B6H12	IgG1	Pharmingen	556044	500
CD49f	GoH3	IgG2a	Pharmingen	555734	500
CD55	IA10	IgG2a	Pharmingen	555691	500
CD59	p282	IgG2a	Pharmingen	555761	500
CD63	H5C6	IgG1	Pharmingen	556019	
CD69	FN50	IgG1	Pharmingen	555529	500
CD66e	C365D3	IgG1	Serotec	MCA1744	1000
CD82	5B5	IgG2a	abcam	ab49292	
CD87	VIM5	IgG1	Pharmingen	555767	500
CD104	450-9D	IgG1	Pharmingen	555721	500
CD151	14A2.H1	IgG1	Pharmingen	556056	500
CD166	3A6	IgG1	Pharmingen	559260	500
CD175s	BRIC111	IgG1	abcam	ab24005	1000
CD227	HMPV	IgG1	Pharmingen	555925	500
CD244	2-69	IgG2a	Pharmingen	550814	500
CD261	DJR1	IgG1	BioLegend	307202	?? undil
CD262	B-37D	IgG2b	Diaclone	990-85487	1000
CD324	MB2	IgG2b	abcam	ab8993	1000
CD326	158206	IgG2b	R&D	MAB9601	500
CD340	191924	IgG2b	R&D	MAB1129	1000
CD98	UM7F8	IgG1	Pharmingen	556074	500
b-catenin		IgG	R&D	AF1329	500
Annexin II	5/Annexin II	IgG1	Pharmingen	610069	800
CA-125	X75	IgG1	abcam	ab1107	1000
Claudin-4	382321	IgG2a	R&D	MAB4219	500
DCC	G92-13	IgG1	Pharmingen	554222	500
EGFR	EGFR.1	IgG2b	Pharmingen	555996	500
FAP	F11-24	IgG1	Calbiochem	OP188	1000
Galectin 3	A3A12	IgG1	abcam	ab27850	1000
Galectin 4	198616	IgG2a	R&D	MAB1227	1000
Galectin 8	210608	IgG2a	R&D	MAB1305	1000
HLA-A,B,C	G46-2.6	IgG1	Pharmingen	555551	500
MICA	159227	IgG2b	R&D	MAB1300	
MMP-14	128527	IgG2b	R&D	MAB9181	
pIgR		IgG	R&D	AF2717	1000
CA19-9	M39026	IgG1	abcam	ab47871	1000
TSP-1	46.4	IgG1	Calbiochem	BA18	500
mIgG1 500			Pharmingen	557273	500

mIgG1 200			Cal-Nova	401122	200
mIgG1 50			Cal-Nova	401122	50
mIgG2a 500			Pharmingen	553454	500
mIgG2a 200			Pharmingen		200
mIgG2a 50			Pharmingen		50
mIgG2b 500			Pharmingen	553472	500
mIgG2b 200			Pharmingen	557351	200
mIgG3 500			Pharmingen	555742	500
mIgM 500	G155-228	IgM, k	Pharmingen	555581	500
mIgM 200	G155-228	IgM, k	Pharmingen	555581	200
mIgM 500	G155-228	IgM, k	Pharmingen	555581	500